The role of microRNA-194 in prostate cancer progression

Rayzel Candida Fernandes

Dame Roma Mitchell Cancer Research Laboratories
Faculty of Health and Medical Sciences
School of Medicine
The University of Adelaide

A thesis submitted to the University of Adelaide in fulfilment of the requirements for the degree of

Doctor of Philosophy

September 2019

Table of Contents

Abstract

Prostate cancer is a major cause of cancer-related mortality in Australia men. Mortality is primarily due to metastasis and the development of resistance to therapy. While prostate cancer is primarily driven by the androgen receptor signalling, a number of other factors play important roles in its growth and progression. In particular, small non-coding RNA molecules called microRNAs (miRNAs) are known to be key regulators of progression in prostate cancer. Our group previously identified one specific miRNA, miR-194-5p (miR-194), as an important driver of prostate cancer metastasis; however, the molecular mechanisms by miR-194 mediates these effects is not fully understood. My PhD project aimed to identify target genes and pathways that miR-194 regulates in order to better understand its role in prostate cancer.

I used cutting-edge genomic techniques and bioinformatics to identify 163 miR-194 target genes in prostate cancer. In Chapter 3, I used this data to identify a new role for miR-194 in prostate cancer. More specifically, I found that miR-194 activity was inversely correlated with androgen receptor (AR) activity in clinical samples, an observation explained mechanistically by AR-mediated repression of miR-194 expression. In concordance with these findings, miR-194 activity was significantly elevated in treatment-induced neuroendocrine prostate cancer (NEPC), an aggressive AR-independent subtype of prostate cancer. Furthermore, miR-194 can enhance transdifferentiation of epithelial LNCaP cells to neuroendocrine-like cells, a function mediated at least in part by its ability to target the FOXA1 transcription factor. Importantly, targeting miR-194 effectively inhibited the growth of aggressive models of NEPC, including patient-derived organoids.

By integrating the miR-194 "targetome" with transcriptomic data, my work has provided important insights into miRNA function in cancer cells (Chapter 4). Specifically, I have found that miR-194 functions potently through canonical interactions and can mediate co-operative repression through targeting multiple sites in the same mRNA transcript. Further, I have demonstrated that miR-194 is associated with widespread non-canonical interactions that can regulate gene expression, albeit to a lesser extent than canonical sites.

Finally, in Chapter 5 I have demonstrated that miR-194 has dichotomous effects on proliferation and invasion in breast and prostate cancer despite both cancers having several underlying biological similarities. Furthermore, in breast cancer I have found that miR-194 inhibits estrogen receptor expression, potentially by targeting FOXA1.

Overall, my work has provided unique insights into the pathobiology of miR-194, demonstrated its role as a potential therapeutic target in aggressive AR-independent prostate cancer subtypes, and identified novel functions for miR-194 in breast cancer.

Declaration

I certify that this work contains no material which has been accepted for the award of any other degree or diploma in my name, in any university or other tertiary institution and, to the best of my knowledge and belief, contains no material previously published or written by another person, except where due reference has been made in the text. In addition, I certify that no part of this work will, in the future, be used in a submission in my name, for any other degree or diploma in any university or other tertiary institution without the prior approval of the University of Adelaide and where applicable, any partner institution responsible for the joint-award of this degree.

I acknowledge that copyright of published works contained within this thesis resides with the copyright holder(s) of those works.

I also give permission for the digital version of my thesis to be made available on the web, via the University's digital research repository, the Library Search and also through web search engines, unless permission has been granted by the University to restrict access for a period of time.

I acknowledge the support I have received for my research through the provision of an Australian Government Research Training Program Scholarship.

Rayzel C. Fernandes

September 2019

Acknowledgements

My deepest thanks to my principal supervisor Dr Luke Selth for his excellent mentorship and the time and effort he has invested in my training. I am fortunate to have had the opportunity to join his lab and learn from him.

I am grateful to my co-supervisors, Dr.Theresa Hickey and Dr.Wayne Tilley for their invaluable guidance, support and advice over the course of my candidature. Their insights into my project were very much appreciated.

A big thank you to members of the Dame Roma Mitchell Cancer Research Labs. I've greatly enjoyed working alongside all of you the last few years.

Special thanks to members of the Goodall lab, without their contributions this project would not have been possible.

To the wonderful people at KLC, especially Dancey, Angus, Victoria, Anisha, Harry, Amanda, Brian and Sreekar. Thanks for the great conversations, board games, trivia, hikes, movie nights and just about everything else. I couldn't have asked for a better group of friends and I'm forever grateful for your endless support these last few months.

Finally, my family who deserve more thanks than I can give them. I couldn't have done it without you!

Chapter 1: Introduction

1.1 The prostate gland

1.1.1 Anatomy of the prostate gland

The prostate is a small, glandular male reproductive organ located within the pelvis. It is situated below the bladder, in front of the rectum and surrounds the first part of the urethra. Structurally, the prostate consists of glandular and stromal components enclosed by a fibromuscular pseudocapsule (Ayala et al. 1989; McNeal 1988).

The prostate is divided into four histologically distinct zones: three glandular zones - central, peripheral, transitional - and the non-glandular anterior fibromuscular stromal zone (Figure 1.1) (McNeal 1981). The distal urethral segment receives the majority of ducts from prostate glandular tissue (McNeal 1988). The peripheral zone, situated at the posterior of the gland, comprises approximately 70% of total prostatic glandular tissue (McNeal 1981). The peripheral zone is most predisposed to the development of cancer, with the majority (70-80%) of prostatic intraepithelial neoplasia and carcinomas arising here (McNeal et al. 1988). The central zone makes up 25% of total prostate glandular tissue and is histologically markedly different from the peripheral zone (McNeal 1981). The ejaculatory ducts are located within the central zone and the seminal vesicle duct fuses with the urethra in this region (McNeal 1988). The transitional zone, comprising only 5% of total prostate glandular tissue, is located directly below the bladder (McNeal 1988). Approximately 25% of cancers arise in the transition zone (McNeal et al. 1988). Non-malignant benign prostatic hyperplasia (BPH) typically occurs due to enlargement of glandular and stromal tissues in the transitional zone (McNeal 1978). The anterior fibromuscular region consists of bundles of smooth muscle fibres (McNeal 1988).

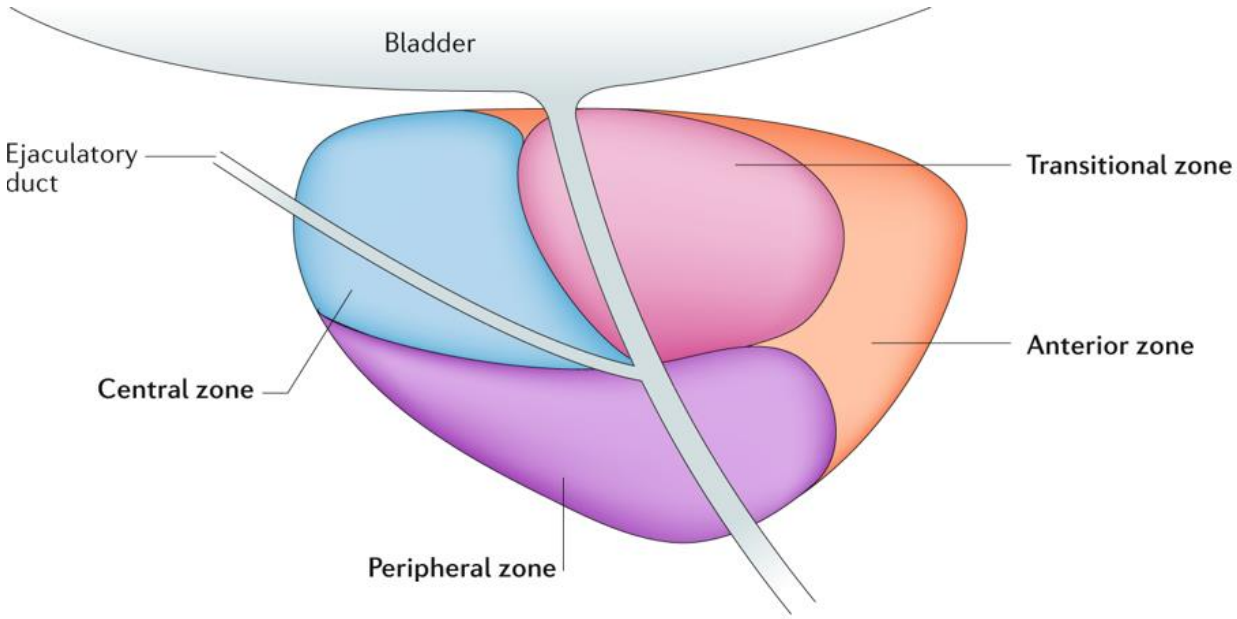

Figure 1.1: Schematic of prostatic zones (Adapted from (Sathianathen et al. 2018)

1.1.2 Histology of the prostate gland

The prostate gland is a highly lobulated structure composed of ducts and acini interspersed in a fibromuscular stroma (McNeal 1988). The ducts and acini are lined with epithelial cells, mainly luminal secretory and basal cells as well as other stem, progenitor or intermediate cells (Figure 1.2). Columnar secretory cells line the lumen whereas flattened basal cells are situated peripherally, separating the secretory cells from the stroma (McNeal 1988; Packer & Maitland 2016). Neuroendocrine (NE) cells are a rare population of cells found in the normal prostate. NE cells have a hybrid of neural and epithelial characteristics and comprise less than 1% of the prostatic epithelium (Abrahamsson & di Sant'Agnese 1993). The prostate epithelium represents a spectrum of differentiation from undifferentiated stem cells to fully mature luminal, basal or neuroendocrine cells. At least 3 models have been proposed for epithelial cell hierarchy in the prostate (Figure 1.3) (Taylor, Toivanen & Risbridger 2010). The linear hierarchal model (Figure 1.3A) hypothesizes that stem cells in the basal layer divide asymmetrically into a stem cell and a progenitor cell. Progenitor cells translocate towards the lumen, differentiating into an intermediate cell that proliferates and terminally differentiates into luminal or neuroendocrine cells (Isaacs & Coffey 1989) (Van Leenders & Schalken 2001). In the non-linear or bidirectional model (Figure 1.3B), stem cells give rise to lineage-specific progenitors that ultimately differentiate into terminal cell lineages (Taylor, Toivanen & Risbridger 2010; Wang et al. 2001). A more recent model (Figure 1.3C) suggests that multiple progenitors (e.g. basal stem cells or castration-resistant Nkx3.1-expressing cells (CARNS), a rare population of prostatic epithelial cells) give rise to differentiated cells (Taylor, Toivanen & Risbridger 2010; Wang et al. 2009). These progenitors may also be bi-potent, giving rise to opposite lineages (Wang et al. 2009).

The terminally differentiated luminal cells express the androgen receptor (AR), described below, and prostate-specific markers such as prostate specific antigen (PSA), prostate-specific acid phosphatase (PAP), prostate-specific membrane antigen (PSMA) and the prostate specific epithelial marker Nkx-3.1 (Shah & Zhou 2012). Mature basal cells are characterized by expression of cytokeratins and p63 and lack AR expression (Shah & Zhou 2012). NE cells, which also lack AR expression, are considered to be fully differentiated and typically express markers such as neural specific enolase, chromogranin A, synaptophysin and CD56 (Abrahamsson 1999). Prostate cancers are

primarily luminal in origin, although a small percentage arise from neuroendocrine cells (0.5-2%) and basal cells (0.01%) (Helpap, Köllermann & Oehler 1999; Kapatia et al. 2018).

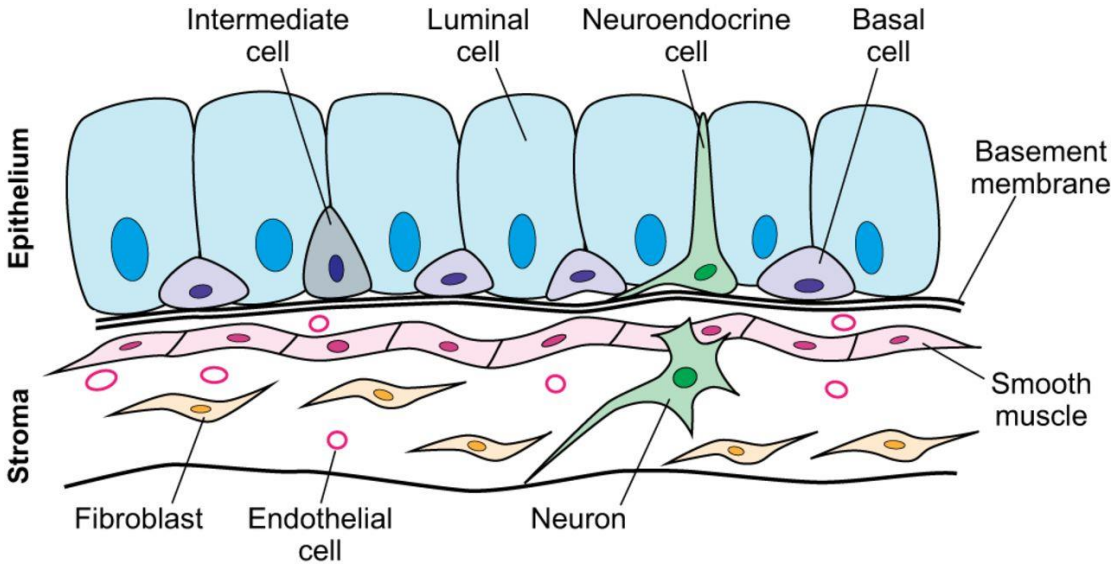

Figure 1.2: Schematic of differentiated cells in the adult prostate duct (Toivanen & Shen 2017).

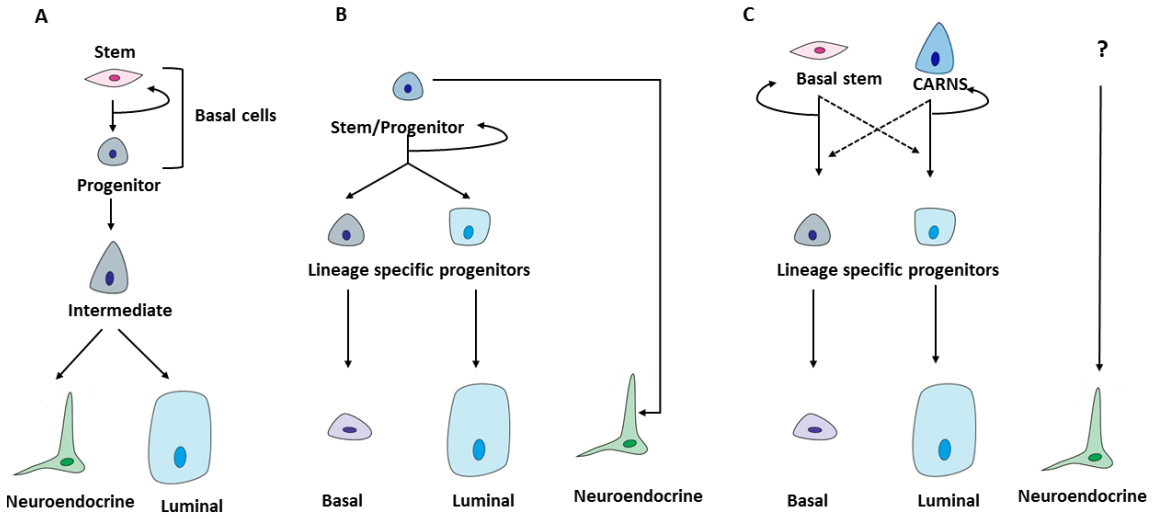

Figure 1.3: Models for prostate epithelial cell hierarchy (A) Linear hierarchical model (B) Non-linear or Bidirectional model (C) Independent arrangement model (Taylor, Toivanen & Risbridger 2010; Toivanen & Shen 2017).

1.2 Androgen receptor (AR): Structure and function

Androgen hormones and androgen receptor (AR) signalling are critical for normal prostatic development as well as prostate carcinogenesis (Heinlein & Chang 2004; Lonergan & Tindall 2011). The AR, a member of the nuclear receptor superfamily, is a ligand-activated transcription factor that is encoded by the *AR* gene on the X chromosome (Lubahn et al. 1988; Van Laar et al. 1989). The AR protein is 110 kDa, made up of 917 amino acids encoded by 2757 nucleotides on eight exons (Brinkmann et al. 1992; Tilley et al. 1989). Similar to other nuclear receptors, the AR protein consists of an N-terminal activation domain (NTD), a DNA binding domain (DBD), a hinge region and a C-terminal ligand binding domain (CTD) (Brinkmann et al. 1989; Jenster et al. 1991).

AR function is modulated by the binding of agonists or antagonists to the CTD. Unliganded AR is generally considered inactive and localised predominantly in the cytoplasm associated with molecular chaperones, co-chaperones and tetratricopeptide repeat (TPR)–containing proteins (Prescott & Coetzee 2006). Androgens such as testosterone and its more active metabolite, dihydrotestosterone (DHT), bind to the AR, which induces conformational changes, dissociation from chaperones, dimerization and translocation to the nucleus (Grino, Griffin & Wilson 1990; Jenster, Trapman & Brinkmann 1993; Wong et al. 1993). In the nucleus, the androgen-bound AR complex binds to specific DNA sequences called AR response elements (AREs) in the regulatory regions of target genes (Claessens et al. 1996).

During embryonic development, the presence of androgens (especially DHT) and a functional AR is necessary for prostate morphogenesis (Bardin et al. 1973; Siiteri & Wilson 1974; Wilson, Griffin & Russell 1993). During early prenatal development, the AR is expressed in the urogenital sinus mesenchyme but not in epithelial cells; AR regulated signals from the mesenchyme promote bud formation, ductal branching, proliferation and differentiation of the prostatic epithelium (Cooke, Young & Cunha 1991). Expression of epithelial AR commences during late prenatal or early neonatal development (Donjacour & Cunha 1993).

During puberty, androgen receptor signalling promotes growth of the prostate to its mature size (Banerjee et al. 2018). Post-puberty, AR signalling maintains homeostasis of the prostatic epithelium, promoting differentiation and maintaining a balance between

proliferation and apotosis, thereby preventing overgrowth of the prostate (Mirosevich et al. 1999). The AR is expressed in both stromal and epithelial cells in the prostate. While stromal cells do not appear to require AR for survival, the release of paracrine factors mediated by AR activity in stromal cells is necessary for the differentiation, growth, survival and function of epithelial cells (Donjacour & Cunha 1993; Prins & Birch 1993). Androgens also act directly via epithelial AR, targeting genes that include those promoting survival of the secretory epithelia, seminal fluid proteins, factors involved in epithelial differentiation and metabolic pathway components (Balk 2014).

1.3 AR co-regulators and pioneer factors

AR activity is modulated by a host of co-regulator proteins, with co-activators enhancing transcriptional activation and co-repressors reducing transactivation (Heinlein & Chang 2002). AR co-regulatory molecules include molecular chaperones, histone modifiers, transcriptional coordinators and chromatin modifiers (Chmelar et al. 2007).

Besides coregulators, pioneer factors play a key role in AR transactivation. Binding of AR to its response elements requires access to DNA, which is mediated by pioneer factors (Mayran & Drouin 2018). Pioneer factors bind to condensed chromatin, initiate chromatin opening and allow AR to access its regulatory elements (Zaret & Carroll 2011). FOXA1, a member of the FOX family of transcription factors, is a pioneer factor for AR and other members of the steroid hormone receptor family, opening chromatin to allow receptor recruitment to genomic loci (Jozwik & Carroll 2012). In the normal prostate, FOXA1 is required for AR gene activation in the prostatic epithelium and for the differentiation of epithelium into mature luminal cells (Gao et al. 2005; Gao et al. 2003). The equilibrium between FOXA1 and AR, important for maintaining the AR transcriptional program, is often lost in prostate cancer (Jin et al. 2014; Yang & Yu 2015).

1.4 Prostate cancer

1.4.1 Incidence

Prostate cancer (PCa) is the second most frequently occuring malignancy and the fifth leading cause of cancer-related mortality in men worldwide (Bray et al. 2018). In Australia, which has one of the highest estimated PCa incidence rates worldwide (86.4 per 100,000), PCa is estimated to be the most commonly diagnosed cancer and the second-leading cause of cancer mortality in 2019 (Bray et al. 2018; AIHW 2019).

1.4.2 Diagnosis of PCa

Two major tests that assist in the diagnosis of PCa are the serum prostate specific antigen (PSA) test and the digital rectal exam (DRE). PSA is encoded by the human kallikrein 3 gene (*KLK3*) and is a well characterised AR target gene in prostate epithelial cells. PSA is generally present at low levels in serum with levels between 0-4ng/ml considered normal. A rise in PSA levels may be due to PCa and or non-malignant conditions like prostatitis and benign prostatic hyperplasia (Kim & Coetzee 2004). PSA or DRE results that are indicative of PCa will often lead to histopathological examination of tissue obtained by biopsy, which is the definitive diagnostic tool for PCa.

Besides being used for diagnosis, PSA levels are also used to monitor patients following surgery or radiation treatment for PCa. A rise in PSA levels following treatment, known as biochemical recurrance (BCR), is used as an indicator of treatment failure, disease progression or metastases (Stephenson et al. 2006).

1.4.3 Gleason grading

The Gleason grading system, based on specific histological patterns of cells, assigns a score to histological sections that is indicative of the aggressiveness of the tumour and its prognosis. The original sytem of clasification, developed in the 1960s, describes 5 histological growth patterns graded from 1 to 5 (Figure 1.4) (Gleason 1992). Gleason grade 1 represents well differentiated cell architecture that is close to normal and associated with favourable prognosis. Grade 5 is indicative of poor differentiation and is correlated with poor prognosis. Since tumours are heterogenous and often contain more than one grade, the two most prevalent grades are added to generate the Gleason score

(Gleason 1992). If only one grade is present or the secondary grade is present in less than 3% of tissue, the primary grade is doubled to give Gleason score (Humphrey 2004). Gleason scores range from 2-10, and have been linked with a number of histopathological and clinical endpoints, including tumour size, pathological stage, margin status, biochemical recurrence, metastasis and survival (Humphrey 2004). The Gleason score remains a powerful prognostic predictor and is used to guide treatment strategies and clinical disease management.

Despite its prognositic utility, the classical Gleason scoring system does have some limitation. For instance, the lowest Gleason score currently assigned to tumours is 6, with scores of 2-5 not being used due to under grading, poor reproducibilty and a lack of correlation between biopsy and prostetectomy samples (Cury, Coelho & Srougi 2008; Epstein 2000). Another drawback is that tumours with patterns 3+4 or 4+3 both have an overall Gleason score of 7 although tumours with primary pattern 4 are likely to be more aggressive (Burdick et al. 2009). To overcome these limitations, modifications have recently been made to the classical Gleason scoring sytem whereby Gleason scores are assigned into grade groups that more accurately predict disease progression (Gordetsky & Epstein 2016).

Figure 1.4: Histological patterns of PCa cells representing gleason grades from 1 to 5 (Gleason 1966).

1.4.4 Tumour staging

Tumour staging classifies tumours based on the extent of spread of disease (Reese 2016). The TNM system is widely used for PCa and evalutes the extent of primary tumour (T), lymph node involvement (N) and presence or absence of metastasis (M) (Figure 1.5). TNM staging in combination with Gleason grade and PSA levels is used to assign patients into prognositic stage groups that guide treatment decisions (Buyyounouski et al. 2017).

1.4.5 Risk stratification

Men with localized or locally advanced PCa, where the cancer is confined within the capsule that surrounds the prostate gland or has extended into surrounding organs, are stratified at diagnosis into groups based on their risk of disease progression. The D'Amico risk stratification system is commonly used for PCa and assesses risk of biochemical recurrance over a 5 year period following treatment (D'Amico et al. 1998). The D'Amico classifier uses pre-treatment, PSA, Gleason score and TNM stage to assign patients into either low, intermediate or high risk groups (D'Amico et al. 1998).

T - Primary Tumour		
TX	Primary tumour cannot be assessed	
T0	No evidence of primary tumour	
T1	Clinically inapparent tumour that is not palpable	
	T1a	Tumour incidental histological finding in 5% or less of tissue resected
	T1b	Tumour incidental histological finding in more than 5% of tissue resected
	T1c	Tumour identified by needle biopsy (e.g. because of elevated prostate-specific antigen (PSA) level)
T2	Tumour that is palpable and confined within the prostate	
	T2a	Tumour involves one half of one lobe or less
	T2b	Tumour involves more than half of one lobe, but not both lobes
	T2c	Tumour involves both lobes
T3	Tumour extends through the prostatic capsule[1]	
	T3a	Extracapsular extension (unilateral or bilateral) including microscopic bladder neck involvement
	T3b	Tumour invades seminal vesicle(s)
T4	Tumour is fixed or invades adjacent structures other than seminal vesicles: external sphincter, rectum, levator muscles, and/or pelvic wall	
N - Regional Lymph Nodes		
NX	Regional lymph nodes cannot be assessed	
N0	No regional lymph node metastasis	
N1	Regional lymph node metastasis	
M - Distant Metastasis		
M0	No distant metastasis	
M1	Distant metastasis	
	M1a	Non-regional lymph node(s)
	M1b	Bone(s)
	M1c	Other site(s)

Figure 1.5: TNM calssification of PCa (Mottet et al. 2017).

1.5 Treatment of localized and locally advanced PCa

At diagnosis, approximately 93% of men have clinically localized or locally advanced disease (National Cancer Control Indicators 2019).With appropriate treatment, localized and locally advanced disease is associated with >98% 5-year overall survival rates in Australia (National Cancer Control Indicators 2019).

Management and treatment decisions for localized and locally advanced PCa are based on disease risk stratification. Low-risk cancers are often slow growing, clinically insignificant and may not require intervention (O'Donnell & Parker 2008). Active surveillance i.e. regular monitoring of disease with selective intervention when there are signs or symptoms of disease progression, is a commonly recommended approach for low-risk tumours (Bellardita et al. 2015; Dall'Era et al. 2008). Active surveillance is also an option for a subset of patients who have favourable intermediate risk PCa (defined as a single intermediate risk factor, Gleason grade of 3 + 4 = 7 or less and <50% of cancer containing biopsies (Zumsteg et al. 2013)), but this carries a higher risk of disease progression (Ward et al. 2015).

Treatment options for intermediate and high-risk PCa include radiation therapy and surgery to remove the prostate and some surrounding tissue (i.e radical prostatectomy). Radiation therapy may involve either external beam radiation therapy (EBRT) or brachytharapy, where radiation source ("seeds") are implanted near the cancer. Both radiation or surgery are effective treatments, with no significant difference in survival irrespective of treatment option (Hamdy et al. 2016). Within the high risk group however, patients with locally advanced disease are at higher risk of treatment failure. For these patients, radical prostatectomy in combination with radiation therapy improves overall survival (Jang et al. 2018).

1.6 Treatment of recurrent and metastatic prostate cancer

Despite high post-treatment survival rates, a subset of men (20-40% post radical prostatetctomy, 30-50% post radiation therapy) experience BCR within 10 years, either due to local disease recurrance or metastasis (Artibani et al. 2018). Local disease recurrance involves the presence of cancer cells in the prostatic bed or pelvic area whereas

metastatic prostate cancer manifests in distant anatomic sites such as bones, lymph nodes, lungs, liver and brain (Logothetis & Lin 2005). Appoximately 10-20% of men develop metastatic disease after treatment, although approximately 5% of men also have metastatic disease at diagnosis (Merseburger et al. 2013; National Cancer Control Indicators 2019). Men with recurrent and metastatic PCa are treated with androgen deprivation therapy (ADT), chemotherapy, radiotherapy, immunotherapy or a combination of these treatments (Miller et al. 2016).

AR is the primary driver of primary and metastatic PCa. The AR-regulated transcriptional program switches from regulating cell differentiation and homeostatsis in the normal prostate to promoting cell proliferation and survival in PCa, resulting in continuous growth (Zhou, Bolton & Jones 2015). Hodges and Huggins first demonstrated that PCa was dependent on androgen hormones in 1941 and supressing AR signalling has since been a mainstay treatment for PCa since that time (Huggins & Hodges 1941). ADT supresses prostate tumour growth by reducing levels of circulating androgens and/or directly blocking the action of the AR with antagonists. ADT is the primary treatment for metastatic PCa and is used as an adjunct to radiotherapy in high-risk and locally advanced disease, where it improves disease-free and overall survival (Kauffmann & Liauw 2017).

Historically, ADT was achieved by orchiectomy (i.e. surgical removal of the testes, which produce the majority of androgens), or chemically using oral estrogen, which supresses testicular androgen production via negative feedback with the hypothalamic–pituitary–testicular axis (Figure 1.6) (Phillips et al. 2014; Turo et al. 2014). Both orchiectomy and oral estrogen have now been replaced in favour of luteinizing hormone releasing hormone (LHRH) agonists and antagonists, and inhibitors of steroid hormone synthesis. LHRH agonists, also known as gonadotrophin-releasing hormone (GnRH) analogues, bind to their receptors in the pituitary, causing an increase in lutenizing hormone (LH) and follicule stimulating hormone (FSH), which act to stimulate testosterone production in the testes. This continuous stimulation of LHRH receptors ultimately downregulates LH/FSH production leading to suppression of testosterone levels (Labrie et al. 1980; Labrie et al. 2005). The rise in serum testosterone levels or ‘flare’ on initial exposure to LHRH agonists can be detrimental to some patients (Thompson 2001). By contrast, LHRH antagonists competitively bind to LHRH receptors to prevent the release of LH/FSH and are not associated with a flare (Gordon & Hodgen 1992). Since the ‘flare’ phenomenon is associated with several side effects including hot

flashes, ureteral obstruction, urinary retention, erectile dysfunction, anaemia and muscle wasting, LHRH antagonists represent a safer therapeutic approach compared to LHRH agonists for treatment of PCa.

In addition to therapeutics that surgically or chemically prevent production of androgens, anti-androgens (also called AR antagonists) are also used to treat advanced PCa. Anti-androgens are a class of steroidal or non-steroidal molecules that inhibit AR signalling by competitively preventing binding of endogenous androgens to the AR (Chen, Clegg & Scher 2009). First generation anti-androgens include such as Flutamide, Bicalutamide and Nilutamide (more accurately termed selective AR modulators (SARMS) (Culig et al. 1999; Kemppainen & Wilson 1996). Antiandrogens can be used in combination with surgical or chemical castration to improve treatment efficacy (Yang et al. 2019).

Castration based therapy and first generation anti-androgens invariably fail, normally after a period of 2-3 years, resulting castration-resistant prostate cancer (CRPC) (Pienta & Bradley 2006; Scher et al. 2004). More than 80% of patients with CRPC develop rapidly progressing metastatic CRPC (mCRPC), which is currently incurable (Albala 2017).

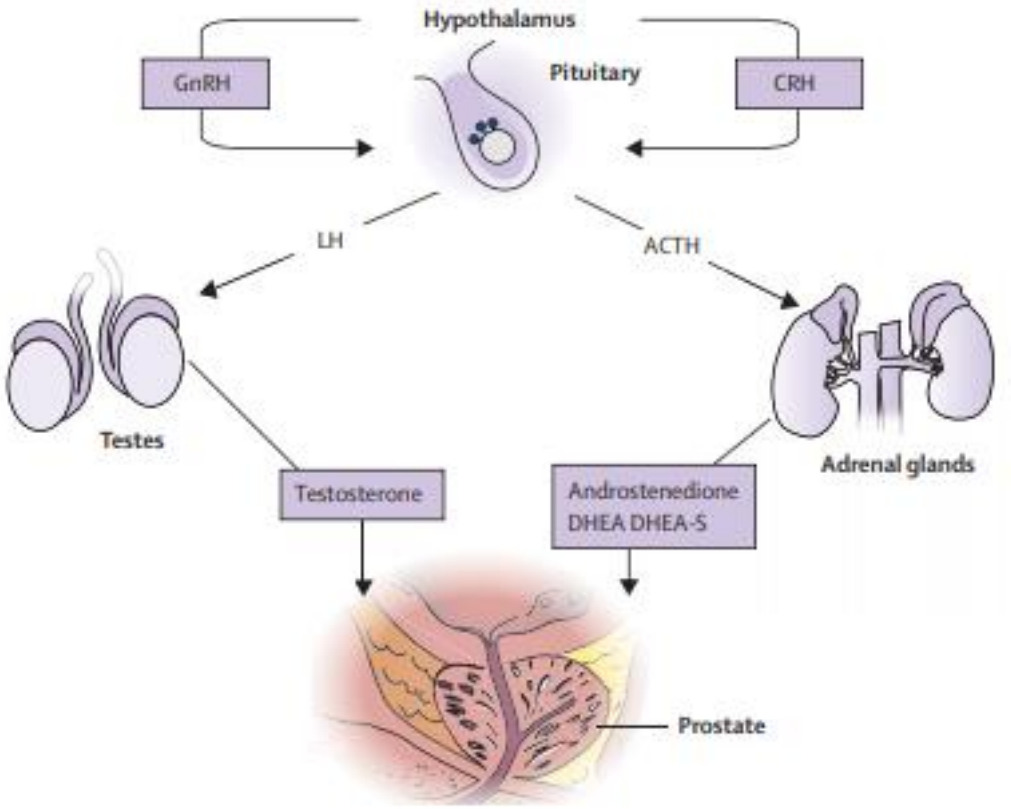

Figure 1.6: Production of androgens by the testes and adrenal glands. Adapted from (Chen, Clegg & Scher 2009).

1.7 Treatment of CRPC

The emergence of CRPC due to the failure of first line treatments has led to the development of second generation anti-androgens (Tran et al. 2009). These include Enzalutamide and Apalutamide, which bind to the AR with high affinity, prevent translocation of receptor into the nucleus and inhibit AR-DNA interaction (Antonarakis 2013; Rathkopf et al. 2017). These anti-androgens significantly improve overall survival and progression free survival in men with CRPC (Chong, Oh & Liaw 2018; Linder et al. 2018).

Although the majority of androgen is produced by the testes, about 1% is produced by the adrenal glands via the corticotropin-releasing hormone (CRH) and adrenocorticotropic hormone (ACTH) signalling axis (Figure 6). Adrenal androgens such as dehydroepiandrosterone (DHEA), dehydroepiandrosterone sulfate (DHEAS) and androstenedione act as precursors for the production of testosterone or DHT and thus contribute to activation of AR signalling. Drugs such as abiraterone acetate are used to inhibit the cytochrome P450 family of enzymes involved in adrenal and gonadal androgen synthesis (Friedlander & Ryan 2010; Mostaghel 2013; Mostaghel & Plymate 2011).

Additional treatment modalities for CRPC and mCRPC includes chemotherapy, radiopharmaceuticals and immunotherapy. These treatments are also used in combination with castration or ADT to aggressively treat non-CRPC metastases for improved clinical outcomes (Sweeney et al. 2015). Commonly used chemotherapeutic agents used for CRPC include docetaxel, cabazitaxel and mitoxantrone. For bone metastasis, the radiopharmaceutical radium-223 dichloride has been found to be effective at improving overall survival (Parker et al. 2013). Radium-223 is a calcium mimetic that is incorporated in stroma formed by bone metastases where it emits cytotoxic alpha radiation (Parker et al. 2013). Immunotherapy, using a dendritic cell vaccine (Sipuleucel-T) is used to treat asymptomatic or minimally symptomatic CRPC.

Despite being incurable, emerging therapies have improved median survival for patients with CRPC. This longer life expectancy is associated with cancer-related complications, particularly related to the urinary tract and skeletal system if bone metastases has occurred. In these instances, palliative treatments are used for symptomatic relief and to improve quality of life (Piper et al. 2014).

1.8 Mechanisms of resistance to ADT

1.8.1 Reactivation of AR signalling

Persistent AR signalling in spite of castrate levels of circulating testosterone is the main driver of CRPC growth in ~70-85% of cases (Bluemn et al. 2017; Coutinho et al. 2016). Persistent AR signalling in CRPC is frequently due to *AR* gene amplification, which occurs at low frequency (~1%) in primary tumours but at high frequency (45-54%) in CRPC (Abida et al. 2019; Cancer Genome Atlas Research 2015; Chen et al. 2004; Grasso et al. 2012; Koivisto et al. 1997; Robinson et al. 2015; Taplin et al. 1995; Visakorpi et al. 1995). Increased AR expression promotes resistance to ADT by sensitizing cells to low levels of serum androgen (Visakorpi et al. 1995). AR gene point mutations, which occur in a proportion of CRPC tumour cells, are also important in resistance to ADT (Steinkamp et al. 2009). AR mutations are found in 5-30% of tumours post-treatment but infrequently in primary PCa prior to treatment (Coutinho et al. 2016). CRPC-associated AR mutations mostly occur within the ligand binding domain of the AR where they promote promiscuous binding and activation by alternative ligands such as estrogens, progesterone or anti-estrogens (Eisermann et al. 2013).

AR splice variants (AR-Vs) represent another strategy adopted by PCa to progress to CRPC (Hörnberg et al. 2011). AR-Vs are alternately spliced isoforms of the AR mRNA that encode the NTD and DBD but lack the CTD (Qu et al. 2015); Approximately 20 AR-Vs have been identified in cell lines and clinical specimens, of which several are constitutively active and can signal in the absence of androgen (Jernberg, Bergh & Wikström 2017; Kallio et al. 2018).

Besides AR alterations, continued AR signalling is maintained by increased expression of steroidogenic enzymes within the tumour, which enhances intratumoral synthesis of testosterone and DHT from adrenal androgens (Armandari et al. 2014; Montgomery et al. 2008). Collectively, mechanisms of resistance to ADT in PCa highlight the central role that AR plays in PCa progression.

Yet another adaptive mechanism in CRPC is the activation of GR signalling (Arora et al. 2013). The GR can act as a surrogate AR by occupying AR DNA binding sites and

regulating expression of some AR target genes to promote therapeutic resistance (Arora et al. 2013).

1.8.2 "AR indifferent" PCa

A subset (20-25%) of prostate tumours are known to shed their reliance on AR and its associated pathways and progress to an "AR indifferent" state, in which AR expression may or may not be retained (Bluemn et al. 2017). The major "AR indifferent" prostate cancer subtypes is neuroendocrine prostate cancer (Ellis & Loda 2018). Neuroendocrine prostate cancer that arises after failure of second generation AR-targeted therapies (i.e. Enzalutamide, Abiraterone) is referred to as treatment emergent NEPC (T-NEPC) (Davies, Beltran & Zoubeidi 2018). T-NEPC is highly aggressive and generally causes death within 2 years from diagnosis (Davies, Beltran & Zoubeidi 2018). Similar to neuroendocrine cells, NEPC express NE markers, such as synaptophysin (SYP), chromogranin A (CHGA), neuronal-specific enolase (NSE) and are defined by loss of AR expression (Beltran et al. 2011). NEPC tumours also originate as *de novo* primary cancers from prostatic neuroendocrine cells but are very rare (~1%).

T-NEPC tumours are suggested to arise as an adaptive response to ADT via lineage plasticity. Lineage plasticity or cellular plasticity refers to the ability of a differentiated cell to revert to a less differentiated state or change to an alternative differentiated state (Aggarwal et al. 2014; Ellis & Loda 2018; Le Magnen, Shen & Abate-Shen 2018). In concordance with this hypothesis, androgen deprivation has been shown to reprogram AR-positive PCa cell lines into a metastable cancer-stem cell like state that can differentiate into a neuroendocrine phenotype (Nouri et al. 2017). Additionally, lineage tracing has determined that neuroendocrine (NE) cells transdifferentiate from prostate luminal cells (Zou et al. 2017). Furthermore, epithelial mesenchymal transition (EMT), a transdifferentiation process utilized by cancer cells for metastasis, has also been associated with T-NEPC (Esposito et al. 2015; McKeithen et al. 2010).

AR targeting therapies have been shown to contribute to the emergence of NEPC via upregulation of AR-repressed genes that can promote transdifferentiation. For example, *BRN2* is a neural transcription factor repressed by AR that is upregulated by the AR antagonist Enzalutamide (Bishop et al. 2017). BRN2 is required for T-NEPC and acts

partly by regulating SOX2, a transcriptional factor required for pluripotency and self-renewal (Bishop et al. 2017). *SOX2*, which is also directly repressed by the AR, promotes lineage plasticity in NEPC (Mu et al. 2017).

In addition to de-repressed AR signalling, multiple genetic, epigenetic and transcriptional events converge to promote plasticity and transdifferentiation in T-NEPC. Common genetic events include allelic loss of *RB1* and *PTEN, Tp53* mutations and amplification of *AURKA* and *MYCN* (Mosquera et al. 2013; Tan et al. 2014). *RB1* loss often occurs in conjunction with *PTEN* and *Tp53* mutations (Tan et al. 2014). Mechanistically, this de-represses the expression of *SOX2* and *EZH2*, to enable lineage switching (Ku et al. 2017). EZH2 is a histone methyltransferase that regulates cell pluripotency by altering gene expression via methylation of histone H3 lysine 27 (H3K27). Other factors implicated in progression to T-NEPC also act via SOX2- and EZH2-regulated gene networks. For instance, MYCN has been shown to drive progression to NEPC by activation of an EZH2 mediated transcriptional program (Dardenne et al. 2016). Besides EZH2, other epigenetic regulators upregulated in NEPC include the RNA splicing factor SRRM4, and non-coding RNAs such as miR-100-5p, miR-652 and lncRNA-p21 (Lee et al. 2018; Luo et al. 2019; Nabavi et al. 2017; Nam et al. 2018).

Another AR indifferent prostate cancer subtype, called double negative prostate cancer (DNPC), is negative for both AR and NEPC markers (Bluemn et al. 2017). DNPC arises in patients after treatment with AR antagonists and is associated with elevated autocrine FGF MAPK signalling which allows these tumours to bypass the requirement for AR signalling(Bluemn et al. 2017) . The DNPC subtype has been suggested to be a transition state to NEPC (Bluemn et al. 2017).

At present, treatment options for AR-indifferent PCa are limited to chemotherapy regimens. Novel molecular targeting therapy against EZH2 and AURKA are currently under development (Akamatsu et al. 2018).

1.9 miRNA

MicroRNAs (miRNAs) are a class of small non coding RNA molecules that post-transcriptionally regulate expression of target genes by (Bartel 2004). miRNAs were first discovered in the nematode *Caenorhabditis elegans* where they were found to interact

with the 3'UTR of developmental genes and negatively regulate their expression (Lee, Feinbaum & Ambros 1993; Reinhart et al. 2000).

miRNA genes encoded in the human genome are located either intergenically or within the introns of protein coding genes (Lee et al. 2004). Approximately 25% of human miRNA genes are organized in clusters of two or more genes (Kabekkodu et al. 2018). Clustered miRNA are co-expressed and transcribed as a single polycystronic unit (Baskerville & Bartel 2005). Transcription of individual or clustered intergenic miRNA genes is generally initiated from their own transcription initiation sites whereas intronic miRNA are either transcribed as part of their host genes or from upstream regulatory elements independent of the host gene (Lee et al. 2004; Monteys et al. 2010; Ozsolak et al. 2008).

Like mRNA, most miRNA are transcribed by RNA polymerase II (Lee et al. 2004). Primary miRNA transcripts (pri-miRNA) are 5' capped and 3' polyadenylated hairpin structures that can range from a few hundred to a few kilobase pairs in size. Within the nucleus, pri-miRNA are processed into a 60-70bp pre-miRNA hairpins by a complex known as the microprocessor, consisting of Drosha and DGCR8 proteins (Figure 1.7) (Han et al. 2004). Pre-miRs are exported into the cytoplasm by the Exportin5 complex where they are processed into 18-22bp mature miRNAs by Dicer (Ha & Kim 2014; Lee et al. 2003; Lund et al. 2004). Mature miRNA are then incorporated into an RNA-induced silencing complex (RISC) along with Argonaute proteins. The RISC ribonucleoprotein complex recognizes and binds to target transcripts by Watson-Crick base pairing between the 5' end of the miRNA and complementary sequences mainly in 3'UTR of the target transcript (Bartel 2009). Gene expression is repressed via transcript degradation or translational repression (Pratt & MacRae 2009). In humans, miRNA-encoding genes make up >5% of the human genome but regulate nearly 60% of protein coding genes (Friedman et al. 2009). As regulators of gene expression, miRNAs play critical roles in normal physiology and in pathological conditions.

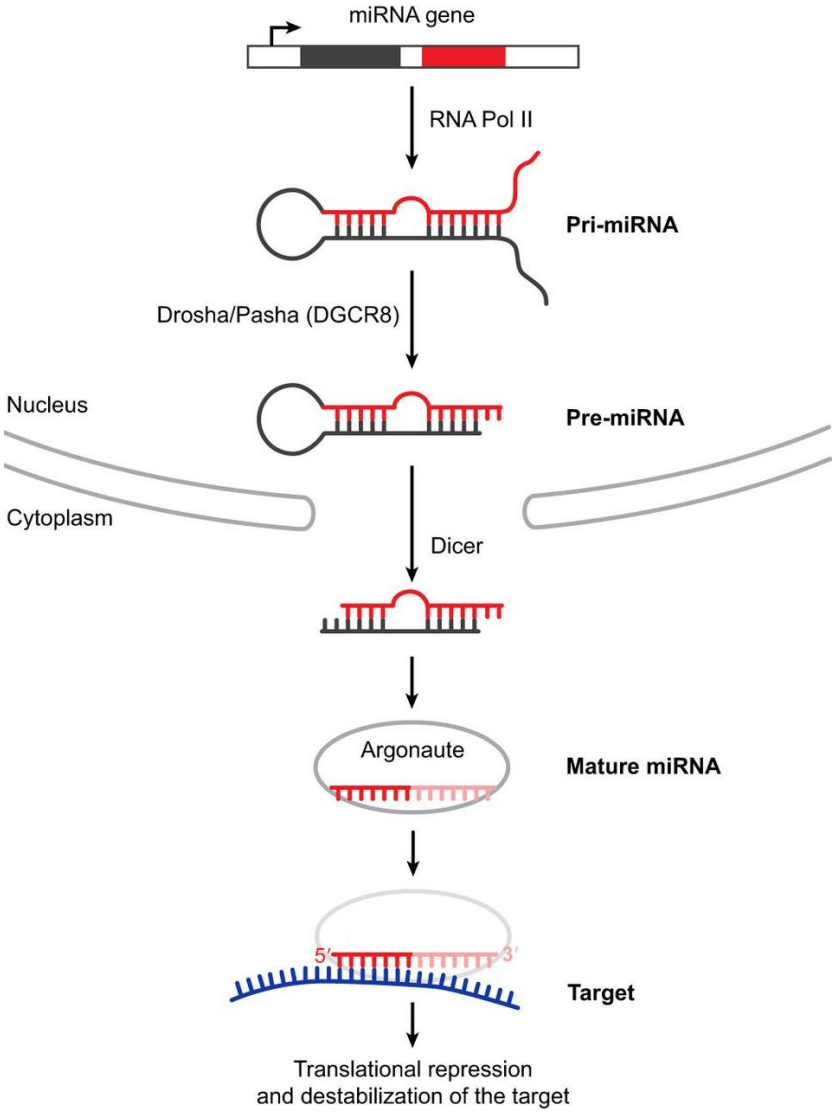

Figure 1.7: miRNA biogenesis (Alberti & Cochella 2017)

1.9.1 MiRNA in PCa

miRNAs were first linked with tumorigenesis when miR-16-1 and 15a were found to be located in a chromosomal region deleted in B cell chronic lymphocytic leukaemia (Calin et al. 2002). Both these miRNA target the anti-apoptotic protein Bcl2 and their loss inhibits apoptosis (Cimmino et al. 2005). Since this initial discovery, dysregulation of miRNAs has been reported in all cancer types (Peng & Croce 2016). Dysregulation of miRNAs in cancer is often a consequence of alteration of miRNA gene loci such amplification, deletion, translocations, copy number variation and epigenetic changes, perturbation of upstream transcriptional regulators or defects in biogenesis (Peng & Croce 2016). Cancer-associated miRNA are either oncogenic (oncomiRs) i.e. they downregulate the expression tumour suppressor genes or act as tumour suppressors by targeting oncogenes (Pang, Young & Yuan 2010).

In PCa, studies comparing miRNA expression in normal prostate epithelium, BPH, primary tumours, metastases, hormone sensitive tumours and CRPC as well as work in animal and cell line models have implicated miRNAs in PCa initiation, progression, therapy resistance, and metastatic dissemination. (Ambs et al. 2008; Goto et al. 2015; Hart et al. 2014; Jalava et al. 2012; Martens-Uzunova et al. 2012; Porkka et al. 2007; Walter et al. 2013). Mechanistically, PCa associated miRNA mediate these effects by regulating cell cycle, apoptosis, migration, invasion and other related pathways. For instance, the oncogenic miR-221/222 family promotes PCa proliferation by repressing the cell cycle inhibitor p27 and inhibits apoptosis by repressing Caspase-10 (Galardi et al. 2007; Wang, Liu, et al. 2015). Other examples of oncomiRs in PCa include miR-21, which targets the cell cycle inhibitor p57(Mishra et al. 2014), miR-9, which regulates metastasis via *SOCS5* and *CDH1*, (Seashols-Williams et al. 2016), miR-32, which regulates the cell cycle and apoptosis via *BTG2* (Jalava et al. 2012), and miR-194, which regulates metastasis via *SOCS2* (Das et al. 2017). Tumour suppressive miRNAs that have frequently been reported as downregulated in PCa include the let-7 family that targeting cell cycle regulators *E2F2* and *CCDN2* (Dong et al. 2010), the miR-15a-16-1 cluster targeting the cell cycle regulator *CCND1* and WNT pathway signalling ligand *WNT3A* (Bonci et al. 2016), and miR-34a which inhibits proliferation by targeting and *MYC* (Yamamura et al. 2012).

Importantly, the downregulation of a number of AR targeting miRNA is partly responsible for increased *AR* expression and activity in PCa. Conversely, the AR signalling axis induces expression of oncogenic miRNA and represses tumour suppressor miRNA. This interplay between the AR signalling axis and miRNA is important in driving PCa growth and progression.

1.9.2 Interplay between the AR signalling axis and microRNAs in PCa

This section of the introduction was published as a review article.

Interplay between the androgen receptor signalling axis and microRNAs in prostate cancer. (2019). Fernandes RC, Hickey TE, Tilley WD, Selth LA. Endocr Relat Cancer. 26(5): R237–R257

https://erc.bioscientifica.com/view/journals/erc/26/5/ERC-18-0571.xml

Statement of Authorship

Title of Paper	Interplay between the AR signalling axis and microRNAs in prostate cancer
Publication Status	● Published ☐ Accepted for Publication ☐ Submitted for Publication ☐ Unpublished and Unsubmitted work written in manuscript style
Publication Details	Interplay between the androgen receptor signaling axis and microRNAs in prostate cancer. (2019). Fernandes RC, Hickey TE, Tilley WD, Selth LA. Endocr Relat Cancer. 26(5): R237–R257

Principal Author

Name of Principal Author (Candidate)	Rayzel C Fernandes		
Contribution to the Paper	Conceptualized manuscript (with Dr.Selth, corresponding author), literature review, prepared tables, wrote manuscript		
Overall percentage (%)	60%		
Certification:	This paper reports on original research I conducted during the period of my Higher Degree by Research candidature and is not subject to any obligations or contractual agreements with a third party that would constrain its inclusion in this thesis. I am the primary author of this paper.		
Signature		Date	20·09·2019

Co-Author Contributions

By signing the Statement of Authorship, each author certifies that:

i. the candidate's stated contribution to the publication is accurate (as detailed above);

ii. permission is granted for the candidate in include the publication in the thesis; and

iii. the sum of all co-author contributions is equal to 100% less the candidate's stated contribution.

Name of Co-Author	Wayne D. Tilley		
Contribution to the Paper	Evaluated and edited Manuscript		
Signature		Date	16/9/2019

Name of Co-Author	Theresa E. Hickey		
Contribution to the Paper	Evaluated and edited Manuscript		
Signature		Date	16/9/2019

Name of Co-Author	Luke A. Selth		
Contribution to the Paper	Supervised development of manuscript, conceptualized and co-wrote manuscript, prepared figures, edited and evaluated manuscript		
Signature		Date	20/9/19

REVIEW

Interplay between the androgen receptor signaling axis and microRNAs in prostate cancer

Rayzel C Fernandes[1,2], **Theresa E Hickey**[1], **Wayne D Tilley**[1,2] and **Luke A Selth**[1,2]

[1]Dame Roma Mitchell Cancer Research Laboratories, Adelaide Medical School, Faculty of Health and Medical Sciences, The University of Adelaide, Adelaide, South Australia, Australia
[2]Freemasons Foundation Centre for Men's Health, Adelaide Medical School, Faculty of Health and Medical Sciences, The University of Adelaide, Adelaide, South Australia, Australia

Correspondence should be addressed to L A Selth: luke.selth@adelaide.edu.au

Abstract

The androgen receptor (AR) is a ligand-activated transcription factor that drives prostate cancer. Since therapies that target the AR are the mainstay treatment for men with metastatic disease, it is essential to understand the molecular mechanisms underlying oncogenic AR signaling in the prostate. miRNAs are small, non-coding regulators of gene expression that play a key role in prostate cancer and are increasingly recognized as targets or modulators of the AR signaling axis. In this review, we examine the regulation of AR signaling by miRNAs and vice versa and discuss how this interplay influences prostate cancer growth, metastasis and resistance to therapy. Finally, we explore the potential clinical applications of miRNAs implicated in the regulation of AR signaling in this prevalent hormone-driven disease.

Key Words

- microRNA
- androgen receptor
- prostate cancer
- biomarkers
- therapy

Endocrine-Related Cancer (2019) **26**, R237–R257

1. INTRODUCTION

The androgen receptor (AR) signaling axis is critical for normal prostatic development and maintenance and is the major driver of prostate cancer (PCa) growth and disease progression. Androgens such as testosterone and its more active metabolite, dihydrotestosterone (DHT), bind to the AR in the cytoplasm of prostate epithelial cells, which elicits its translocation into the nucleus. Ligand-activated AR binds to specific DNA sequences termed AR response elements (AREs) in regulatory regions of target genes, resulting in transcriptional activation or, less commonly, repression (Wang, et al. 2009). In normal prostate epithelial cells, a key function of AR target genes is to maintain luminal differentiation; by contrast, in malignant prostate cells an aberrant AR transcriptional program promotes cell proliferation and survival (Coutinho, et al. 2016).

Given the critical role of AR in PCa, androgen deprivation therapy (ADT) is the primary treatment for metastatic disease (Feldman and Feldman 2001). ADT encompasses multiple agents that: i) decrease circulating androgen levels by inhibiting pituitary signals that stimulate testicular androgen production i.e. lutenizing hormone releasing hormone (LHRH) and gonadotropin releasing hormone (GnRH) agonists that; ii) diminish biosynthesis of androgens i.e. inhibitors of androgen biosynthetic enzymes; and/or iii) inhibit AR activity i.e. agents that block androgen binding to the AR, termed AR antagonists. Unfortunately, these treatments inevitably fail, normally after a period of 2-3 years. The resultant disease is termed castration-resistant prostate cancer (CRPC) (Scher, et al. 2004). AR remains the key driver of most cases of CRPC. Maintenance of AR activity despite low levels of circulating androgens can be achieved through amplification or mutation of the *AR* gene, alternative splicing to produce constitutively-active AR splice variants, altered expression of AR co-regulators and/or enhanced intra-tumoral androgen production (Coutinho et al. 2016).

MicroRNAs (miRNAs) are a class of small non-coding RNAs, approximately 22nt in length, that post-transcriptionally silence target messenger RNAs (mRNAs). An estimated 60% of all protein coding mRNAs are targeted by miRNAs (Friedman, et al. 2009), highlighting the powerful influence these small transcripts can have on the transcriptome and how it is interpreted by the cell. Primary transcripts of miRNA genes (pri-miRNAs), transcribed primarily by RNA polymerase II, can be encoded by sequences within (intragenic) or outside of (intergenic) protein-coding genes (Lee, et al.

2004; Rodriguez, et al. 2004). Following transcription of a miRNA gene (or host gene), pri-miRNAs are processed into precursor miRNAs (pre-miRNAs) that fold into a stem loop structure and are exported from the nucleus (Kim 2005). Within the cytoplasm, pre-miRNAs are cleaved into a miRNA duplex that is then separated; one strand is the final mature form of approximately 22bp and the other strand is degraded (Kim 2005). As part of the RNA induced silencing complex (RISC) that includes Argonaute (Ago) proteins, miRNAs bind to target mRNAs and promote transcript degradation and/or translational inhibition (Fabian and Sonenberg 2012). MiRNAs generally bind to the 3'UTR of their target genes through complementarity with a region called the seed sequence, consisting of nucleotides 2-8 on the 5′ to 3′ ends of a miRNA sequence (Lewis, et al. 2005), although an increasing number of studies have also identified functional miRNA seed sites in the coding and 5'UTR regions of genes (Brummer and Hausser 2014; Ito, et al. 2017; Zhang, et al. 2018; Zhou and Rigoutsos 2014).

Dysregulated miRNA expression is a hallmark of cancer development and metastasis (Calin and Croce 2006; Jackson, et al. 2014). PCa-associated miRNAs were initially reported by Porkka and colleagues, who identified differential expression of miRNAs between benign and malignant prostatic tissue (Porkka, et al. 2007). MiRNAs have since been implicated in all aspects of prostate carcinogenesis and progression to metastatic and therapy-resistant disease (Kojima, et al. 2017; Luu, et al. 2017). Moreover, since some PCa-associated miRNAs exist stably in the circulation of patients, there is considerable interest in their utility as blood-based biomarkers to improve PCa diagnosis, prognosis and treatment management (Fabris, et al. 2016; Kanwal, et al. 2017; Matin, et al. 2018).

In this review we explore the significance of the interplay between the AR signaling axis and miRNAs as it relates to PCa growth and progression. Finally, we speculate on the potential clinical applications of miRNAs implicated in the regulation of AR.

2. REGULATION OF AR BY MICRORNAS

Direct targeting of AR by miRNAs

Mechanisms by which miRNAs influence the AR signalling axis are depicted in Figure 1. One prominent feature of this interplay is direct targeting of the *AR* 3'UTR by miRNAs. Indeed, a recent study predicted that the *AR* 3'UTR is likely to be more heavily

regulated by miRNAs than all other PCa driver genes and in the top 5% of regulated genes overall (Hamilton, et al. 2016). This elegant work exploited photoactivatable ribonucleoside-enhanced cross-linking immunoprecipitation of the Argonaute protein (Ago-PAR-CLIP) to identify 147 miRNA seed sides corresponding to 71 miRNA families in the *AR* 3'UTR (Table 1). Importantly, 4 of the miRNAs identified by Hamilton and colleagues – miR-9, miR-34c, miR-185 and miR-488 –had been previously discovered in 2 high-throughput screens aimed at identifying AR-targeting miRNAs (Kumar, et al. 2016; Östling, et al. 2011) (Table 1). In addition to these unbiased approaches, many other studies have characterized specific AR-targeting miRNAs in a more directed manner. Interestingly, in addition to classical targeting of the 3'UTR, miRNA regulation of the *AR* via 5'UTR (miR-31) and the coding region (miR-421, miR-449a, miR-449b, miR-646, miR-371, miR-193a and miR-9) has also been reported (Kumar et al. 2016; Lin, et al. 2013; Östling et al. 2011). A list of putative AR-targeting miRNAs and their putative modes of action is provided in Table 1.

We propose that the biological relevance of these AR-targeting miRNAs can be prioritized using a set of discrete parameters. First, miRNAs that have been identified in multiple studies using multiple *in vitro* models are likely to have greater biological relevance in PCa. Second, it is known that transfection of cells with miRNA mimics can yield non-physiological miRNA activity; therefore, we prioritize studies that have demonstrated AR targeting using both miRNA mimics and inhibitors. Third, given that prostate tumors are "addicted" to AR (Coutinho et al. 2016), one would expect oncogenic selection pressure to down-regulate biologically relevant AR-targeting miRNAs. Indeed, a number of AR-targeting miRNAs have been reported to be down-regulated in prostate tumors compared to non-malignant prostate tissues. However, it is worth noting that our own analyses of miRNA expression in The Cancer Genome Atlas (TCGA) and Memorial Sloan-Kettering Cancer Center (MSKCC) (Taylor, et al. 2010) often contradict the published associations with cancer (Figures 2A-B). Finally, it would be expected that biologically relevant miRNAs are inversely correlated with AR protein levels in clinical samples. Indeed, our analysis of the TCGA cohort revealed such a correlation for miR-145, miR-205, miR-34a and miR-31 (Figure 2C). Using these parameters for prioritization and taking into account both published findings and our new analyses, we have generated a list of candidate AR-targeting miRNAs, shown in Table 2, which are ranked by predicted relevance in PCa. We propose that down-regulation of at least a

subset of these miRNAs is a key enabler of enhanced AR expression and activity in this disease.

When considering targeting of AR by miRNAs, it is worth noting that the reference *AR* 3'UTR sequence is annotated as being 6,777 nucleotides in length (NM_000044.4), but other isoforms have been reported. For example, LNCaP cells have been reported to express an AR isoform with the canonical ~6.8kb 3'UTR and another alternatively spliced version that lacks a 3kb region in the 3'UTR (Faber, et al. 1991). Moreover, Ostling and colleagues delineated a 6,680 nucleotide *AR* 3'UTR in VCaP cells, a sequence that was also identified in LNCaP, LAPC-4, 22Rv1, and MDA-PCa-2b cell line models (Östling et al. 2011). In addition to variation in length, 5 single nucleotide polymorphisms (SNPs) were identified in the *AR* 3'UTR in PCa cell lines (Waltering, et al. 2006). Interestingly, SNPs have been reported to influence miRNA targeting of multiple genes in PCa (Stegeman, et al. 2015a; Stegeman, et al. 2015b), although our analyses indicate that none of the *AR* 3'UTR SNPs occur within conserved miRNA recognition sequences (not shown). Nevertheless, we believe that reported variations in the length and sequence of the AR 3'UTR warrants further consideration in relation to interplay with miRNAs, especially since 3'UTR sequences are often overlooked in genomic and transcriptomic studies.

Direct targeting of AR splice variants by miRNAs

AR splice variants (ARVs) are truncated isoforms of the AR that lack part or all of the C-terminal ligand binding domain (LBD) (Antonarakis, et al. 2016). ARV mRNAs were first identified in PCa cell lines (Dehm, et al. 2008; Guo, et al. 2009) but have since been detected in patient specimens including primary tumors and metastases, circulating tumor cells and whole blood (Antonarakis, et al. 2014; Hornberg, et al. 2011; Hu, et al. 2009; Liu, et al. 2016). Recent RNA-seq data indicates the presence of at least 16 distinct *ARV* mRNA species in primary PCa (TCGA 2015) and 23 in metastatic CRPC (Robinson, et al. 2015). A subset of these ARVs are constitutively active (i.e. they can regulate transcription in the absence of androgen) and are therefore resistant to therapies that target the LBD (Chan, et al. 2015). Although the relevance of ARVs in driving the growth of CRPC remains to be definitively proven (Luo, et al. 2018), it is worth noting that high expression of certain ARVs, such as AR-V7 and AR-V9, correlates with resistance to

AR-targeted therapies and worse survival (He, et al. 2018; Kohli, et al. 2017; Qu, et al. 2015).

Given the clinical relevance of ARVs, it is important to understand how they are regulated by miRNAs in PCa. Of note, ARVs possess 3'UTR sequences distinct from the canonical *AR* transcript (Hu, et al. 2011; Shi, et al. 2015) (Figure 3A). Recent studies have begun to decipher miRNA regulation of ARVs. Interestingly, a number of miRNAs regulate both canonical AR and specific ARVs through different target sites. For example, miR-124 targets the *AR* transcript via a 3'UTR site that is distinct from another functional targeting site in the 3'UTRs of *AR-V3, AR-V4* and *AR-V7* (Figure 3B) (Shi et al. 2015; Shi, et al. 2013). Although the complete repertoires of ARV-targeting miRNAs remain to be determined, the identification of miRNAs that target both AR and ARVs via distinct sequences is intriguing and may suggest co-evolution of miRNAs and alternative AR splicing. Another mechanism by which miRNAs target both AR and ARV transcripts is via shared sequences in coding regions, as exemplified by translational regulation of *AR* and *AR-V7* by miR-646, miR-371-3p and miR-193a-3p (Kumar et al. 2016).

Importantly, differences in the 3'UTRs of *ARV*s and *AR* suggest that many of the identified AR-targeting miRNAs would not influence ARV expression, and vice versa. While this remains to be proven for most miRNAs, a recent study provided proof of concept by showing that miR-181c-5p effectively suppresses AR-V7 expression by targeting its 3'UTR but has no effect on the levels of the prototypical AR (Wu, et al. 2019). Interestingly, AR-V7 and ARv567es exhibit greater post-transcriptional stability than AR in CRPC bone metastases (Hornberg et al. 2011); it is tempting to speculate that this may be (at least partly) explained by differential miRNA targeting.

Indirect modulation of AR expression and activity by miRNAs

As well as direct regulation of AR, miRNAs can indirectly influence the expression and activity of AR via multiple mechanisms (Figure 1), including targeting AR co-regulators. Approximately 200 AR co-regulators – broadly classed as co-activators and co-repressors – have been identified, comprising a highly complex and potent system for shaping AR function in PCa (Liu, et al. 2017) . The co-repressor small heterodimer partner (SHP) is downregulated by miR-141, which is frequently elevated in PCa, thereby indirectly contributing to activation of AR's transcriptional activity (Xiao, et al. 2012). Another AR

corepressor, Prohibitin (PHB), is targeted by miR-27a, leading to increased expression of AR target genes and PCa cell growth (Fletcher, et al. 2012). Interestingly, miR-27a is an androgen-regulated miRNA, creating a feedback loop that represents a novel mechanism by which AR enhances its own activity.

Concomitant with enhanced miRNA-mediated targeting of AR co-repressors in PCa is the frequent loss or down-regulation of miRNAs that target AR co-activators. For example, miR-137 targets a suite of AR co-activators and is progressively lost with tumor grade due to DNA methylation of the *MIR137* locus (Nilsson, et al. 2015). Loss of miR-331-3p, which targets the *ERBB2* (HER2) oncogene, another AR co-activator (Craft, et al. 1999), also enhances AR signaling in PCa (Epis, et al. 2009). The AR co-activators p300/CBP-associated factor and bromodomain containing 8 isoform 2 are targeted by miR-17-5p and miR-185, respectively, leading to reduced AR transcriptional activity in PCa cells (Jiang, et al. 2016; Xiao et al. 2012). Interestingly, miR-185 also directly targets AR, enabling this miRNA to mediate a dual mode of inhibition of the AR signaling axis (Jiang et al. 2016).

Another mechanism by which miRNAs indirectly influence the AR signaling axis is by targeting factors that regulate *AR* gene expression. For example, miR-let-7c targets the oncogenic transcription factor Myc, thereby indirectly down-regulating *AR* expression (Nadiminty, et al. 2012). Similarly, by directly targeting fibronectin type III domain containing 1, miR-1207-3p reduces fibronectin 1 and subsequently *AR* expression (Das, et al. 2016). Todorova and colleagues reported that miR-204 targeting of the DNA methyltransferase DNMT1 results in decreased methylation of, and hence increased transcription from, the *AR* gene promoter (Todorova, et al. 2017). The nuclear matrix protein hnRNPH1, which is upregulated in prostate tumors and promotes expression of AR and AR-V7, AR transactivation and binding to AREs, is a target of miR-212 (Yang, et al. 2016); miR-212 is downregulated in prostate tumors and its ectopic expression in PCa cell lines results in decrease in hnRNPH1 and AR expression (Yang et al. 2016). In summary, targeting AR co-regulators and upstream regulators of AR expression allows miRNAs to exert an additional layer of regulation on this key oncogenic signaling axis (Figure 1).

3. REGULATION OF MICRORNAS BY THE AR SIGNALING AXIS

Direct regulation of miRNA gene expression by AR

The AR can directly regulate the PCa "miRNAome" by binding to androgen response elements (AREs) within cis-regulatory regions that regulate miRNA gene expression (Figure 4). The integration of AR genome-wide DNA binding profiles ("cistromes") with androgen-regulated transcriptomes has greatly facilitated the identification of direct miRNA target genes (e.g. (Pasqualini, et al. 2015; Takayama, et al. 2011)). This strategy has been used successfully irrespective of whether miRNAs are encoded in an intragenic or intergenic manner (Pasqualini et al. 2015). In general, AR induces oncogenic miRNAs, which act as downstream effectors of AR signaling, and represses tumor suppressor miRNAs (Table 3), although exceptions to this rule exist (see paragraph immediately below). Key oncogenic miRNAs that are directly upregulated by AR's transcriptional activation function include miR-19a, miR-27a, miR-133b and miR-185-5p, all of which can promote PCa cell growth and/or survival (Mo, et al. 2013; Yao, et al. 2016), whereas tumor suppressor miRNAs directly repressed by AR include miR-221/222 and miR-421 (Gui, et al. 2017; Meng, et al. 2016).

While AR is the major driver of PCa, it also plays an essential role in normal prostate physiology, where it primarily regulates a differentiative rather than proliferative transcriptional program (Coutinho et al. 2016). This concept may explain the observation that AR also promotes the expression of miRNAs that inhibit proliferation (e.g. miR-101, miR-135a and miR-1, which target the oncogenic factors EZH2, ROCK1/2 and SRC respectively (Cao, et al. 2010; Kroiss, et al. 2015; Liu, et al. 2015)) and promote epithelial differentiation (e.g. miR-200b, which targets factors that drive epithelial-mesenchymal transition, such as ZEB1 (Williams, et al. 2013)).

Indirect regulation of miRNA expression and/or activity by the AR signaling axis

Indirect regulation of miRNAs by the AR can occur through a variety of mechanisms (Figure 4). First, AR appears to play an important regulatory role in miRNA biogenesis (Fletcher et al. 2012) by upregulating expression of DICER (Mo et al. 2013) and also, at least for certain miRNA transcripts, modulating the activity of Drosha (Fletcher et al. 2012). The latter mechanism was elegantly elucidated by Fletcher and colleagues, who demonstrated a dual mode by which AR regulates miR-27a: AR induced expression of the primiR-23a27a24-2 cluster and concomitantly accelerated Drosha-mediated

processing of this cluster to generate mature miR-27a (Fletcher et al. 2012). The biological significance of AR's role in regulating the PCa miRNAome was highlighted by the observation that treatment of LNCaP cells with the AR antagonist Enzalutamide results in a ~25% reduction in the number of miRNAs associated with gene 3'UTRs (Hamilton et al. 2016).

AR-mediated regulation of the epigenome – more specifically, interplay between the AR and DNA methylation machinery – also modulates miRNA expression. As an example, by negatively regulating DNMT1, AR elicits hypomethylation and activation of the *MIR375* promoter (Chu, et al. 2014). Similarly, AR appears to regulate the DNA methylation levels of genomic elements that regulate the expression of miR-22 and miR-29a, although the mechanism by which it achieves this is unclear (Pasqualini et al. 2015).

Androgen receptor-mediated rewiring of microRNA/mRNA transcriptional networks

The androgen-regulated transcriptome has been examined in many different PCa models and contexts (Massie, et al. 2011; Nelson, et al. 2002; Ngan, et al. 2009; Pomerantz, et al. 2015; Velasco, et al. 2004). However, it is often difficult to identify which of these transcripts are directly regulated by AR, largely due to the fact that AR often binds to enhancers that are distal to its target genes (Wang, et al. 2007). Carefully assessing the temporality of androgen-mediated gene regulation (Massie et al. 2011), integrating transcriptomic data with AR cistromes (Pomerantz et al. 2015) and/or using more sophisticated transcriptomic techniques such as global run-on sequencing (GRO-seq) (Toropainen, et al. 2016), which is designed to identify nascent transcription, have improved the detection of *bona fide* AR targets in PCa cell lines and tissues. Nevertheless, accurately differentiating direct versus indirect targets of the AR remains challenging.

We propose that indirect regulation of protein-coding genes by androgens/AR is heavily influenced by the same genes being direct targets of AR-regulated miRNAs. Sun and colleagues explored this concept by evaluating the AR-repressed miR-99a/let7c/125b-2 cluster and discovered significant enrichment of AR-induced genes that are putative targets of these miRNAs (Sun, et al. 2014). Importantly, this *in silico* finding was validated for select candidate targets of each miRNA (Sun et al. 2014). We have expanded on this earlier work by intersecting TargetScan-predicted targets (Agarwal, et al. 2015) of AR-induced miRNAs with a panel of androgen-repressed genes, and vice versa

(Massie et al. 2011) (Table 4). Androgen-repressed genes are significantly over-represented in the putative targets of certain AR-induced miRNAs, whereas androgen-induced genes are over-represented in the targets of certain AR-repressed miRNAs. Our analysis provides strong evidence that protein-coding genes can be regulated by AR signaling via AR-mediated rewiring of miRNA/mRNA transcriptional networks. This phenomenon should be considered when undertaking genomic analysis of AR activity as it may facilitate the elucidation of the direct versus indirect transcriptional regulation.

Regulation of AR and miRNA expression by feedback loops

Feedback loops are a common feature of the interplay between AR and miRNAs. For example, the *MIR21* gene is directly activated by the AR; conversely, miR-21 increases expression of AR in PCa cell lines, potentially by targeting *PTEN* – although the precise mechanism remains unclear (Mishra, et al. 2014; Ribas, et al. 2009). Since miR-21 potently stimulates prostate tumor growth and metastasis, this feedback loop is likely to play a key role in PCa progression by maintaining expression and activity of 2 oncogenic factors (i.e. AR and miR-21) (Bonci, et al. 2016; Li, et al. 2009; Reis, et al. 2012). Conversely, the AR-repressed miRNAs miR-31 and miR-421 both target the AR directly (Lin et al. 2013; Meng et al. 2016; Östling et al. 2011). In the case of miR-31, this negative feedback loop is shifted in favor of the AR during disease progression, since DNA hypermethylation and subsequent down-regulation of miR-31 is a feature of aggressive prostate tumors (Lin et al. 2013; Meng et al. 2016).

Indirect regulatory loops between miRNAs and the AR also exist. For example, miR-190a is directly repressed via an AR binding site in its promoter, and in turn it suppresses AR expression and activity by targeting the 3'UTR of *YB1* (Xu, et al. 2015), a transcription factor that acts to enhance *AR* gene transcription and also as an AR co-activator (Shiota, et al. 2011; Xu et al. 2015).

4. MICRORNAS AS REGULATORS OF THERAPY RESISTANCE IN PROSTATE CANCER

A key feature of CRPC is the acquisition of miRNA activity that promotes cell survival in androgen-depleted conditions. Given the central role of AR in CRPC, it is not surprising that many of these miRNAs act, at least in part, by enhancing AR expression and/or activity. The feedback loop between miR-21 and AR has already been described

above; in the context of CRPC, it is worth noting that over-expression of miR-21 alone is sufficient to impart androgen-independent growth (Ribas et al. 2009). Unlike miR-21, miR-221/22 is repressed by AR signalling, yet it plays a similar role in promoting CRPC growth; upon castration, it is immediately upregulated and acts to enhance the expression of key cell cycle genes (Gui et al. 2017). Another example of a CRPC-relevant miRNA that influences AR is miR-125b, which was found to be elevated in androgen-independent derivatives of the LNCaP model (Shi, et al. 2007). By targeting the AR co-repressor NCoR2, miR-125b enhances AR signalling and thereby promotes androgen-independent growth (Yang, et al. 2012) .

Concomitant with gain of oncomiRs in CRPC is loss of miRNAs that inhibit survival, proliferation and other oncogenic properties, including: miR-146a, which targets the oncogene Rho activated protein kinase (Lin, et al. 2007; Lin, et al. 2008); let-7c, which targets the oncogenes *Myc* and *Lin28* (Nadiminty et al. 2012); miR-145-3p, which targets cell cycle associated genes (Goto, et al. 2017); and the *AR*-targeting miRNAs miR-30c-5p and 30d-5p (Kumar et al. 2016).

While the aforementioned miRNAs appear to play important roles in the progression of PCa to a castration-resistant state, it is noteworthy that studies evaluating expression of miRNAs in CRPC tissues are poorly concordant. Nevertheless, by comparing miRNAs putatively associated with CRPC in 3 published genome-wide miRNA profiling studies (Goto, et al. 2015; Goto et al. 2017; Jalava, et al. 2012) and combining this with our own analysis of the Memorial Sloan-Kettering Cancer Center cohort (Taylor et al. 2010), we have identified a set of miRNAs that are reproducibly dysregulated in CRPC. MiRNAs that were not reproducibly altered in these studies may be false positives, or alternatively may simply reflect differences in experimental design; for example, one study compared miRNA expression between benign prostatic hyperplasia and CRPC (Jalava et al. 2012), while the others compare normal prostate tissues or hormone naïve PCa with CRPC (Goto et al. 2015; Goto et al. 2017; Taylor et al. 2010). Moreover, only the latest of these employed RNA-seq (Goto et al. 2017), while the earlier studies used PCR arrays (Goto et al. 2015) or miRNA microarrays (Jalava et al. 2012; Taylor et al. 2010).

5. CLINICAL POTENTIAL OF AR-ASSOCIATED MICRORNAS IN PROSTATE CANCER

AR-associated miRNAs as biomarkers

Circulating miRNAs can be detected in many body fluids – most notably serum, plasma and urine – and have shown promise as biomarkers for PCa diagnosis and prognosis and predicting therapy response. Since this topic has been comprehensively encapsulated in recent reviews (Fabris et al. 2016; Kanwal et al. 2017), here we will briefly touch on the relevance of the AR signalling axis to these putative biomarkers. Several PCa-associated circulating miRNAs are known to be regulated by AR, suggesting that – like the classic PCa marker prostate specific antigen (Catalona, et al. 1991) – their release into circulation is likely increased in PCa due to elevated AR activity. One prominent example is miR-375, which has consistently been identified as a potential marker of PCa, with higher levels in serum or plasma being associated with shorter overall survival and metastasis (Brase, et al. 2011; Huang, et al. 2015; Mitchell, et al. 2008; Selth, et al. 2012). AR indirectly promotes miR-375 transcription by suppressing DNA methylation of its promoter (Chu et al. 2014), and we have previously shown that miR-375 levels are positively correlated with androgen signalling in multiple tumor datasets (Selth, et al. 2017). The release of miR-375 from LNCaP cells into culture medium is stimulated by DHT (Gezer, et al. 2015; Tiryakioglu, et al. 2013), suggesting that its levels in the blood of patients would be increased in PCa due to elevated AR activity. Other AR-regulated miRNAs that have been proposed as potential serum- or plasma-based biomarkers of PCa include miR-21 (Zhang, et al. 2011), miR-125b (Fredsoe, et al. 2017), miR-141 (Gonzales, et al. 2011), miR-19a (Stuopelyte, et al. 2016), miR-27a (Gao, et al. 2018) and miR-221/222 (Santos, et al. 2014).

Potentially the most useful application of circulating miRNAs would be in predicting response to therapies for CRPC. Given that an important subset of circulating miRNAs are AR-regulated, it is conceivable that one or more of these may be useful in predicting response to AR-targeted therapies. Supporting this concept, elevated circulating miR-141 could predict clinical progression in a small cohort of CRPC patients with a sensitivity of 78.9% and specificity of 68.8%, although the therapies they received were mixed (chemotherapy, hormone therapy, or novel agents such as vaccines and kinase inhibitors) (Gonzales et al. 2011). Additionally, high levels of miR-221 in peripheral blood is predictive of early CRPC development (Santos et al. 2014). These examples suggest that

circulating miRNAs could be useful additions to the biomarker armamentarium, although robust retrospective and prospective validation studies are required to move this field forward (Tavallaie, et al. 2015; Wang, et al. 2016)

Exploiting AR-modulating microRNAs as a therapeutic strategy

MiRNA-based therapies are being actively pursued for a multitude of diseases, as eloquently described in several recent reviews (Hong, et al. 2016; Van der Ree, et al. 2016; van der Ree, et al. 2017). In cancer, such therapies are focused on increasing levels of tumor suppressor miRNAs by delivery of miRNAs mimics or decreasing levels of oncogenic miRNAs by delivery of antisense oligonucleotides (termed antimiRs or antagomiRs) (D'Angelo, et al. 2016). Since a single miRNA can regulate multiple cancer-related pathways, miRNA-based therapies possess considerable promise. However, like other nucleic acid-based strategies, issues related to stability in biofluids, delivery to the tissue of interest and toxicity of mimics and antimiRs have hindered their clinical development (Rupaimoole and Slack 2017). While recent advances in formulation and delivery have led to miRNA-based therapies being tested in a range of clinical studies (Matin, et al. 2016), it is worth noting that none are yet used in the treatment of patients.

With these caveats in mind, the application of a miRNA-based therapy in PCa remains a distant goal. Nevertheless, it is clear that opportunities in this area exist, especially given the importance of the interplay between miRNAs and the AR. For example, miR-34a reduces PCa cell viability, at least in part by targeting *AR* (Östling et al. 2011), but it also downregulates the expression of >30 oncogenes across multiple oncogenic pathways (Beg, et al. 2017). Cancer therapies based on master tumor suppressor miRNAs such as miR-34 are attractive because they would be expected to have high efficacy and at the same time reduce opportunities for resistance to develop. In pre-clinical studies, systemic delivery of a miR-34a mimic to mice harbouring orthotopic PCa xenografts led to decreased tumor growth and metastasis (Liu, et al. 2011). A liposomal formulation of miR-34a, termed MRX34, was evaluated in a Phase 1 clinical trial of patients with primary liver cancer, advanced solid tumors and hematological malignancies. Unfortunately, this trial was terminated due to immune-related serious adverse side effects (Hong et al. 2016; Van Roosbroeck and Calin 2017). Nevertheless, the promising anti-tumor activity of MRX34 observed in a subset of patients (Beg et al. 2017) provides incentive to continue investigating miRNA-based therapies for cancer. Indeed, new

strategies to more precisely deliver miRNA-based payloads to solid tumors are already showing promise: exciting findings from a recent phase I clinical trial in mesothelioma demonstrated that miR-16-loaded, EGFR-targeted "minicells" demonstrated an acceptable safety profile and early signs of activity (van Zandwijk, et al. 2017).

As an alternative to therapies based on miRNA mimics or antimiRs, other strategies to regulate miRNA expression can be envisioned. Indeed, epigenetic therapies are being intensively investigated for a multitude of diseases, and we propose that an important aspect of their activity relates to miRNA biology. As specific examples associated with the AR signalling axis, re-activation of miR-124 using DNA demethylating agents or miR-320a with the histone deacetylase inhibitor OBP-801 lead to decreased AR expression and activity in PCa (Sato, et al. 2016; Shi et al. 2013)

SUMMARY

MiRNAs and the AR are involved in an intricate dance mediated by direct interactions or complex indirect mechanisms involving transcription factors, co-regulators and epigenetic machinery (Figures 1 and 4). Despite the complexity of this interplay, one overarching theme is that miRNAs play a major role in enhancing and maintaining AR activity throughout the course of PCa progression; miRNAs that antagonize AR expression and activity are frequently lost, whereas miRNAs that facilitate AR signaling are frequently gained. This phenomenon may be particularly relevant in CRPC, where miRNAs can play key roles in establishing and maintaining resistance to AR-targeted therapies. With this in mind, and given the continued focus on targeting AR in PCa, we propose that exploitation of miRNAs – potentially as biomarkers or therapeutic targets – warrants further consideration as a strategy to manage and/or treat this common disease. Finally, since AR is a key player and being investigated as a target in other solid tumours, including breast, bladder and hepatocellular, the value of understanding its interplay with miRNAs is increased; indeed, recent studies indicate that such interplay may be crucial to the progression of these other cancer types (Xiao, et al. 2019; Xiong, et al. 2017; Yang, et al. 2018).

DECLARATION OF INTEREST

The authors declare that there is no conflict of interest that could be perceived as prejudicing the impartiality of the research reported.

FUNDING

This work was supported by funding from the National Health and Medical Research Council of Australia (IDs 1083961 and 1121057 to LAS and WDT).

ACKNOWLEDGEMENTS

The authors wish to thank Dr John Toubia for providing processed miRNA expression data from The Cancer Genome Atlas cohort. The results published here are in part based on data generated by The Cancer Genome Atlas, established by the National Cancer Institute and the National Human Genome Research Institute, and we are grateful to the specimen donors and relevant research groups associated with this project.

FIGURES AND LEGENDS

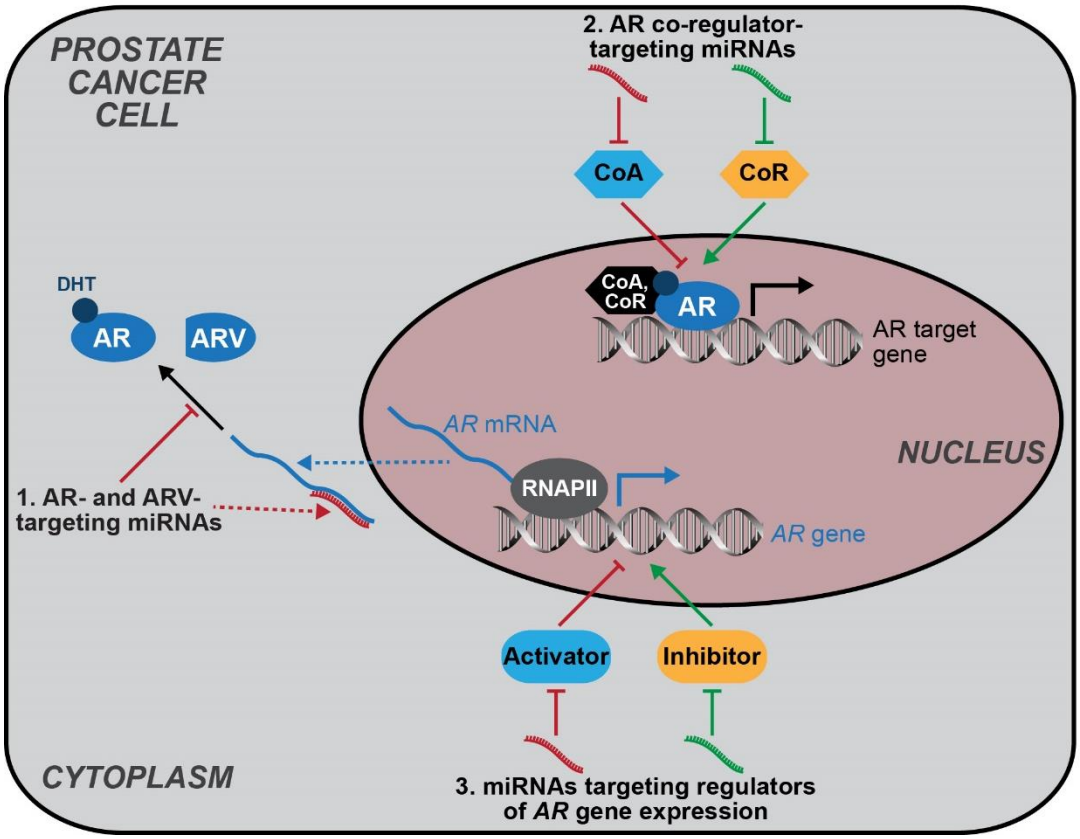

Figure 1. Key mechanisms by which microRNAs regulate AR expression and activity in prostate cancer, including direct targeting of the AR transcript (1), targeting of AR co-regulators (2) and targeting of factors that influence expression of the *AR* gene (3).

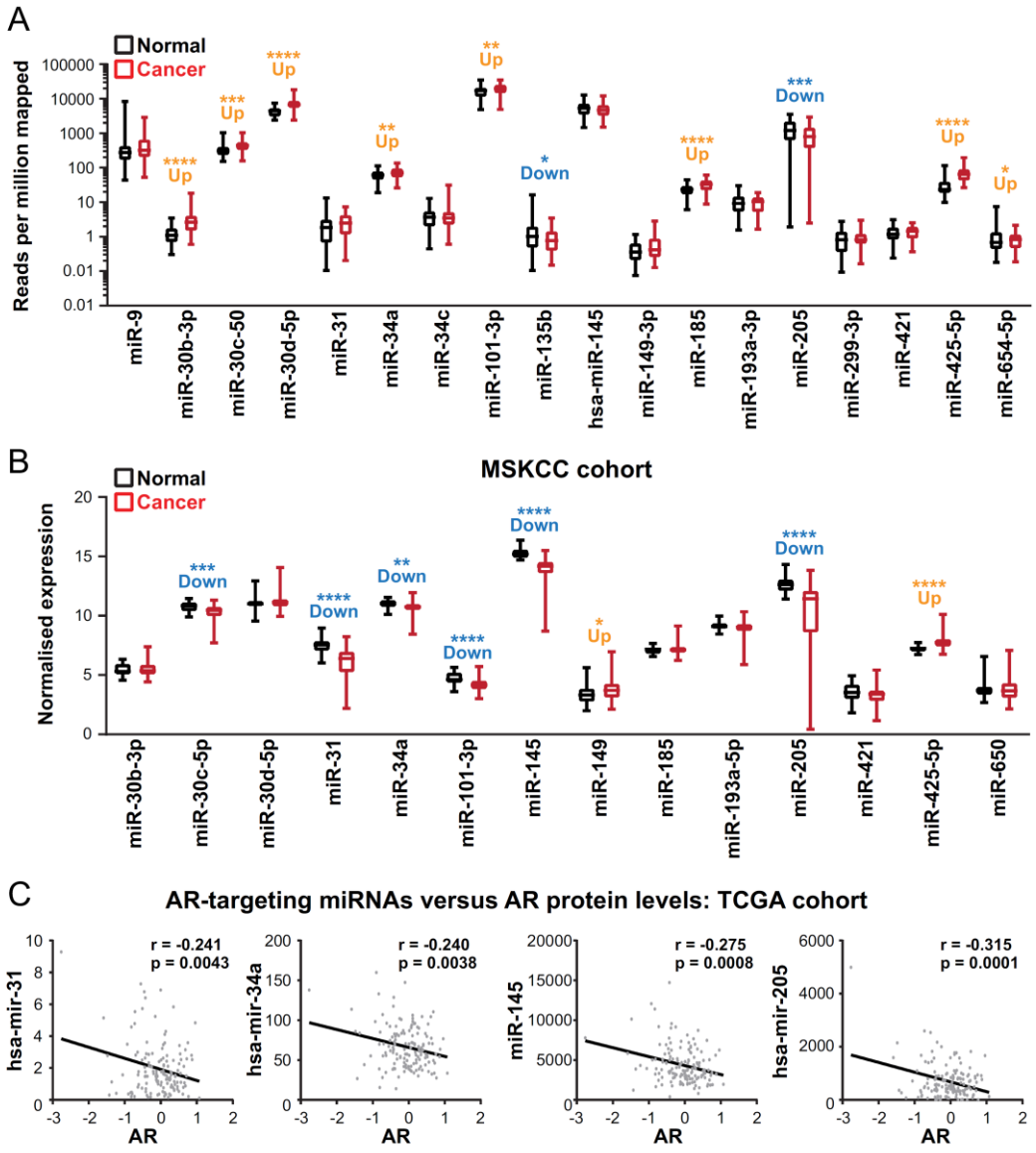

Figure 2. Expression of putative AR-targeting miRNAs in clinical samples. **(A)** Expression of putative AR-targeting miRNAs in matched normal and primary prostate cancers from The Cancer Genome Atlas (TCGA). TCGA miRNA expression data was obtained from Genomic Data Commons, which uses miRBase v21 as miRNA reference; miRNA names were derived miRBase v21 and converted where necessary. MiRNA abundance (reads-per-million-miRNA-mapped) was calculated by taking the sum of all counts per miRNA (unique MIMAT ID), and the MIMAT ID was then converted to its appropriate miRNA name. Only miRNAs that were expressed in more than 50% of samples were included in this analysis. P values were determined using paired t tests; *, $p < 0.05$; **, $p < 0.01$; ***, $p < 0.001$; ****, $p < 0.0001$. **(B)** Expression of putative AR-

targeting miRNAs in normal and prostate cancer (primary and metastatic) in the Memorial Sloan-Kettering Cancer Center (MSKCC) cohort. Normalized miRNA expression data for the MSKCC cohort was obtained from cBioPortal (www.cbioportal.org). P values were determined using unpaired t tests; *, $p < 0.05$; **, $p < 0.01$; ***, $p < 0.001$; ****, $p < 0.0001$. **(C)** Correlation between putative AR-targeting miRNAs and AR protein levels in the TCGA cohort. AR protein levels are from reverse phase protein array data, obtained from the Broad Institute's GDAC Firehose. RPPA data was available for 145 primary prostate tumors. Only AR-targeting miRNAs that exhibited a significant ($p < 0.05$) negative Pearson correlation with AR protein levels in these 145 tumors are shown.

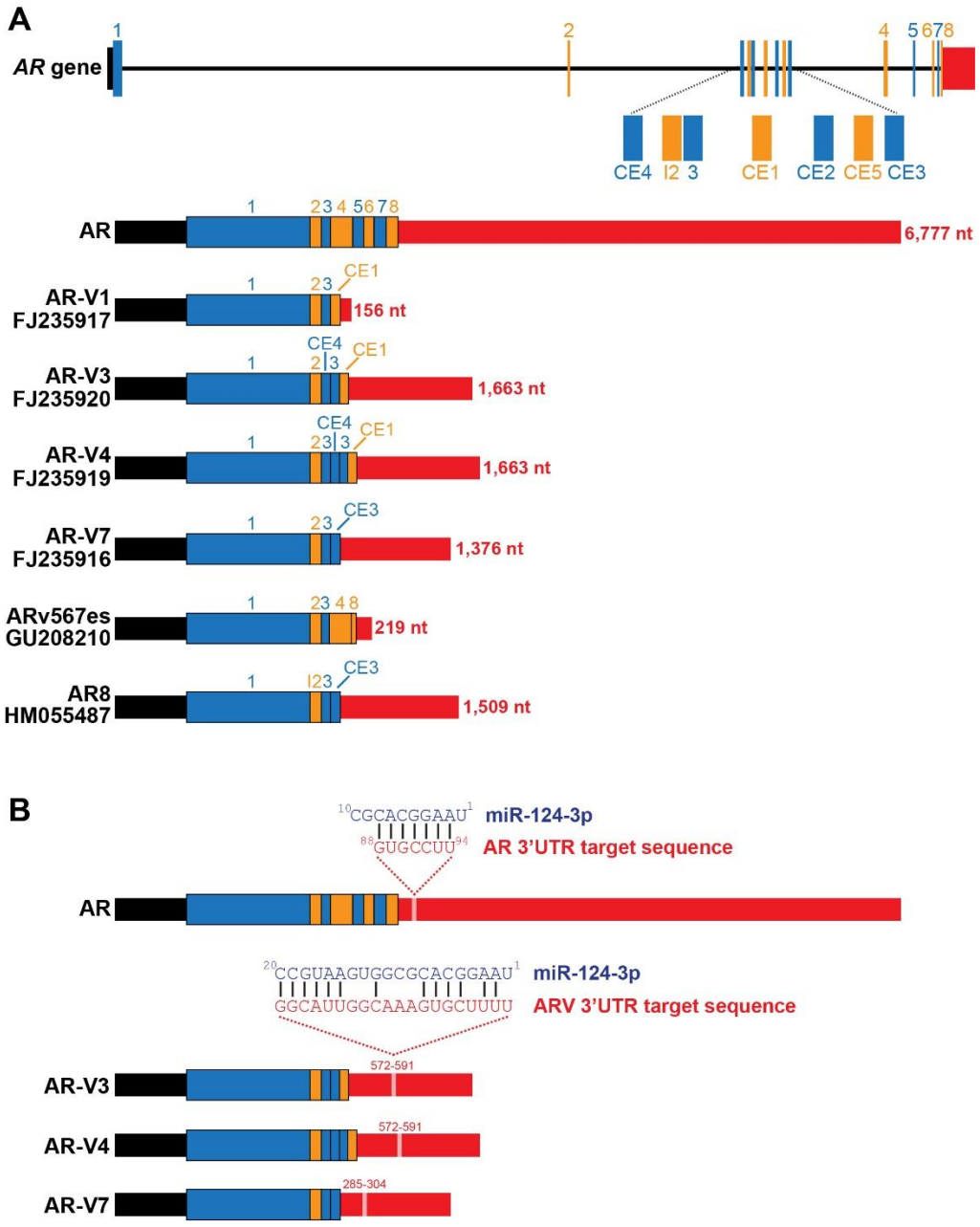

Figure 3. Differential 3'UTRs of AR and AR variants in prostate cancer influence their regulation by miRNAs. **(A)** Graphical representation of 3'UTR sequences for the canonical AR transcript and 6 AR variants. Genbank accession IDs are shown; 3'UTR length was calculated as the number of nucleotides from after to the stop codon to the end of the annotated transcript. **(B)** miR-124 target sites in the canonical AR transcript and AR variants V3, V4 and V7.

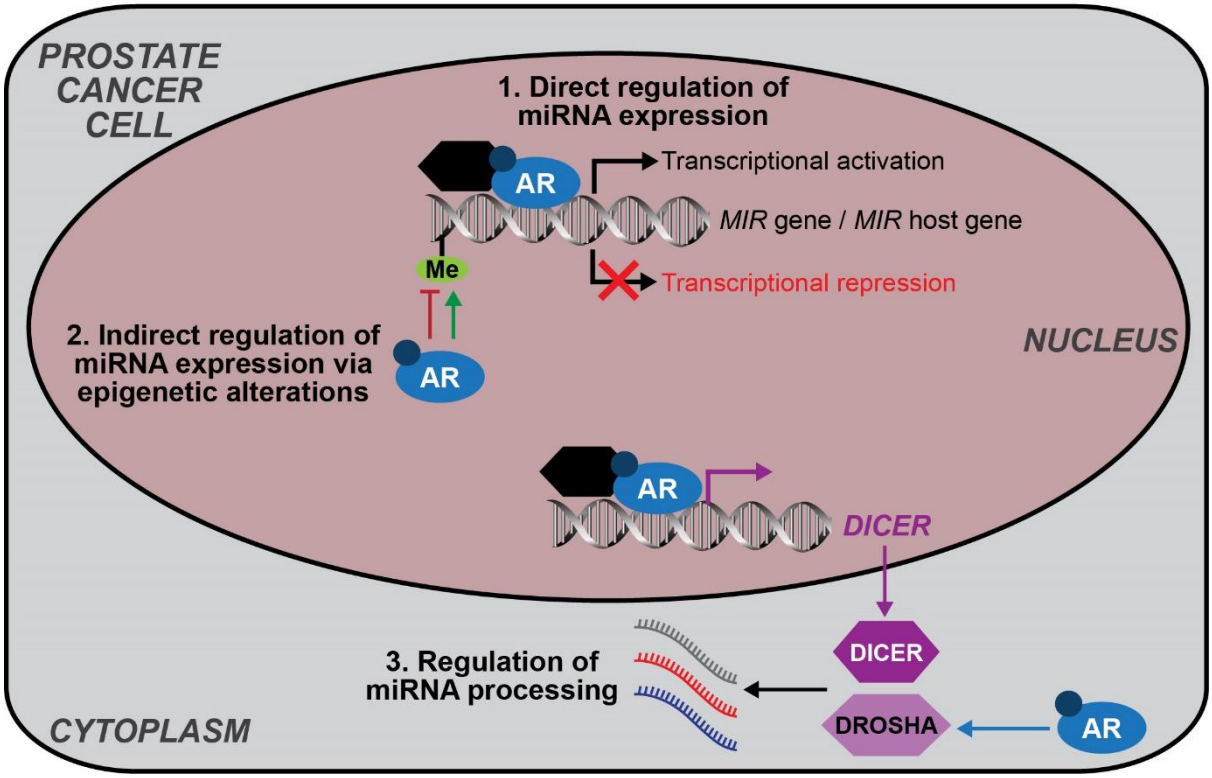

Figure 4. Key mechanisms by which AR controls the miRNAome in prostate cancer, including direct regulation of miRNA expression (1), regulating epigenetic machinery that modulates expression of miRNAs (2) and regulating the expression and activity of the miRNA biogenesis machinery (3).

TABLES

Table 1. Putative AR- and AR variant-targeting miRNAs.

miRNA	Target	Mechanism of regulation	Mimic and/or inhibitor used	Ago-PAR-CLIP binding site/s in 3'UTR*	Readouts	Reference
miR-9	AR	3'UTR and coding region	Mimic	Yes	AR protein and mRNA, AR luciferase reporter (wild-type only)	Hamilton et al. 2016; Kumar et al. 2016; Östling et al. 2011
miR-30b-3p	AR	3'UTR	Mimic and Inhibitor		AR protein and mRNA, AR 3'UTR luciferase reporter (wild-type and mutant)	Kumar et al. 2016
miR-30c-5p	AR	3'UTR	Mimic		AR protein, AR 3'UTR luciferase reporter (wild-type)	Kumar et al. 2016
miR-30d-5p	AR	3'UTR	Mimic and Inhibitor		AR protein and mRNA, AR 3'UTR luciferase reporter (wild-type and mutant)	Kumar et al. 2016
miR-31	AR	5'UTR and coding region	Mimic		AR protein, AR 3'UTR luciferase reporter (wild-type and mutant)	Lin et al. 2013
miR-34a	AR	3'UTR	Mimic	Yes	AR protein and mRNA, AR luciferase reporter (wild-type only)	Hamilton et al. 2016; Östling et al. 2011
miR-34c	AR	3'UTR	Mimic	Yes	AR protein and mRNA, AR luciferase reporter (wild-type only)	Hamilton et al. 2016; Kumar et al. 2016; Östling et al. 2011
miR-101-3p	AR and AR-V7	3'UTR	Mimic	Yes	AR protein, AR 3'UTR luciferase reporter (wild-type only)	Hamilton et al. 2016; Kumar et al. 2016; Östling et al. 2011
miR-124-3p	AR, AR-V7, AR-V4	3'UTR	Mimic	Yes	AR protein, AR 3'UTR luciferase reporter (wild-type and mutated)	Hamilton et al. 2016; Kumar et al. 2016; Shi et al. 2015; Shi et al. 2013
miR-135b	AR and AR-V7	3'UTR	Mimic		AR protein and mRNA, AR luciferase	Östling et al. 2011

					reporter (wild-type only)	
miR-145	AR	3’UTR	Mimic		AR protein and mRNA	Hamilton et al. 2016; Larne et al. 2015
miR-149-3p	AR	3'UTR	Mimic		AR protein, AR 3'UTR luciferase reporter (wild-type only)	Kumar et al. 2016
miR-181c-5p	AR-V7	3’UTR	Mimic	Yes	AR protein and mRNA, AR luciferase reporter (wild-type and mutated)	Wu et al. 2019
miR-193a-3p	AR and AR-V7	Coding region	Mimic		AR protein, AR 3'UTR luciferase reporter (wild-type only)	Kumar et al. 2016
miR-205	AR	3'UTR	Mimic	Yes	AR protein, AR luciferase reporter (wild-type)	Hagman et al. 2013; Hamilton et al. 2016; Kumar et al. 2016
miR-297	AR	3'UTR	Mimic		AR mRNA, AR luciferase reporter (wild-type)	Fang et al. 2016
miR-298	AR	3'UTR	Mimic		AR protein and mRNA, AR luciferase reporter (wild-type only)	Östling et al. 2011
miR-299	AR	3'UTR	Mimic	Yes	AR protein and mRNA, AR luciferase reporter (wild-type only)	Hamilton et al. 2016; Östling et al. 2011
miR-371	AR and AR-V7	Coding region	Mimic		AR protein, AR luciferase reporter (wild-type only)	Kumar et al. 2016; Östling et al. 2011
miR-421	AR	3'UTR and coding region	Mimic	Yes	AR protein and mRNA, AR luciferase reporter (wild-type only)	Hamilton et al. 2016; Östling et al. 2011
miR-425-5p	AR	3'UTR	Mimic		AR protein, AR 3'UTR luciferase reporter (wild-type)	Kumar et al. 2016
miR-449a	AR	3'UTR and coding region	Lentiviral miRNA overexpression		AR protein and mRNA	Zheng et al. 2015a
miR-449b	AR	3'UTR and coding region	Mimic		AR protein, AR 3'UTR luciferase	Kumar et al. 2016;

					reporter (Wild-type)	Östling et al. 2011
mir-488	AR and AR-V7	3'UTR	Mimic	Yes	AR protein and mRNA, AR luciferase reporter (wild-type and mutated)	Hamilton et al. 2016; Kumar et al. 2016; Östling et al. 2011; Sikand et al. 2011
miR-541	AR	3'UTR	Mimic		AR protein and mRNA, AR 3'UTR luciferase reporter (wild-type)	Kumar et al. 2016; Östling et al. 2011
miR-634	AR	3'UTR	Mimic		AR protein and mRNA, AR luciferase reporter (wild-type only)	Kumar et al. 2016; Östling et al. 2011
miR-635	AR	3'UTR	Mimic		AR protein, AR 3'UTR luciferase reporter (wild-type)	Kumar et al. 2016
miR-646	AR and AR-V7	Coding region	Mimic		AR protein, AR 3'UTR luciferase reporter (wild-type)	Kumar et al. 2016
miR-650	AR	3'UTR	Mimic		AR protein, AR 3'UTR luciferase reporter (wild-type)	Kumar et al. 2016
miR-654	AR	3'UTR	Mimic		AR protein and mRNA, AR luciferase reporter (wild-type only)	Kumar et al. 2016; Östling et al. 2011

*Ago-PAR-CLIP, photoactivatable ribonucleoside-enhanced cross-linking immunoprecipitation of the Argonaute protein (Hamilton et al. 2016).

Table 2. Assessing the biological relevance of microRNAs reported to target the androgen receptor

miRNA	No of studies reporting association between miRNA and AR	Reference (Score: 1 if 2 or more references)	Inverse correlation between AR protein and miRNA (Score: 1 if yes, 0 if N/A or no)	Downregulated in cancer compared to normal tissues (Score: 0.5 for yes in each of MSKCC and TCGA datasets, 0 if no)	Inverse correlation between AR and miR in PCa tissues (Score: 1 if yes, 0 if unknown)	miRNA status in PCa tissues (Score: 1 if downregulated, 0 if unknown)	Reported role of miRNA in PCa (Score: 1 if tumor suppressor, 0 unknown)	Rank (sum of score)	References
miR-205	3	Hagman et al. 2013; Hamilton et al. 2016; Kumar et al. 2016	Yes	Downregulated in TCGA and MSKCC	Yes, AR transcript and protein	Downregulated in PCa tissues	Tumor suppressor	6	Gandellini et al. 2009; Hagman et al. 2013; Kumar et al. 2016
miR-145	2	Hamilton et al. 2016; Larne et al. 2015	Yes	Downregulated in MSKCC	Yes	Downregulated in PCa metastases	Tumor suppressor	5.5	Larne et al. 2015
miR-34a	2	Hamilton et al. 2016; Östling et al. 2011	Yes	Downregulated in MSKCC, Upregulated in TCGA	Yes, AR protein	Unknown	Tumor suppressor	4.5	Leite et al. 2015; Liu et al. 2011; Östling et al. 2011
miR-34c	4	Fang et al. 2016; Hamilton et al. 2016; Kumar et al. 2016; Östling et al. 2011	No	N/A	Yes, AR transcript and protein	Downregulated in PCa tissues	Tumor suppressor	4	Hagman et al. 2010; Östling et al. 2011
miR-101-3p	2	Hamilton et al. 2016; Östling et al. 2011	N/A	Downregulated in MSKCC, Upregulated in TCGA	Yes, AR protein	Unknown	Tumor suppressor	3.5	Cao et al. 2010
miR-299-3p	2	Hamilton et al. 2016; Östling et al. 2011	No	N/A	Unknown	Unknown	Unknown	2	

miR-421	2	Hamilton et al. 2016; Östling et al. 2011	No	N/A	Unknown	Downregulated in PCa tissues	Tumor suppressor	3	Meng et al. 2016
miR-124-3p	4	Hamilton et al. 2016; Kumar et al. 2016; Shi et al. 2015; Shi et al. 2013	N/A	N/A	Unknown	Unknown	Tumor suppressor	2	Shi et al. 2015
miR-185	4	Hamilton et al. 2016; Kumar et al. 2016; Östling et al. 2011	No	Upregulated in TCGA	Unknown	Downregulated in PCa tissues	Tumor suppressor	2	Qu et al. 2013
miR-371	3	Kumar et al. 2016; Leite et al. 2015; Östling et al. 2011	N/A	N/A	Unknown	Downregulated in PCa tissues	Unknown	2	Leite et al. 2015
mir-488	4	Hamilton et al. 2016; Kumar et al. 2016; Östling et al. 2011; Sikand et al. 2011	N/A	N/A	Unknown	Unknown	Tumor suppressor	2	Sikand et al. 2011
miR-449a	2	Östling et al. 2011; Zheng et al. 2015	N/A	N/A	Unknown	Unknown	Tumor suppressor	2	Noonan et al. 2009; Zheng et al. 2015b
miR-297	2	Fang et al. 2016; Östling et al. 2011	N/A	N/A	Unknown	Unknown	Unknown	1	N/A
miR-449b	2	Kumar et al. 2016; Östling et al. 2011	N/A	N/A	Unknown	Unknown	Unknown	1	N/A
miR-541	2	Kumar et al. 2016; Östling et al. 2011	No	N/A	Unknown	Unknown	Unknown	1	N/A
miR-634	2	Kumar et al. 2016; Östling et al. 2011	N/A	N/A	Unknown	Unknown	Unknown	1	N/A
miR-654	2	Kumar et al. 2016; Östling et al. 2011	No	N/A	Unknown	Unknown	Unknown	1	N/A
miR-9	3	Hamilton et al. 2016; Kumar et al. 2016; Östling et al. 2011	N/A	N/A	Unknown	Upregulated in high grade tumors	OncomiR	1	Seashols-Williams et al. 2016

Table 3 MicroRNAs directly regulated by the AR signaling axis.

miRNA	Regulation by AR / androgens	miRNA expression in PCa tissues	Effect of modulating miRNA on PCa growth	No of studies reporting association between miRNA and AR	References
miR-1	Induced	Downregulated	Tumour suppressor	1	(Liu et al. 2015)
miR-19a	Induced	Upregulated in CRPC	OncomiR	1	(Lu et al. 2015; Mo et al. 2013)
miR-21	Induced	Upregulated	OncomiR	4	(Murata et al. 2010; Ribas et al. 2009; Takayama et al. 2011; Waltering et al. 2011)
miR-22	Induced	Downregulated in PCa	Tumor suppressor	3	(Murata et al. 2010; Pasqualini et al. 2015; Waltering et al. 2011)
miR-27a	Induced	Unknown	OncomiR (Fletcher et al. 2012)/Tumour suppressor (Wan et al. 2016)	3	(Fletcher et al. 2012; Mo et al. 2013; Murata et al. 2010)
miR-29a	Induced	Downregulated in PCa	Tumor suppressor	3	(Pasqualini et al. 2015; Ribas et al. 2009; Waltering et al. 2011)
miR-32	Induced	Upregulated	OncomiR	2	(Jalava et al. 2012; Waltering et al. 2011)
miR-99a	Induced (Takayama et al 2011) / Repressed (Sun et al 2014)	Downregulated	Tumor suppressor	2	(Sun et al. 2014a; Sun et al. 2011; Takayama et al. 2011)
miR-125b-2	Induced (Murata et al. 2010; Takayama et al. 2011) / Repressed (Sun et al. 2014b)	Unknown	OncomiR	3	(Murata et al. 2010; Shi et al. 2007; Sun et al. 2014b; Takayama et al. 2011)
miR-133b	Induced	Unknown	Unknown	1	(Mo et al. 2013)
miR-135a	Induced	Downregulated	Tumor suppressor	1	(Kroiss et al. 2015)

miR-148a	Induced	Upregulated	OncomiR	4	(Jalava et al. 2012; Murata et al. 2010; Ribas et al. 2009; Waltering et al. 2011)
miR-182-5p	Induced	Upregulated	OncomiR	1	(Yao et al. 2016)
miR-193a-3p	Induced	Unknown	OncomiR	2	(Jia et al. 2017; Waltering et al. 2011)
miR-203	Induced	Upregulated	Tumor suppressor	1	(Jalava et al. 2012; Siu et al. 2017)
miR-221/222	Repressed	Downregulated / Upregulated	OncomiR	3	(Jalava et al. 2012; Takayama et al. 2011; Waltering et al. 2011)
miR-421	Repressed	Unknown	Tumor suppressor	1	(Meng et al. 2016)
miR-4496	Induced	Unknown	Tumor suppressor	1	(Wang et al. 2018)

Table 4: Intersection between AR regulated miRNA (by binding to ARBS) and AR regulated genes.

Overlap between miRNA upregulated by AR and genes downregulated by AR			
miRNA	No of predicted miRNA target genes	Genes in overlap	p value
miR-19	1338	43	0.02581
miR-21	384	13	0.12688
miR-22	620	22	0.03987
miR-27a	1421	56	0.00012
miR-29a	1264	34	0.24447
miR-32	1041	36	0.01505
miR-133b	711	18	0.42141
miR-135a	847	26	0.10774
miR-148a	802	26	0.06667
miR-182-5p	1329	44	0.011979
miR-193a-3p	286	12	0.041
miR-203	960	25	0.342
miR-4496	5975	168	0.004
Overlap between miRNA downregulated by AR and genes upregulated by AR			
miRNA	No of predicted targets	Genes in overlap	p value
miR-221/222	504	26	0.023
miR-421	450	27	0.003

[a]Predicted target genes for each miRNA were downloaded from TargetScan (release 7.2; Agarwal et al. 2015). [b]P values were calculated using hypergeometric probability tests. Genes in universe = 18,393 i.e. total number of genes in Targetscan database. AR-repressed genes (n = 436) and AR-upregulated genes (n = 625) are from (Massie et al. 2011).

Table 5. Dysregulated miRNA in CRPC

miRNA	Up/Down	# of studies reporting differential expression	References
miR-7	Upregulated	2	Jalava et al. 2012; Taylor et al. 2010
miR-18a	Upregulated	2	Jalava et al. 2012; Taylor et al. 2010
miR-23b	Downregulated	3	Goto et al. 2015; Goto et al. 2017; Taylor et al. 2010
miR-24	Downregulated	4	Goto et al. 2015; Goto et al. 2017; Jalava et al. 2012; Taylor et al. 2010
miR-25	Upregulated	2	Jalava et al. 2012; Taylor et al. 2010
miR-27a	Downregulated	3	Goto et al. 2015; Goto et al. 2017; Taylor et al. 2010
miR-30a*	Downregulated	3	Goto et al. 2015; Jalava et al. 2012; Taylor et al. 2010
miR-30b-3p	Upregulated	2	Jalava et al. 2012; Taylor et al. 2010
miR-30e-3p	Downregulated	3	Goto et al. 2015; Goto et al. 2017; Taylor et al. 2010
miR-95	Upregulated	2	Jalava et al. 2012; Taylor et al. 2010
miR-99a	Downregulated	4	Goto et al. 2015; Goto et al. 2017; Jalava et al. 2012; Taylor et al. 2010
miR-100	Downregulated	3	Goto et al. 2017; Jalava et al. 2012; Taylor et al. 2010
miR-125a-5p	Downregulated	3	Goto et al. 2015; Goto et al. 2017; Taylor et al. 2010
miR-125b	Downregulated	4	Goto et al. 2015; Goto et al. 2017; Jalava et al. 2012; Taylor et al. 2010
miR-125b-2*	Downregulated	3	Goto et al. 2017; Jalava et al. 2012; Taylor et al. 2010
miR-130b	Upregulated	2	Jalava et al. 2012; Taylor et al. 2010
miR-133a	Downregulated	4	Goto et al. 2015; Goto et al. 2017; Jalava et al. 2012; Taylor et al. 2010
miR-143	Downregulated	3	Goto et al. 2015; Goto et al. 2017; Taylor et al. 2010
miR-143*	Downregulated	3	Goto et al. 2017; Jalava et al. 2012; Taylor et al. 2010
miR-145	Downregulated	3	Goto et al. 2017; Jalava et al. 2012; Taylor et al. 2010
miR-145*	Downregulated	3	Goto et al. 2015; Goto et al. 2017; Taylor et al. 2010
miR-150	Downregulated	3	Goto et al. 2015; Goto et al. 2017; Taylor et al. 2010
miR-152	Downregulated	3	Goto et al. 2015; Jalava et al. 2012; Taylor et al. 2010
miR-181c	Downregulated	3	Goto et al. 2017; Jalava et al. 2012; Taylor et al. 2010
miR-182	Upregulated	2	Jalava et al. 2012; Taylor et al. 2010
miR-183	Upregulated	2	Jalava et al. 2012; Taylor et al. 2010
miR-185	Upregulated	2	Jalava et al. 2012; Taylor et al. 2010
miR-196b	Downregulated	3	Goto et al. 2015; Goto et al. 2017; Taylor et al. 2010

miR-199a-5p	Downregulated	3	Goto et al. 2017; Jalava et al. 2012; Taylor et al. 2010
miR-205	Downregulated	4	Goto et al. 2015; Goto et al. 2017; Jalava et al. 2012; Taylor et al. 2010
miR-214	Downregulated	3	Goto et al. 2017; Jalava et al. 2012; Taylor et al. 2010
miR-221	Downregulated	4	Goto et al. 2015; Goto et al. 2017; Jalava et al. 2012; Taylor et al. 2010
miR-222	Downregulated / Upregulated	4	Goto et al. 2015; Goto et al. 2017; Jalava et al. 2012; Taylor et al. 2010
miR-425	Upregulated	2	Jalava et al. 2012; Taylor et al. 2010
miR-452	Downregulated	3	Goto et al. 2017; Jalava et al. 2012; Taylor et al. 2010
miR-625	Upregulated	2	Jalava et al. 2012; Taylor et al. 2010

[a]The studies referred to in the above table encompass 32 CRPC (18 metastases and 14 localized CRPC), 109 primary prostate tumor, 7 benign prostatic hyperplasia and 38 normal prostate samples. Downregulated miRNA were listed in Table 5 if they were reproducibly altered in >50% i.e. 3 out of 4 studies. Upregulated miRNA were listed if they were reproducibly altered in >50% i.e. 2 out of 2 studies. Goto et al 2015 and Goto et al 2017 only report miRNA downregulated in CRPC and were excluded when listing upregulated miRNA. Comparisons were done between benign prostatic hyperplasia and CRPC (Jalava et al. 2012), normal prostate tissues or primary prostate tumours with CRPC (Goto et al. 2015; Goto et al. 2017; Taylor et al. 2010).

REFERENCES

Agarwal V, Bell GW, Nam JW & Bartel DP 2015 Predicting effective microRNA target sites in mammalian mRNAs. *elife* **4**.
Antonarakis ES, Armstrong AJ, Dehm SM & Luo J 2016 Androgen receptor variant-driven prostate cancer: clinical implications and therapeutic targeting. *Prostate Cancer Prostatic Dis* **19** 231-241.
Antonarakis ES, Lu C, Wang H, Luber B, Nakazawa M, Roeser JC, Chen Y, Mohammad TA, Chen Y, Fedor HL, et al. 2014 AR-V7 and resistance to enzalutamide and abiraterone in prostate cancer. *N Engl J Med* **371** 1028-1038.
Beg MS, Brenner AJ, Sachdev J, Borad M, Kang YK, Stoudemire J, Smith S, Bader AG, Kim S & Hong DS 2017 Phase I study of MRX34, a liposomal miR-34a mimic, administered twice weekly in patients with advanced solid tumors. *Invest New Drugs* **35** 180-188.
Bonci D, Coppola V, Patrizii M, Addario A, Cannistraci A, Francescangeli F, Pecci R, Muto G, Collura D, Bedini R, et al. 2016 A microRNA code for prostate cancer metastasis. *Oncogene* **35** 1180-1192.
Brase JC, Johannes M, Schlomm T, Falth M, Haese A, Steuber T, Beissbarth T, Kuner R & Sultmann H 2011 Circulating miRNAs are correlated with tumor progression in prostate cancer. *Int J Cancer* **128** 608-616.
Brummer A & Hausser J 2014 MicroRNA binding sites in the coding region of mRNAs: extending the repertoire of post-transcriptional gene regulation. *Bioessays* **36** 617-626.
Calin GA & Croce CM 2006 MicroRNA signatures in human cancers. *Nat Rev Cancer* **6** 857-866.
Cao P, Deng Z, Wan M, Huang W, Cramer SD, Xu J, Lei M & Sui G 2010 MicroRNA-101 negatively regulates Ezh2 and its expression is modulated by androgen receptor and HIF-1α/HIF-1β. *Molecular cancer* **9** 108.
Catalona WJ, Smith DS, Ratliff TL, Dodds KM, Coplen DE, Yuan JJ, Petros JA & Andriole GL 1991 Measurement of prostate-specific antigen in serum as a screening test for prostate cancer. *N Engl J Med* **324** 1156-1161.
Chan SC, Selth LA, Li Y, Nyquist MD, Miao L, Bradner JE, Raj GV, Tilley WD & Dehm SM 2015 Targeting chromatin binding regulation of constitutively active AR variants to overcome prostate cancer resistance to endocrine-based therapies. *Nucleic Acids Res* **43** 5880-5897.
Chu M, Chang Y, Li P, Guo Y, Zhang K & Gao W 2014 Androgen receptor is negatively correlated with the methylation-mediated transcriptional repression of miR-375 in human prostate cancer cells. *Oncology reports* **31** 34-40.
Coutinho I, Day TK, Tilley WD & Selth LA 2016 Androgen receptor signaling in castration-resistant prostate cancer: a lesson in persistence. *Endocr Relat Cancer* **23** T179-T197.
Craft N, Shostak Y, Carey M & Sawyers CL 1999 A mechanism for hormone-independent prostate cancer through modulation of androgen receptor signaling by the HER-2/neu tyrosine kinase. *Nature medicine* **5** 280-285.
D'Angelo B, Benedetti E, Cimini A & Giordano A 2016 MicroRNAs: A Puzzling Tool in Cancer Diagnostics and Therapy. *Anticancer Res* **36** 5571-5575.
Das DK, Naidoo M, Ilboudo A, Park JY, Ali T, Krampis K, Robinson BD, Osborne JR & Ogunwobi OO 2016 miR-1207-3p regulates the androgen receptor in prostate cancer via FNDC1/fibronectin. *Exp Cell Res* **348** 190-200.
Dehm SM, Schmidt LJ, Heemers HV, Vessella RL & Tindall DJ 2008 Splicing of a novel androgen receptor exon generates a constitutively active androgen receptor that mediates prostate cancer therapy resistance. *Cancer research* **68** 5469-5477.

Epis MR, Giles KM, Barker A, Kendrick TS & Leedman PJ 2009 miR-331-3p regulates ERBB-2 expression and androgen receptor signaling in prostate cancer. *J Biol Chem* **284** 24696-24704.
Faber PW, van Rooij HC, van der Korput HA, Baarends WM, Brinkmann AO, Grootegoed JA & Trapman J 1991 Characterization of the human androgen receptor transcription unit. *J Biol Chem* **266** 10743-10749.
Fabian MR & Sonenberg N 2012 The mechanics of miRNA-mediated gene silencing: a look under the hood of miRISC. *Nat Struct Mol Biol* **19** 586-593.
Fabris L, Ceder Y, Chinnaiyan AM, Jenster GW, Sorensen KD, Tomlins S, Visakorpi T & Calin GA 2016 The Potential of MicroRNAs as Prostate Cancer Biomarkers. *Eur Urol* **70** 312-322.
Feldman BJ & Feldman D 2001 The development of androgen-independent prostate cancer. *Nat Rev Cancer* **1** 34-45.
Fletcher CE, Dart DA, Sita-Lumsden A, Cheng H, Rennie PS & Bevan CL 2012 Androgen-regulated processing of the oncomir MiR-27a, which targets Prohibitin in prostate cancer. *Human molecular genetics* **21** 3112-3127.
Fredsoe J, Rasmussen AKI, Thomsen AR, Mouritzen P, Hoyer S, Borre M, Orntoft TF & Sorensen KD 2017 Diagnostic and Prognostic MicroRNA Biomarkers for Prostate Cancer in Cell-free Urine. *Eur Urol Focus*.
Friedman RC, Farh KKH, Burge CB & Bartel DP 2009 Most mammalian mRNAs are conserved targets of microRNAs. *Genome research* **19** 92-105.
Gao W, Hong Z, Huang H, Zhu A, Lin S, Cheng C, Zhang X, Zou G & Shi Z 2018 miR‐27a in serum acts as biomarker for prostate cancer detection and promotes cell proliferation by targeting Sprouty2. *Oncology letters* **16** 5291-5298.
Gezer U, Tiryakioglu D, Bilgin E, Dalay N & Holdenrieder S 2015 Androgen Stimulation of PCA3 and miR-141 and Their Release from Prostate Cancer Cells. *Cell Journal* **16** 488-493.
Gonzales JC, Fink LM, Goodman OB, Jr., Symanowski JT, Vogelzang NJ & Ward DC 2011 Comparison of circulating MicroRNA 141 to circulating tumor cells, lactate dehydrogenase, and prostate-specific antigen for determining treatment response in patients with metastatic prostate cancer. *Clin Genitourin Cancer* **9** 39-45.
Goto Y, Kojima S, Nishikawa R, Kurozumi A, Kato M, Enokida H, Matsushita R, Yamazaki K, Ishida Y, Nakagawa M, et al. 2015 MicroRNA expression signature of castration-resistant prostate cancer: the microRNA-221/222 cluster functions as a tumour suppressor and disease progression marker. *British journal of cancer* **113** 1055-1065.
Goto Y, Kurozumi A, Arai T, Nohata N, Kojima S, Okato A, Kato M, Yamazaki K, Ishida Y, Naya Y, et al. 2017 Impact of novel miR-145-3p regulatory networks on survival in patients with castration-resistant prostate cancer. *Br J Cancer* **117** 409-420.
Gui B, Hsieh CL, Kantoff PW, Kibel AS & Jia L 2017 Androgen receptor-mediated downregulation of microRNA-221 and-222 in castration-resistant prostate cancer. *PloS one* **12** e0184166.
Guo Z, Yang X, Sun F, Jiang R, Linn DE, Chen H, Chen H, Kong X, Melamed J & Tepper CG 2009 A novel androgen receptor splice variant is up-regulated during prostate cancer progression and promotes androgen depletion–resistant growth. *Cancer research* **69** 2305-2313.
Hamilton MP, Rajapakshe KI, Bader DA, Cerne JZ, Smith EA, Coarfa C, Hartig SM & McGuire SE 2016 The Landscape of microRNA Targeting in Prostate Cancer Defined by AGO-PAR-CLIP. *Neoplasia* **18** 356-370.

He Y, Lu J, Ye Z, Hao S, Wang L, Kohli M, Tindall DJ, Li B, Zhu R, Wang L, et al. 2018 Androgen receptor splice variants bind to constitutively open chromatin and promote abiraterone-resistant growth of prostate cancer. *Nucleic Acids Res* **46** 1895-1911.
Hong DS, Kang YK, Brenner AJ, Sachdev JC, Ejadi S, Borad MJ, Kim TY, Lim HY, Park K, Becerra C, et al. 2016 MRX34, a liposomal miR-34 mimic, in patients with advanced solid tumors: Final dose-escalation results from a first-in-human phase I trial of microRNA therapy. *Journal of Clinical Oncology* **34**.
Hornberg E, Ylitalo EB, Crnalic S, Antti H, Stattin P, Widmark A, Bergh A & Wikstrom P 2011 Expression of Androgen Receptor Splice Variants in Prostate Cancer Bone Metastases is Associated with Castration-Resistance and Short Survival. *PloS one* **6** e19059.
Hu R, Dunn TA, Wei S, Isharwal S, Veltri RW, Humphreys E, Han M, Partin AW, Vessella RL, Isaacs WB, et al. 2009 Ligand-independent androgen receptor variants derived from splicing of cryptic exons signify hormone-refractory prostate cancer. *Cancer Res* **69** 16-22.
Hu R, Isaacs WB & Luo J 2011 A snapshot of the expression signature of androgen receptor splicing variants and their distinctive transcriptional activities. *The Prostate* **71** 1656-1667.
Huang X, Yuan T, Liang M, Du M, Xia S, Dittmar R, Wang D, See W, Costello BA, Quevedo F, et al. 2015 Exosomal miR-1290 and miR-375 as prognostic markers in castration-resistant prostate cancer. *Eur Urol* **67** 33-41.
Ito Y, Inoue A, Seers T, Hato Y, Igarashi A, Toyama T, Taganov KD, Boldin MP & Asahara H 2017 Identification of targets of tumor suppressor microRNA-34a using a reporter library system. *Proceedings of the National Academy of Sciences of the United States of America* **114** 3927-3932.
Jackson BL, Grabowska A & Ratan HL 2014 MicroRNA in prostate cancer: functional importance and potential as circulating biomarkers. *BMC cancer* **14** 1.
Jalava SE, Urbanucci A, Latonen L, Waltering KK, Sahu B, Janne OA, Seppala J, Lahdesmaki H, Tammela TLJ & Visakorpi T 2012 Androgen-regulated miR-32 targets BTG2 and is overexpressed in castration-resistant prostate cancer. *Oncogene* **31** 4460-4471.
Jiang CY, Ruan Y, Wang XH, Zhao W, Jiang Q, Jing YF, Han BM, Xia SJ & Zhao FJ 2016 MiR-185 attenuates androgen receptor function in prostate cancer indirectly by targeting bromodomain containing 8 isoform 2, an androgen receptor co-activator. *Mol Cell Endocrinol* **427** 13-20.
Kanwal R, Plaga AR, Liu X, Shukla GC & Gupta S 2017 MicroRNAs in prostate cancer: Functional role as biomarkers. *Cancer Lett* **407** 9-20.
Kim VN 2005 MicroRNA biogenesis: coordinated cropping and dicing. *Nat Rev Mol Cell Biol* **6** 376-385.
Kohli M, Ho Y, Hillman DW, Van Etten JL, Henzler C, Yang R, Sperger JM, Li Y, Tseng E & Hon T 2017 Androgen receptor variant AR-V9 is co-expressed with AR-V7 in prostate cancer metastases and predicts abiraterone resistance. *Clinical Cancer Research* clincanres. 0017.2017.
Kojima S, Goto Y & Naya Y 2017 The roles of microRNAs in the progression of castration-resistant prostate cancer. *J Hum Genet* **62** 25-31.
Kroiss A, Vincent S, Decaussin-Petrucci M, Meugnier E, Viallet J, Ruffion A, Chalmel F, Samarut J & Allioli N 2015 Androgen-regulated microRNA-135a decreases prostate cancer cell migration and invasion through downregulating ROCK1 and ROCK2. *Oncogene* **34** 2846-2855.

Kumar B, Khaleghzadegan S, Mears B, Hatano K, Kudrolli TA, Chowdhury WH, Yeater DB, Ewing CM, Luo J, Isaacs WB, et al. 2016 Identification of miR-30b-3p and miR-30d-5p as direct regulators of Androgen Receptor Signaling in Prostate Cancer by complementary functional microRNA library screening. *Oncotarget* **7** 72593-72607.
Lee Y, Kim M, Han J, Yeom KH, Lee S, Baek SH & Kim VN 2004 MicroRNA genes are transcribed by RNA polymerase II. *The EMBO journal* **23** 4051-4060.
Lewis BP, Burge CB & Bartel DP 2005 Conserved seed pairing, often flanked by adenosines, indicates that thousands of human genes are microRNA targets. *Cell* **120** 15-20.
Li T, Li D, Sha J, Sun P & Huang Y 2009 MicroRNA-21 directly targets MARCKS and promotes apoptosis resistance and invasion in prostate cancer cells. *Biochem Biophys Res Commun* **383** 280-285.
Lin PC, Chiu YL, Banerjee S, Park K, Mosquera JM, Giannopoulou E, Alves P, Tewari AK, Gerstein MB, Beltran H, et al. 2013 Epigenetic repression of miR-31 disrupts androgen receptor homeostasis and contributes to prostate cancer progression. *Cancer Res* **73** 1232-1244.
Lin SL, Chang D & Ying SY 2007 Hyaluronan stimulates transformation of androgen-independent prostate cancer. *Carcinogenesis* **28** 310-320.
Lin SL, Chiang A, Chang D & Ying SY 2008 Loss of mir-146a function in hormone-refractory prostate cancer. *RNA* **14** 417-424.
Liu C, Kelnar K, Liu B, Chen X, Calhoun-Davis T, Li H, Patrawala L, Yan H, Jeter C, Honorio S, et al. 2011 The microRNA miR-34a inhibits prostate cancer stem cells and metastasis by directly repressing CD44. *Nat Med* **17** 211-215.
Liu S, Kumari S, Hu Q, Senapati D, Venkadakrishnan VB, Wang D, DePriest AD, Schlanger SE, Ben-Salem S, Valenzuela MM, et al. 2017 A comprehensive analysis of coregulator recruitment, androgen receptor function and gene expression in prostate cancer. *elife* **6**.
Liu XC, Ledet E, Li DY, Dotiwala A, Steinberger A, Feibus A, Li JZ, Qi Y, Silberstein J, Lee B, et al. 2016 A Whole Blood Assay for AR-V7 and AR(v567es) in Patients with Prostate Cancer. *Journal of Urology* **196** 1758-1763.
Liu YN, Yin J, Barrett B, Sheppard-Tillman H, Li D, Casey OM, Fang L, Hynes PG, Ameri AH & Kelly K 2015 Loss of Androgen-Regulated MicroRNA 1 Activates SRC and Promotes Prostate Cancer Bone Metastasis. *Mol Cell Biol* **35** 1940-1951.
Luo J, Attard G, Balk SP, Bevan C, Burnstein K, Cato L, Cherkasov A, De Bono JS, Dong Y, Gao AC, et al. 2018 Role of Androgen Receptor Variants in Prostate Cancer: Report from the 2017 Mission Androgen Receptor Variants Meeting. *Eur Urol* **73** 715-723.
Luu HN, Lin HY, Sorensen KD, Ogunwobi OO, Kumar N, Chornokur G, Phelan C, Jones D, Kidd L, Batra J, et al. 2017 miRNAs associated with prostate cancer risk and progression. *BMC Urol* **17** 18.
Massie CE, Lynch A, Ramos-Montoya A, Boren J, Stark R, Fazli L, Warren A, Scott H, Madhu B, Sharma N, et al. 2011 The androgen receptor fuels prostate cancer by regulating central metabolism and biosynthesis. *EMBO J* **30** 2719-2733.
Matin F, Jeet V, Clements JA, Yousef GM & Batra J 2016 MicroRNA Theranostics in Prostate Cancer Precision Medicine. *Clin Chem* **62** 1318-1333.
Matin F, Jeet V, Moya L, Selth LA, Chambers S, Australian Prostate Cancer B, Clements JA & Batra J 2018 A Plasma Biomarker Panel of Four MicroRNAs for the Diagnosis of Prostate Cancer. *Sci Rep* **8** 6653.

Meng D, Yang S, Wan X, Zhang Y, Huang W, Zhao P, Li T, Wang L, Huang Y, Li T, et al. 2016 A transcriptional target of androgen receptor, miR-421 regulates proliferation and metabolism of prostate cancer cells. *Int J Biochem Cell Biol* **73** 30-40.
Mishra S, Deng JJ, Gowda PS, Rao MK, Lin CL, Chen CL, Huang T & Sun LZ 2014 Androgen receptor and microRNA-21 axis downregulates transforming growth factor beta receptor II (TGFBR2) expression in prostate cancer. *Oncogene* **33** 4097-4106.
Mitchell PS, Parkin RK, Kroh EM, Fritz BR, Wyman SK, Pogosova-Agadjanyan EL, Peterson A, Noteboom J, O'Briant KC, Allen A, et al. 2008 Circulating microRNAs as stable blood-based markers for cancer detection. *Proceedings of the National Academy of Sciences of the United States of America* **105** 10513-10518.
Mo WJ, Zhang JY, Li X, Meng DL, Gao Y, Yang S, Wan XC, Zhou CH, Guo FH, Huang Y, et al. 2013 Identification of Novel AR-Targeted MicroRNAs Mediating Androgen Signalling through Critical Pathways to Regulate Cell Viability in Prostate Cancer. *PloS one* **8** e56592.
Nadiminty N, Tummala R, Lou W, Zhu Y, Zhang J, Chen X, eVere White RW, Kung HJ, Evans CP & Gao AC 2012 MicroRNA let-7c suppresses androgen receptor expression and activity via regulation of Myc expression in prostate cancer cells. *J Biol Chem* **287** 1527-1537.
Nelson PS, Clegg N, Arnold H, Ferguson C, Bonham M, White J, Hood L & Lin B 2002 The program of androgen-responsive genes in neoplastic prostate epithelium. *Proc Natl Acad Sci U S A* **99** 11890-11895.
Ngan S, Stronach E, Photiou A, Waxman J, Ali S & Buluwela L 2009 Microarray coupled to quantitative RT–PCR analysis of androgen-regulated genes in human LNCaP prostate cancer cells. *Oncogene* **28** 2051-2063.
Nilsson EM, Laursen KB, Whitchurch J, McWilliam A, Odum N, Persson JL, Heery DM, Gudas LJ & Mongan NP 2015 MiR137 is an androgen regulated repressor of an extended network of transcriptional coregulators. *Oncotarget* **6** 35710-35725.
Östling P, Leivonen S-K, Aakula A, Kohonen P, Mäkelä R, Hagman Z, Edsjö A, Kangaspeska S, Edgren H & Nicorici D 2011 Systematic analysis of microRNAs targeting the androgen receptor in prostate cancer cells. *Cancer research* **71** 1956-1967.
Pasqualini L, Bu H, Puhr M, Narisu N, Rainer J, Schlick B, Schafer G, Angelova M, Trajanoski Z, Borno ST, et al. 2015 miR-22 and miR-29a Are Members of the Androgen Receptor Cistrome Modulating LAMC1 and Mcl-1 in Prostate Cancer. *Mol Endocrinol* **29** 1037-1054.
Pomerantz MM, Li FG, Takeda DY, Lenci R, Chonkar A, Chabot M, Cejas P, Vazquez F, Cook J, Shivdasani RA, et al. 2015 The androgen receptor cistrome is extensively reprogrammed in human prostate tumorigenesis. *Nature genetics* **47** 1346-+.
Porkka KP, Pfeiffer MJ, Waltering KK, Vessella RL, Tammela TL & Visakorpi T 2007 MicroRNA expression profiling in prostate cancer. *Cancer Res* **67** 6130-6135.
Qu Y, Dai B, Ye D, Kong Y, Chang K, Jia Z, Yang X, Zhang H, Zhu Y & Shi G 2015 Constitutively active AR-V7 plays an essential role in the development and progression of castration-resistant prostate cancer. *Sci Rep* **5** 7654.
Reis ST, Pontes J, Antunes AA, Dall'Oglio MF, Dip N, Passerotti CC, Rossini GA, Morais DR, Nesrallah AJ, Piantino C, et al. 2012 miR-21 may acts as an oncomir by targeting RECK, a matrix metalloproteinase regulator, in prostate cancer. *BMC urology* **12** 14.
Ribas J, Ni X, Haffner M, Wentzel EA, Salmasi AH, Chowdhury WH, Kudrolli TA, Yegnasubramanian S, Luo J & Rodriguez R 2009 miR-21: an androgen receptor–regulated microRNA that promotes hormone-dependent and hormone-independent prostate cancer growth. *Cancer research* **69** 7165-7169.

Robinson D, Van Allen EM, Wu Y-M, Schultz N, Lonigro RJ, Mosquera J-M, Montgomery B, Taplin M-E, Pritchard CC & Attard G 2015 Integrative clinical genomics of advanced prostate cancer. *Cell* **161** 1215-1228.
Rodriguez A, Griffiths-Jones S, Ashurst JL & Bradley A 2004 Identification of mammalian microRNA host genes and transcription units. *Genome Res* **14** 1902-1910.
Rupaimoole R & Slack FJ 2017 MicroRNA therapeutics: towards a new era for the management of cancer and other diseases. *Nat Rev Drug Discov* **16** 203-222.
Santos JI, Teixeira AL, Dias F, Mauricio J, Lobo F, Morais A & Medeiros R 2014 Influence of peripheral whole-blood microRNA-7 and microRNA-221 high expression levels on the acquisition of castration-resistant prostate cancer: evidences from in vitro and in vivo studies. *Tumour Biol* **35** 7105-7113.
Sato S, Katsushima K, Shinjo K, Hatanaka A, Ohka F, Suzuki S, Naiki-Ito A, Soga N, Takahashi S & Kondo Y 2016 Histone Deacetylase Inhibition in Prostate Cancer Triggers miR-320-Mediated Suppression of the Androgen Receptor. *Cancer Res* **76** 4192-4204.
Scher HI, Buchanan G, Gerald W, Butler LM & Tilley WD 2004 Targeting the androgen receptor: improving outcomes for castration-resistant prostate cancer. *Endocr Relat Cancer* **11** 459-476.
Selth LA, Das R, Townley SL, Coutinho I, Hanson AR, Centenera MM, Stylianou N, Sweeney K, Soekmadji C, Jovanovic L, et al. 2017 A ZEB1-miR-375-YAP1 pathway regulates epithelial plasticity in prostate cancer. *Oncogene* **36** 24-34.
Selth LA, Townley S, Gillis JL, Ochnik AM, Murti K, Macfarlane RJ, Chi KN, Marshall VR, Tilley WD & Butler LM 2012 Discovery of circulating microRNAs associated with human prostate cancer using a mouse model of disease. *Int J Cancer* **131** 652-661.
Shi XB, Ma AH, Xue L, Li M, Nguyen HG, Yang JC, Tepper CG, Gandour-Edwards R, Evans CP, Kung HJ, et al. 2015 miR-124 and Androgen Receptor Signaling Inhibitors Repress Prostate Cancer Growth by Downregulating Androgen Receptor Splice Variants, EZH2, and Src. *Cancer Res* **75** 5309-5317.
Shi XB, Xue L, Ma AH, Tepper CG, Gandour-Edwards R, Kung HJ & deVere White RW 2013 Tumor suppressive miR-124 targets androgen receptor and inhibits proliferation of prostate cancer cells. *Oncogene* **32** 4130-4138.
Shi XB, Xue L, Yang J, Ma AH, Zhao J, Xu M, Tepper CG, Evans CP, Kung HJ & deVere White RW 2007 An androgen-regulated miRNA suppresses Bak1 expression and induces androgen-independent growth of prostate cancer cells. *Proc Natl Acad Sci U S A* **104** 19983-19988.
Shiota M, Takeuchi A, Song Y, Yokomizo A, Kashiwagi E, Uchiumi T, Kuroiwa K, Tatsugami K, Fujimoto N, Oda Y, et al. 2011 Y-box binding protein-1 promotes castration-resistant prostate cancer growth via androgen receptor expression. *Endocr Relat Cancer* **18** 505-517.
Stegeman S, Amankwah E, Klein K, O'Mara TA, Kim D, Lin HY, Permuth-Wey J, Sellers TA, Srinivasan S, Eeles R, et al. 2015a A Large-Scale Analysis of Genetic Variants within Putative miRNA Binding Sites in Prostate Cancer. *Cancer Discov* **5** 368-379.
Stegeman S, Moya L, Selth LA, Spurdle AB, Clements JA & Batra J 2015b A genetic variant of MDM4 influences regulation by multiple microRNAs in prostate cancer. *Endocr Relat Cancer* **22** 265-276.
Stuopelyte K, Daniunaite K, Jankevicius F & Jarmalaite S 2016 Detection of miRNAs in urine of prostate cancer patients. *Medicina (Kaunas)* **52** 116-124.
Sun D, Layer R, Mueller AC, Cichewicz MA, Negishi M, Paschal BM & Dutta A 2014 Regulation of several androgen-induced genes through the repression of the miR-99a/let-7c/miR-125b-2 miRNA cluster in prostate cancer cells. *Oncogene* **33** 1448-1457.

Takayama K, Tsutsumi S, Katayama S, Okayama T, Horie-Inoue K, Ikeda K, Urano T, Kawazu C, Hasegawa A, Ikeo K, et al. 2011 Integration of cap analysis of gene expression and chromatin immunoprecipitation analysis on array reveals genome-wide androgen receptor signaling in prostate cancer cells. *Oncogene* **30** 619-630.
Tavallaie R, De Almeida SRM & Gooding JJ 2015 Toward biosensors for the detection of circulating microRNA as a cancer biomarker: an overview of the challenges and successes. *Wiley Interdisciplinary Reviews-Nanomedicine and Nanobiotechnology* **7** 580-592.
Taylor BS, Schultz N, Hieronymus H, Gopalan A, Xiao Y, Carver BS, Arora VK, Kaushik P, Cerami E, Reva B, et al. 2010 Integrative genomic profiling of human prostate cancer. *Cancer Cell* **18** 11-22.
TCGA 2015 The molecular taxonomy of primary prostate cancer. *Cell* **163** 1011-1025.
Tiryakioglu D, Bilgin E, Holdenrieder S, Dalay N & Gezer U 2013 miR‐141 and miR‐375 induction and release are different from PSA mRNA and PCA3 upon androgen stimulation of LNCaP cells. *Biomedical reports* **1** 802-806.
Todorova K, Metodiev MV, Metodieva G, Mincheff M, Fernandez N & Hayrabedyan S 2017 Micro-RNA-204 Participates in TMPRSS2/ERG Regulation and Androgen Receptor Reprogramming in Prostate Cancer. *Horm Cancer* **8** 28-48.
Toropainen S, Niskanen EA, Malinen M, Sutinen P, Kaikkonen MU & Palvimo JJ 2016 Global analysis of transcription in castration-resistant prostate cancer cells uncovers active enhancers and direct androgen receptor targets. *Sci Rep* **6** 33510.
Van der Ree M, Van Der Meer A, Van Nuenen A, de Bruijne J, Ottosen S, Janssen H, Kootstra N & Reesink H 2016 Miravirsen dosing in chronic hepatitis C patients results in decreased micro RNA-122 levels without affecting other micro RNA s in plasma. *Alimentary pharmacology & therapeutics* **43** 102-113.
van der Ree MH, de Vree JM, Stelma F, Willemse S, van der Valk M, Rietdijk S, Molenkamp R, Schinkel J, van Nuenen AC, Beuers U, et al. 2017 Safety, tolerability, and antiviral effect of RG-101 in patients with chronic hepatitis C: a phase 1B, double-blind, randomised controlled trial. *Lancet* **389** 709-717.
Van Roosbroeck K & Calin GA 2017 Cancer hallmarks and MicroRNAs: the therapeutic connection. In *Advances in cancer research*, pp 119-149: Elsevier.
van Zandwijk N, Pavlakis N, Kao SC, Linton A, Boyer MJ, Clarke S, Huynh Y, Chrzanowska A, Fulham MJ, Bailey DL, et al. 2017 Safety and activity of microRNA-loaded minicells in patients with recurrent malignant pleural mesothelioma: a first-in-man, phase 1, open-label, dose-escalation study. *Lancet Oncol* **18** 1386-1396.
Velasco AM, Gillis KA, Li Y, Brown EL, Sadler TM, Achilleos M, Greenberger LM, Frost P, Bai W & Zhang Y 2004 Identification and validation of novel androgen-regulated genes in prostate cancer. *Endocrinology* **145** 3913-3924.
Waltering KK, Wallen MJ, Tammela TL, Vessella RL & Visakorpi T 2006 Mutation screening of the androgen receptor promoter and untranslated regions in prostate cancer. *Prostate* **66** 1585-1591.
Wang J, Chen JY & Sen S 2016 MicroRNA as Biomarkers and Diagnostics. *Journal of cellular physiology* **231** 25-30.
Wang Q, Li W, Liu XS, Carroll JS, Janne OA, Keeton EK, Chinnaiyan AM, Pienta KJ & Brown M 2007 A hierarchical network of transcription factors governs androgen receptor-dependent prostate cancer growth. *Mol Cell* **27** 380-392.
Wang Q, Li W, Zhang Y, Yuan X, Xu K, Yu J, Chen Z, Beroukhim R, Wang H, Lupien M, et al. 2009 Androgen receptor regulates a distinct transcription program in androgen-independent prostate cancer. *Cell* **138** 245-256.

Williams LV, Veliceasa D, Vinokour E & Volpert OV 2013 miR-200b inhibits prostate cancer EMT, growth and metastasis. *PloS one* **8** e83991.
Wu G, Sun Y, Xiang Z, Wang K, Liu B, Xiao G, Niu Y, Wu D & Chang C 2019 Preclinical study using circular RNA 17 and micro RNA 181c-5p to suppress the enzalutamide-resistant prostate cancer progression. *Cell Death Dis* **10** 37.
Xiao J, Gong AY, Eischeid AN, Chen D, Deng C, Young CY & Chen XM 2012 miR-141 modulates androgen receptor transcriptional activity in human prostate cancer cells through targeting the small heterodimer partner protein. *The Prostate* **72** 1514-1522.
Xiao Y, Sun Y, Liu G, Zhao J, Gao Y, Yeh S, Gong L & Chang C 2019 Androgen receptor (AR)/miR-520f-3p/SOX9 signaling is involved in altering hepatocellular carcinoma (HCC) cell sensitivity to the Sorafenib therapy under hypoxia via increasing cancer stem cells phenotype. *Cancer letters* **444** 175-187.
Xiong Y, Wang L, Li Y, Chen M, He W & Qi L 2017 The Long Non-Coding RNA XIST Interacted with MiR-124 to Modulate Bladder Cancer Growth, Invasion and Migration by Targeting Androgen Receptor (AR). *Cell Physiol Biochem* **43** 405-418.
Xu S, Wang T, Song W, Jiang T, Zhang F, Yin Y, Jiang SW, Wu K, Yu Z, Wang C, et al. 2015 The inhibitory effects of AR/miR-190a/YB-1 negative feedback loop on prostate cancer and underlying mechanism. *Sci Rep* **5** 13528.
Yang F, Shen Y, Zhang W, Jin J, Huang D, Fang H, Ji W, Shi Y, Tang L, Chen W, et al. 2018 An androgen receptor negatively induced long non-coding RNA ARNILA binding to miR-204 promotes the invasion and metastasis of triple-negative breast cancer. *Cell Death Differ* **25** 2209-2220.
Yang X, Bemis L, Su LJ, Gao D & Flaig TW 2012 miR-125b Regulation of Androgen Receptor Signaling Via Modulation of the Receptor Complex Co-Repressor NCOR2. *Biores Open Access* **1** 55-62.
Yang YJ, Jia DW, Kim H, Elmageed ZYA, Datta A, Davis R, Srivastav S, Moroz K, Crawford BE, Moparty K, et al. 2016 Dysregulation of miR-212 Promotes Castration Resistance through hnRNPH1-Mediated Regulation of AR and AR-V7: Implications for Racial Disparity of Prostate Cancer. *Clinical Cancer Research* **22** 1744-1756.
Yao J, Xu C, Fang Z, Li Y, Liu H, Wang Y, Xu C & Sun Y 2016 Androgen receptor regulated microRNA miR-182-5p promotes prostate cancer progression by targeting the ARRDC3/ITGB4 pathway. *Biochem Biophys Res Commun* **474** 213-219.
Zhang HL, Yang LF, Zhu Y, Yao XD, Zhang SL, Dai B, Zhu YP, Shen YJ, Shi GH & Ye DW 2011 Serum miRNA-21: elevated levels in patients with metastatic hormone-refractory prostate cancer and potential predictive factor for the efficacy of docetaxel-based chemotherapy. *Prostate* **71** 326-331.
Zhang J, Zhou W, Liu Y, Liu T, Li C & Wang L 2018 Oncogenic role of microRNA-532-5p in human colorectal cancer via targeting of the 5'UTR of RUNX3. *Oncol Lett* **15** 7215-7220.
Zhou H & Rigoutsos I 2014 MiR-103a-3p targets the 5' UTR of GPRC5A in pancreatic cells. *RNA* **20** 1431-1439.

1.10 miR-194

1.10.1 Genomic location and regulation of expression

Mature miR-194 is derived from two precursors originating from the miR-215/miR-194-1 cluster and the miR-192/miR-194-2 cluster, on chromosome 1 and 11 respectively (Hino et al. 2008). While the miR-215/194-1 cluster is located within an intron of the *IARS2* gene, the miR-192/miR-194-2 cluster is encoded by the *miR-194-2HG* gene located ~1.25kb downstream of the *ATG2A* gene.

As with many miRNA, miR-194 has context dependant roles in cancer, and its regulation reflects its role in that tumour type. In hepatocellular carcinoma for instance, where miR-194 is tumour suppressive, its expression is downregulated by NF-κB mediated suppression of Hepatocyte nuclear factor-1 alpha (HNF-1α) (Bao et al. 2015). HNF-1α is a key transcriptional upregulator of miR-194 that induces expression by binding to a highly conserved element within the promoter region of the miR-192/miR-194-2 cluster (Hino et al. 2008; Krützfeldt et al. 2012; Wang et al. 2014). In multiple myeloma, hypermethylation of the miR-194-2-192 cluster corresponding to inhibition of expression has been reported (Pichiorri et al. 2010). Consistent with its tumour suppressive role in some cancers, both miR-194-containing clusters have response elements for the p53 tumour suppressor protein (Braun et al. 2008; Pichiorri et al. 2010). In prostate cancer, where miR-194 is oncogenic, expression is upregulated by GATA2 (Das et al. 2017).

Only a few factors that regulate the expression of miR-194 have been reported so far. In general, upstream signalling events either up/downregulate miR-194 expression based on its role in cancer. Elucidating other factors, like genetic alterations and dysregulation of biogenesis, is important for further understanding how miR-194 might be affected and affect carcinogenesis.

1.10.2 miR-194 in PCa

miR-194 is known to have cellular context-dependent role in tumorigenesis (Xu et al. 2012; Zhang et al. 2014). Several studies have indicated that miR-194 acts as a tumour suppressor, with its downregulation being linked to hepatocellular carcinoma (HCC)

(Bao et al. 2015), bladder cancer (Zhang, Zhuang & Cui 2016), oral squamous cell carcinoma (Chia et al. 2015), renal cell carcinoma (Khella et al. 2013), gastric cancer (Song et al. 2012), non-small cell lung cancer (Zhou et al. 2016) and myelodysplastic syndrome (Choi et al. 2015). In certain other cancer types, like oesophageal and pancreatic cancer, upregulation of miR-194 contributes to increased tumour growth and invasion (Mathé et al. 2009; Zhang et al. 2014).

Work from our laboratory and others have shown that in prostate cancer, elevated miR-194 is associated with early biochemical recurrence, metastasis and poor prognosis (Selth et al. 2013; Tong et al. 2009). Tong et al reported a >40% increase in miR-194 in prostatectomy sections of individuals who relapsed after to surgery compared to those who did not (Tong et al. 2009). Selth et al showed that miR-194 is elevated in the serum of men who experienced early biochemical recurrence (BCR) after prostatectomy versus those who did not, suggesting its utility as a circulating prognostic biomarker (Selth et al. 2013). This study also found that tumour miR-194 levels were prognostic for BCR and that miR-194 is more highly expressed in metastases compared to normal prostate or primary tumours (Selth et al. 2013).

Based on these earlier finding from our laboratory, we further investigated the role of miR-194 in prostate cancer metastasis and progression. I contributed to this study (Das et al. 2017) , which was completed during the early stages of my PhD, by assessing levels of miR-194 and its targets in tumour tissues, analysing data and participating in discussions. In this study, we showed that in cell line models, overexpression of miR-194 can enhance migration, invasion and stimulate epithelial-mesenchymal transition. MiR-194 was found to mediate these effects partly by targeting SOCS2. SOCS2 inhibits metastasis in prostate cancer by suppressing the STAT3 and ERK signalling pathways (Das et al. 2017). Although this study identifies one target through which miR-194 promotes metastasis, a complete description of miR-194 regulated genes and signalling networks remains lacking and is necessary to better understand the molecular mechanisms underlying its pro-metastatic function in PCa.

1.11 Hypothesis and aims

Previous studies in our laboratory have defined an oncogenic, metastasis-promoting role for miR-194 in prostate cancer. While our previous study identified one target gene by which miR-194 promotes metastasis, miR-194 is likely to act via multiple genes and pathways. We hypothesised that identifying all miR-194 target genes and associated signalling pathways, would be crucial to understanding its role in EMT, metastasis and prostate cancer progression.

Aims:

1. Identify a complete set of miR-194 target genes ("targetome") in prostate cancer
2. Identify and validate pathways by which the miR-194 targetome promotes prostate cancer metastasis and progression
3. Define mechanisms of miR-194 specific target gene interactions

Chapter 2: Materials and methods

2.1 Materials

Table 2.1: Chemicals and reagents

Reagent	Supplier	Catalogue number
Advanced DMEM	Thermo Fischer Scientific	12491023
Anti-microRNA-194 inhibitors (LNA)	Qiagen	YI04101208-DFA
Anti-microRNA negative control LNA inhibitors	Qiagen	YI00199006-DFA
Anti-microRNA FAM labelled negative control LNA inhibitors	Qiagen	339136 YI00199006-DDB
Bradford assay reagent	BioRad	500-0006
BSA (bovine serum albumin)	Sigma Aldrich	A9647
Cell Titre Glo reagent	Promega	G7572
Chloroform	Sigma Aldrich	C2432
DMEM	Thermo Fischer Scientific	11995073
DMSO (dimethyl sulfoxide)	BDG Laboratory Supplies	D2650
Ethanol, molecular grade	Scharlau	ET00110500
FBS (fetal bovine serum)	Sigma Aldrich	14M357
Glycerol	Chem Supply	GA010-2.5L-P
Glycine	Sigma Aldrich	G8898
iScript cDNA synthesis kit	BioRad	170-8891
iQ SYBR Green Supermix	BioRad	170-8885
Lipofectamine RNA iMAX	Thermo Fisher Scientific	13778150
Matrigel	Corning Scientific	BD 354234
Matrigel Growth Factor Reduced	Corning Scientific	BD 356231
Methanol	Chem Supply	MA004-2.5L-P
Nitrocellulose membrane (0.4 µm)	Amersham	GEHE10600016

mirVana® miRNA mimic hsa-miR-194-5p	Ambion	4464066
mirVana® miRNA mimic negative control	Ambion	4464058
Optimem	Thermo Fisher Scientific	31985070
PBS (phosphate buffered saline)	Gibco	14190
Ponceau S	Sigma Aldrich	P3504
Pre-microRNA-194 precursors	GenePharma	B02001
Pre-microRNA precursors negative control	GenePharma	B04002
Propidium Iodide	Sigma Aldrich	P4864
RPMI 1640 liquid media	Sigma Aldrich	R8758
RPMI 1640 phenol red free	Sigma Aldrich	R7509
SDS (sodium dodecyl sulphate)	Sigma Aldrich	75746
Tris	Sigma Aldrich	T1378
Triton-X 100	Sigma Aldrich	T8787
TRI Reagent	Sigma Aldrich	T9424
Trypsin EDTA solution	Sigma Aldrich	T4049
TrypLE Express Enzyme	Gibco	12605010
Tween 20	Sigma Aldrich	P7949

Table 2.2: Western Blot Buffers

Buffer Name	Buffer Components
Loading Buffer (6x) for western blot	0.27M Tris base 10.3% SDS 35% Glycerol 6% β-mercaptoethanol 0.05% bromophenol blue
RIPA (Radioimmunoprecipitation assay) Buffer	10 mM Tris base 150 mM NaCl 1 mM EDTA 1% Triton X-100 Volume to 500 mL with water pH 7.4
Running Buffer (10x)	77.5 g Tris base 360 g Glycine 25 g SDS Volume to 2.5 L with water
TBS (Tris-buffered saline) (10x)	151.5 g Tris base 219 g NaCl Volume to 2.5 L with water pH 7.4
TBST (Tris-buffered saline, 0.1% Tween 20) (1x)	2.5 mL Tween20 250 mL 10x TBS Volume to 2.5 L with water
Transfer Buffer (10x)	77.5 g Tris base 360 g Glycine Volume to 2.5 L with water

Table 2.3: qPCR Primers

Primer Name	Sequence	Annealing Temp
AHR F	AGTTATCCTGGCCTCCGTTT	55˚C
AHR R	TCAGTTCTTTAGGCTCAGCGTC	
ARHGAP1 F	GCGGAAATGGTTGGGGATAG	62˚C
ARHGAP1 R	CCTTAAGAGAAACCGCGCTC	
ARL6IP5 F	GATTTCTTCCCGGGTTCCGA	55˚C
ARL6IP5 R	GATTTCTTCCCGGGTTCCGA	
ATXN1 F	GATCCAAAACAAGCCCCGTG	58˚C
ATXN1 R	GCACGATGCTCTGTAAAGTGT	
BTF34L F	GATAGGGGGCAAGGGTACAG	55˚C
BTF34L R	TTGGCTTCTGCATGACCAGT	
BRN2 F	ACACTGACCGATCTCCACGCAGTA	60˚C
BRN2 R	GAGGGTGTGGGACCCTAAATATGAC	
CHGA F	CTCAAGAACCTCTGAGAGTTCATC	55˚C
CHGA R	CTCAAGAACCTCTGAGAGTTCATC	
CHGB F	CGAGGGGAAGATAGCAGTGAA	60˚C
CHGB R	CAGCATGTGTTTCCGATCTGG	
DUSP6 F	GAGTCTGACCTTGACCGAGACCCCAA	55˚C
DUSP6 R	TTCCTCCAACACGTCCAAGTTGGTGGAGTC	
EGR1 F	CACGAACGCCCTTACGCT	60˚C
EGR1 R	CATCGCTCCTGGCAAACT	
ENO2 F	CTGGCTAAATACAACCAGCTCA	60˚C
ENO2 R	CACAGCACACTGGGATTACG	
ER F	ATCATCAACTGGGCGAAGAG	55˚C
ER R	GATCTCCACCATGCCCTCTG	
ERGIC2 F	AAAGAGTGGCAGAGGATGCTG	55˚C
ERGIC2 R	TGCCTTGCCCACTGTTATGT	
ETV4 F	CCACCAGGATCAAGAAGGAA	60˚C
ETV4 R	CCCTGAGGAGATGTGAAGGA	
EZH2 F	TGCAGTTGCTTCAGTACCCATAAT	55˚C
EZH2 R	ATCCCCGTGTACTTTCCCATCATAAT	
FAM63B F	TCTACACAGGCTCAGCAGGG	62˚C
FAM63B R	AGGAAATCAGGCACAGACGG	
FLRT2 F	ACCCTTGGTTTTGTGACTGC	62˚C
FLRT2 R	AGGACCTTGGCACATGAAAC	
FOXA1 F	GGGGGTTTGTCTGGCATAGC	60˚C
FOXA1 R	GCACTGGGGGAAAGGTTGTG	
GAPDH F	TGCACCACCAACTGCTTAGC	55˚C
GAPDH R	GGCATGGACTGTGGTCATGAG	
IQGAP1 F	GGAGCACAATGATCCAATCC	58˚C
IQGAP1 R	ATGGTTCGA GCATCCATTTC	
NACC2 F	ACGCTGTGAAATTGTACTGTC	55˚C
NACC2 R	CAGCATGGACTTGATCTTGG	
MAPK1 F	GAAGCATTATCTTGACCAGC	55˚C

MAPK1 R	TCCATGGCACCTTATTTTTG	
MET F	TGAAATTCATCCAACCAAATCTT	60˚C
MET R	AATAGAAAACTGACAATGTTGAGAGG	
PAK2 F	TGGTCGGAACGCCATACTG	55˚C
PAK2 R	TTCTGGGGTTCCATTAGTTGC	
QKI F	CCTTGCCTTTTCTCTTGCAG	55˚C
QKI R	TATTGCAGCAGTTGGGTGAG	
REEP5 F	AAGAACTGCATGACTGACCTTC	55˚C
REEP5 R	GAGGCTCCATAACCGAACACC	
REST F	GCCGCACCTCAGCTTATTATG	60˚C
REST R	CCGGCATCAGTTCTGCCAT	
RHEB F	TACCGGTCTGTGGGGAAATC	62˚C
RHEB R	CCCGGCTGTGTCTACAAGTT	
STEAP2 F	TGGAATGAGGAAGAAGTTTGGA	55˚C
STEAP2 R	GCAAGAACAAAGTTTGGTGGTGTA	
SYP F	TTAGTTGGGGACTACTCCTCG	60˚C
SYP R	GGCCCTTTGTTATTCTCTCGGTA	
SSH2 F	GGGGAAATGGCTCATCCACA	55˚C
SSH2 R	TTCCAGTCTTACAGCCAGCC	
TJP1 F	GCCTCAGAAATCCAGCTTCACGAA	55˚C
TJP1 R	GCAGCTAGCCAGTGTACAGTATAC	
TRAF6 F	GCGCACTAGAACGAGCAAG	55˚C
TRAF6 R	TTTCCAGGGGTGGGTCAAAC	
ZBTB10 F	GCTGGATAGTAGTTATGTTGC	60˚C
ZBTB10 R	CTGAGTGGTTTGATGGACAGAG	

Table 2.4: Published prostate cancer datasets

Identifier	Description	Microarray/Sequencing/CNV	Number of samples	Reference
GSE77930	Metastatic prostate tumours	Microarray/CNV	171	(Kumar et al. 2016)
SU2C	Metastatic prostate tumours	RNA-seq/CNV	444	(Robinson et al. 2015)
TCGA PRAD	Primary prostate tumours	RNA-seq (mRNA &miRNA)/CNV	414	(Cancer Genome Atlas Research 2015)
MSKCC	Normal prostate tissue, Primary and metastatic prostate tumours	Microarray (mRNA&miRNA)/CNV	210	(Taylor et al. 2010)
Beltran et al 2016	Metastatic prostate tumours	RNA-seq/CNV	50	(Beltran et al. 2016)
Grasso et al 2012	Normal prostate tissue, Primary and metastatic prostate tumours	Microarray/CNV	89	(Grasso et al. 2012)
Bluemn et al 2018	Metastatic prostate tumours	RNA-seq	87	(Bluemn et al. 2017)
Armenia et al 2018	Primary and metastatic prostate tumours	CNV	1013	(Armenia et al. 2018)

2.2 Methods

2.2.1 Cell culture

2.2.1.1 Reviving, maintaining, passaging and freezing of cell lines

The human prostate carcinoma cell lines 22Rv1, LNCaP, and PC-3, were obtained from the American Type Culture Collection (ATCC). The LNCaP-V16D, LNCaP-MR42D and LNCaP-MR49F cell lines were obtained from the Zoubeidi lab at the Vancouver Prostate Centre. 22Rv1, LNCaP-V16D LNCaP cell lines were maintained in RPMI-1640 containing 10% Fetal Bovine Serum (FBS). PC3 cell line was maintained in RPMI-1640 containing 5% FBS. LNCaP-MR42D and LNCaP-MR49F were maintained in RPMI-1640 containing 10% Fetal Bovine Serum (FBS) and 10μM Enzalutamide.

All cell lines cultures regularly underwent mycoplasma testing. All cell lines underwent verification by short tandem repeat profiling by CellBank Australia.

For revival of cell lines, vials from liquid nitrogen were rapidly thawed in a 37°C water bath and gently mixed with 9ml of appropriate cell culture media. Cells were centrifuged at 1500rpm for 5 minutes, pellets were resuspended in 8ml of media and transferred to a T25 culture flask. Flasks were incubated at 37°C and 5%CO_2 and passaged when 80% confluency was reached.

For passaging, media was removed from cell culture flask followed by a PBS wash. Harvest of cells for passaging was performed using 0.25% trypsin and incubating at 37˚C and 5%CO_2 for 2 minutes or until cells detached from flask. Trypsin was neutralized with media containing FBS and collected in a 50ml tube. Cells were pelleted by centrifuging at 1500rpm for 5 minutes and reseeded at appropriate density in a new flask.

For freezing cells, T75 or T150 flasks at 80% confluency were trypsinized and counted. Cells were pelleted by centrifuging at 1500rpm for 5 minutes and resuspended in freezing media (10% DMSO, 40% FBS, 50% culture media) at a concentration of 1-2 million cells/ml. 1ml of suspension was added to each labelled cryo-vial, and placed in an isopropanol filled freezing container at -80°C. Cells were transferred to liquid nitrogen once frozen.

2.2.1.2 MicroRNA (miR) mimic or inhibitor transfection

Prostate cancer cells were transfected in solution with 20nM of pre-miR microRNA precursors or microRNA locked nucleic acid (LNA) inhibitors (6.25nM, 12.5nM or 50nM depending on experiment) or negative controls using the RNAiMax transfection agent. Briefly, an RNAiMax -Opti-MEM mix was made and incubated for 10 min at RT. The miRNA precursors/inhibitors were diluted in Opti-MEM. RNAiMax-Opti-MEM mix was added to precursors/inhinitors and incubated for an additional 10 min at RT to form complexes. The transfection complexes were added drop-wise to the cell cultures at the time of seeding. The cells were incubated for 48h, 72h, 96h or longer depending on the assay being performed.

2.2.2 Cell viability assay

Growth assays were performed over a period of 7 days. Cells were transfected with miR-194 LNA or negative controls and a known number of cells was seeded at into the wells of a 12 well plate. Cell numbers were counted at 2, 4 and 7 days to assess proliferation. Number of live cells was assessed using trypan blue exclusion assay. Briefly, 20µl of 0.4% trypan blue solution was added to 20µl of cell suspension, mixed and loaded onto a haemocytometer. Cells were examined under a microscope. If cells take up trypan blue, they are considered non-viable. The number of unstained and stained cells were counted and total number of live cells was assessed as follows:

Total cells/ml = Average number of cells in corner squares×dilution factor×10000 cells/ml

2.2.3 Inverse invasion assay

100µl of Matrigel diluted in a 1:1 ratio with ice-cold PBS was pipetted into 8µm pore, 6.5mm diameter uncoated transwells. Matrigel was allowed to solidify by incubating for 30 min at 37°C. Transwells were then inverted and 100µl of cell suspension with $5x10^5$ cells per mL was pipetted onto the underside of each transwell. Transwells were covered with the base of their 24 well culture plate and incubated inverted for 4 h to allow cells to adhere to the transwell membrane. Transwells were then returned to their original orientation and washed twice with 1mL serum free medium. Transwells were left to incubate in 1mL serum free media containing indicated treatments. 100µl appropriate

media containing 10% FBS was added to each transwell on top of the matrigel layer. Plates were incubated for 5 days at 37°C and 5% CO_2. Cells were stained in culture wells filled with 1 mL PBS containing 10 μg per mL propidium iodide for 30 min at RT in the dark followed by PBS washes. Images were collected by confocal microscopy using the Leica SP5 microscope microscope. Transwells were placed onto a large coverslip covered in a small amount of PBS ensuring no bubbles were present for imaging with non-immersion 20x objective. 10 Z-stack sections of Matrigel were captured at set intervals beginning at the transwell membrane (0 μm). Florescence intensity of PI staining at individual z-stack sections was quantified by Image J software. Average measure of all slices was calculated and indicates proportion of cells that invaded.

2.2.4 Organoid culture

2.2.4.1 Reviving, maintaining, passaging and freezing of organoids

The organoid cell lines 201.1 Dura and 201.2 Lung representing prostate adenocarcinoma and neuroendocrine prostate cancer respectively, were obtained from the Melbourne Urology Research Alliance (MURAL) and are described in (Lawrence et al. 2018). Organoid cell lines were generated from patient derived xenografts (PDX) of CRPC metastases from rapid autopsy specimens. The 201. Dura and 201.2 Lung lines were derived from metastases in the dura and lung, respectively (Lawrence et al. 2018).

201.1 Dura and 201.2 Lung cells were seeded in growth factor reduced, phenol red-free, LDEV-free Matrigel (Corning). 201.1 organoids were cultured in advanced DMEM/F-12 media (Gibco) containing 0.1ml Primocin (Invivogen), 2 mM Glutamax (Sigma), 10mM HEPES (Sigma), 1nM DHT (Sigma), 1.25mM N-acetylcysteine (Sigma), 5nM NRG1 Heregulinβ-1 (Peprotech), 500 nM A83-01, 10 mM nicotinamide (Sigma), 10μM SB202190 (Sigma), 2% B27 (Thermo), 10ng/ml FGF10 (Peprotech), 5ng/ml FGF2 (Peprotech), 1μM prostaglandin E2 (Tocris), 10% noggin conditioned media and 10% R-spondin conditioned media. 10μM Y-27632 dihydrochloride (Selleck Chemicals) was added to culture medium during organoid establishment and following passage.

201.2 Lung organoids were grown were cultured in PrENR -p38i -NAC media (Beshiri et al. 2018), which is similar to the media described above with the following modifications: 5ng/ml EGF was added to the medium but NRG1 Heregulinβ-1, SB202190 and N-acetylcysteine were not added to this medium.

For revival, frozen vials were thawed in a 37°C water bath. Cell suspension was centrifuged at 1200rpm for 4 minutes, pellet was washed with organoid culture media. Pellets were resuspended in growth factor reduced Matrigel (Corning) at a concentration of 100,000-50,000 cells per 30µl of Matrigel in 24 well plates. Plates were inverted at 37°C for 15 minutes to allow Matrigel to solidify, then overlaid with 500mL of human organoid culture medium containing 10µM Y27632. Media was replaced every 3-4 days.

At the time of passage, organoids were washed in PBS, 250µl of TrypLE (GIBCO) was added and Matrigel broken up by pipetting. Plates were incubated at 37°C for 5 minutes. Once the Matrigel was digested, the cells were transferred to 1.5ml Eppendorf tubes and centrifuged to form a pellet, washed and reseeded in Matrigel.

For freezing organoids, cells were digested out of Matrigel as described above and pelleted. Pellets were resuspended in freezing media (90% human organoid culture medium containing 10µM Y27632, 10% DMSO). 1ml of suspension was added to each labelled cryo-vial, and placed in an isopropanol filled freezing container at -80°C. Cells were transferred to liquid nitrogen once frozen.

2.2.2.2 Organoid transduction

Organoid cells were digested out of 3 Matrigel discs and centrifuged as described above. Cell pellets were washed and resuspended in 350ul of organoid culture media containing 10µM Y27632 in one well of a 24 well plate. 100ul of pJS309 lentivirus was added and cells were incubated at 37°C , 5%CO_2 overnight in suspension. The following day, cells were collected and spun down. The cell pellet was washed, resuspended in 90ul Matrigel and seeded out in 30ul matrigel discs. Plates were inverted at 37°C for 15 minutes to allow Matrigel to solidify, then overlaid with 500mL of human organoid culture medium. Cells were observed at 24h-48h post transduction for expression of Tomato. At 48h, 2ug/ml puromycin was added to the media to select for transduced cells.

2.2.2.3 Organoid transfection

Organoid transfections were carried out essentially as described (Broutier et al. 2016). Organoid cells were digested out of Matrigel discs as described above, counted and resuspended in at appropriate concentration in 450µl of organoid culture media. The transfection mix was prepared by adding 25µl of Opti-MEM per tube to two 1.5ml microcentrifuge tubes for each transfection condition. 0.5µl of LNA at 50mM (for a final

concentration of 50nM) was added to one of the tubes and 1.5µl of RNAiMAX reagent to the other tube and incubated at room temperature (RT) for 5min. The contents of the two tubes were mixed together and incubated at RT for a further 5-15min. 50µl of the LNA:RNAiMAX mixture was added to 450µl of single cell suspension and centrifuged in a pre-warmed centrifuge at 32°C, 600g for 1h. Cells were then incubated in a tissue culture incubator at 37°C for 4h. Cells were collected in a 1.5ml centrifuge tube and centrifuged at 1200rpm for 5min at RT. Pellet was resuspended in 90ul Matrigel and seeded out in 30ul Matrigel discs. Plates were inverted at 37°C for 15 minutes to allow Matrigel to solidify, then overlaid with 500mL of human organoid culture medium.

Organoid forming efficiency was assessed as described previously (Lawrence et al. 2018). At seven days post transfection, ≥5 sets of images were taken per treatment. Images were taken at different depths in order to get all the organoids for each field of view. Number of organoids per μm^2 was determined by manually counting number of organoids from each field of view and dividing by area. Images of the Matrigel disc were taken at 2x magnification with scale bar and diameter was estimated using measure function in ImageJ. Average number of organoids per μm^2 was multiplied by area of disc to estimate average number of organoids per disc. Organoid forming efficiency was calculated as average number of organoids divided by number of cells originally seeded.

2.2.2.4 Organoid viability using Cell Titer-Glo

Oganoid cells were transfected as described above. Briefly, organoid were collected and 50,000 cells were resuspended in 450µl of organoid culture media and 50µl of transfection mix containing RNAiMAX with 25, 100, and 250nM miR-194 or NC LNA inhibitor. Cells were centrifuged in a pre-warmed centrifuge at 32°C, 600g for 1h. After centrifuging, cells were incubated in a tissue culture incubator at 37°C for 2-4h and then collected in 1.5ml centrifuge tubes by centrifugation at 300 g for 5 min at room temperature. Cell pellets were resuspended in 5 µl Matrigel and seeded out in 10µl matrigel discs in 96-well plates. Plates were inverted and incubated at 37°C for 15 minutes to allow Matrigel to solidify, then overlaid with 100mL of organoid culture medium.

Organoid viability was assessed at 7 days post-transfection using the Cell Titer-Glo® Luminescent Cell Viability Assay kit (Promega). Media was removed from wells and 70µl fresh media was added to each well. 80µl of Cell Titer-Glo reagent was added to

each well and contents of the well were mixed by pipetting up and down several times. Plate was wrapped in foil and contents were then mixed on an orbital shaker for 5 minutes. The plate was incubated at room temperature for 25 minutes. Luminescence was measured using a BMG Lumistar Optima luminometer.

2.2.5 Western blotting

2.2.5.1 Preparation of cell lysates

Cells were generally grown in 6 well plates for protein extraction. Cells were washed with PBS, 100µl of RIPA buffer was added to each well followed by incubation on ice for 10 minutes. Cells were scraped from wells and collected in 1.5ml Eppendorf tubes. Lysates were centrifuged for 10 min at 10000g at 4°C and supernatant containing protein was collected. Protein concentration was assessed using Bradford assay. Lysates were stored at -80°C.

2.2.5.2 Bradford assay

Total protein concentration of cell lysates was determined using the Bradford assay. The assay was performed in 96 well flat bottomed culture plates. 1 µl of BSA standards from 0-6mg/ml and samples were pipetted in duplicates into the plate. 20% Bradford reagent was added to each well to a total of 200µl. The plate was mixed and incubated at RT for 5min before being read at 595 nm on a PolarStar microplate reader. The protein concentration of a test sample was calculated using a standard curve.

2.2.5.3 Sodium Dodecyl Sulfate Polyacrylamide Gel Electrophoresis (SDS-PAGE)

Protein lysates containing 25ug of total protein were mixed with 6x loading dye and heated at 95°C for 5 minutes. Lysates were loaded on precast SDS-PAGE gels (Criterion or TGX) and run with appropriate running buffer at 100V for 1.5 hours using a Biorad Criterion electrophoresis cell or Biorad Mini-protean tetra cell. 8µl of Precision Plus Protein Dual Color Standards was used as size marker.

2.2.5.4 Western Transfer and Immunoblot

Proteins were transferred from SDS-PAGE gel to a nitrocellulose membrane with transfer buffer using a BioRad Criterion Blotter at 400 mA for 60 minutes. Ponceau staining was used to confirm transfer of proteins to the membrane. Membranes were de-stained by washing with 1x TBST for 10 minutes. Nitrocellulose membranes were then blocked for

60 minutes on a rocking tray using 3% skim milk powder dissolved in 1x TBST. Membranes were probed using primary and HRP-conjugated secondary antibodies. HRP-conjugates were detected using ECL solution and imaged on a BioRad Chemidoc MP imaging system and processed using Image Lab Software. Protein expression was determined by densitometry using Image Lab Software.

2.2.6 RNA extraction

2.2.6.1 RNA extraction from tissues

RNA samples in *RNA later* were thawed on ice. Samples were placed in a Precellys tube (Sapphire BioScience) on ice with 500µl Qiazol and homogenized in a Precellys24 homogenizer: 2x 6500 – 2x30 – 30sec break i.e. samples were homogennized twice at 6500rpm for two cycles at 30 seconds per cycle with a 30 second break between cycles. Homogenates were transferred to a 1.5ml tube and 200µl Qiazol was added for a total volume 700µl. Samples were incubated at RT for 5 minutes. 140 µl chloroform was added, shaken vigorously for 15s and incubated at RT for 3 minutes. Samples were centrifuged at 12000g at 4°C for 15 min and upper aqueous layer was transferred to a new tube, making sure not to disturb the interphase layer. 1.5 volume 100% ethanol was added and mixed thoroughly by pipetting. 700µl sample, including precipitate, was pipetted into an RNeasy® Mini column in a 2 ml collection tube. Lid was closed and centrifuged at ≥8000g for 15s at RT. Flow-through was discarded. Remainder of sample was pipetted into column and spun.700 µl Buffer RWT was added to the RNeasy Mini column and centrifuged for 15s at ≥8000g. Flow-through was discarded. Pipet 500 µl Buffer RPE was pipetted onto the RNeasy Mini column and centrifuged for 15s at ≥8000g. Flow-through was discarded. 500 µl Buffer RPE was added to the RNeasy Mini column and centrifuged for 2 min at ≥8000 x g. Column was centrifuged at full speed for 1 min to further dry the membrane. RNeasy Mini column was transferred to a new 1.5 ml collection tube. 30 µl RNase free water was added directly onto the RNeasy Mini column membrane. Columns were centrifuge for 1 min at ≥8000 x g to elute. This step was repeated to maximise amount of RNA eluted. RNA concentration and purity was determined by spectrophotometry using a Thermo Scientific NanoDrop 2000.

2.2.6.2 RNA extraction from cells grown in 2D culture

Cells in 6 well plates were washed with 1x PBS and harvested using 1 mL Trizol per well. Trizol samples were incubated at 37°C for 15 minutes then mixed with 200µl of chloroform and shaken vigorously for 15s followed by incubation for 3 mins at RT. Samples were centrifuged at 12000rpm at 4°C for 15 min and upper aqueous layer was transferred to a new tube, making sure not to disturb the interphase layer. The aqueous layer was mixed with 2.5 volume 100% ethanol, 10mM $MgCl_2$, 0.1 volume 5M NaCl and 2µl Glyco-blue, mixed and for 2h to overnight at -20˚C. RNA was pelleted by centrifugation at 12000rpm at 4°C for 30 min, washed in 80% EtOH and resuspended in nuclease free water. RNA concentration and purity were determined by spectrophotometry using a Thermo Scientific NanoDrop 2000.

2.2.7 qPCR

2.2.7.1 DNase Treatment

RNA samples were DNase treated using TURBO DNA-free™ DNase Treatment kits (Ambion cat#AM1907). 2µg RNA was diluted in RNase free water to a total volume of 44µl, gently mixed with 5µl of 10xTurbo DNAse Buffer and 1µl TURBO DNase*free.* Samples were incubated at 37°C for 30 min. 5µl of DNase inactivation reagent was added to each sample, mixed and incubated for 5 min at RT. Samples were centrifuged at 10000g for 1.5 min and supernatant was collected. 50µl 75% isopropanol and 2µl Glycoblue was added to each sample. Samples were incubated overnight at -80˚C. RNA was pelleted by centrifugation at 12000rpm at 4°C for 30 min, washed in 80% EtOH and resuspended in nuclease free water. The resulting RNA concentration and purity were determined by spectrophotometry using a Thermo Scientific NanoDrop 2000.

2.2.7.2 Reverse Transcription

After DNAse treatment, cDNA was made from RNA samples using the iScript™ Reverse Transcription kit or TaqMan® MicroRNA Reverse Transcription Kit. For the iScript reaction, 500ng RNA was diluted with nuclease free water to a volume of 15µl. 5µl iScript reaction mix and 1µl of reverse transcriptase enzyme was added to each sample. A control containing all components except reverse transcriptase was also made to confirm complete DNAse treatment. iScript reactions were run in an iCycler thermocycler using

the following conditions: 25˚C for 5 min, 42°C for 30 min, 85°C for 5 min and 4°C hold. Resultant cDNA samples were diluted 1:4 and stored at -20°C until further use. For Taqman reactions, 100ng RNA was combined with 0.15µl dNTPs, 1µl MultiScribe Reverse Transcriptase, 1.5µl Reverse Transcriptase buffer , 0.19µl RNase inhibitor, 0.75µl each of miRNA primers and NFW for a total volume of 15µl. Taqman reactions were run in the iCycler thermocycler using the following conditions: 16°C for 30 min, 42°C for 30 min, 85°C for 5 min and 4°C hold. Resultant cDNA samples were diluted 1:4and stored at -20°C until further use.

2.2.7.3 Quantitative Reverse Transcriptase Polymerase Chain Reaction (qRT-PCR)

RNA expression was examined via qRT-PCR using a BioRad C1000 Thermal Cycler and CFX384TM Real-Time System. RNA expression of target genes was expressed relative to GAPDH as the reference gene. For SYBR Green based PCRs, reactions contained 0.5µl primer mix (Forward+reverse primer at 10pmol each) (Table 2.3), 5µl iQ SYBR Green Supermix, 2.5µl RNase free water, and 2µl cDNA. Three technical replicates were performed for all samples. qRT-PCR reaction conditions were as follows: 3 min at 95°C, 40 cycles of 15 sec at 95°C, 15 sec at 55°C-62˚C (Annealing temperature-May change dependent on primer set used), 30 sec at 72°C and 1 cycle of 95°for 1 minute, 1 min at 55°C and 10 sec at 60°C. Melt curve was determined by a temperature increase from 60˚C to 95˚C in 0.5˚C increments. Data was analysed using CFX Manager Software Version 3.0 (Bio-Rad Laboratories, Inc.).

For Taqman based PCRs, reactions contained 0.5µl primer (20x), 5µl TaqMan Universal Master Mix II, no UNG, 2.5µl RNase free water, and 2µl cDNA. Three technical replicates were performed for all samples. qRT-PCR reaction conditions were as follows: 2 min at 50°C, 10 minutes at 95°C, 15 sec at 95˚C and 1 min at 60°C . Data was analysed using CFX Manager Software Version 3.0 (Bio-Rad Laboratories, Inc.).

2.2.8 Computational analyses

2.2.8.1 Gene set enrichment Analysis (GSEA)

GSEA was performed using GSEA preranked module on GenePattern (https://cloud.genepattern.org/gp/pages/index.jsf). Ranked lists were generated from RNA-Seq counts using the signal-to noise metric. Genesets were obtained from MSigDB or from specific published studies.

2.2.8.2 Single Sample Gene Set Enrichment Analysis (ssGSEA)

ssGSEA was performed using ssGSEA Projection module on GenePattern (https://cloud.genepattern.org/gp/pages/index.jsf). GCT files were generated from relevant microarray or RNA-seq data. Genesets were obtained from MSigDB or generated specific published studies. Rank normalization was used to normalize gene expression data.

2.2.8.3 Bioinformatic Analysis for HITS-CLIP and RNA-seq

Detailed methods are described in Chapter 3

2.2.9 Statistical analyses

Results were analysed using GraphPad Prism 7.02 or appropriate functions in R. Detailed methods for statistical analysis are included in figure legends or in the individual Chapter methods.

Chapter 3: MicroRNA-194 promotes lineage plasticity in advanced prostate cancer

The following chapter includes a manuscript submitted for publication to Nature Communications, followed by supplementary figures. Supplementary tables are available on Figshare https://adelaide.figshare.com/s/98cb3b341a7f554bae0d. This chapter makes up a significant proportion of the work completed as a part of this PhD. A general discussion of this chapter had been included in Chapter 6.

Statement of Authorship

Title of Paper	MicroRNA-194 promotes lineage plasticity in advanced prostate cancer
Publication Status	☐ Published ☐ Accepted for Publication ☑ Submitted for Publication ☐ Unpublished and Unsubmitted w ork w ritten in manuscript style
Publication Details	Submitted to Nature Communications

Principal Author

Name of Principal Author (Candidate)	Rayzel C Fernandes
Contribution to the Paper	Performed experiments (Cell and organoid culture, transfections, western blots, qPCR), data mining, analyzed and interpreted data, designed experiments, assisted with manuscript preparation
Overall percentage (%)	65%
Certification:	This paper reports on original research I conducted during the period of my Higher Degree by Research candidature and is not subject to any obligations or contractual agreements with a third party that would constrain its inclusion in this thesis. I am the primary author of this paper.
Signature	Date 20.09.2019

Co-Author Contributions

By signing the Statement of Authorship, each author certifies that:

i. the candidate's stated contribution to the publication is accurate (as detailed above);

ii. permission is granted for the candidate in include the publication in the thesis; and

iii. the sum of all co-author contributions is equal to 100% less the candidate's stated contribution.

Name of Co-Author	John Toubia
Contribution to the Paper	Processed and analysed HITS-CLIP and RNA-seq data
Signature	Date 30/08/2019

Name of Co-Author	Scott Townley
Contribution to the Paper	Carried out experiments (Cell line treatments, qRT-PCT)
Signature	Date 30/8/2019

Name of Co-Author	Adrienne R. Hanson		
Contribution to the Paper	Assisted with cell line experiments		
Signature		Date	3-9-19

Name of Co-Author	B. Kate Dredge		
Contribution to the Paper	Performed HITS-CLIP experiment		
Signature		Date	06/09/2019

Name of Co-Author	Katherine A. Pillman		
Contribution to the Paper	EISA analysis of RNA-Seq data		
Signature		Date	9/9/19

Name of Co-Author	Andrew G. Bert		
Contribution to the Paper	Performed HITS-CLIP experiment		
Signature		Date	30/8/19

Name of Co-Author	Richard Iggo		
Contribution to the Paper	Assisted with organoid culture		
Signature		Date	30.8.2019

Name of Co-Author	Rajdeep Das		
Contribution to the Paper	Generated preliminary data, edited/evaluated manuscript		
Signature		Date	8/30/2019

Name of Co-Author	Daisuke Obinata		
Contribution to the Paper	Immunohistochemistry of organoids		
Signature		Date	11/09/2019

Name of Co-Author	Shahneen Sandhu		
Contribution to the Paper	Recruited patients for for generation PDX/organoid models		
Signature		Date	17/9/2019

Name of Co-Author	MURAL Investigators		
Contribution to the Paper	Established and maintained PDX models		
Signature		Date	**25/09/2019**

Name of Co-Author	Gail P. Risbridger		
Contribution to the Paper	Provided Organoid, PDX and serum samples, evaluated/edited manuscript		
Signature		Date	4/9/2019

Name of Co-Author	Mitchell G. Lawrence		
Contribution to the Paper	Provided organoid, PDX and serum samples and technical assistance, edited/evaluated manuscript		
Signature		Date	4/9/2019

Name of Co-Author	Renea A. Taylor		
Contribution to the Paper	Provided organoid,PDX and serum samples, edited/evaluated manuscript		
Signature		Date	02/09/19

Name of Co-Author	Lisa M. Butler		
Contribution to the Paper	Analyzed data, evaluated/edited manuscript		
Signature		Date	August 30, 2019

Name of Co-Author	Amina Zoubeidi		
Contribution to the Paper	Analyzed data, evaluated/edited manuscript		
Signature		Date	30/08/2019

Name of Co-Author	Philip A. Gregory		
Contribution to the Paper	Designed experiments, assisted in data analysis and interpretation, evaluated/edited manuscript		
Signature		Date	30/8/2019

Name of Co-Author	Wayne D. Tilley		
Contribution to the Paper	Project supervision,assisted in data analysis and interpretation, evaluated/edited manuscript		
Signature		Date	02/09/2019

Name of Co-Author	Theresa E. Hickey		
Contribution to the Paper	Project supervision, assisted in data analysis and interpretation, evaluated/edited manuscript		
Signature		Date	02/09/2019

Name of Co-Author	Gregory J. Goodall		
Contribution to the Paper	Designed experiments, assisted in data analysis and interpretation, evaluated/edited manuscript		
Signature		Date	30 August 2019

Name of Co-Author	Luke A. Selth		
Contribution to the Paper	Project supervision, conceived project, designed experiments, analysed data, made figures and wrote the manuscript		
Signature		Date	20/9/19

MicroRNA-194 promotes lineage plasticity in advanced prostate cancer

Rayzel C. Fernandes[1,2], John Toubia[3], Scott Townley[1,2], Adrienne R. Hanson[1,2], B. Kate Dredge[4], Katherine A Pillman[4], Andrew G. Bert[4], Richard Iggo[1,5], Rajdeep Das[6], Daisuke Obinata[7,8], MURAL investigators[8,9], Shahneen Sandhu[9,10], Gail P. Risbridger[8,9,10], Renea A. Taylor[9,11], Mitchell G. Lawrence[8,9], Lisa M. Butler[2,12], Amina Zoubeidi[13], Philip A. Gregory[3,14], Wayne D. Tilley[1,2], Theresa E. Hickey[1], Gregory J. Goodall[3,15] and Luke A. Selth[1,2*]

[1]Dame Roma Mitchell Cancer Research Laboratories, Adelaide Medical School, The University of Adelaide, Adelaide, South Australia, Australia.

[2]Freemasons Foundation Centre for Men's Health, Adelaide Medical School, The University of Adelaide, Adelaide, South Australia, Australia.

[3]ACRF Cancer Genomics Facility, Centre for Cancer Biology, An alliance of SA Pathology and University of South Australia, Frome Road, Adelaide, South Australia, Australia.

[4]Centre for Cancer Biology, An alliance of SA Pathology and University of South Australia, Adelaide, South Australia, Australia.

[5]Institut Bergonié Unicancer, INSERM U1218, Bordeaux, France.

[6]Department of Radiation Oncology, University of California San Francisco, San Francisco, California.

[7]Department of Urology, Nihon University School of Medicine, Tokyo, Japan.

[8]Department of Anatomy and Developmental Biology, Monash Partners Comprehensive Cancer Consortium, Monash Biomedicine Discovery Institute, Prostate Cancer Research Group, Monash University, Clayton, Victoria, Australia.

[9]Cancer Research Program, Cancer Research Division, Peter MacCallum Cancer Centre, University of Melbourne, Melbourne, Victoria, Australia.

[10]Sir Peter MacCallum Department of Oncology, The University of Melbourne, Parkville, Victoria, Australia.

[11]Department of Physiology, Monash Partners Comprehensive Cancer Consortium, Monash Biomedicine Discovery Institute, Prostate Cancer Research Group, Monash University, Clayton, Victoria, Australia.

[12]South Australian Health and Medical Research Institute, Adelaide, South Australia, Australia.
[13]The Vancouver Prostate Centre, University of British Columbia, Vancouver, British Columbia, Canada.
[14]Faculty of Health and Medical Sciences, The University of Adelaide, Adelaide, South Australia, Australia.
[15]School of Biological Sciences, The University of Adelaide, Adelaide, South Australia, Australia.

* To whom correspondence should be addressed. Tel: +618 83137860. Email: luke.selth@adelaide.edu.au

ABSTRACT

MicroRNA-194 (miR-194) promotes prostate cancer metastasis, but the precise molecular mechanisms by which it achieves this are unknown. Here, by integrating cutting-edge molecular (Ago-HITS-CLIP and RNA sequencing) and bioinformatic (exon-intron split analysis) techniques, we defined a 163-gene miR-194 "targetome" in prostate cancer. MiR-194 target genes were predominantly down-regulated through canonical 3'UTR recognition sites and were enriched within pathways involved in cytoskeletal organisation and cell movement. In clinical prostate cancer samples, miR-194 activity was inversely correlated with the androgen receptor (AR) signalling axis. At a mechanistic level, this inverse correlation was explained by down-regulation of miR-194 expression by AR. Accordingly, miR-194 expression and activity was significantly elevated in neuroendocrine prostate cancer (NEPC), an aggressive AR-independent disease subtype. MiR-194 enhanced the transdifferentiation of prostate adenocarcinoma cells to a neuroendocrine-like state, at least in part by targeting FOXA1, a transcription factor with a key role in maintaining the prostate epithelial lineage. Importantly, a miR-194 inhibitor effectively inhibited the growth of cell lines and patient-derived organoids with neuroendocrine features. Overall, our study reveals a novel post-transcriptional mechanism regulating the plasticity of prostate cancer cells and provides a rationale for targeting miR-194 in NEPC.

INTRODUCTION

Cellular plasticity, also referred to as lineage plasticity or lineage switching, is a process whereby cells exhibit reversible changes in properties and phenotypes. Cancer cells exploit this phenomenon in response to a targeted therapy, acquiring the phenotypic characteristics of another lineage that does not depend on the drug target for survival[1]. This phenomenon allows cancer cells to adapt to new or stressful conditions and is increasingly recognised as a key feature of cancer progression[2].

As first-line treatment for metastatic prostate cancer (PCa), androgen deprivation therapy targets the exquisite dependence of tumours on the androgen receptor (AR) for their growth. While initially effective, patients inevitably develop resistance and progress to castration-resistant prostate cancer (CRPC). Most CRPC tumours exhibit adaptive changes that maintain AR activity despite the low androgen environment, an understanding that led to the development of highly potent second-generation AR-targeted therapies (e.g. Enzalutamide and Abiraterone). However, response to these newer agents is also limited in most cases[3]. It has become increasingly clear that prolonged targeting of the AR, particularly with the more potent second-generation therapies, can drive cellular plasticity in CRPC. This plasticity is characterised by cells losing dependence on AR and gaining new phenotypes (i.e. aggressive variant PCa), with the most well recognised of these being a neuroendocrine (NE)-like state that is characterised by the expression of neuroendocrine, neuronal, developmental and stem cell markers[1]. Neuroendocrine prostate cancer (NEPC) is evident in ~15-25% of CRPC tumours[4, 5] and exhibits aggressive clinical features; indeed, patients with NEPC have a median overall survival time of <1 year[4]. A deeper understanding of how AR-targeted therapies promote lineage plasticity and the emergence of aggressive disease phenotypes such as NEPC is essential to improve patient outcomes.

Genomic comparisons of NEPC and CRPC adenocarcinoma (CRPC-Adeno) have revealed surprisingly few genetic differences between these disease subtypes; reproducible alterations in NEPC include higher incidences of *RB1* and *TP53* loss and more frequent amplification of *MYCN* and *AURKA*[6, 7]. The similarities in mutational landscapes between NEPC and CRPC-Adeno suggest that the plasticity underlying transdifferentiation from adenocarcinoma to an NE-like state is predominantly mediated by changes in epigenetics, transcriptional programs and protein function in the tumour cells, as opposed to selection and outgrowth of rare genetic variants[1].

In this study, we identified miR-194 as a novel post-transcriptional regulator of transdifferentiation in PCa. By targeting genes that suppress plasticity, such as *FOXA1*, miR-194 drives the emergence and growth of NEPC, a finding that justifies further investigation of miRNA-based therapies for this aggressive CRPC subtype.

RESULTS

Global identification of transcripts targeted by miR-194 in prostate cancer

Our earlier work demonstrated that miR-194 can promote epithelial-mesenchymal transition (EMT) and metastasis, at least in part by targeting the tumour suppressor SOCS2[8]. However, miRNAs target tens to hundreds of genes, so we hypothesised that elucidating additional miR-194 targets would shed further light on its oncogenic functions in PCa. Thus, we performed Ago-HITS-CLIP on control- and miR-194-transfected 22Rv1 prostate cancer cells to decode miRNA-mRNA interactions. The 22Rv1 model was chosen for this experiment since it exhibits increased metastatic capacity upon transient delivery of miR-194[8]. After immunoprecipitation of Argonaute, co-immunoprecipitating RNA was isolated and evaluated by high-throughput sequencing. Argonaute binding sites (i.e. peaks) that were enriched in cells transfected with miR-194 compared to control transfected cells were identified using MACS2[9], yielding 7,772 peaks associated with 3,326 genes (Supplementary Table S2). An example peak at the *ZBTB10* gene is shown in Fig. 1a. Highlighting the robustness of the data, the vast majority (94%) of peaks were within genes, most commonly in exons, 3'UTRs and introns (Fig. 1b). Furthermore, unbiased *de novo* motif analysis revealed that the most strongly enriched sequence within the peaks was a seed recognition site for miR-194 (Supplementary Table S3), which was concentrated within the centres of peaks (Fig. 1c).

MiRNAs typically reduce the levels of their target mRNAs[10]. Therefore, we conducted RNA-seq of cells transfected with miR-194 mimic or a control. MiR-194 elicited significant changes to the transcriptome, causing down-regulation of 2,626 and up-regulation of 2,485 transcripts (Fig. 1d). We identified a strong bias toward down-regulation of mRNAs with miR-194 Ago-HITS-CLIP peaks in 3'UTRs, whereas mRNAs with peaks in coding regions were less strongly biased toward down-regulation and those with peaks in introns were collectively unchanged (Fig. 1e; Supplementary Fig. S1a). This is consistent with previous studies demonstrating that 3'UTRs are the key sequences through which miRNAs exert their activity[10]. Similarly, transcripts with 3'UTR peaks

containing miR-194 seed recognition sequences tended to be more robustly down-regulated than those lacking such sequences (Fig. 1f; Supplementary Fig. S1b).

miR-194 expression and activity is negatively correlated with AR signalling

Gene ontology analysis of the miR-194 targetome revealed enrichment for genes associated with cytoskeletal remodelling, cell adhesion and cell motility (Supplementary Table S4), which likely relates to the ability of miR-194 to enhance prostate cancer cell migration and invasion and elicit an EMT[8]. To more specifically evaluate the targetome in clinical prostate cancer, we used single sample gene set enrichment analysis (ssGSEA) of our high-confidence targetome to generate miR-194 activity scores in clinical cohorts, which were then compared to equivalent scores generated from the same cohorts for the "Hallmark" biological gene sets[13]. Amongst other robust associations, one striking finding was that miR-194 activity was strongly inversely correlated with AR signalling across all cohorts examined (Fig. 2a; Supplementary Table S5). This observation was validated using a more refined set of AR target genes (Fig. 2b) recently generated by Sowalsky and colleagues[14].

The strength of this negative association led us to examine whether the miR-194 targetome was enriched for AR target genes, but there was only a limited overlap between these gene sets (Fig. 2c). Moreover, our Ago-HITS-CLIP and transcriptomic data indicated that miR-194 does not target the *AR* transcript (Supplementary Fig. S2). An alternative (and/or additional) explanation for this inverse relationship could be that AR regulates the expression of miR-194. Indeed, levels of miR-194 in the androgen-sensitive LNCaP model were decreased by the potent androgen DHT but increased by the AR antagonist Enzalutamide (Fig. 2d). In accordance with these findings, extended culture of cells in androgen-depleted conditions led to upregulation of miR-194 (Fig. 2e). Collectively, these data reveal that AR represses expression of miR-194, which (at least partly) explains the negative association between these factors in clinical prostate cancer.

Fig 1

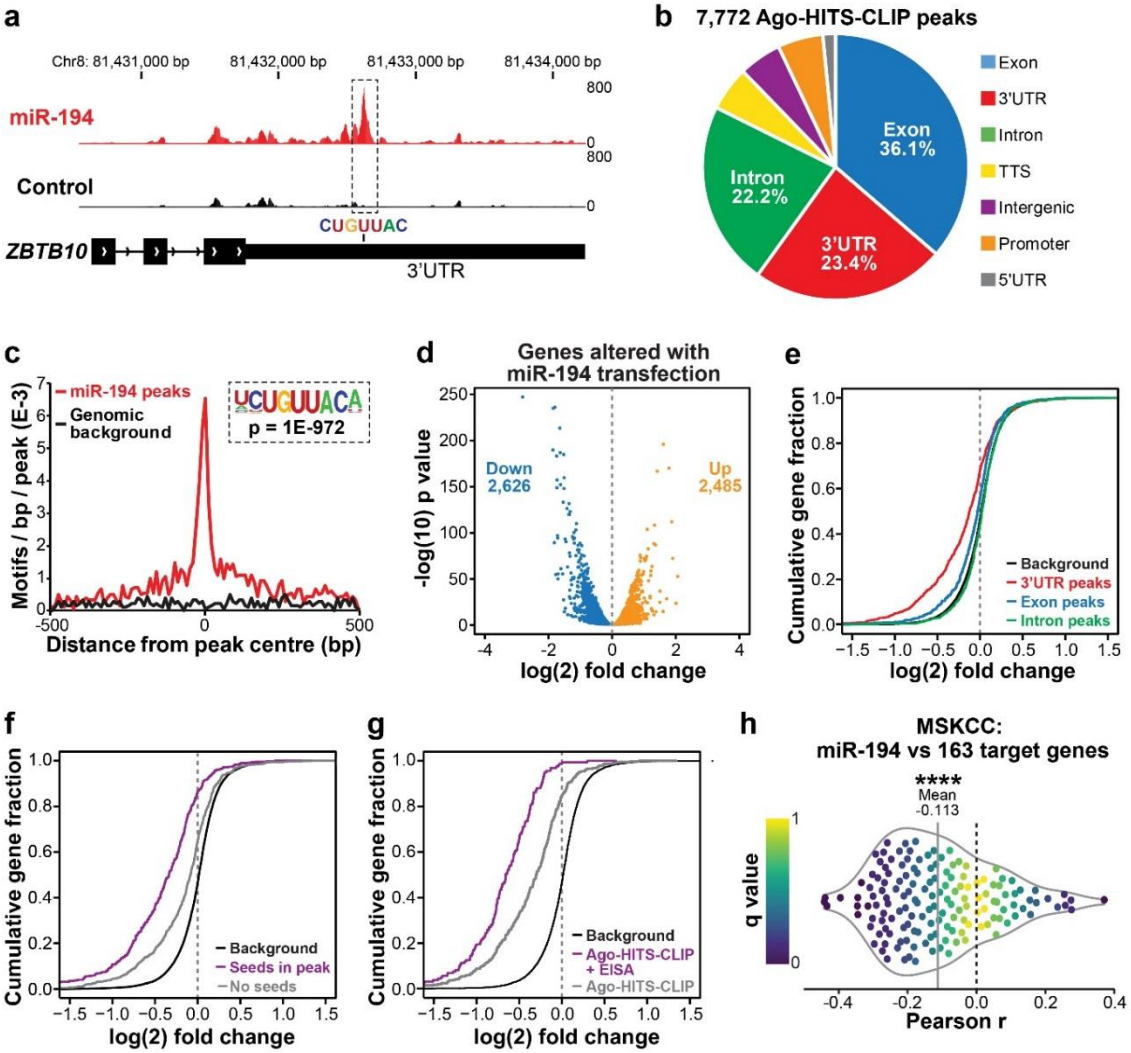

Fig 1. Integrative omics identifies a miR-194 "targetome" in prostate cancer. (a) Example of an Ago-HITS-CLIP peak with a miR-194 seed recognition sequence in the *ZBTB10* gene. Genome tracks depict the average read density of all replicates for each treatment condition (i.e. cells transfected with miR-194 (red) or a scrambled control (black)). (b) Distribution of 7,772 Ago-HITS-CLIP peaks mapped to their genomic regions. (c) Distribution of miR-194 recognition sequences within Ago-HIT-CLIP peaks. Background represents occurrence of the motif on the opposite strand of the peak. (d) Volcano plot showing expression of genes altered by miR-194 transfection in 22RV1 cells. Blue dots indicate significantly downregulated genes and orange dots indicate significantly upregulated genes (FDR ≤ 0.05). (e) Cumulative distribution of log2 fold change for genes containing peaks in the 3'UTR, CDS and Introns compared to a

background of all genes with no peaks. (f) Cumulative distribution of log2 fold change for genes with a 3'UTR Ago-HITS-CLIP peak containing miR-194 seed matches or no seed matches in peaks compared to a background of all genes with no peaks. (g) Cumulative distribution of log2 fold change for all genes with a 3'UTR Ago-HITS-CLIP peak containing a miR-194 seed match (Ago-HITS-CLIP) or both a 3'UTR peak with miR-194 seed match and down-regulation at the post-transcriptional level (Ago-HITS-CLIP + EISA). (h) Correlations between miR-194 expression and its "targetome" in 72 primary and metastatic prostate cancers (MSKCC cohort[11]). For each target identified, the Pearson correlation coefficient and its q value was calculated and plotted as −log q (on y-axis) versus correlation coefficient (on x-axis). To indicate the bias towards negative correlations, the mean correlation coefficient is indicated by a vertical black line. P value was determined using a one-sided t test (****, $p < 0.0001$).

Fig 2

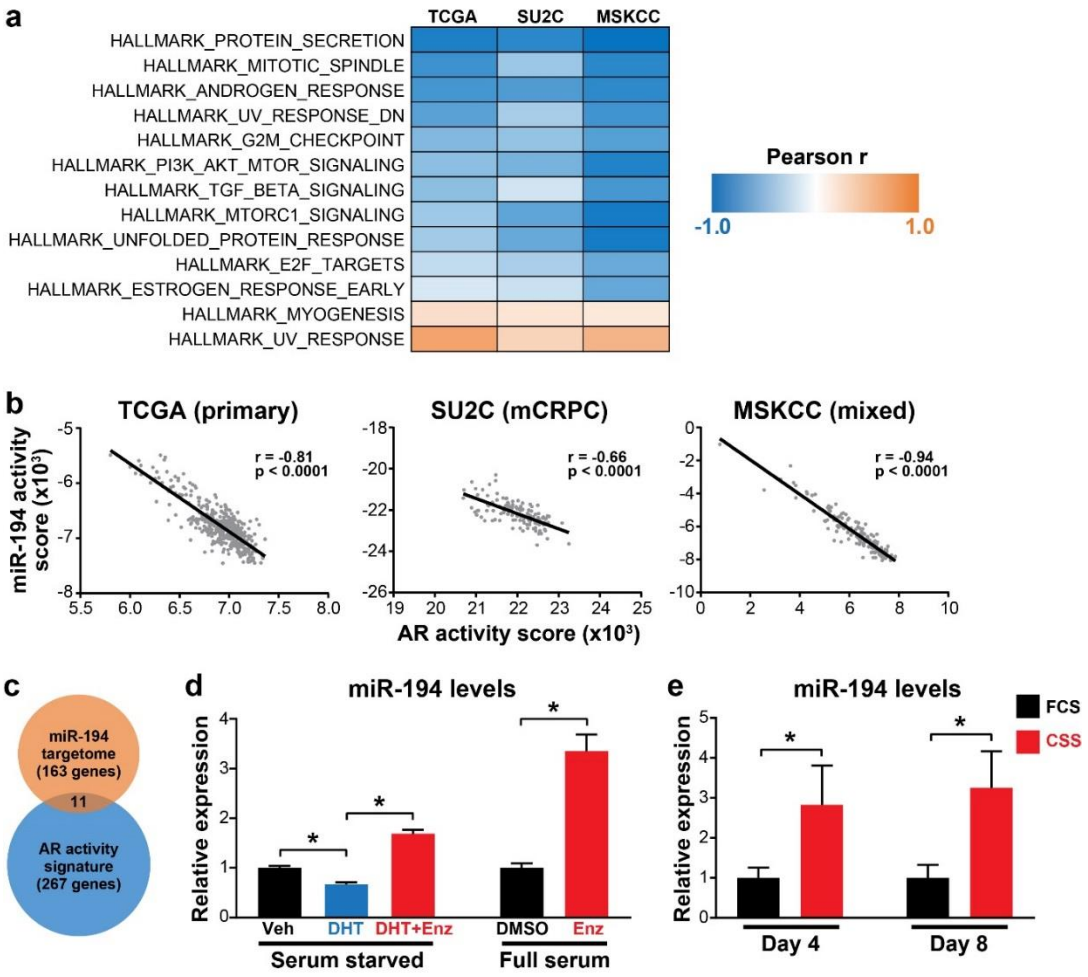

Fig 2. MiR-194 expression is suppressed by AR. (a) Correlation of miR-194 activity score with activity scores of "Hallmark" biological gene sets in the TCGA, SU2C and MSKCC cohorts. P and r values were determined using Pearson's correlation tests. Only gene sets that were significantly correlated ($p < 0.05$) in all three cohorts are shown in the heatmap. (b) MiR-194 activity is inversely correlated with AR activity in primary prostate cancer (TCGA cohort, left[15]), metastatic prostate cancer (SU2C cohort, centre[16]) and a cohort comprising both primary and metastatic prostate cancer (MSKCC cohort, right[11]). P and r values were determined using Pearson's correlation tests. (c) Overlap between the miR-194 targetome and an AR target gene set[14]. (d) Relative miR-194 expression in LNCaP cells treated with the androgen DHT and AR antagonist Enzalutamide (Enz). Cells grown in serum starved conditions were treated with vehicle control (Veh) or 10 nM DHT in the presence or absence of 10 μM Enz for 48 hours. Cells

grown in full serum were treated with vehicle (DMSO) or 10μM Enz for 48 hours. Expression of miR-194 was normalised to the reference small RNA U6. P values were determined using unpaired two-sided t tests (*, $p < 0.05$). (e) Relative miR-194 expression in LNCaP cells grown in fetal calf serum (FCS) or charcoal stripped serum (CSS) for 4 or 8 days. Expression of miR-194 was normalised to the reference small RNA U6. P value was determined using an unpaired two-sided t test (*, $p < 0.05$).

miR-194 activity and expression is elevated in neuroendocrine prostate cancer

NEPC is associated with loss of canonical AR activity[1]. Given the inverse relationship between miR-194 and AR, we therefore hypothesised that its activity would be elevated in clinical NEPC. Indeed, miR-194 activity (estimated by ssGSEA) was significantly higher in NEPC compared to CRPC-Adeno tumours in clinical samples (Fig. 3a) and patient-derived xenograft (PDX) models (Supplementary Fig. S3). Moreover, miR-194 activity was correlated with established NEPC gene sets (Fig. 3b).

We next examined whether miR-194 itself was over-expressed in NEPC. In the absence of miRNA expression data from clinical samples, we turned to a panel of 13 PDXs established through the Melbourne Urological Research Alliance (MURAL), 6 of which have features of NEPC[17]. Importantly, miR-194 expression was higher in the NEPC versus AR-positive adenocarcinoma PDXs (Fig. 3c), further demonstrating its association with this disease subtype.

Loss of AR expression and/or activity during the transition to NEPC likely explains – at least partly - increased miR-194 expression in this disease state. However, since we have also noted elevated miR-194 expression and activity in metastases and "poor outcome" primary tumours[18], we speculated that other alterations may underlie dysregulation of miR-194 in PCa. MiR-194 is encoded by two separate loci on chromosomes 1 and 11; the *MIR194-1* gene clusters with *MIR215* within intron 12 of the *IARS2* gene on chromosome 1, while the *MIR194-2* gene clusters with *MIR192* approximately 3kb downstream of the *ATG2A* gene on chromosome 11. By interrogating clinical genomic datasets, we found that *MIR194-1*/*IARS2* and *MIR194-2*/*ATG2A* are more frequently gained/amplified in metastatic compared to primary PCa and in NEPC compared to CRPC-Adeno (Fig. 3d). Importantly, gain/amplification of these loci were associated with elevated levels of miR-194 (Fig. 3e). These data suggest that copy number gain can result in increased miR-194 expression in aggressive prostate tumours and NEPC.

miR-194 promotes the emergence of a neuroendocrine features in prostate cancer

To determine whether miR-194 can directly influence the emergence of a NE-like state, we examined the response of adenocarcinoma PCa cells to transfection with a miR-194 mimic. Exogenous miR-194 led to upregulation of NE marker genes (Fig. 4a) and increased neurite length in LNCaP cells (Fig. 4b), an effect that was recapitulated in the 22Rv1 cell line model (Fig. 4a-b, Supplementary Fig. S4).

The ability of miR-194 to enhance NE transdifferentiation was further tested using a locked nucleic acid (LNA) inhibitor that specifically inhibits the activity of this oncogenic miRNA. In these experiments, we exploited the fact that the LNCaP model can be transdifferentiated from adenocarcinoma-like to NE-like cells by androgen deprivation[19]. As expected, growth of cells in charcoal-stripped serum (CSS) resulted in upregulation of NE markers *ENO2* (encoding neuron-Specific Enolase) and *SYP* (encoding synaptophysin) and increased the length of neurite-like extensions (Fig. 4c-d). Importantly, the miR-194 LNA inhibitor effectively blocked this transdifferentiation (Fig. 4c-d). Collectively, these data reveal that miR-194 can drive the acquisition of NE features, which corresponds with its increased activity in clinical NEPC.

Fig 3

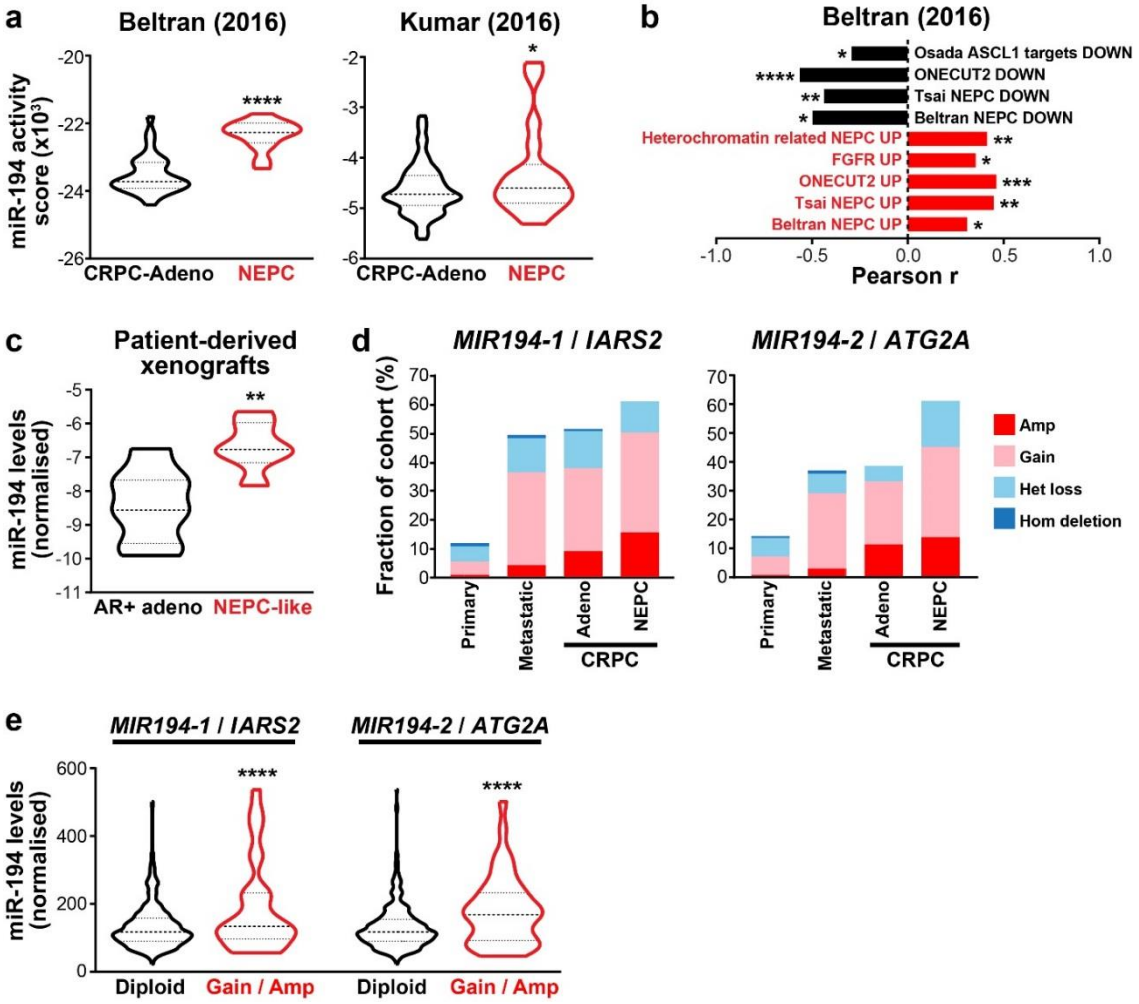

Fig 3. MiR-194 is associated with the AR independent NEPC subtype. (a) MiR-194 activity is higher in neuroendocrine prostate cancer (NEPC) compared to adenocarcinoma CRPC (CRPC-Adeno) in 2 distinct cohorts[6, 20]. Dashed middle line, median; dotted lines above and below, upper and lower quartiles. P values were determined using unpaired two-sided t tests (*, P < 0.05; ****, P< 0.0001). (b) Correlation between miR-194 activity and published NEPC associated gene signatures[21, 22, 23, 24, 25, 26]. P and r values were determined using Pearson's correlation tests (*, p < 0.05; **, p < 0.01; ***, p < 0.001; ****, p < 0.0001). (c) Expression of miR-194 is higher in NEPC PDXs compared to PDXs derived from AR-positive adenocarcinoma tumours. Expression of miR-194 was normalised to two reference small RNAs (U6 and RNU44). Dashed middle line, median; dotted lines above and below, upper and lower quartiles. P value was determined using an unpaired two-sided t test (**, P < 0.01). (d) *MIR194-1/IARS2* and *MIR194-2/ATG2A* are more frequently gained/amplified in metastatic

compared to primary PCa and in NEPC compared to CRPC-Adeno. Copy number data is combined from multiple clinical cohorts[24, 27, 28, 29, 30]. (e) Expression of miR-194 is higher in primary prostate tumours with *MIR194-1*/*IARS2* or *MIR194-2*/*ATG2A* copy number gain or amplification compared to tumours with no change in copy number (diploid). Data is from the TCGA cohort. Dashed middle line, median; dotted lines above and below, upper and lower quartiles. P values were determined using unpaired two-sided t tests. (****, $p<0.0001$).

Fig 4

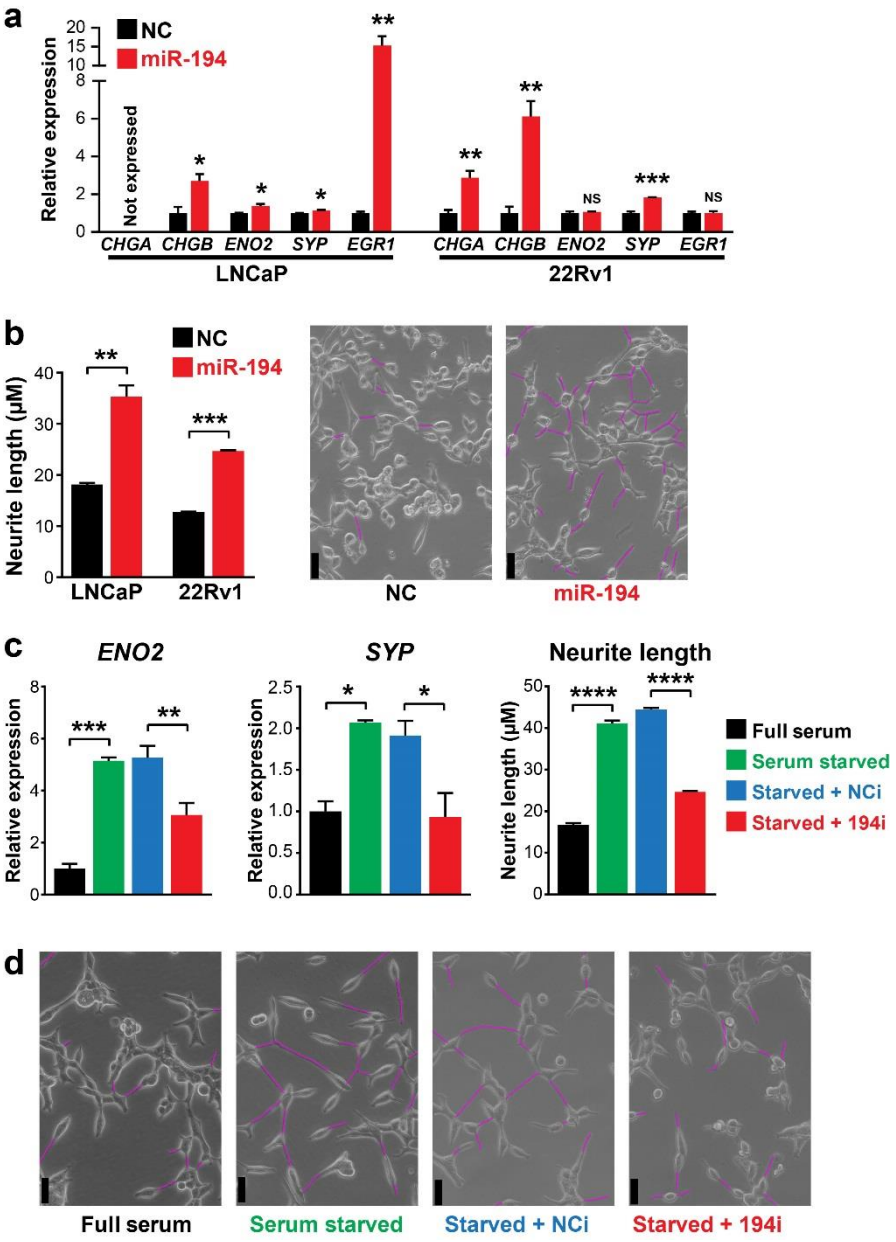

Fig 4. MiR-194 promotes prostate cancer transdifferentiation. (a) Expression of NEPC marker genes is upregulated in response to transfection of a miR-194 mimic in LNCaP and 22RV1 cells. Gene expression was normalised to GAPDH. Expression for the negative control (NC) was set to 1, and error bars are SEM. (b) MiR-194 increases neurite length in LNCaP and 22RV1 cells compared to cells transfected with a negative control miRNA mimic (NC). Expression for NC was set to 1, and error bars are SEM. P values were determined using unpaired two-sided t tests (**, $p < 0.01$). Representative

phase contrast images (on the right) are of LNCaP cells transfected with miR-194 mimic or NC. Neurite outgrowths are traced on images in magenta. Scale bars, 25 μm. (c) A miR-194 inhibitor (194i) blocks neuroendocrine transdifferentiation of LNCaP cells mediated by androgen deprivation, as determined by expression of Neuron specific enolase (*ENO2*), Synaptophysin (*SYP*) and changes in neurite length. Gene expression was normalised to GAPDH. Gene expression or neurite length for cells grown in full serum were set to 1, and error bars are SEM. P values were determined using ANOVA (*, $p < 0.05$; **, $p < 0.01$; ***, $p < 0.001$; ****, $p < 0.0001$). (d) Representative phase contrast images of LNCaP cells grown in full or stripped serum conditions with or without a miR-194 inhibitor (194i) or negative control inhibitor (NCi). Neurite outgrowths are traced in magenta. Scale bars, 25 μm.

FOXA1, an inhibitor of neuroendocrine transdifferentiation, is targeted by miR-194

To understand at a mechanistic level how miR-194 promotes PCa transdifferentiation, we searched the targetome for genes with a known role in PCa progression. Of particular interest was FOXA1, a transcription factor with a critical role in maintaining epithelial lineage in the prostate[31]. Consistent with this function, a recent report demonstrated that loss of FOXA1 leads to NE differentiation in prostate cancer[32]. Multiple miR-194 Ago-HITS-CLIP peaks were found within the *FOXA1* 3'UTR, one of which contains a perfect 7-mer seed match (Fig. 5a). We confirmed that miR-194 decreases the levels of *FOXA1* mRNA and FOXA1 protein in the LNCaP and 22Rv1 models (Fig. 5b-c). Importantly, the activity of FOXA1 and miR-194 is inversely correlated in clinical PCa (NEPC and primary PCa; Fig. 5d). Collectively, these findings reveal a functional interaction between miR-194 and FOXA1.

A recently described mechanism by which FOXA1 suppresses NE differentiation is by directly repressing the *IL8* gene, a chemokine elevated in NEPC, which results in dampening of the MAPK/ERK pathway, a known driver of NEPC[32, 33]. Supporting the relevance of this mechanism in miR-194's mode of action, transfection of prostate cancer cells (LNCaP and 22Rv1) with miR-194 caused upregulation of *IL8* (Fig. 5e). Moreover, miR-194 also enhanced MAPK/ERK pathway activity (Fig. 5f), and miR-194 activity was positively correlated with MAPK/ERK gene signatures in clinical NEPC (Fig. 5g and Supplementary Fig. S5). Collectively, these data reveal that miR-194 promotes the emergence of NEPC at least in part by targeting FOXA1, which leads to upregulation of IL8 and enhanced MAPK/ERK pathway activity.

Targeting miR-194 suppresses the growth of prostate cancer with neuroendocrine features

Although miR-194 mediates the acquisition of an NE-like phenotype in prostate cancer, whether it represented a therapeutic target in this disease context is unclear. To investigate this possibility, we measured the growth of PCa cells treated with the miR-194 LNA inhibitor. Interestingly, the growth of all 4 cell line models tested could be suppressed by the inhibitor, but the models with NE features (PC3 and LNCaP-MR42D) were more sensitive than those with a more typical adenocarcinoma phenotype (LNCaP, LNCaP-MR49F) (Fig. 6a). The miR-194 inhibitor was cytotoxic as revealed by cell viability assays (Fig. 6b) and by counting dead cells (Fig. 6c).

To examine the potential of targeting miR-194 in a more clinically-relevant setting, we turned to patient-derived CRPC organoids recently described by our team[17]. Models 201.1 and 201.2 were derived from dura and lung metastases, respectively, from a patient who died after receiving second-generation AR-targeted therapies (Enzalutamide, Abiraterone) and chemotherapies (Docetaxel, Cabazitaxel)[17]. 201.1 is a model of PSA-positive adenocarcinoma that expresses a mutated form of the AR (C687Y and T878A) that mediates resistance to Enzalutamide. In contrast, 201.2 has no AR or PSA expression but exhibits high expression of a neuroendocrine gene signature, focal staining of CD56, and concurrent genomic loss of *TP53*, *PTEN* and *RB1*[17]. Representative IHC images of the expression of various markers in each model are shown in Fig. 6D. As expected, miR-194 levels were higher in 201.2 compared to 201.1 (Fig. 6e). The effect of the miR-194 LNA inhibitor on the growth of these 2 patient-derived models was evaluated by measuring organoid forming efficiency (OFE) and cell viability. Both models exhibited reduced OFE and cell viability in response to transfection with the inhibitor (Fig. 6f-g). However, similarly to the cell lines, the AR-null, NEPC-like 201.2 model was more sensitive to miR-194 inhibition than the adenocarcinoma-like 201.1 model (Fig. 6f-g). Collectively, these findings - in both traditional cell lines and contemporary patient-derived models - provide evidence that targeting miR-194 has potential as a novel therapy for prostate cancer with NE features.

Fig 5

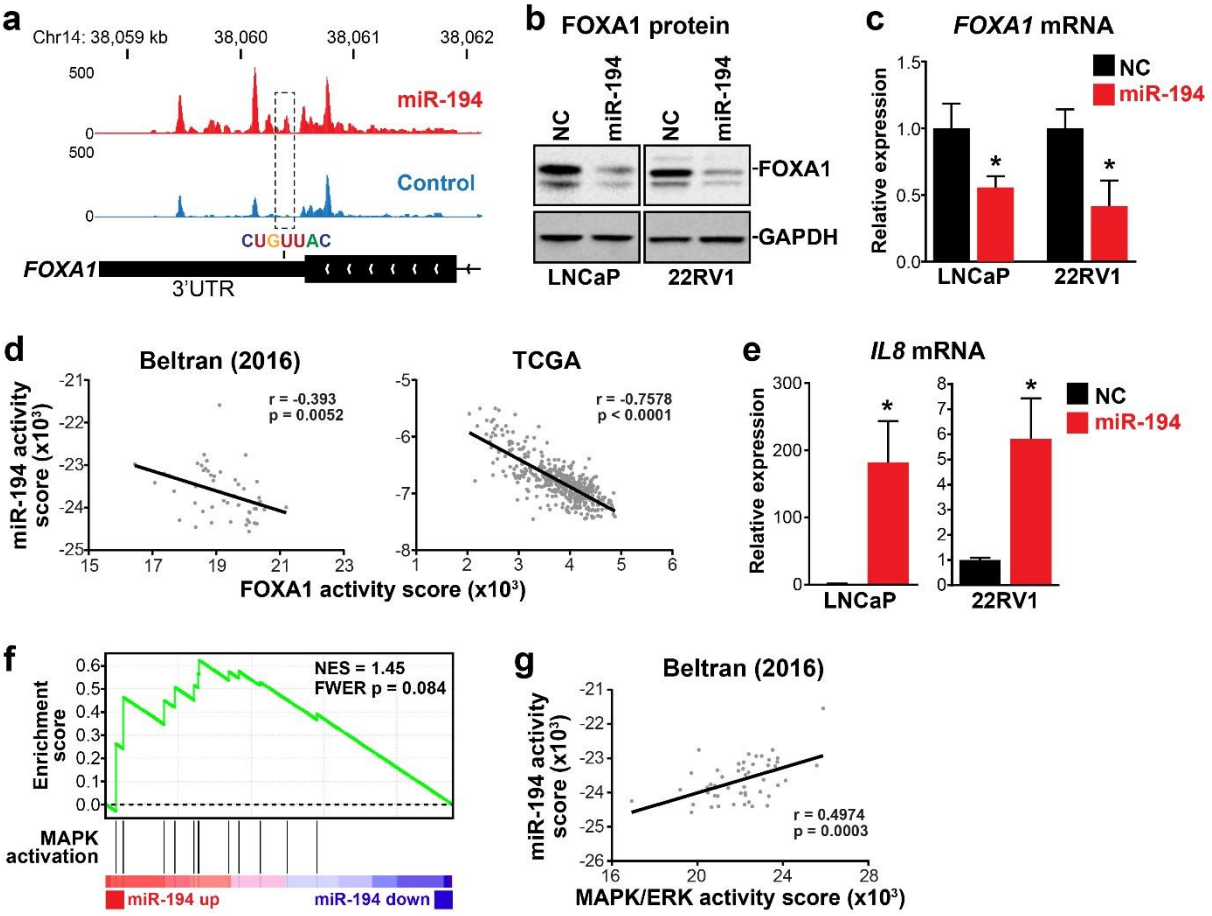

Fig 5. MiR-194 targets *FOXA1* and activates the MAPK/ERK pathway. (a) Ago-HITS-CLIP peaks (including one indicated with a miR-194 seed recognition) sequence in the *FOXA1* gene. Genome tracks depict the average read density of all replicates for each treatment condition (i.e. cells transfected with miR-194 (red) or a scrambled control (black)). (b) Western blot showing FOXA1 protein levels following transfection of a miR-194 mimic or negative control mimic (NC) in 22RV1 and LNCaP cells. (c) Expression of *FOXA1* mRNA, as determined by qRT-PCR, following transfection of miR-194 mimic or NC in 22RV1 and LNCaP cells. Gene expression was normalised to GAPDH. Expression for NC was set to 1, and error bars are SEM. P values were determined using unpaired two-sided t tests (*, $p < 0.05$). (d) FOXA1 activity is negatively correlated with miR-194 activity in clinical cohorts[6, 15]. P and r values were determined using Pearson's correlation tests. (e) Expression of *IL8* is upregulated in response to miR-194 in 22RV1 and LNCaP cells. Gene expression was normalised to

GAPDH. Expression for NC was set to 1, and error bars are SEM. P values were determined using unpaired two-sided t tests (*, $p < 0.05$). (f) MiR-194 causes increased MAPK activity in 22Rv1 cells, as determined by GSEA. The MAPK activation signature has been described previously[34]. (g) MAPK/ERK activity is positively correlated with miR-194 activity in a clinical cohort comprised of NEPC and CRPC-Adeno samples[6]. P and r values were determined using a Pearson's correlation test.

Fig 6

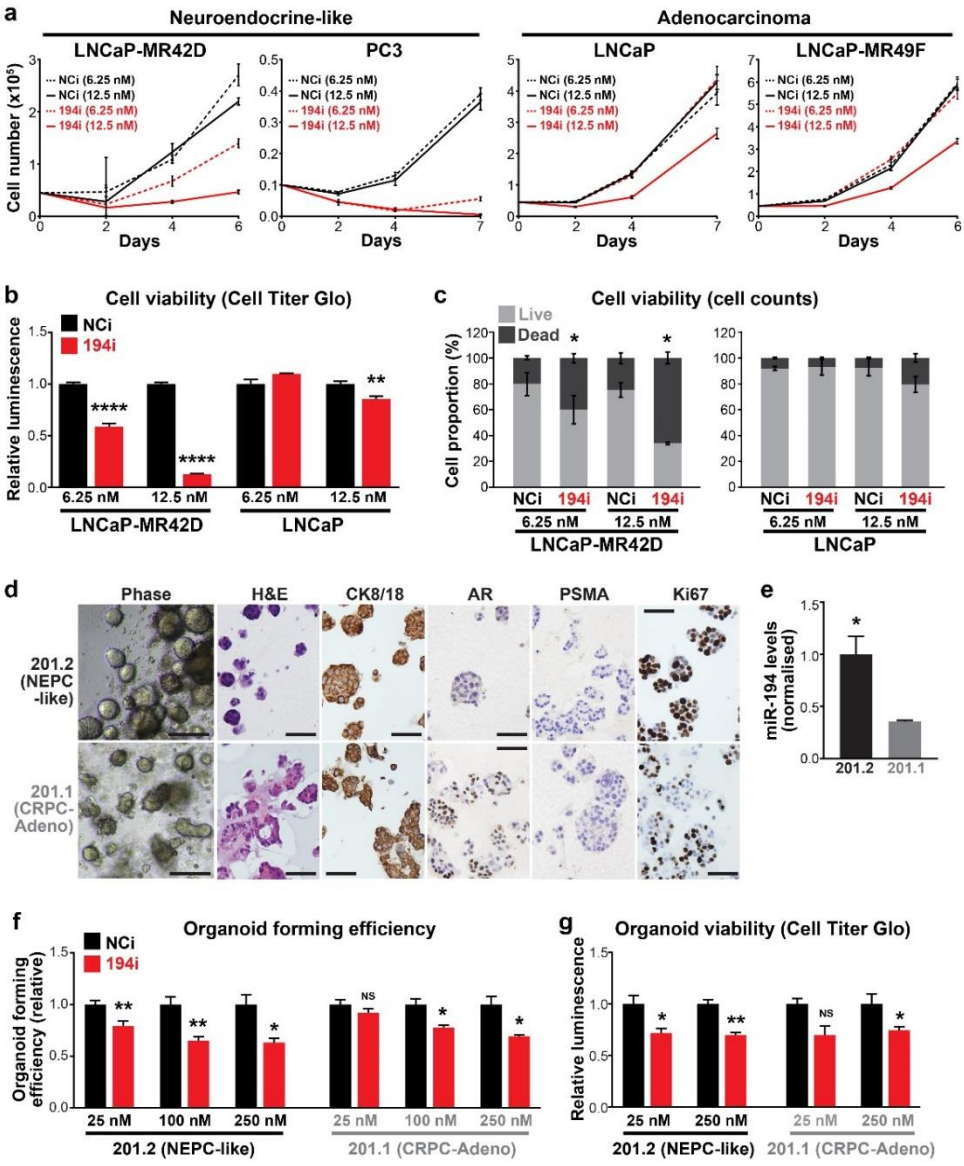

Fig 6. Inhibiting miR-194 blocks the growth of NEPC. (a) Blocking miR-194 activity with an LNA inhibitor (miR-194i) supresses the growth of cell lines with neuroendocrine features (LNCaP-MR42D, PC3) more potently than AR-driven adenocarcinoma cell lines (LNCaP-MR49F, LNCaP), as determined by Trypan blue growth assays. Error bars are SEM. Negative control inhibitor, NCi. (b) Blocking miR-194 activity with an LNA inhibitor supresses cell viability more potently in neuroendocrine-like LNCaP-MR42D cells compared to LNCaP adenocarcinoma cells, as determined by Cell Titer Glo cell viability assay. P values were determined using unpaired two-sided t tests (**, $p < 0.01$; ****, $p < 0.0001$). (c) Proportion of live and dead cells in LNCaP-MR42D and LNCaP cells transfected with 194i or NCi. P values were determined using unpaired two-sided t tests (*, $p < 0.05$). (d) Representative phase contrast, haematoxylin and eosin (H&E) and

immunohistochemistry (IHC) of 201.1 and 201.2 organoid models growing as colonies in Matrigel. Scale bars: phase images = 100 μm; H&E and IHC = 50 μm. (e) Levels of miR-194 in 201.1 and 201.2 organoids. Expression of miR-194 was normalised to 2 reference small RNAs (U6 and RNU44). P value was determined using an unpaired two-sided t test (*, $p < 0.05$). (f-g) Blocking miR-194 activity with 194i inhibits organoid forming efficiency (f) and organoid viability (g) of the 201.1 and 201.2 models. P values were determined using unpaired two-sided t test. (*, $p < 0.05$; **, $p < 0.01$).

DISCUSSION

Epigenetic and transcriptional alterations are known to mediate prostate cancer cell plasticity during adenocarcinoma-neuroendocrine transdifferentiation. Most drivers of these alterations identified to date are transcription factors and chromatin modifiers, such as SOX2[35, 36], EZH2[35], REST[37], BRN2[38] and FOXA2[39]. By identifying miR-194 as a mediator of this transdifferentiation, our work reveals that post-transcriptional gene regulation is another mechanism by which transcriptional networks are altered during progression to NEPC.

Our study suggests that miR-194 is elevated in NEPC via 2 key mechanisms. First, by evaluating PCa cells treated with androgens and anti-androgens, we found that miR-194 is negatively regulated by the AR signalling axis. Interrogation of published cistromic data revealed no evidence for association of AR with regulatory elements proximal to *MIR194* genes (data not shown); thus, we do not believe that the inverse relationship between AR and miR-194 represents a direct mode of transcriptional repression. Rather, we hypothesise that AR indirectly inhibits miR-194 expression through a mechanism that is yet to be elucidated. One possibility is that the transcription factor GATA2 serves as an intermediary: expression of GATA2 is known to be down-regulated by AR[40], and we previously demonstrated that GATA2 enhances the levels of miR-194[8]. Future studies should investigate the role of this putative pathway in NEPC, particularly since GATA2 has been identified as a mediator of PCa metastasis and drug resistance previously[41]. Second, we found that gain or amplification of genomic regions encompassing the *MIR194* genes is another mechanism that can result in elevated expression of miR-194 in aggressive forms of prostate cancer, including NEPC. MiR-194 is unusual in that it is encoded by 2 genes (*MIR194-1* and *MIR194-2*), and the observation that both are frequently gained further supports the relevance of this miRNA in disease progression.

Using an integrative approach that exploited cutting-edge biochemical (Ago-HITS-CLIP), molecular (RNA-seq) and bioinformatics (EISA) techniques, we identified ~160 genes that miR-194 putatively targets in PCa. Of note, gene signatures enriched in this targetome include those involved in cell movement, cytoskeletal organisation (including axon guidance) and focal adhesion. We propose that dysregulation of these networks by elevated miR-194 during PCa progression promotes EMT[8] and transdifferentiation from an adenocarcinoma-like cell to an NE-like cell (this study).

While this hypothesis remains to be proven, we note the EMT and emergence of NE features are manifestations of cell plasticity that share many fundamental characteristics; indeed, it appears as if the re-activation of a developmental EMT program is a crucial strategy by which PCa cells evolve towards a NE lineage[1, 42].

In addition to a miR-194 targetome enriched for cell movement, structure and attachment, we identified *FOXA1* as a key target gene via which miR-194 influences the emergence of NEPC. Supporting our findings, *FOXA1* has been previously identified as a target of miR-194 in non-small cell lung cancer (NSCLC); interestingly, in this context it appeared to act as a tumour suppressor, with upregulation of miR-194 suppressing tumour proliferation, invasion and metastasis [43]. The divergent outcomes of targeting FOXA1 by miR-194 in PCa and NSCLC reflects a common phenomenon in miRNA biology whereby context-dependent roles are mediated by the relative expression of key miRNA target genes in a particular cell or tissue environment. Our data suggest that targeting of FOXA1 by miR-194 in PCa leads to de-repression of IL8 and subsequent upregulation of the MAPK/ERK pathway[32]. Both IL8 and the MAPK/ERK pathway are known drivers of NEPC[33, 44, 45]; our work defines a new mechanism by which these factors are elevated in this disease context.

The relevance of the miR-194:*FOXA1* pathway in PCa likely goes beyond its consequent impact on IL8 and MAPK/ERK, since FOXA1 is a pioneer factor for AR and a major regulator of its transcriptional outputs[46]. Like FOXA1, AR is also vital for maintenance of the epithelial phenotype; therefore, the consequent disruption of AR signalling by down-regulation of FOXA1 could be another mechanism by which miR-194 enhances lineage plasticity in PCa. Combined with our finding that miR-194 is repressed by AR signalling and the identification of up to 11 AR downstream genes as miR-194 targets (Fig. 2c), our study reveals a complex and intimate interplay between miR-194 and this key pathway in PCa. In addition to being the likely explanation for the extremely strong negative correlation between miR-194 and AR in clinical PCa, this interplay may also influence response to AR-targeted therapies.

Given the increasing frequency of treatment-emergent NEPC tumours and their aggressiveness, the development of therapies that selectively target this CRPC subtype is critically important. Indeed, strategies to target AURKA (which promotes the activity of MYCN, a known driver of NEPC), EZH2 (which enhances adenocarcinoma-NEPC transdifferentiation) and the Wnt and NOTCH pathways (both of which promote stem cell maintenance in NE-like tumours) are being evaluated in clinical trials[1]. Our study

identifies miR-194 as a novel therapeutic target in this disease setting. Although a recent study found that miR-652 can promote the acquisition of NE features in PCa cells[47], to our knowledge ours is the only study to date demonstrating that targeting a miRNA can inhibit NE transdifferentiation and block the growth of NEPC. Moreover, the sensitivity of patient-derived CRPC organoids and PCa cell lines to nanomolar doses of a miR-194 inhibitor highlights the potential of such a therapeutic strategy. While miRNA-based therapies have proven difficult to translate to the clinic[48], at least 2 antagomiRs are currently being evaluated in trials: a miR-122 antagomiR ("Miravirsen") showed activity in a phase IIa trial of hepatitis C (in which no adverse side effects were reported), while a miR-155 antagomiR is in phase I trials for lymphoma[49]. The attraction of targeting miRNAs in cancer comes from the potential to concurrently modulate multiple pathways involved in tumour growth and progression. In the case of miR-194, an inhibitor could stabilise multiple plasticity suppressing factors (e.g. FOXA1) and tumour suppressors (e.g. SOCS2[8]), leading to inhibition of multiple plasticity- and metastasis-promoting pathways (e.g. MAPK/ERK, IL8 and STAT3). We aim to undertake further pre-clinical evaluation of a miR-194-targeted therapy to treat NEPC and/or re-sensitise NEPC tumours to AR-targeted therapies.

In addition to its potential as a therapeutic target, it is worth noting that miR-194 was first linked to PCa as a serum marker of poor prognosis in a patients with localised disease[18]. In this earlier disease context, high levels of serum miR-194 likely demarcates tumours with increased plasticity and hence a propensity to metastasize. However, whether miR-194 is a marker of advanced PCa and CPRC is unknown. Given the strong inverse correlation between miR-194 and AR activity, it is tempting to speculate that circulating miR-194 could be used to identify CRPC patients with AR-independent tumours (e.g. NEPC) and therefore guide therapy, but this concept remains to be tested in patient cohorts.

In summary, our study demonstrates that miR-194 can promote adenocarcinoma-NE transdifferentiation and the growth of NEPC by targeting a network of genes including the lineage-defining transcription factor FoxA1. These findings deliver new molecular insights into lineage plasticity in PCa, and provide impetus to further investigate the potential of targeting miR-194 as a novel therapy for NEPC.

MATERIAL AND METHODS

Cell lines and cell culture

LNCaP, PC3 and 22RV1 cell lines were purchased from the American Type Culture Collection (ATCC). LNCaP-MR42D and LNCaP-MR49F cell lines have been described previously[38]. LNCaP and 22RV1 cell lines were maintained in RPMI-1640 (Sigma) containing 10% Fetal Bovine Serum (FBS) (Sigma). PC3 cell lines were maintained in RPMI-1640 containing 5% FBS. LNCaP-MR42D and LNCaP-MR49F cells were maintained in RPMI-1640 containing 10% FBS and 10μM Enzalutamide. For serum starvation experiments, cells were grown in phenol red-free RPMI-1640 containing 10% dextran-coated charcoal (DCC) stripped serum. Cell lines were subjected to regular mycoplasma testing. All cell lines underwent verification by short tandem repeat profiling by CellBank Australia.

Cell line transfections

Transient transfection of cell lines were performed using RNAiMAX Transfection Reagent (Life Technologies) according to the manufacturer's instructions. For HITS-CLIP and RNA-seq experiments, 22RV1 cells were transfected with 20nM miRVana mimic (miR-194 or negative control; Ambion). For all other experiments, cells were transfected with 20nM miRNA mimics from Shanghai GenePharma. For miR-194 inhibition, cells were transfected with 12.5 or 6.25nM locked nucleic acid (LNA) miRNA inhibitors (miR-194 LNA inhibitor or negative control inhibitor; Qiagen).

Argonaute high-throughput sequencing of RNA isolated by crosslinking immunoprecipitation (Ago-HITS-CLIP)

The Ago-HITS-CLIP method was adapted from published methods[50, 51], incorporating modifications from eCLIP[52, 53]. 22RV1 cells were seeded in 10 cm cell culture dishes and transfected in suspension with 20 nM miRVana mimic (miR-194 or negative control, 3 replicates of each; Ambion) using RNAiMAX (Life Technologies). After 24 h, transfected 22RV1 cells were rinsed once with ice-cold PBS and UV irradiated with 600 mJ/cm2, 254 nm, in ice-cold PBS using a UV Stratalinker-1800 (Agilent). Cells were collected by scraping, and cell pellets stored at -80°C as one pellet per 100mm plate. One pellet per CLIP IP was lysed in 500 μl of 1 X PXL (1 X PBS, 0.1% SDS, 0.5% deoxycholate, 0.5% Igepal) + EDTA-free Complete protease inhibitor cocktail (PIC;

Roche) for 15 min on ice, followed by trituration through a 21G needle and syringe 5 times. DNA was digested with 20 µl RQ1 DNAse (Promega) at 37°C for 10 min on a Thermomixer (750 rpm, Eppendorf). RNA was partially digested with RNase 1 (ThermoFisher) by adding 5 µl of 1:40 diluted RNase 1 in 1 X PBS at 37°C for 5 min on a Thermomixer (750 rpm), then returned to ice. Lysates were centrifuged at 21,000 g for 20 min at 4°C and supernatant transferred to a fresh tube.

AGO-RNA complexes were immunoprecipitated using mouse IgA2 monoclonal anti-Ago2 antibody 4F9[54]; hybridoma sourced from University of Florida ICBR) with a mouse IgA antibody (GeneTex S107) used as a control. Antibodies (8 µg) were conjugated to 20 µl protein L Dynabeads (ThermoFisher, 88849) in PBS-Tw (1 X PBS, 0.05% Tween-20) for 45 min and washed three times with 1 X PXL (1 X PBS, 0.1% SDS, 0.5% sodium deoxycholate, 0.5% Igepal) before resuspending the beads with 450 µl of prepared lysate and rotating for 2 hr at 4°C. Bound AGO-RNA complexes were washed twice each consecutively with ice cold 1 X PXL, 5 X PXL (5 X PBS, 0.1% SDS, 0.5% sodium deoxycholate, 0.5% Igepal), and 1 X PNK (50 mM Tris-Cl pH 7.5, 10 mM MgCl2, and 0.5% Igepal). Beads were first treated with T4 PNK (NEB, M0201L; 20 U in 80 µl reaction volume) in the absence of ATP (37°C, 850 rpm for 20 min) to dephosphorylate 3' RNA ends followed by washes with 1 X PNK, 5 X PXL, and two washes with 1 X PNK at 4°C. The 3' preadenylated linker (NEBNext 3'SR adaptor for Illumina; /5rApp/AGA TCG GAA GAG CAC ACG TCT /3AmMO/) was ligated to the RNA fragments on bead using T4 RNA ligase 2 truncated KQ (NEB M0373; 100 U in a 40 µl reaction volume, 12% PEG8000, 1x RNA ligase buffer, 0.125 µM adaptor) in the absence of ATP at 16°C, overnight with periodic mixing. Beads were washed consecutively with ice cold 1 X PXL, 5 X PXL, and twice with 1 X PNK. Bound RNAs were then labelled with P32 γ-ATP using T4 PNK, 20 min at 37°C, and washed as above.

AGO-RNA complexes were eluted with 40 µl 1 X Bolt LDS sample buffer (ThermoFisher) + 1% β-mercaptoethanol at 70°C for 10 min on a Thermomixer (1200 rpm). Samples were separated through Bolt 8% Bis-tris Plus gels (ThermoFisher) using BOLT MOPS SDS running buffer at 200 V for 75 min. Complexes were then transferred to nitrocellulose (Schleicher&Schuell, BA-85) by wet transfer using 1 X BOLT transfer buffer with 10% methanol. Filters were placed on a phosphor screen and exposed using a Typhoon imager (GE). 115-160 kDa regions (corresponding to RNA tags > 30 nt) were excised from the nitrocellulose. RNA was extracted by proteinase K digestion (2 mg/mL proteinase K, 100 mM Tris-HCl pH 7.5, 50 mM NaCl, 10 mM EDTA, 0.2% SDS) at

50°C for 60 min on a Thermomixer (1200 rpm) followed by extraction with acid phenol (ThermoFisher, AM9712) and precipitation with 1:1 isopropanol:ethanol. RNA was pelleted by centrifugation then separated on a 15% denaturing polyacrylamide gel (1:19 acrylamide, 1 X TBE, 7 M urea). The wet gel was wrapped in plastic wrap and exposed to a phosphor screen and imaged using a Typhoon. Gel slices were cut corresponding to the expected size of the cross-linked RNA eluted by the "crush and soak" method as previously described[51].

Reverse transcription, 5' linker ligation and amplification were performed essentially as previously described[52] using SR-RT primer for reverse transcription (IDT, AGACGTGTGCTCTTCCGATCT) with SuperScript IV, and a custom synthesised 5' linker (IDT, 5'SRdeg /5Phos/NN NNN NNN NNG ATC GTC GGA CTG TAG AAC TCT GAA C/3SpC3/). Products were amplified for 20 cycles using a common forward primer (NEBNext SR primer for Illumina) and barcoded reverse primers for each sample (NEBNext Index primers for Illumina). PCR products were purified using Qiagen Qiaquick PCR purification kit, separated on an 8% acrylamide (29:1) TBE non-denaturing gel, stained with SYBR Gold nucleic acid gel stain (ThermoFisher) and imaged on a ChemiDoc (BioRad). Products corresponding to an insert size of ~30 – 70 nt were excised from the gel and extracted by the "crush and soak" method as previously described[51]. Library quality and quantity was assessed by Bioanalyzer (Agilent) and qPCR, pooled and sequenced on an Illumina NextSeq 500 (1 x 75bp).

RNA libraries generated by HITS-CLIP were sequenced on the Illumina Nextseq 500 platform using the single end protocol with a read length of 75. Raw reads were adapter trimmed and filtered for short sequences using cutadapt v1.8.1[55] setting minimum-length option to 18, error-rate 0.2, and overlap 5. The resulting FASTQ files (averaging 41.6 million reads per sample) were analysed and quality checked using the FastQC (http://www.bioinformatics.babraham.ac.uk/projects/fastqc) program. Filtered reads were mapped against the human reference genome (hg19) using the Tophat2 alignment algorithm (version 2.0.9 with default parameters)[56], returning an average alignment rate of 43.8%. Unique molecular identifiers (UMIs) were used to de-duplicate reads that mapped to the same start site, possessed identical CIGAR strings and UMI barcodes sequences ≤1 edit distance apart. Enriched regions of the genome were identified from Samtools quality-filtered alignments[57] (-q 5) with the MACS2 peak caller (version 2.1.1)[9] (setting; --nomodel, --shift -15, --extsize 50, -B, --slocal 0, --llocal 0, --fe-cutoff 10, -q 0.05). Peak calling was performed using pooled alignment files and

carried out separately for each strand. The resulting peak files from each strand were merged. Features in the vicinity of peak loci and enrichment of motifs within peaks were determined and analysed using Homer[58]. Alignments were visualised and interrogated using IGV[59].

CLIP using a control antibody was performed on a single biological replicate of control transfected cells but yielded very little sequence data and was excluded from the analysis.

RNA sequencing

22RV1 cells were seeded in 6-well plates and transfected in solution with 20nM miRVana mimic (miR-194 or negative control; Ambion) using RNAiMAX (Life Technoloies). At 36 hours post-transfection, cells were collected in Qiazol (Qiagen) and total RNA was extracted using a miRNeasy Mini Kit (Qiagen) according to the manufacturer's instructions. RNA seq was performed on 4 biological replicates each of 22RV1 cells transfected with miR-194 or negative control. RNA sequencing libraries were constructed with the mRNAseq Library prep kit and libraries were sequenced on the Illumina NextSeq 500 platform.

RNA-seq libraries were multiplexed and sequenced on the Illumina NextSeq 500 platform using the stranded, paired-end protocol with a read length of 150. Raw reads were adapter trimmed and filtered for short sequences using cutadapt v1.8.1[55], setting minimum-length option to 18, error-rate 0.2, quality cut-off 28, overlap 5 and trim N's on. The resulting FASTQ files (averaging 60.2 million read pairs per sample) were analysed and quality checked using the FastQC program (http://www.bioinformatics.babraham.ac.uk/projects/fastqc). Reads were mapped against the human reference genome (hg19) using the STAR spliced alignment algorithm[60] (version 2.5.3a with default parameters and --chimSegmentMin 20, --quantMode GeneCounts), returning an average unique alignment rate of 92.9%. Differential expression analysis was evaluated from TMM normalised gene counts using R (version 3.2.3) and edgeR[61] (version 3.3), following protocols as described[62]. Graphical representations of differentially expressed genes were generated using Glimma[63]. Alignments were visualised and interrogated using the Integrative Genomics Viewer v2.3.80[59].

Exon Intron Split analysis (EISA) was performed as described previously[64]. To refine the miR-194 targetome, only post-transcriptionally downregulated genes (i.e.

genes with log2FC(dExon-dIntron) < 0) and a FDR cutoff of 0.05) were considered as targets.

Gene set enrichment analysis

Genes were ranked according to expression using the Signal2Noise metric. Gene Set Enrichment Analysis (Preranked analysis)[65] was implemented using the Broad Institute's public GenePattern server with default parameters.

Analysis of miR-194 activity in published datasets single sample GSEA (ssGSEA)

Expression data was downloaded from GEO (Kumar 2016 (GSE77930)[20]), cBioportal (MSKCC[29] and SU2C[66]), TCGA[67] and dbGAP (Beltran 2016[24]). ssGSEA[68] was implemented using the Broad Institute's public GenePattern server, using rank normalisation and default parameters. Since miRNAs repress expression of their target genes, miR-194 activity was calculated as the inverse value of ssGSEA scores for the miR-194 targetome.

RNA extractions from cell lines and patient-derived xenograft (PDX) tissues

Total RNA from cell lines was extracted using TRI Reagent (Sigma), as described previously[8]. PDX tissues preserved in RNALater were provided by the Melbourne Urology Research Alliance (MURAL)[17]. Tissues were homogenised in Qiazol (Qiagen) with a Precellys24 Tissue Homogeniser (Bertin Technologies) and total RNA was extracted using a miRNeasy Mini Kit (Qiagen), according to the manufacturer's instructions.

Quantitative RT-PCR (qRT-PCR) analysis of mRNA

Total RNA was treated with Turbo DNA-free kit (Invitrogen), and reverse transcribed using iScript Reverse Transcriptase Supermix kit (Bio-Rad). qRT-PCR was performed in triplicate as described previously[69]. GAPDH levels were used for normalization of qRT-PCR data. Primer sequences are available on request.

qRT-PCR analysis of miR-194

Total RNA (100 ng) was reverse transcribed using the TaqMan MicroRNA Reverse Transcription Kit (Applied Biosystems) and Taqman Microarray Assays (Thermo Fisher Scientific). Quantitation of miR-194, U6 and RNU44 was done by qRT-PCR using Taqman Microarray Assays (Thermo Fisher Scientific) and TaqMan™ Universal Master

Mix II, no UNG (Applied Biosystems) on a CFX384 real-time PCR detection system (Bio-Rad). MiR-194 expression was normalised to expression of U6 (cell lines) or the geometric mean of U6 and RNU44 (PDX tissues).

Proliferation and cell viability assays

Proliferation curves for cell lines treated with LNA miRNA inhibitors were performed using the Trypan blue exclusion assay. Cells were seeded at 1×10^4 (PC3) or 4.5×10^4 (LNCaP-MR42D, LNCaP-MR49F, LNCaP) in 12-well plates and transfected in suspension with 12.5 or 6.25 nM miR LNA inhibitor using RNAiMAX (Life Technologies). Live and dead cells were quantified at indicated time points using Trypan blue.

For cell viability assays, LNCaP-MR42D or LNCaP cells were seeded at 4×10^3 cells/well in 96-well plates and transfected in suspension with 12.5 or 6.25nM miR LNA inhibitor using RNAiMAX (Life Technologies). Cell viability was assesses using the Cell Titer-Glo Luminescent Cell Viability Assay (Promega) according to manufacturer's recommendations.

Neurite length measurement

Length of neurite extensions were measured using the Simple Neurite Tracer plugin [70] for Fiji/ImageJ . Neurite lengths were measured from $\geq$ 3 images per replicate. Representative images with overlaid traces were generated using the NeuronJ plugin[71] for Fiji/ImageJ

Western blots

Protein extraction from cells using RIPA buffer and western blotting was done as described in [69]. Primary antibodies used in western blotting were FOXA1 (Abcam, Ab23738) and GAPDH (Millipore, MAB374). Immunoreactive bands were visualised using Clarity Western ECL Substrate (Bio-Rad).

Organoid culture and transfections

PDXs were established by the Melbourne Urology Research Alliance (MURAL) (Monash University Human Research Ethics Committee approval 12287). The established PDXs were grown as subcutaneous grafts in male NSG mice supplemented with testosterone implants according to animal ethics approval (17963), as previously

described[17, 72]. PDXs were routinely authenticated using short tandem repeat profiling (GenePrint 10, Promega) at the Australian Genome Research Facility. Tissue from PDXs 201.1 dura (adenocarcinoma) and 201.2 lung (AR-null) was digested and grown as organoids in growth factor reduced, phenol red-free, ldEV-free Matrigel (Corning). 201.1 organoids were cultured in advanced DMEM/F-12 media (Gibco) containing 0.1 mg/ml Primocin (Invivogen), 1x Glutamax (Gibco), 10 mM HEPES (Gibco), 1 nM DHT (Sigma), 1.25mM N-acetylcysteine (Sigma), 5nM NRG1 Heregulinβ-1 (Peprotech), 500 nM A83-01 (Sigma), 10 mM nicotinamide (Sigma), 0.5 μM SB202190 (Sigma), 2% B27 (Thermo), 20 ng/ml FGF10 (Peprotech), 5 ng/ml FGF7 (Peprotech), 10ng/ml Amphiregulin (Peprotech), 1 μM prostaglandin E2 (Tocris), 10% noggin conditioned media and 10% R-spondin conditioned media. 201.2 Lung organoids were cultured in PrENR -p38i -NAC media[73]. 10 μM Y-27632 dihydrochloride (Selleck Chemicals) was added to culture medium during organoid establishment and following passage.

Phase contrast images of organoids were obtained with a Leica DM IL LED microscope with Leica DFC425 C digital camera. For immunohistochemistry, organoids were pelleted in agar, then formalin-fixed and paraffin embedded. Sections were stained using a Leica BOND-MAX-TM autostainer with BondTM epitope retrieval 1 or 2 and the Bond Refine Detection Kit (Leica). Primary antibodies are listed in Supplementary Table S1.

Organoids were transfected with miR LNA inhibitors essentially as described previously [74]. Briefly, organoid were collected and 50,000 cells were resuspended in 450μl of organoid culture media and 50μl of transfection mix containing RNAiMAX with 25, 100, and 250 nM miR-194 or NC LNA inhibitor. Cells were centrifuged in a pre-warmed centrifuge at 32°C, 600g for 1h. After centrifuging, cells were incubated in a tissue culture incubator at 37°C for 2-4h and then collected in 1.5ml centrifuge tubes by centrifugation at 300 g for 5 min at room temperature. Cell pellets were resuspended in 50 ul Matrigel and seeded out in 10 μl matrigel discs in 96-well plates. Plates were inverted and incubated at 37°C for 15 minutes to allow Matrigel to solidify, then overlaid with 100mL of organoid culture medium. Organoid forming efficiency was determined at 7 days post-transfection as described previously[17]. Organoid viability was assessed at 7 days post-transfection using the CellTiter-Glo® Luminescent Cell Viability Assay kit (Promega), as per the manufacturer's instructions.

Statistical Analysis

Statistical analysis for grouped quantitative data were carried out using two-tailed unpaired t-test or ANOVA (GraphPad Prism 7). The relationships between activity scores were determined using Pearson's correlation coefficient (Graphpad Prism 7).

DATA AVAILIBILITY

Ago-HITS-CLIP and RNA-seq data have been deposited with NCBI's Gene Expression Omnibus (accession number GSE137072).

SUPPLEMENTARY INFORMATION

SUPPLEMENTARY TABLES

Supplemetary tables are available in Figshare:
https://adelaide.figshare.com/s/98cb3b341a7f554bae0d

SUPPLEMENTARY FIGURES

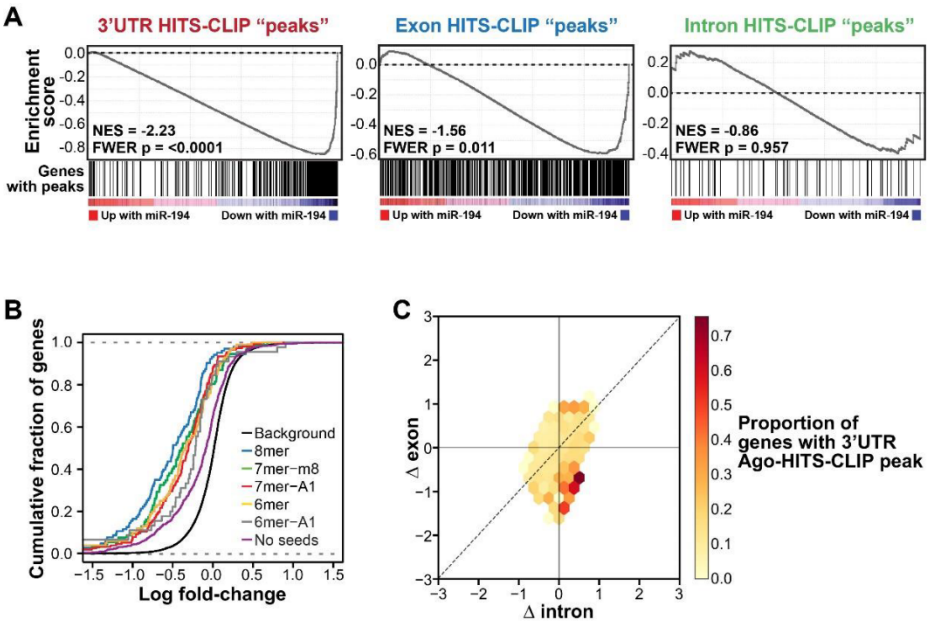

Supplementary Figure S1. Defining a miR-194 targetome. (A) Ago-HITS-CLIP peaks in the 3'UTR of genes are associated with their down-regulation, as determined by GSEA. Genes with peaks in exons were biased towards down-regulation, whereas genes with peaks in introns were not collectively down-regulated. (B) Cumulative distribution of log2 fold change for 3'UTR Ago-HITS-CLIP peaks containing different miR-194 seed recognition sequences or no seeds, compared to a background of all genes with no peaks. (C) Post-transcriptionally downregulated genes will have a negative delta exon (Δ exon) and a positive/no delta intron (Δ intron) or a Δ exon-Δ intron < 0. Post-transcriptionally downregulated genes are mainly concentrated in the bottom right quadrant and close to the y-axis in the bottom left quadrant. Genes that have a negative Δ exon but also a negative Δ intron (such that Δ exon-Δ intron = ≥ 0) are likely to be downregulated at the transcriptional level. The colour of the hexamers indicates percentage of genes with Ago-HITS-CLIP peaks in the 3'UTR.

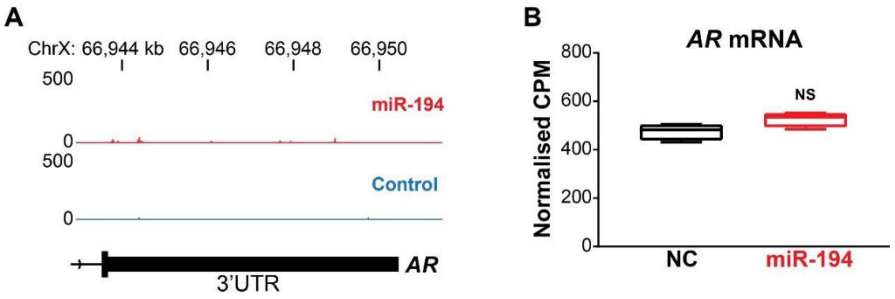

Supplementary Figure S2. No evidence for direct targeting of *AR* by miR-194. (A) Genome tracks from the Ago-HITS-CLIP experiment depicting the average read density of all replicates for each treatment condition (i.e. cells transfected with miR-194 (red) or a scrambled control (black)) at the *AR* 3'UTR. No Ago-HITS-CLIP peaks are evident. (B) *AR* mRNA expression is not altered with miR-194 transfection, as determined by RNA-seq.

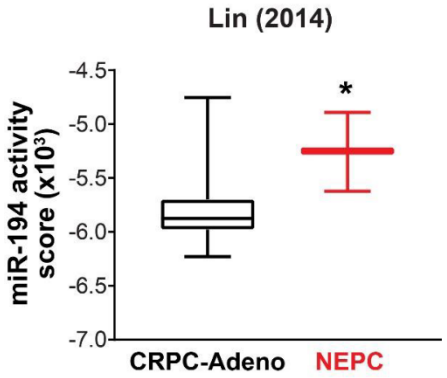

Supplementary Figure S3. MiR-194 activity is higher in neuroendocrine prostate cancer (NEPC) patient-derived xenografts (PDXs) compared to adenocarcinoma CRPC (CRPC-Adeno) PDXs (GSE41192) (Lin et al 2014).

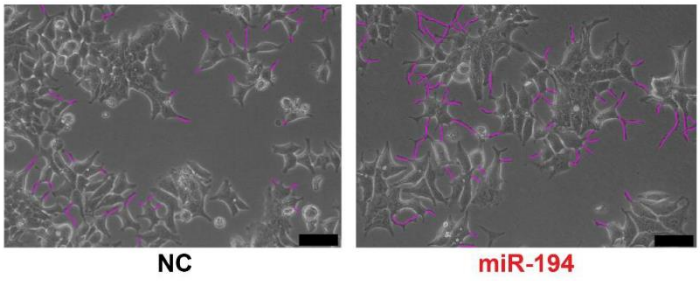

Supplementary Figure S4. Representative phase contrast images of 22Rv1 cells transfected with a miR-194 mimic or a negative control (NC) mimic. Neurite outgrowths are traced in magenta. Scale bars, 25 µm.

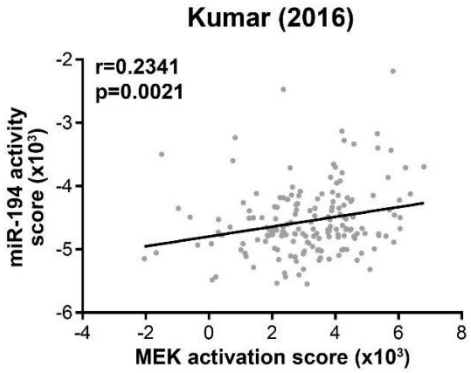

Supplementary Figure S5. MiR-194 activity is positively correlated with MAPK pathway activation in a clinical cohort prostate cancer (Kumar et al 2016).

ACKNOWLEDGEMENTS

This work was supported by the National Health and Medical Research Council of Australia (1121057 to WDT, LAS, RAT and GPR; 1083961 to LAS, WDT, GJG and PAG; 1138242 to GPR, WDT, LAS and MGL; 1002648 to GPR; 1118170 to GJG). PAG is supported by a Beat Cancer Project fellowship from the Cancer Council of South Australia. T.E.H. currently is supported by an NBCF Fellowship (IIRS-19-009). MGL and RAT are supported by Fellowships from the Victorian Government through the Victorian Cancer Agency (MCRF18017 and MCRF15023). The research programs of LMB, WDT and LAS are supported by the Movember Foundation and the Prostate Cancer Foundation of Australia through a Movember Revolutionary Team Awards. Funding for open access charge: National Health and Medical Research Council of Australia.

The authors thank: the Australian Cancer Research Foundation (ACRF) Cancer Genomics Facility for assistance with Ago-HITS-CLIP and RNA-seq; Nicholas Choo (Monash University), Birunthi Niranjan (Monash University), Roxanne Toivanen (Monash University) and Susan Woods (University of Adelaide) for expert technical assistance with organoid culture; Jindan Yu (Northwestern University) for providing a FOXA1 activity gene set; Peter Nelson and Ilsa Coleman (Fred Hutchinson Cancer Research Center) for providing transcriptomic data[75]; and Emily Hackett-Jones (University of South Australia) for assistance with analysis of the Ago-HITS-CLIP data. We acknowledge the team that generated transcriptomic data from CRPC-Adeno and NEPC tumours[6], which we obtained from dbGaP (accession number phs000909). The results published here are in part based on data generated by The Cancer Genome Atlas, established by the National Cancer Institute and the National Human Genome Research Institute, and we are grateful to the specimen donors and relevant research groups associated with this project. Finally, we thank the patients and clinicians who have generously supported the MURAL research platform.

AUTHOR CONTRIBUTIONS

R.C.F, G.J.G. and L.A.S. conceived the project. R.C.F., P.A.G., W.D.T., T.E.H., G.J.G. and L.A.S. designed experiments. R.C.F., S.T., A.R.H., B.K.D., A.G.B. and D.O. performed experiments and acquired data. J.T. and K.A.T. performed bioinformatics analysis. R.I. provided technical assistance. R.D. generated preliminary data. S.S.

recruited patients for generation of PDXs. MURAL investigators established and maintained PDXs. G.P., R.A.T. and M.G.L. provided PDX, organoid and serum samples. R.C.F. and L.A.S. interpreted and analysed all data. L.M.B., A.Z., P.A.G., W.D.T., T.E.H. and G.J.H. contributed to interpreting the data. L.A.S wrote the manuscript. All of the authors have read, edited, and approved the paper

COMPETING INTERESTS

The authors have no conflicts of interest to disclose.

REFERENCES

1. Davies AH, Beltran H, Zoubeidi A. Cellular plasticity and the neuroendocrine phenotype in prostate cancer. *Nat Rev Urol*, (2018).

2. Yuan S, Norgard RJ, Stanger BZ. Cellular Plasticity in Cancer. *Cancer Discov*, (2019).

3. Recine F, Sternberg CN. Hormonal therapy and chemotherapy in hormone-naive and castration resistant prostate cancer. *Transl Androl Urol* **4**, 355-364 (2015).

4. Aggarwal R, *et al.* Clinical and Genomic Characterization of Treatment-Emergent Small-Cell Neuroendocrine Prostate Cancer: A Multi-institutional Prospective Study. *J Clin Oncol* **36**, 2492-2503 (2018).

5. Aparicio A, Logothetis CJ, Maity SN. Understanding the lethal variant of prostate cancer: power of examining extremes. *Cancer Discov* **1**, 466-468 (2011).

6. Beltran H, *et al.* Divergent clonal evolution of castration-resistant neuroendocrine prostate cancer. *Nat Med* **22**, 298-305 (2016).

7. Beltran H, *et al.* Molecular characterization of neuroendocrine prostate cancer and identification of new drug targets. *Cancer Discov* **1**, 487-495 (2011).

8. Das R, *et al.* MicroRNA-194 Promotes Prostate Cancer Metastasis by Inhibiting SOCS2. *Cancer Res* **77**, 1021-1034 (2017).

9. Zhang Y, *et al.* Model-based analysis of ChIP-Seq (MACS). *Genome biology* **9**, R137 (2008).

10. Hafner M, *et al.* Transcriptome-wide identification of RNA-binding protein and microRNA target sites by PAR-CLIP. *Cell* **141**, 129-141 (2010).

11. Taylor BS, *et al.* Integrative genomic profiling of human prostate cancer. *Cancer cell* **18**, 11-22 (2010).

12. Gaidatzis D, Burger L, Florescu M, Stadler MB. Analysis of intronic and exonic reads in RNA-seq data characterizes transcriptional and post-transcriptional regulation. *Nat Biotechnol* **33**, 722-729 (2015).

13. Liberzon A, Birger C, Thorvaldsdottir H, Ghandi M, Mesirov JP, Tamayo P. The Molecular Signatures Database (MSigDB) hallmark gene set collection. *Cell Syst* **1**, 417-425 (2015).

14. Sowalsky AG, *et al.* Neoadjuvant-Intensive Androgen Deprivation Therapy Selects for Prostate Tumor Foci with Diverse Subclonal Oncogenic Alterations. *Cancer research* **78**, 4716-4730 (2018).

15. Cancer Genome Atlas Research Network. Electronic address scmo, Cancer Genome Atlas Research N. The Molecular Taxonomy of Primary Prostate Cancer. *Cell* **163**, 1011-1025 (2015).

16. Robinson D, *et al.* Integrative clinical genomics of advanced prostate cancer. *Cell* **161**, 1215-1228 (2015).

17. Lawrence MG, *et al.* Patient-derived Models of Abiraterone- and Enzalutamide-resistant Prostate Cancer Reveal Sensitivity to Ribosome-directed Therapy. *European urology* **74**, 562-572 (2018).

18. Selth LA, *et al.* Circulating microRNAs predict biochemical recurrence in prostate cancer patients. *Br J Cancer* **109**, 641-650 (2013).

19. Shen R, Dorai T, Szaboles M, Katz AE, Olsson CA, Buttyan R. Transdifferentiation of cultured human prostate cancer cells to a neuroendocrine cell phenotype in a hormone-depleted medium. *Urol Oncol* **3**, 67-75 (1997).

20. Kumar A, *et al.* Substantial interindividual and limited intraindividual genomic diversity among tumors from men with metastatic prostate cancer. *Nat Med* **22**, 369-378 (2016).

21. Guo H, *et al.* ONECUT2 is a driver of neuroendocrine prostate cancer. *Nature communications* **10**, 278 (2019).

22. Osada H, *et al.* Roles of achaete-scute homologue 1 in DKK1 and E-cadherin repression and neuroendocrine differentiation in lung cancer. *Cancer Research* **68**, 1647-1655 (2008).

23. Tsai HK, Lehrer J, Alshalalfa M, Erho N, Davicioni E, Lotan TL. Gene expression signatures of neuroendocrine prostate cancer and primary small cell prostatic carcinoma. *BMC cancer* **17**, 759 (2017).

24. Beltran H, *et al.* Divergent clonal evolution of castration-resistant neuroendocrine prostate cancer. *Nature medicine* **22**, 298 (2016).

25. Ci X, *et al.* Heterochromatin protein 1α mediates development and aggressiveness of neuroendocrine prostate cancer. *Cancer research* **78**, 2691-2704 (2018).

26. Delpuech O, *et al.* Identification of pharmacodynamic transcript biomarkers in response to FGFR inhibition by AZD4547. *Molecular cancer therapeutics* **15**, 2802-2813 (2016).

27. Abida W, *et al.* Genomic correlates of clinical outcome in advanced prostate cancer. *Proceedings of the National Academy of Sciences* **116**, 11428-11436 (2019).

28. Armenia J, *et al.* The long tail of oncogenic drivers in prostate cancer. *Nature genetics* **50**, 645 (2018).

29. Taylor BS, *et al.* Integrative genomic profiling of human prostate cancer. *Cancer cell* **18**, 11-22 (2010).

30. Grasso CS, *et al.* The mutational landscape of lethal castration-resistant prostate cancer. *Nature* **487**, 239 (2012).

31. Bernardo GM, Keri RA. FOXA1: a transcription factor with parallel functions in development and cancer. *Biosci Rep* **32**, 113-130 (2012).

32. Kim J, *et al.* FOXA1 inhibits prostate cancer neuroendocrine differentiation. *Oncogene* **36**, 4072-4080 (2017).

33. Kim J, Adam RM, Freeman MR. Activation of the Erk mitogen-activated protein kinase pathway stimulates neuroendocrine differentiation in LNCaP cells independently of cell cycle withdrawal and STAT3 phosphorylation. *Cancer research* **62**, 1549-1554 (2002).

34. Dry JR, *et al.* Transcriptional pathway signatures predict MEK addiction and response to selumetinib (AZD6244). *Cancer research* **70**, 2264-2273 (2010).

35. Ku SY, *et al.* Rb1 and Trp53 cooperate to suppress prostate cancer lineage plasticity, metastasis, and antiandrogen resistance. *Science* **355**, 78-83 (2017).

36. Mu P, *et al.* SOX2 promotes lineage plasticity and antiandrogen resistance in TP53- and RB1-deficient prostate cancer. *Science* **355**, 84-88 (2017).

37. Li Y, *et al.* SRRM4 Drives Neuroendocrine Transdifferentiation of Prostate Adenocarcinoma Under Androgen Receptor Pathway Inhibition. *European urology* **71**, 68-78 (2017).

38. Bishop JL, *et al.* The Master Neural Transcription Factor BRN2 Is an Androgen Receptor-Suppressed Driver of Neuroendocrine Differentiation in Prostate Cancer. *Cancer Discov* **7**, 54-71 (2017).

39. Qi J, *et al.* Siah2-dependent concerted activity of HIF and FoxA2 regulates formation of neuroendocrine phenotype and neuroendocrine prostate tumors. *Cancer cell* **18**, 23-38 (2010).

40. He B, *et al.* GATA2 facilitates steroid receptor coactivator recruitment to the androgen receptor complex. *Proceedings of the National Academy of Sciences of the United States of America* **111**, 18261-18266 (2014).

41. Vidal SJ, *et al.* A targetable GATA2-IGF2 axis confers aggressiveness in lethal prostate cancer. *Cancer cell* **27**, 223-239 (2015).

42. Dicken H, Hensley PJ, Kyprianou N. Prostate tumor neuroendocrine differentiation via EMT: The road less traveled. *Asian J Urol* **6**, 82-90 (2019).

43. Zhu X, *et al.* miR-194 inhibits the proliferation, invasion, migration, and enhances the chemosensitivity of non-small cell lung cancer cells by targeting forkhead box A1 protein. *Oncotarget* **7**, 13139-13152 (2016).

44. Zhang XQ, Kondrikov D, Yuan TC, Lin FF, Hansen J, Lin MF. Receptor protein tyrosine phosphatase alpha signaling is involved in androgen depletion-induced neuroendocrine differentiation of androgen-sensitive LNCaP human prostate cancer cells. *Oncogene* **22**, 6704-6716 (2003).

45. Chen H, *et al.* Pathogenesis of prostatic small cell carcinoma involves the inactivation of the P53 pathway. *Endocrine-related cancer* **19**, 321-331 (2012).

46. Labbe DP, Brown M. Transcriptional Regulation in Prostate Cancer. *Cold Spring Harb Perspect Med* **8**, (2018).

47. Nam RK, *et al.* MicroRNA-652 induces NED in LNCaP and EMT in PC3 prostate cancer cells. *Oncotarget* **9**, 19159-19176 (2018).

48. Fernandes R, Hickey T, Tilley WD, Selth LA. Interplay between the androgen receptor signalling axis and microRNAs in prostate cancer. *Endocrine-related cancer*, (2019).

49. Kreth S, Hubner M, Hinske LC. MicroRNAs as Clinical Biomarkers and Therapeutic Tools in Perioperative Medicine. *Anesth Analg* **126**, 670-681 (2018).

50. Chi SW, Zang JB, Mele A, Darnell RB. Argonaute HITS-CLIP decodes microRNA–mRNA interaction maps. *Nature* **460**, 479 (2009).

51. Jensen KB, Darnell RB. CLIP: crosslinking and immunoprecipitation of in vivo RNA targets of RNA-binding proteins. In: *RNA-Protein Interaction Protocols* (ed^(eds). Springer (2008).

52. Van Nostrand EL, *et al.* Robust transcriptome-wide discovery of RNA-binding protein binding sites with enhanced CLIP (eCLIP). *Nature methods* **13**, 508 (2016).

53. Pillman KA, *et al.* miR-200/375 control epithelial plasticity-associated alternative splicing by repressing the RNA-binding protein Quaking. *The EMBO journal* **37**, (2018).

54. Ikeda K, Satoh M, Pauley KM, Fritzler MJ, Reeves WH, Chan EK. Detection of the argonaute protein Ago2 and microRNAs in the RNA induced silencing complex (RISC) using a monoclonal antibody. *Journal of immunological methods* **317**, 38-44 (2006).

55. Martin M. Cutadapt removes adapter sequences from high-throughput sequencing reads. *EMBnet journal* **17**, 10-12 (2011).

56. Kim D, Pertea G, Trapnell C, Pimentel H, Kelley R, Salzberg SL. TopHat2: accurate alignment of transcriptomes in the presence of insertions, deletions and gene fusions. *Genome biology* **14**, R36 (2013).

57. Li H, *et al.* The sequence alignment/map format and SAMtools. *Bioinformatics* **25**, 2078-2079 (2009).

58. Heinz S, *et al.* Simple combinations of lineage-determining transcription factors prime cis-regulatory elements required for macrophage and B cell identities. *Molecular cell* **38**, 576-589 (2010).

59. Thorvaldsdóttir H, Robinson JT, Mesirov JP. Integrative Genomics Viewer (IGV): high-performance genomics data visualization and exploration. *Briefings in bioinformatics* **14**, 178-192 (2013).

60. Dobin A, *et al.* STAR: ultrafast universal RNA-seq aligner. *Bioinformatics* **29**, 15-21 (2013).

61. Robinson MD, McCarthy DJ, Smyth GK. edgeR: a Bioconductor package for differential expression analysis of digital gene expression data. *Bioinformatics* **26**, 139-140 (2010).

62. Lun AT, Chen Y, Smyth GK. It's DE-licious: a recipe for differential expression analyses of RNA-seq experiments using quasi-likelihood methods in edgeR. In: *Statistical Genomics* (ed^(eds). Springer (2016).

63. Su S, Law CW, Ah-Cann C, Asselin-Labat M-L, Blewitt ME, Ritchie ME. Glimma: interactive graphics for gene expression analysis. *Bioinformatics* **33**, 2050-2052 (2017).

64. Pillman KA, *et al.* Extensive transcriptional responses are co-ordinated by microRNAs as revealed by Exon–Intron Split Analysis (EISA). *Nucleic acids research*, (2019).

65. Subramanian A, *et al.* Gene set enrichment analysis: a knowledge-based approach for interpreting genome-wide expression profiles. *Proceedings of the National Academy of Sciences* **102**, 15545-15550 (2005).

66. Robinson D, *et al.* Integrative clinical genomics of advanced prostate cancer. *Cell* **161**, 1215-1228 (2015).

67. Abeshouse A, *et al.* The molecular taxonomy of primary prostate cancer. *Cell* **163**, 1011-1025 (2015).

68. Barbie DA, *et al.* Systematic RNA interference reveals that oncogenic KRAS-driven cancers require TBK1. *Nature* **462**, 108 (2009).

69. Moore NL, *et al.* An androgen receptor mutation in the MDA-MB-453 cell line model of molecular apocrine breast cancer compromises receptor activity. *Endocrine related cancer* **19**, 599 (2012).

70. Longair MH, Baker DA, Armstrong JD. Simple Neurite Tracer: open source software for reconstruction, visualization and analysis of neuronal processes. *Bioinformatics* **27**, 2453-2454 (2011).

71. Meijering E, Jacob M, Sarria JC, Steiner P, Hirling H, Unser M. Design and validation of a tool for neurite tracing and analysis in fluorescence microscopy images. *Cytometry Part A: the journal of the International Society for Analytical Cytology* **58**, 167-176 (2004).

72. Porter LH, *et al.* Establishing a cryopreservation protocol for patient-derived xenografts of prostate cancer. *The Prostate* **79**, 1326-1337 (2019).

73. Beshiri ML, *et al.* A PDX/organoid biobank of advanced prostate cancers captures genomic and phenotypic heterogeneity for disease modeling and therapeutic screening. *Clinical Cancer Research* **24**, 4332-4345 (2018).

74. Broutier L, *et al.* Culture and establishment of self-renewing human and mouse adult liver and pancreas 3D organoids and their genetic manipulation. *Nature protocols* **11**, 1724 (2016).

75. Bluemn EG, *et al.* Androgen Receptor Pathway-Independent Prostate Cancer Is Sustained through FGF Signaling. *Cancer cell* **32**, 474-489 e476 (2017).

Chapter 4: Mechanisms underlying miR-194 regulation of target genes in prostate cancer

Introduction

MiRNAs, as post-transcriptional regulators of gene expression, are key players in numerous biological processes. MiRNA precursors are processed in the nucleus and cytoplasm into mature miRNA, which are then incorporated into an RNA-induced silencing complex (RISC) (Ha & Kim 2014; Kobayashi & Tomari 2016). Target recognition depends on base pairing between complementary sequences in mRNA transcripts and mature miRNA in the RISC (Ha & Kim 2014).

Structurally, mature miRNA strands can be divided into 5 domains: 5′ anchor (nucleotide 1), seed sequence (nucleotides 2–8), central region (nucleotides 9–12), 3′ supplementary region (nucleotides 13–16) and 3′ tail (nucleotides 17–22) (Figure 4.1A) (Wee et al. 2012). Canonical target recognition occurs via base pairing between miRNA seed sequences and conserved complementary sequences in the target transcript, although interactions with seed distal regions (i.e. 3'region of miRNA) can also be important for miRNA mediated silencing (Bartel 2009; Moore et al. 2015). Seed matches on target transcripts can be separated into 4 main types based on the extent of complementarity to the miRNA seed: "6mer" sites have perfect complementarity with the miRNA seed, "7mer-m8" sites match with the seed and nucleotide 8 on the miRNA, "7mer-A1" sites have a perfect seed math and a supplementary A across from nucleotide 1 on the miRNA and "8mer" sites have a match with nucleotide 8 and A at position 1 in addition to a perfect seed match (Figure 4.1B) (Grimson et al. 2007). Additional seed types include "offset 6mer" which have a perfect match with nucleotides 3-8 on the miRNA and "6mer-A1" sites matching nucleotides 1-6 on miRNA (Ellwanger et al. 2011; Friedman et al. 2009). Efficiency of target downregulation is generally dependent on the seed match type, with 8mer>7mer-m8>7mer-A1>6mer>offset-6mer>6mer-A1 (Agarwal et al. 2018; Grimson et al. 2007).

Non-canonical targeting by miRNA includes imperfect seed matches or weak pairing at the 5'end supplemented by strong pairing at the 3'end (Figure 4.1C), bulged sites involving the nucleotide opposite position 6 bulging out (Figure 4.1D) (Liu et al. 2011) and centered sites where there is complementarity between nucleotides in the centre of the miRNA and the target (Figure4.1E) (Bartel 2009; Shin et al. 2010).

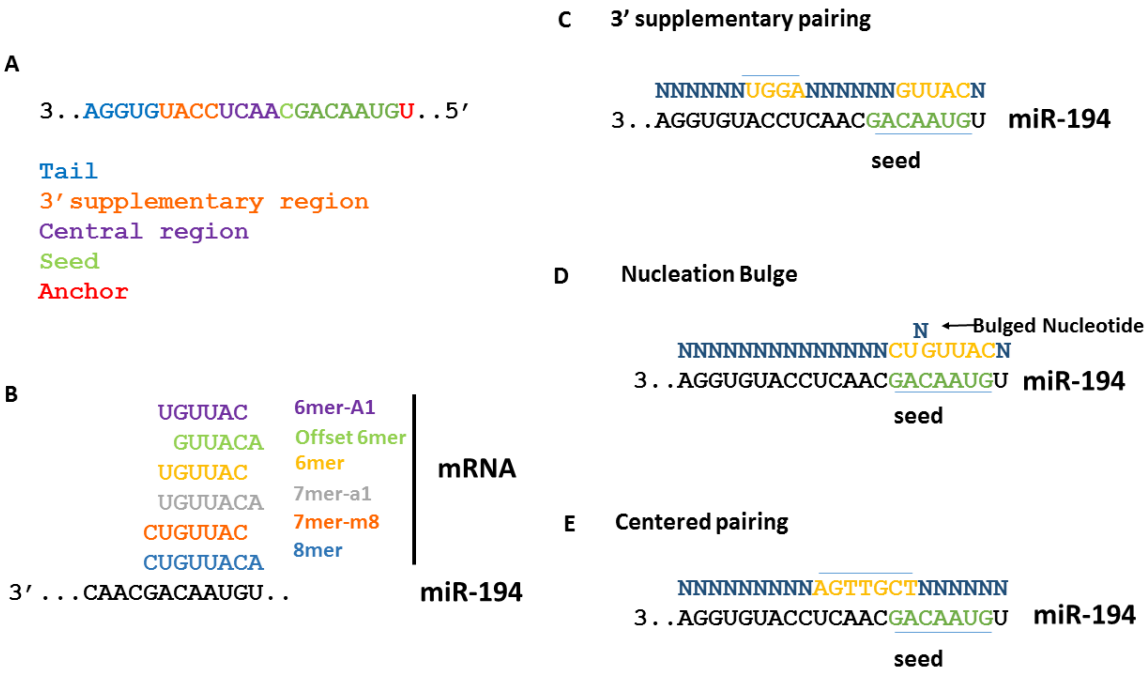

Figure 4.1: (A) miR-194 sequence depicting different regions. (B) Types of miR-194 canonical seed sequences. (C-E). Putative non-canonical target recognition by miR-194 (B-D).

MiRNA:mRNA interactions are usually characterized as occurring at the 3'UTR of target transcripts and resulting in post-transcriptional repression, however miRNAs can bind to other regions of a transcript and induce post-transcriptional upregulation in some instances (Chi et al. 2009; Forman & Coller 2010; Vasudevan 2012). An abundance of miRNA binding sites have been found in coding sequences (CDS) but generally do not lead to downregulation of target mRNAs as effectively as 3'UTR sites. As another point of difference, CDS sites appear to always act by repressing translation rather than destabilizing mRNA (Hausser et al. 2013).

Predicting functional miRNA binding sites is difficult. A key component of computational prediction tools is that they also incorporate the evolutionary conservation of predicted sites; sites that are conserved are more likely to be biologically relevant (Bartel 2009). Besides conservation, prediction algorithms also rely on stringent seed pairing rules, free energy analysis of hybridization between miRNA and its target, and site accessibility (Peterson et al. 2014). Despite these features, predictions algorithms are associated with several drawbacks including high rate of false positives and negatives, a tendency to focus only on 3'UTR sites and canonical sites, and a failure to account for tissue specificity of miRNA (M Witkos, Koscianska & J Krzyzosiak 2011; Ovando-

Vázquez, Lepe-Soltero & Abreu-Goodger 2016). To overcome these limitations, crosslinking immunoprecipitation (CLIP)-based methods combined with bioinformatics analysis are being used to experimentally map functional miRNA binding sites. One such method, Ago-HITS-CLIP (high-throughput sequencing of RNAs isolated by crosslinking immunoprecipitation), uses UV-irradiation to covalently crosslink miRNA:mRNA:Argonaute complexes within cells. These complexes are purified using antibodies against the Argonaute protein and bound mRNA fragments are identified by sequencing. Ago-HITS-CLIP has high specificity and low false positive and false negative rates (Chi et al. 2009; Neame 2009).

CLIP in combination with gene expression changes following miRNA perturbation has been used to elucidate targetomes and functionally characterize specific miRNA and their role in disease (Bracken et al. 2014; Loeb et al. 2012; Xu et al. 2010). Changes in gene expression caused by miRNA overexpression or knockdown are often assessed using RNA sequencing (RNA-seq). One drawback of using this method, however, is that miRNAs alter levels of target genes transcripts at the post-transcriptional level but standard RNA-seq outputs do not distinguish if expression changes occur at the transcriptional or post-transcriptional level. Standard RNA-seq is therefore unable to distinguish between direct and indirect effects of miRNA on gene expression. Exon Intron Split Analysis (EISA), a powerful computational method that can use sequencing reads for RNA-seq to identify transcriptional or post-transcriptional expression changes, can be used to overcome this issue (Gaidatzis et al. 2015). Across experimental conditions, EISA quantitates the difference between intronic reads (dIntron) which is a measure transcriptional changes or between exon and intron reads (dExon-dIntron) a measure of post-transcriptional regulation (Gaidatzis et al. 2015). EISA has been previously used to determine direct post-transcriptionally downregulated miRNA target genes (Gaidatzis et al. 2015; Pillman et al. 2019).

In the previous Chapter, I described how we used Ago-HITS-CLIP and EISA to identify miR-194 target genes in prostate cancer (PCa). In this Chapter, I examine this data in more detail to provide insights into the function of this miRNA, and miRNA biology more broadly.

Materials and methods

Details of cell lines, transfections, qPCR, HITS-CLIP, RNA-seq and EISA are described in Chapter 3.

Identification of miR-194 non-canonical binding in the 3'UTR

Genomic sequences for peaks without miR-194 seed matches ("seedless peaks") were obtained from peak coordinates using bedtools GetFastaBed in Galaxy (https://usegalaxy.org/). Genomic sequences were assessed for presence of enriched motifs using the SeqPos motif tool in Cistrome (http://cistrome.org/ap/). In a set of sequences, SeqPos finds motifs enriched near the centre of the regions i.e. motifs enriched near peak summits. The FIMO tool in Meme Suite (http://meme-suite.org) was used to scan for de-novo motif identified by SeqPos and specific motifs in seedless peaks.

ECDF curves and Kolmogorov–Smirnov (KS) tests

Cumulative distribution function graphs, to represent changes in expression of genes of interest, were plotted using the ecdf function in R. Statistical significance of differences in cumulative distribution function were calculated using the Kolmogorov–Smirnov (KS) test. KS tests were performed in R.

3'complementary binding analysis for CDS sites

RNAduplex was used to determine base pairing interaction between miR-194 and CDS peak regions. Only interactions with a binding energy ΔD of <-15 and base pairing of 6 perfect matches at the 3' end of the miR, with a possible mismatch at the very end were considered.

Results

Functional effects of miR-194 binding sites identified by Ago-HITS-CLIP

To identify miR-194:target interactions in PCa, we performed Ago-HITS-CLIP analysis on 22RV1 cells transfected with a miR-194 mimic or a control mimic, as described in Chapter 3. Genomic annotation of the peaks revealed that the majority occurred in the coding regions (36%), followed by the 3'UTR (23.4%) and introns (22%). Other regions with miR-194 binding included promoters (5.5%), transcription termination sites (TTS) (5.4%), intergenic regions (5.2%), 5'UTRs (1.5%), non-coding RNAs (0.6%) and pseudogenes (0.1%). Since binding in the 3'UTR, 5'UTR, CDS and introns has been associated with miRNA functional effects (Bartel 2009; Hausser et al. 2013; Meng et al. 2013; Ørom, Nielsen & Lund 2008), we have focussed primarily on these regions in this study.

To determine the effect of miR-194 binding on transcript levels, we have used RNA-seq to compare changes in gene expression between 22RV1 cells transfected with a miR-194 mimic or a control mimic. RNA-seq data was further processed by EISA to obtain post-transcriptional changes (dExon-dIntron) in gene expression. Post-transcriptional changes in gene expression (from EISA) were used for all analyses in this chapter.

Changes in transcript levels for genes with Ago-HITS-CLIP peaks in different regions of the transcript were plotted as a cumulative distribution. As expected, we found that genes with Ago binding sites in the 3'UTR have a very strong bias towards downregulation ($p< 2.2\times10^{16}$), whereas CDS ($p= 2.58\times10^{12}$) and 5'UTR (2.821×10^{05}) peaks are associated with modest changes in transcript downregulation (Figure 4.2B). Interestingly, changes in gene expression for intron peaks (p=0.03196) had a small bias towards upregulation (Figure 4.2B).

A panel of sixteen genes, with Ago-HITS-CLIP peaks in the 3'UTR and showing post-transcriptional downregulation with EISA, were validated by qPCR in the 22RV1 cell line. 14 out of the 16 genes tested were downregulated with 9 genes showing significant downregulation (Figure 4.2C).

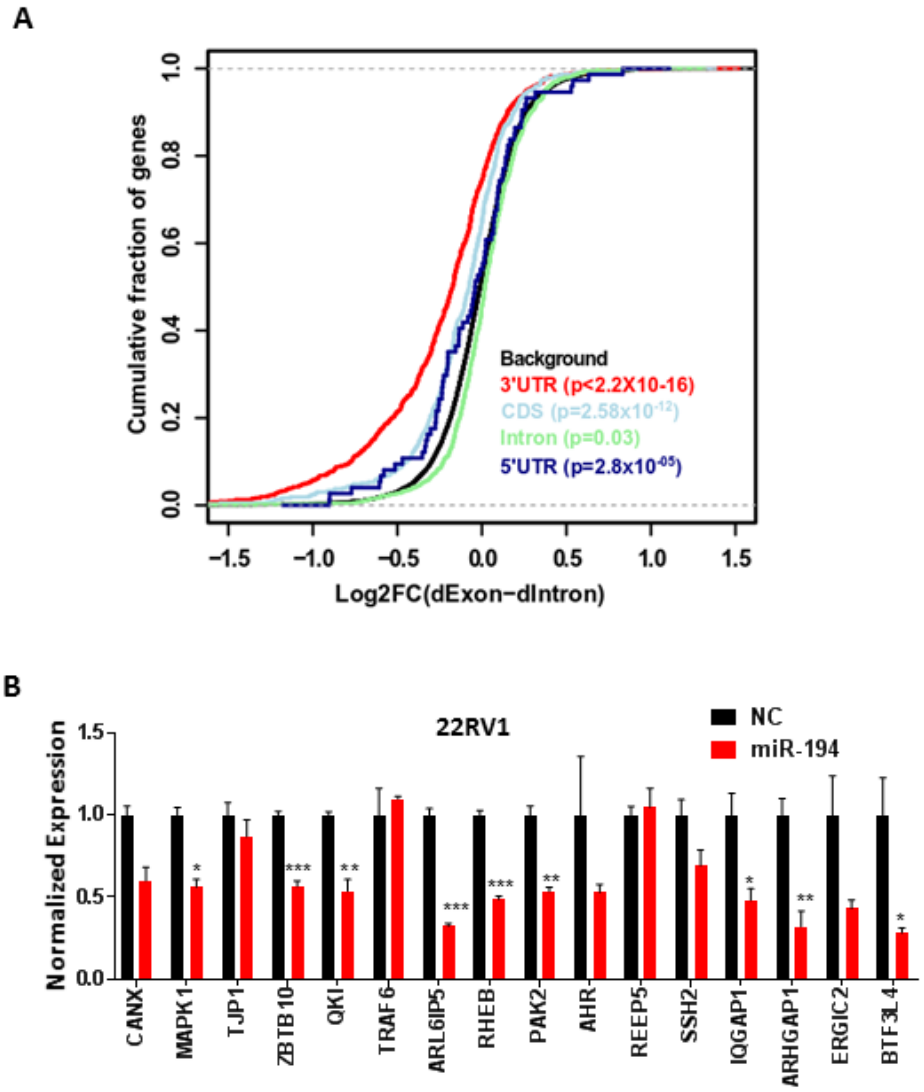

Figure 4.2: miR-194 binding sites are associated with reduced transcript levels. (A) Cumulative distribution of log2 fold change for genes with peaks in the 3'UTR, CDS, Introns and 5'UTR compared to background of all genes with no peaks. Numbers in parenthesis indicate p value compared to background. P values were determined by KS test. (B) Validation of miR-194 target genes identified by HITS-CLIP and EISA in the 22RV1 cell line. Cell lines were transiently transfected with a miR-194 mimic or negative control (NC) for 36h. p-values were determined by two tailed student's t test. (*, $p < 0.05$; **, $p < 0.01$;***, $p<0.001$; ****, $p<0.0001$).

Association of seed match with repression in 3'UTR and CDS binding sites

The efficacy of miRNA downregulation often correlates with the target transcript's seed type, with longer seed matches resulting in stronger repression (Grimson et al. 2007). To evaluate the impact of seed match on miR-194 target gene repression, we identified all canonical 8mer, 7mer and 6mer seed matches in Ago-HITS-CLIP peaks. Of the canonical miR-194 seed matches (Figure 4.3A), 7mer-A1 sites were the most enriched in both the 3'UTR and the CDS (Figure 4.3A) (Table 4.1). In the 3'UTR, 8mer, 7mer-m8 and 6mer sites were almost equally enriched whereas 6mer-A1 sites were less common. In the CDS, 7mer-m8, 6mer and 6mer-A1 sites were more common compared to 8mer sites (Figure 4.3A). The CDS also had five offset 6mer sites which were not seen in the 3'UTR. MiR-194 seed matches were rare in 5'UTR and intron peaks. In the 5'UTR, only 7 out of 120 peaks had miR-194 seed matches whereas in the intron, 84 out of 1730 peaks had seed matches. 5'UTR and intron seed matches were mainly 8mer, 7mer-m8 and 7mer-A1 (Figure 4.3A) (Table 4.1).

To test how different seed types were associated with changes in target mRNA levels, we plotted post-transcriptional changes in gene expression as cumulative distribution fractions for transcripts containing single seed matches (Figure 4.3C,D). All miR-194 seed types in the 3'UTR were significantly associated with downregulation of target transcripts compared to background (KS test, $p<10^{-5}$). Similar to what has been reported for other miRNAs (Bracken et al. 2014; Grimson et al. 2007), targets with 8-mer 3'UTR sites were associated with significantly more robust target downregulation compared to targets with 7mer-A1 (p=0.0001536) and 6-mer (p=0.006177) sites; there appeared to be a trend towards stronger repression of 8-mer sites compared to 7mer-m8 and 6mer-a sites, but the differences between these groups were not significant. In summary, for miR-194 sites in the 3'UTR, seed associated repression efficacy was 8mer>7mer-m8=6mer-A1>6mer>7mer-A1.

Repression of target genes with seed matches in the CDS occurred to a much smaller extent than 3'UTR sites, with only 8mer (p=0.03007), 7-mer-m8 (p=0.004165) and 7-mer-A1 ($1.66\times10\text{^}0^{-5}$) sites significantly repressing target genes over background (Figure 4.3B). Both CDS 6mer and 6mer-A1 sites repress expression to a lesser extent than other seed matches, and as a whole do not significantly reduce transcript levels.

Seed matches occurred infrequently in the 5'UTR and introns. Out of 1,107 genes with intronic peaks, only 71 had a canonical seed match in these regions. More than half of these genes were downregulated (Table 4.1) but strong downregulation was only observed for genes that also had a 3'UTR or CDS peak. Only 7 out of 95 genes were associated with a canonical seed match in the 5'UTR (Table 4.1).

In summary, although miR-194 can binds to the 3'UTR, CDS, 5'UTR and introns, the strongest effects on transcript levels are observed for binding at 8mer sites in the 3'UTR of target genes.

	8mer	7mer-m8	7mer-A1	6mer	6mer-A1	Offset 6mer	No seed
3'UTR	108 (93DN, 2UP)	98 (71DN, 12UP)	159 (122DN, 20UP)	99 (77DN, 9UP)	46 (38DN, 5UP)	-	713 (426DN, 162UP)
CDS	106 (68DN, 24UP)	127 (79DN, 34UP)	147 (97DN, 36UP)	131 (70DN, 51UP)	123 (62DN, 44UP)	5 (2DN, 2UP)	1280 (590DN, 478UP)
Intron	41 (21DN, 15UP)	5 (4DN, 1UP)	22 (15DN, 5UP)	-	-	2 (2DN)	1036 (369DN, 453UP)
5'UTR	3 (3DN)	2 (1DN, 1UP)	2 (1DN)	-	-	-	91 (37DN, 34UP)

Table 4.1: Distribution of genes with canonical seed matches or no seeds in the 3'UTR, CDS, introns and 5'UTR regions of transcripts. Number in parenthesis indicates number of genes that are post-transcriptionally downregulated (DN) or upregulated (UP). Expression values not available for some genes.

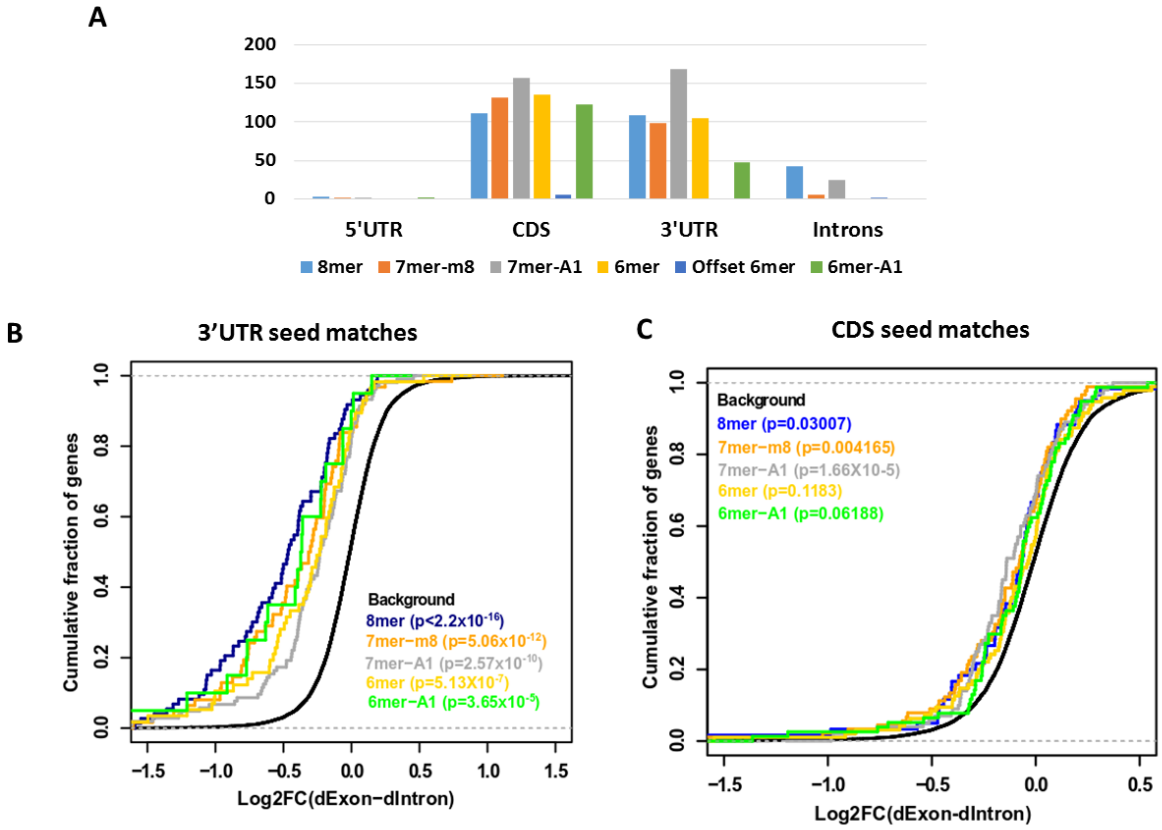

Figure 4.3: 3'UTR seed matches are more functional than CDS seed matches. (A) Distribution of miR-194 canonical seed matches in 5'UTR, CDS, 3'UTR and intron peaks. (B) Cumulative distribution of log2 fold change for genes with canonical seed matches in the 3'UTR. Numbers in parenthesis indicate p value compared to background. P values were determined by KS test. (C) Cumulative distribution of log2 fold change for genes with canonical seed matches in the CDS. Numbers in parenthesis indicate p value compared to background. P values were determined by KS test.

Multiple miR-194 sites work cooperatively to repress target genes

The presence of multiple seeds within a single transcript has previously been shown to increase the effective of miRNA repression (Fang & Rajewsky 2011; Grimson et al. 2007). Previous reports have found that 8mer seed matches in combination with other seed matches are more effective at reducing target mRNA stability than combinations of other seed types (Grimson et al. 2007). In addition, seed matches in the CDS have been shown to act additively with 3'UTR sites (Fang & Rajewsky 2011).

We determined the number of canonical seeds in all miR-194 targets and found that the majority of target transcripts harbour single seeds in the 3'UTR or the CDS (Figure 4.4A), with only 16% and 12% of target transcripts having multiple seed sites in the 3'UTR and CDS, respectively. The presence of seeds in both the 3'UTR and CDS of a single transcript is much more uncommon (~2.5% of targets). In the 3'UTR, 7mer-A1 and 6mer seed matches are more likely to be present in combination with other seeds (Figure 4.4B). In the CDS, 7mer-a1 and 6mer sites are most likely to occur in combination with other sites (Figure 4.4C).

To test if multiple miR-194 seed matches can act cooperatively to repress targets, we assessed changes in expression of genes containing 2 or more seed sequences vs genes with single sites (Figure 4.4D). 8mers in combination with 7mers or 6mers were not in general associated with stronger mRNA dysregulation than 8mers alone ($p=0.4428$) (Figure 4.4D), but it must be noted that there is only a few transcripts in this group ($n=20$). Combinations of 7 or 6-mer sites, however, were significantly more effective than single 7-mer or 6-mer sites alone ($p=0.008857$). Multiple sites in the CDS moderately increased target repression compared to single CDS sites ($p=0.005813$) (Figure 4.4E). However, combination of a 3'UTR site and a CDS site do not significantly downregulate expression compared to transcripts with single 3'UTR seeds ($p=0.5151$) (Figure 4.4F).

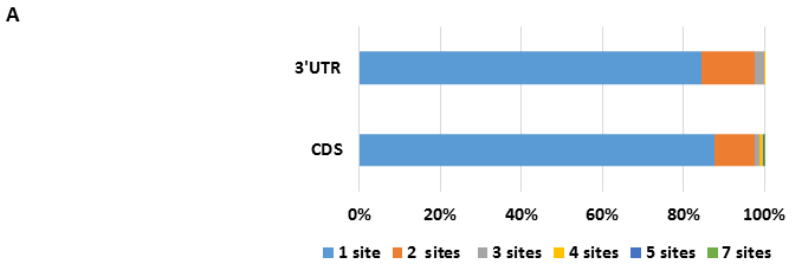
A
3'UTR
CDS
0%
20%
40%
60%
80%
100%
1 site
2 sites
3 sites
4 sites
5 sites
7 sites

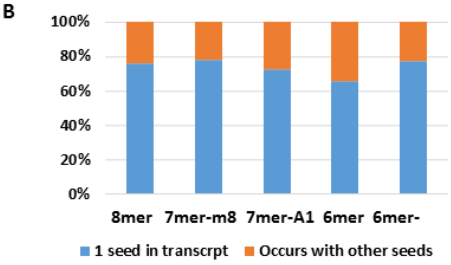
B
100%
80%
60%
40%
20%
0%
8mer
7mer-m8
7mer-A1
6mer
6mer-
1 seed in transcrpt
Occurs with other seeds

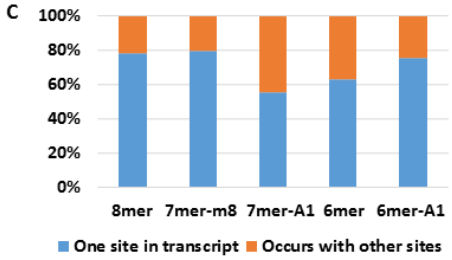
C
100%
80%
60%
40%
20%
0%
8mer
7mer-m8
7mer-A1
6mer
6mer-A1
One site in transcript
Occurs with other sites

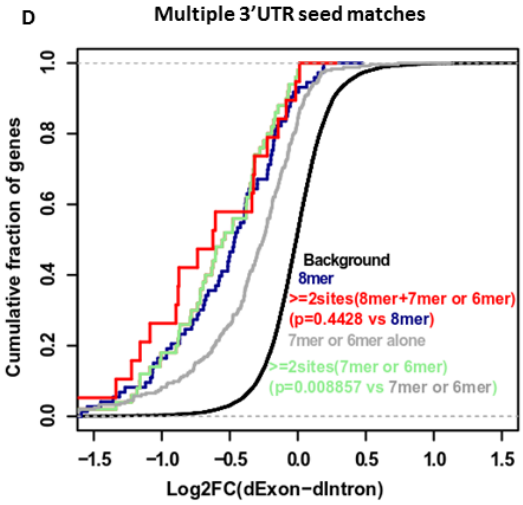
D
Multiple 3'UTR seed matches
Cumulative fraction of genes
Log2FC(dExon−dIntron)
Background
8mer
>=2sites(8mer+7mer or 6mer)
(p=0.4428 vs 8mer)
7mer or 6mer alone
>=2sites(7mer or 6mer)
(p=0.008857 vs 7mer or 6mer)

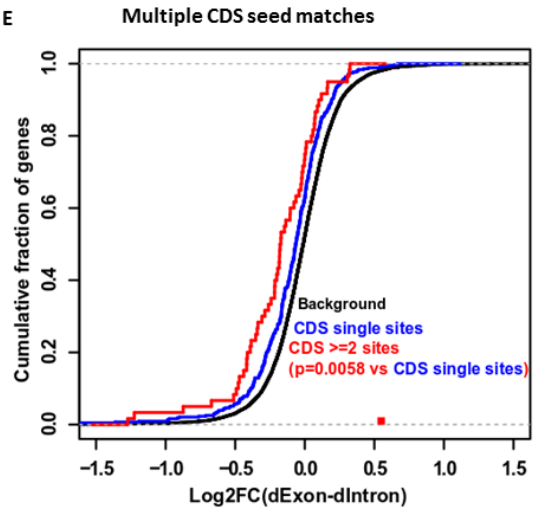
E
Multiple CDS seed matches
Cumulative fraction of genes
Log2FC(dExon-dIntron)
Background
CDS single sites
CDS >=2 sites
(p=0.0058 vs CDS single sites)

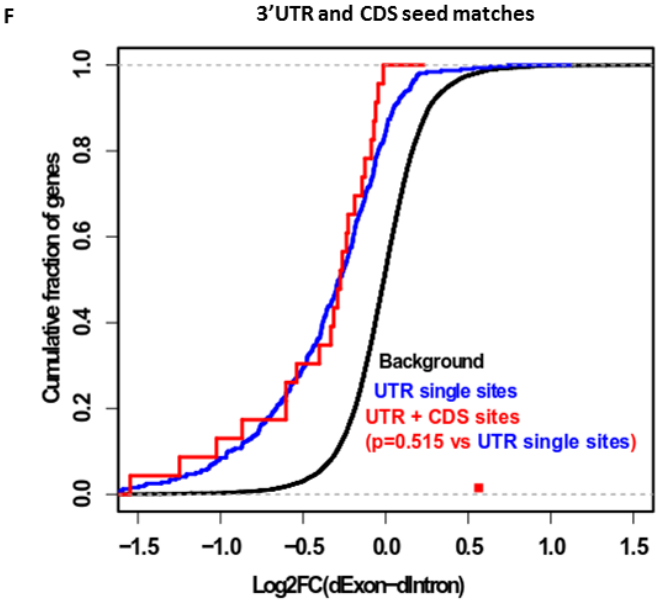
F
3'UTR and CDS seed matches
Cumulative fraction of genes
Log2FC(dExon−dIntron)
Background
UTR single sites
UTR + CDS sites
(p=0.515 vs UTR single sites)

Figure 4.4: miR-194 binding sites work cooperatively to reduce target mRNA stability. (A) Distribution of transcripts with 1 or more miR-194 seeds in the 3'UTR and CDS. (B) Occurrence of different seed matches per transcript in the 3'UTR. (C) Occurrence of different seed matches per transcript in the CDS. (D) Cumulative distribution of log2 fold change for genes for genes with single or multiple seed matches in the 3'UTR of the same transcript. (E) Cumulative distribution of log2 fold change for genes for genes with single or multiple seed matches in the CDS. (F) Cumulative distribution of log2 fold change for genes for genes with a single 3'UTR seed match or combinations of a 3'UTR seed with one or more CDS seed matches in the same transcript.

MiR-194 is associated with non-canonical binding in the 3'UTR and CDS

MiRNA CLIP experiments have helped identify a range of non-canonical miRNA: target interactions that do not rely on perfect seed matches but are associated with nucleation bulges, mismatches, wobbles, centred pairing and/ or complementarity with the 3' and 5' ends of miRNA. Non-canonical interactions are widespread and may occur for up to 60% of miRNA: target interactions in the 3'UTR (Helwak et al. 2013; Moore et al. 2015).

Approximately 70% (1,314 peaks) of 3'UTR Ago-HITS-CLIP peaks did not have a canonical seed match for miR-194 (Figure 4.5A). To determine whether miR-194 was associated with non-canonical binding in these sites, we used the SeqPos tool on Cistrome (Liu et al. 2011) to search for enriched sequences. SeqPos identified 2 motifs (p-value > 0.001), with the most significant motif (-log10 pvalue=102) resembling a miR-194 7mer-m8 seed sequence with mismatches at nucleotide positions position 8 and 4 (Figure 4.5B). The other enriched motif (-log10 pvalue=74.929) (Figure 4.5C) did not correspond to any part of the miR-194 sequence. We next used the FIMO tool (Find Individual Motif Occurrences) on MEME suite (Bailey et al. 2009) to scan all 1314 "seedless" peaks for presence of the "mismatched" miR-194 motif, with a p-value filter of 0.001 for output, shown in Figure 4.5B, and found 199 occurrences. To assess effects of the mismatched motif on gene regulation, we evaluated expression of targets with one or more mismatched sites in the 3'UTR but no canonical 3'UTR seed sequence against background. Our results indicate that sites with a mismatched miR-194 seed sites are indeed functional based on reduced transcript levels ($p=6.482\times10^{-5}$) (Figure 4.5D). The other identified motif (Figure 4.5C) was not associated with decreased transcript levels.

In addition to mismatches, we used FIMO to scan for complementarity to the central region (centred sites) of the miRNA, nucleation bulges, and other possible mismatches to the miR-194 seed sequence that might occur at low frequency (Figure 4.5E). No evidence for centred pairing was found in any of the seedless peaks, suggesting that miR-194 does not function through this mode of non-canonical binding. A perfect nucleation bulge was found in only 6 seedless peaks, indicating this is not a major mode of miR-194 action. We also found evidence for multiple seed mismatch sequences at low frequency within seedless peaks.

A recent study has identified a novel miRNA recognition element in the CDS of target genes that is dependent on extensive binding to the 3' end of the miRNA rather than the seed sequence and only functions in the context of the CDS (Zhang et al. 2018). This mode of miRNA regulation does not result in transcriptional repression but inhibits translation (Zhang et al. 2018). We found 106 sites that meet the criteria for this type of miRNA: target interaction in our HITS-CLIP dataset. An example of this type of interaction between miR-194 and the CDS of the *LAPTM4A* transcript is depicted in Figure 4.5F. Figure 4.5G depicts Ago-HITS-CLIP peaks in the non-canonical binding site in the *LAPTM4A* CDS. These transcripts showed a trend towards downregulation at the transcript level (p=0.07) compared to background (Figure 4.5H). The functional relevance of this interaction remains to be assessed.

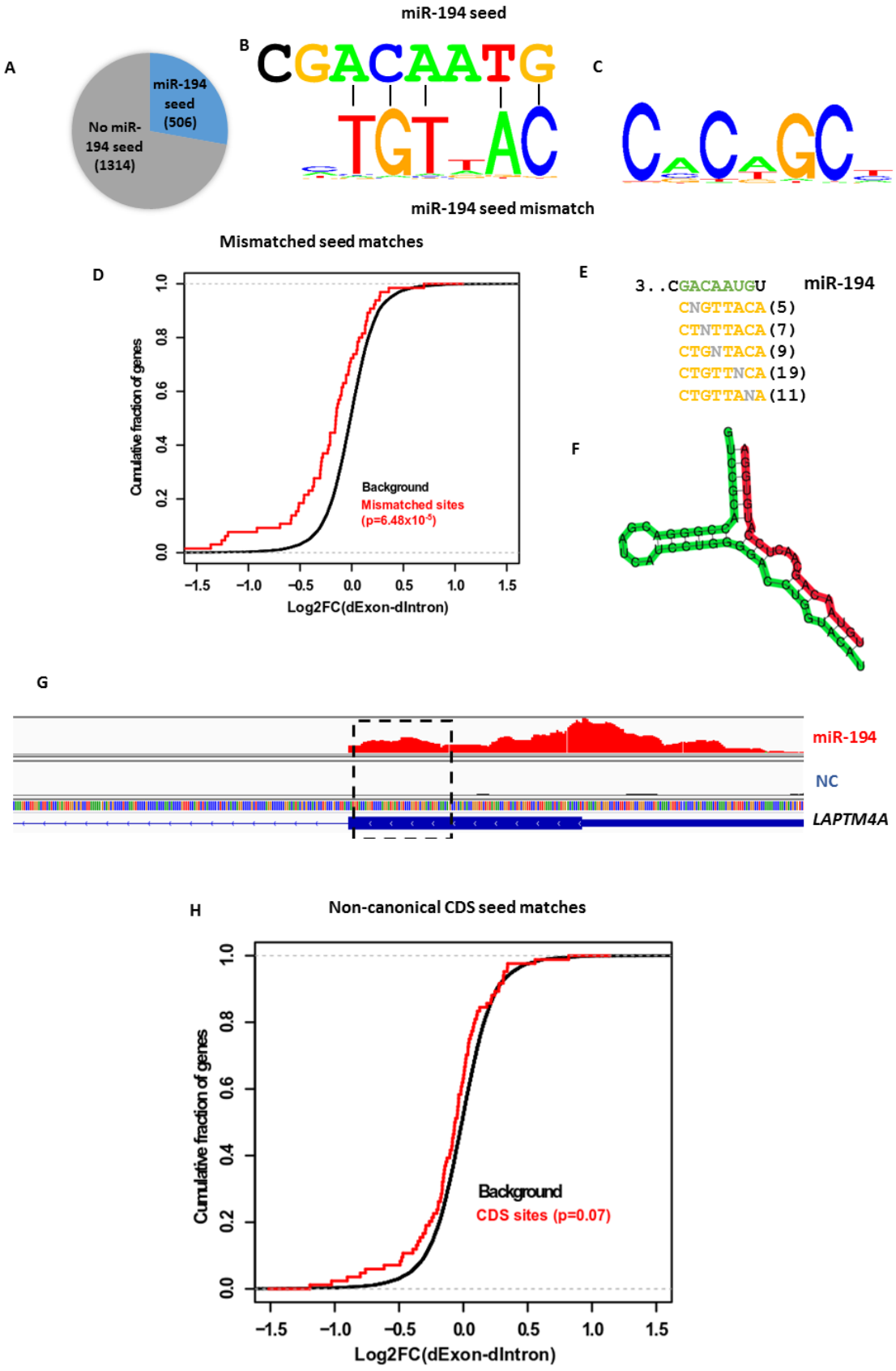
A
miR-194 seed (506)
No miR-194 seed (1314)
B
miR-194 seed
C
miR-194 seed mismatch
D
Mismatched seed matches
Cumulative fraction of genes
Background
Mismatched sites (p=6.48x10-5)
Log2FC(dExon-dIntron)
E
3..CGACAAUGU miR-194
CNGTTACA(5)
CTNTTACA(7)
CTGNTACA(9)
CTGTTNCA(19)
CTGTTANA(11)
F
G
miR-194
NC
LAPTM4A
H
Non-canonical CDS seed matches
Cumulative fraction of genes
Background
CDS sites (p=0.07)
Log2FC(dExon-dIntron)

Figure 4.5: miR-194 is associated with non-canonical binding to target genes. (A) Distribution of peaks with and without miR-194 seed motifs in the 3'UTR. (B) Motif found enriched in seedless peaks using the SeqPos tool represents a mismatched miR-194 seed match sequence. (C) Motif found enriched in seedless peaks using the SeqPos tool that does not match any region of miR-194. (D) Cumulative distribution of log2 fold change for genes with a mismatched miR-194 seed match in the 3'UTR.Numbers in parenthesis indicate p value versus background. (E) Examples of other non-canonical miR-194 seed mismatches found in 3'UTR peaks. 'N' represents mismatched nucleotide. Numbers in parentheses represent number of peaks with corresponding mismatched site. (F) Example of non-canonical binding with extensive complementarity to the miRNA 3' region for a site in the *LAPTM4A* CDS. Red strand represents miR-194, green strand represents mRNA. (G) Example of a CDS region with non-canonical 3' binding. Genome tracks depict the average read density of all replicates for each treatment condition (i.e. cells transfected with miR-194 (red) or a negative control (NC) (black)).(H) Cumulative distribution of log2 fold change for genes with a non-canonical CDS seed match in the 3'UTR. Numbers in parenthesis indicate p-value versus background.

Discussion

CLIP-based high-throughput studies combined with transcriptomic datasets are increasingly being used for high confidence detection of miRNA: target interactions (Hoefert et al. 2018; Loeb et al. 2012; Luna et al. 2017). This approach is advantageous over computational prediction tools, which are often limited to sites in the 3'UTR, cannot predict non-canonical interactions and do not take tissue specific miRNA interactions into account. In the present study, we have used an integrated approach combining Ago-HITS-CLIP and transcriptomics to identify hundreds of functional binding sites for miR-194 in PCa. We further refined our transcriptomic data using EISA, which allowed us to match miR-194 bound sites specifically with genes that were post-transcriptionally regulated. This strategy allowed us to ignore genes that were likely to be indirectly altered in response to miR-194 (i.e. downstream of direct targets). Notably, ours is one of only two studies (Pillman et al. 2019) that has used EISA to specifically identify direct miRNA targets.

Consistent with other CLIP studies (Chi et al. 2009; Moore et al. 2015), we have found that miR-194 binds predominantly in the 3'UTR and CDS. MiR-194 target genes with 3'UTR peaks were significantly more down-regulated at the mRNA level than targets with CDS sites. Strong 3'UTR-associated repressive effects on mRNA suggest that miRNA binding at this location is highly biologically relevant. The weaker repressive effects observed for genes with CDS binding sites are possibly due to CDS effects being mediated primarily at the translational rather than transcriptional level (Hausser et al. 2013). We cannot assess translational effects as we have not evaluated the effect of miR-194 on the proteome of PCa cells. Such an experiment would be extremely useful to more precisely dissect the mechanism by which miR-194 regulates its target genes.

Besides CDS and 3'UTR binding, our study also identified extensive binding of miR-194 to introns. Interestingly, genes associated with introns peaks show a small bias towards upregulation (Figure 4.2A). One reason for this could be that transcripts indirectly upregulated by miR-194 have been misannotated as intronic sequences. Alternately, miR-194 could be downregulating a splicing factor responsible for intron retention, a process where specific introns are not spliced out of mRNA transcripts. Retained introns are often found in 3'UTRs and harbour numerous miRNA binding sites (Bicknell et al. 2012; Schmitz et al. 2017; Tan et al. 2007). Downregulation of a splicing factor that regulates

this process might result in introns not being retained in transcripts, resulting in loss of functional miRNA binding sites and consequently gene upregulation.

Our study indicated that miR-194 does not follow the general hierarchy for seed repression but instead has a seed repression efficacy of 8mer>7mer-m8=6mer-A1>6mer>7mer-A1. Such differences have been attributed to sequence of the miRNA which affects relative affinity with targets and thus affects efficacy of gene repression (McGeary et al. 2018).

Our results indicate that multiple seed matches on a transcript are more potent than single seed matches. The occurrence of multiple seed match sites in single transcripts has been proposed to enhance miRNA-based repression, for at least 2 reasons: i) by increasing the probability of having at least one site bound at any one time, and ii) by one bound site promoting binding at the secondary site (Grimson et al. 2007). Interestingly, our data with miR-194 indicates that 7mer-A1 and 6mer sites, which are less efficient at gene repression than 8mer or 7mer-m8 sites, are more likely to occur in combination with another seed match on the same transcript within 3'UTRs and CDSs. When co-occurring in 3'UTRs, these combinations are nearly as effective at decreasing transcript levels as single 8mer sites.

Canonical miR-194 seed sequences were only detected in ~30% of 3'UTR peaks, indicating that a significant fraction of interaction occur via non-canonical sites. Non-canonical binding is widespread among miRNA and is made up of a variety of interaction types (Bartel 2009). While miR-194 is not associated with centered sites and very few nucleation bulge sites, mismatched sites appear to be a major form of miR-194 non-canonical interaction. Besides their role in repressing gene expression, non-canonical sites have been suggested to act as evolutionary midpoints that will eventually form canonical sites (Loeb et al. 2012).

In addition to a mismatch motif, our search in seedless peaks detected a motif (Figure 4.5C) that does not have complementarity to the miR-194 sequence. Two previous studies have found non-functional sequences that bind to miRNA with high affinity but without significant complementarity (Leung et al. 2011; McGeary et al. 2018). The motif we identified did not reduce transcript levels and likely falls into this category.

Non-canonical miRNA binding has been primarily studied in the context of 3'UTR peaks (Loeb et al. 2012; Seok et al. 2016). Recently, however, a novel non-canonical miRNA recognition element (MRE) was reported for miR-20a binding in the CDS of its target genes (Zhang et al. 2018). This miRNA:target interaction relies on extensive binding at the 3'end of the miRNA, minimal pairing at the 5'seed region and results in translational repression with no effect on transcript levels (Zhang et al. 2018). We have found evidence for a similar MRE interaction in miR-194 "seedless" CDS peaks, which were associated with a trend towards decreased mRNA stability at the transcript level, but may be associated with stronger repression at the protein level and it remain to be experimentally validated.

In summary, this work provides mechanistic insights into miR-194 and its interactions with target genes in the context of PCa. In particular, we demonstrate that effectiveness of different seed matches, co-operative repression by binding to multiple sites and show that miR-194 is associated with functional non-canonical binding. These findings raise the possibility of expanding the miR-194 targetome beyond canonical 3'UTR targets by further evaluating non-canonical and CDS binding sites. In addition to the miR-194 specific findings, this study provides broader insights into how miRNA exert their actions, reinforcing earlier findings and providing further evidence for the utility of non-canonical targeting in miRNA targetomes.

Chapter 5: The role of miR-194 in breast cancer

5.1 Introduction

Breast cancer (BCa) is the most common cause of cancer in women and a leading cause of cancer mortality worldwide (Bray et al. 2018). Despite arising in different organs, BCa and prostate cancer (PCa) share many biological similarities. Like PCa, BCa is a hormone dependant malignancy that is driven by a steroid hormone receptor, the estrogen receptor (ER). AR and ER belong to the nuclear hormone receptor superfamily, have similar mechanisms of action and can be regulated by the same factors (Risbridger et al. 2010). These factors include SRC3, UBE3A (Risbridger et al. 2010) and FOXA1 (Bernardo et al. 2010; Jin et al. 2014). Therapies directed against hormone receptor signalling are the mainstays treatments for both cancers and mutations of AR/ER are major therapy resistance mechanisms (Coutinho et al. 2016; Jeselsohn et al. 2015).

Based on gene expression profiling, BCa can be subdivided into several molecular subtypes. These subtypes largely cluster into the ER-positive and -negative groups (Perou et al. 2000). ER positive subtypes, which make up ~70% of all BCa cases, are termed luminal as they have expression signatures consistent with secretory epithelial cells that line the lumen of breast ducts (i.e. mammary luminal epithelial cells) (Perou et al. 2000). The luminal subtypes, called Luminal A and Luminal B, differ mainly in expression of the progesterone receptor (PR) and the oncogenic human epidermal growth factor 2 (HER2) with Luminal B expressing lower levels of PR and higher levels of HER2 (Perou et al. 2000). The ER negative subgroups, which include HER2-enriched, basal-like, and normal breast-like, are more aggressive than the luminal subgroups (Perou et al. 2000). Breast cancers can be subtyped into the groups described above using the PAM50 gene expression signature. The PAM50 signature was recently applied to cohorts of prostate tumours (Zhao et al. 2017). Based on PAM50 gene expression, PCa samples could be stratified into groups with expression profiles concordant with BCa (Zhao et al. 2017). Additionally, while luminal BCa is characterized by ER expression, luminal PCa demonstrated increased AR expression and signalling (Zhao et al. 2017).

Although similarities between PCa and BCa are largely related to hormone receptor signalling, both cancers also share genetic features such as mutations in the *BRCA1* and *BRCA2* genes which predispose to breast cancer and are also linked to increased risk of prostate cancer (López-Otín & Diamandis 1998; Oh et al. 2019).

5.2 Rationale for assessing the role of miR-194 in BCa

The preceding sections of this thesis have focussed on the role and mechanisms of action of miR-194 in PCa. In those chapters, I identified a targetome for miR-194, discovered that miR-194 targets FOXA1 to promotes progression to an aggressive subtype of PCa and defined PCa specific miR-194:target gene interactions. Given the underlying biological parallels between BCa and PCa, including similar roles for FOXA1 in these malignancies, I hypothesized that miR-194 may be an oncomiR in BCa akin to its role in PCa. Supporting an oncogenic role for miR-194, high levels of miR-194 in serum and tissue are proposed to predict recurrence in BCa (Hironaka-Mitsuhashi et al. 2017; Huo et al. 2016). In this chapter, I aimed to determine if miR-194 played an oncogenic metastasis-promoting role in BCa.

Materials and methods

Analysis of miR-194 expression in clinical datasets

miR-194 expression was analysed in The Cancer Genome Atlas (TCGA) cohort, GSE40525 and GSE22216. TCGA data was obtained from the TCGA data portal (https://gdac.broadinstitute.org/). GSE40525 and GSE22216 were retrieved from NCBI GEO (https://www.ncbi.nlm.nih.gov/geo/). The TCGA dataset consists of 995 primary breast cancer and 102 normal samples. 73% of tumours in the TCGA dataset were ER positive. The GSE40525 consists of 56 primary breast tumours with matched peritumour tissue, with 77% of the tumours showing ER expression. GSE22216 consists of 210 early primary breast cancers with 63% ER positivity. Recurrence free survival was assessed at 10 years.

Cell lines and transfections

MCF7 and ZR-75-1 cell lines were purchased from ATCC. MCF7 cells were maintained in DMEM-High Glucose supplemented with 10% FBS. ZR-75-1 cells were maintained in RPMI supplemented with 10% FBS. Cell lines were subjected to regular mycoplasma testing. All cell lines were regularly checked for identity using STR testing by CellBank Australia.

Detailed methods for transfection are provided in Chapter 2.

Cell viability assay

For cell viability assays, cells were seeded at 2×10^5 (MCF7) or 1.5×10^5 (ZR-75-1) cells/well in 6-well plates and transfected in suspension with 20nM miR-194 mimic using RNAiMax reagent. Live and dead cells were subsequently quantified at days 2, 4 and 6 using Trypan blue and manual cell counting

Detailed methods for cell viability assay are provided in Chapter 2.

Inverse Invasion assay

Detailed methods for invasion assay are provided in Chapter 2.

qPCR

Total RNA was extracted from cells using TRIzol and qPCRs were done as described as in Chapter 2. Primer sequences are listed in Chapter 2.

Western blot

Protein extraction and western blotting was done as described in Chapter 2. Antibodies used in this study were FOXA1 (Abcam, Ab23738; 1:500), ER (Novocastra, NCL-ER-6F11;1:500) and GAPDH (MERCK Ab2305; 1:1000).

Results

miR-194 is upregulated in BCa and is a predictor of metastasis free survival

To determine whether miR-194 is associated with BCa subtypes and clinic-pathological parameters, we assessed its expression in clinical cohorts with associated miRNA expression data. To determine the expression of miR-194 in breast tumours relative to non-tumour tissue, we made use of two clinical datasets: the GSE40525 cohort consisting of 56 matched tumour and peritumoural tissues; and the TCGA cohort, with 995 tumour samples and 102 normal breast tissue samples. We found that miR-194 is highly expressed in tumour tissue compared to normal /peritumoural tissues (Figure 5.1A, B).

We next determined if miR-194 is associated with specific breast cancer subtypes in the TCGA cohort. We found that miR-194 expression is significantly higher in HER2-enriched tumours compared to the basal and Luminal A subtypes (Figure 5.1C). Among luminal sub-groups, expression was higher in Luminal B tumours (Figure 5.1C).

In PCa, we have found that increased miR-194 expression is associated with increasing tumour grade and poor metastasis-free survival (Das et al. 2017). To determine if such an association existed in BCa, we assessed miR-194 in GSE22216 (Buffa et al. 2011), a clinical cohort of 210 primary breast tumours that has associated grade and metastasis free survival information over a ten year follow-up period. In this cohort, miR-194 was lower in Grade 3 tumours compared to Grade 1 and 2 tumours (Figure 5.1D). Furthermore, high expression of miR-194 was associated with longer time to distant metastasis compared to patients with low expression of miR-194 (Figure 5.1E). Collectively, these data suggest that elevated expression of miR-194 may be associated with tumorigenesis, but a reduction in expression occurs with disease progression.

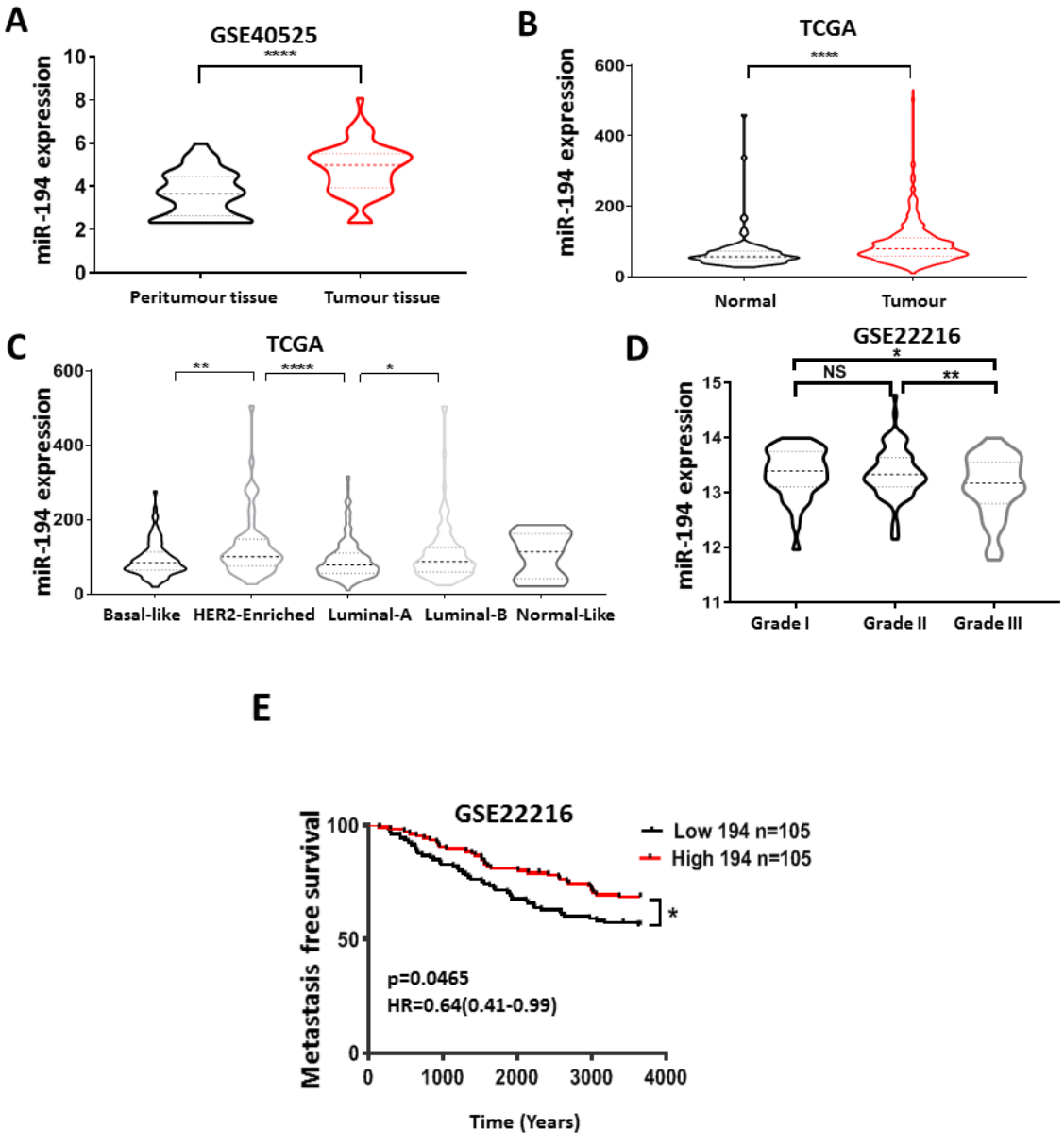

Figure 5.1: miR-194 is upregulated in BCa and is a predictor of metastasis. (A) miR-194 expression analysis in the GSE40525 dataset (Biagioni et al. 2012) containing matched patient peri-tumour and tumour samples. Middle dashed line represents median. Dotted lines above and below represent upper and lower quartiles. p-values were determined by two tailed student's t test (****, $p<0.00001$). (B) miR-194 expression analysis between matched and unmatched normal and tumour samples in the TCGA dataset. Middle dashed line represents median. Dotted lines above and below represent upper and lower quartiles. p-values were determined by two tailed student's t test (****, $p<0.00001$). (C) Differential expression of miR-194 occurs between the PAM50 breast cancer subtypes. Middle dashed line represents median. Dotted lines above and below represent upper and lower quartiles. p-values were determined by ANOVA (*, $p < 0.05$;

**, $p < 0.01$; ****, $p<0.00001$). (D) miR-194 expression in patients from the GSE22216 dataset (Buffa et al. 2011) grouped according to tumour grade. Middle dashed line represents median. Dotted lines above and below represent upper and lower quartiles. p-values were determined by ANOVA (*, $p < 0.05$). (E) Correlation between miR-194 expression and metastasis free survival in patients with breast cancer from the GSE22216 dataset. p-value was determined by Log Rank test (*, $p < 0.05$).

MiR-194 inhibits proliferation and invasion of ER-positive BCa cell lines

To explore the functional effects of miR-194 in BCa, we assessed cell proliferation and invasion following transient transfection of a miR-194 mimic into the MCF7 and ZR-75-1 cell lines. MCF7 and ZR-75-1 are models of Luminal A breast cancer expressing ER, PR and HER2. Luminal A models of breast cancer were chosen because (i) ER is the main driver of approximately 70% of breast cancers; (ii) Luminal breast cancers have a gene expression profile similar to AR-expressing prostate cancers (Zhao et al. 2017); and (iii) miR-194 has the lowest expression in this subtype.

In both cell lines, the miR-194 mimic significantly inhibited proliferation, as measured by a trypan blue cell viability assay (Figure 5.2A, B). We next determined whether miR-194 influenced invasion, a key measure of the metastatic capacity of cancer cells. The ability to invade is also a proxy measure of plasticity in cells since this requires cells to activate plasticity-related pathways such as epithelial mesenchymal transition (EMT). In the MCF7 cell line, transient expression of the mimic significantly inhibited invasion through Matrigel compared to a negative control (Figure 5.2C); there was a trend towards this phenotype in the ZR-75-1 cell line, but it was not significant (Figure 5.2D). Additionally, MCF7 cells did not undergo any morphological changes characteristic of acquisition of a plastic phenotype (Figure 5.2E). These results indicate that miR-194 inhibits tumourigenic potential (growth, invasion) in BCa.

MiR-194 targets FOXA1 in BCa

We assessed expression of FOXA1 in our BCa cell line models in response to miR-194 mimic transfection. Although we did not see a significant reduction of *FOXA1* mRNA (Figure 5.3A), FOXA1 protein (Figure 5.3B) levels were reduced by miR-194 overexpression in both cell lines. Since miRNAs can act by translational inhibition rather than transcript degradation (Hausser et al. 2013), these results support the concept that FOXA1 is a target of miR-194 in the context of the ER-positive subtype of breast cancer. Supporting this idea, transfection of a miR-194 locked nucleic acid (LNA) inhibitor increased endogenous levels of FOXA1 protein in the MCF7 cell line (Figure 5.3C).

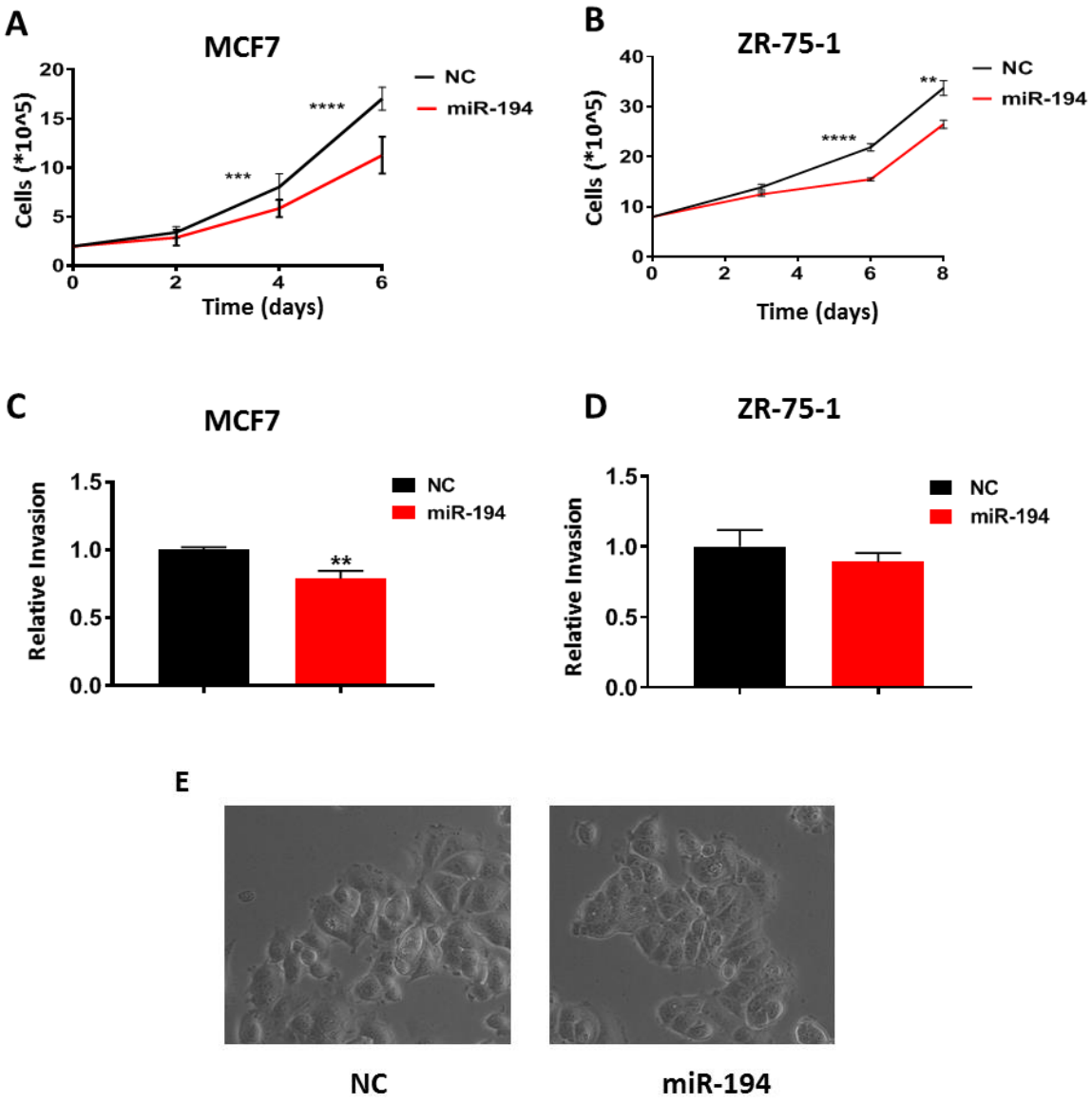

Figure 5.2: The effect of miR-194 on proliferation and invasion of ER positive BCa cells. (A,B) Ectopic expression of a miR-194 mimic inhibits proliferation of MCF7 and ZR-75-1 cell lines compared to a negative control (NC). Error bars represent SEM. p-values were determined by two tailed student's t test (**, $p < 0.01$;***, $p<0.001$; ****, $p<0.00001$). (C, D) Ectopic expression of a miR-194 mimic inhibits invasion of MCF7 but not ZR-75-1 cells. Error bars represent SEM. p-values were determined by two tailed student's t test (**, $p < 0.01$). (E) MCF7 cells transfected with a miR-194 mimic or negative control (NC).

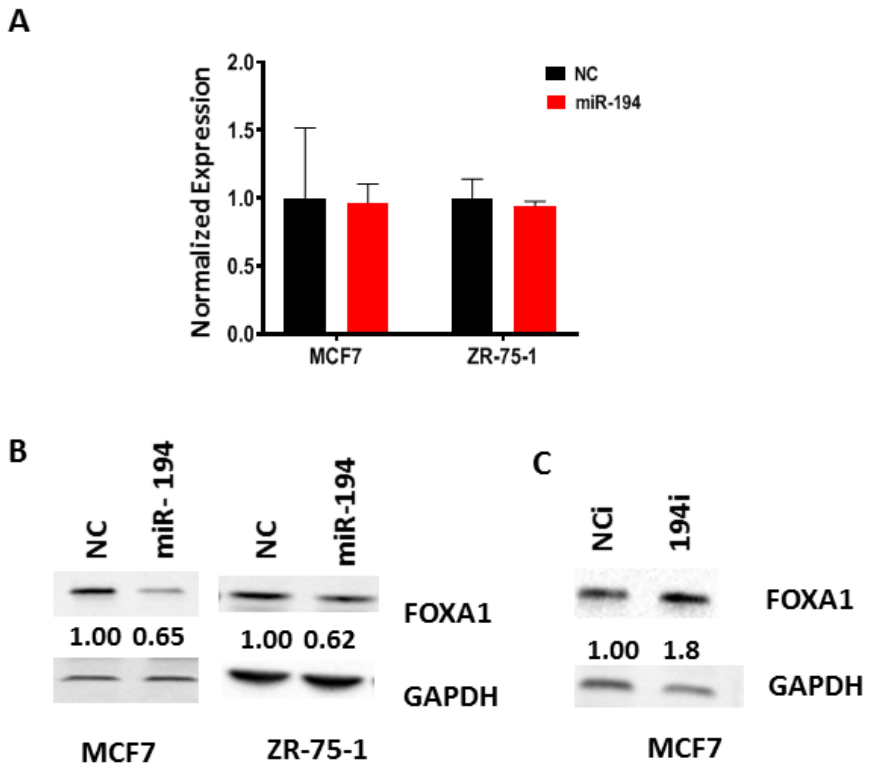

Figure 5.3: miR-194 targets FOXA1 in BCa. (A) *FOXA1* mRNA levels following transient transfection of a miR-194 mimic or negative control (NC) into the MCF7 and ZR-75-1 BCa cell lines. Error bars represent SEM. (B) FOXA1 protein levels following transient transfection of a miR-194 mimic or negative control (NC) into the MCF7 and ZR-75-1 BCa cell lines. Normalized FOXA1 protein levels are shown below the lanes. (C) FOXA1 protein levels following transient transfection of a miR-194 locked nucleic acid (LNA) inhibitor (194i) or negative control inhibitor (NCi) into the MCF7 cell line. Normalized FOXA1 protein levels are shown below the lanes.

ER expression is downregulated by miR-194

FOXA1 is an upstream regulator of *ESR1* gene expression, binding to a regulatory element within the *ESR1* promoter to promote expression of this gene (Bernardo et al. 2010). Since overexpression of miR-194 reduced FOXA1 expression in our cancer cell line models (Figure 5.3C), we speculated that this would result in consequent reduction in ER expression. Indeed, overexpression of miR-194 significantly reduced expression of ER at both the protein and RNA level (Figure 5.4 A, B). *ESR1* is not predicted to have a binding site for miR-194 in its 3'UTR, thus the downregulation we have observed is unlikely to be a direct effect of miR-194.

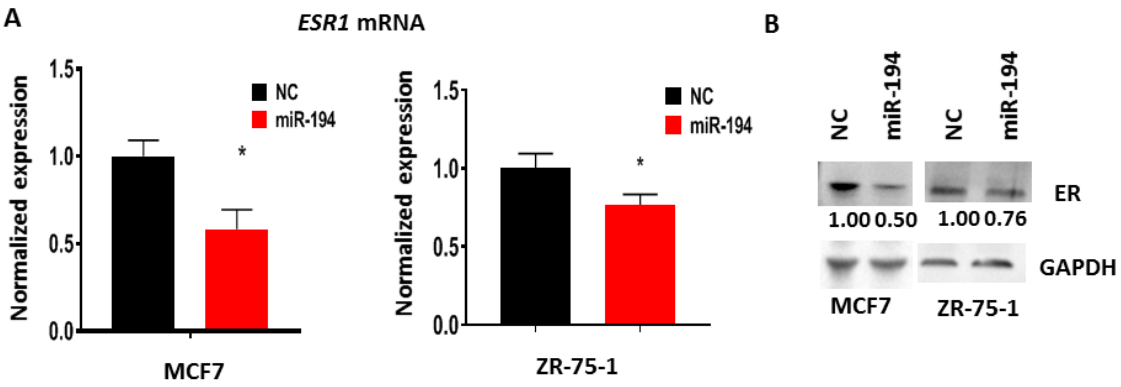

Figure 5.4: miR-194 downregulates expression of the estrogen receptor. (A) *ESR1* mRNA levels after transient transfection of a miR-194 mimic or negative control (NC) into two ER-positive BCa cell lines. Error bars represent SEM. p-values were determined by two tailed student's t test (*, $p < 0.05$). (B) ER protein levels after transient transfection of a miR-194 mimic or negative control into two Luminal A breast cancer cell lines.

Discussion

MiR-194 has context-dependent roles in different cancer types, and can act as an oncomiR or a tumour suppressor (Das et al. 2017; Wang, Shen, et al. 2015). In PCa, miR-194 has been shown to have an metastasis-promoting role (Das et al. 2017). In this study, we aimed to determine if miR-194's role in BCa mirrors its role in PCa.

Similar to PCa, we have found that in clinical cohorts miR-194 expression is elevated compared to normal tissue. Unlike PCa, however, we show that miR-194 expression is reduced in higher grade tumours, and higher expression is associated with better outcomes. This suggests that while high levels of miR-194 is linked to the initial states of carcinogenesis it may repress disease progression in later stages. Such a phenomenon is not without precedent: for example, miR-221/-222 is reported to have oncogenic or tumour suppressive roles in different phases of prostate cancer (Gui et al. 2017). Supporting a tumour suppressive function of miR-194, we found that ectopic expression of miR-194 decreased growth and invasion in BCa cell line models. Altogether, these results suggest that miR-194 has dichotomous roles in PCa and BCa, acting as an oncomiR in the former and a tumour suppressor in the latter.

In this study we have specifically assessed expression of FOXA1 as a miR-194 target in BCa. FOXA1 is a miR-194 target in PCa (Chapter 3) and is important for steroid receptor transcriptional function, acting as a pioneer factor for both AR and ER (Bernardo et al. 2010; Clarke & Graham 2012; Sahu et al. 2013). Additionally, FOXA1 directly upregulates expression of ER in breast cancer (Bernardo et al. 2010). Since our study indicated that FOXA1 is a target of miR-194 in ER-positive BCa cell lines, we speculated it may have an effect on ER expression. Our study provides evidence for miR-194 downregulating ER at the protein and RNA level. Since *ESR1* is not predicted to have a binding site for miR-194 in its 3'UTR, downregulation is likely to be an indirect effect via FOXA1. ER is a key driver of luminal BCa, promoting proliferation, invasion and migration of cells (Fuqua 2001; Pike et al. 1993; Sanchez et al. 2010). The downregulation of ER by miR-194 therefore likely explains the effects we observe on growth and invasion as well as the positive outcomes for tumours expressing high levels of miR-194.

One of the major findings of our study in PCa was the role of miR-194 in mediating plasticity via EMT and promoting neuroendocrine transdifferentiation. While I did not address this in detail in relation to BCa in the current study, the invasion data as well as the inability of miR-194 to induce morphological changes in BCa cells suggests that this miRNA does not promote plasticity in ER-positive breast cancer cells.

The obvious explanation for the differences in the action of miR-194 in PCa versus BCa are that it targets different genes in these 2 distinct cancer types. However, in the absence of transcriptomic data in response to miR-194 delivery to BCa cells, we are unable to assess the extent to which our miR-194 PCa targetome (defined in Chapter 3) compares with its targetome in BCa. Determining the miR-194 targetome in BCa and its contribution to the divergent effects on this cancer type compared to PCa is an obvious avenue for future investigation.

While my work indicates that miR-194 is tumour suppressive, earlier studies found it to have an oncogenic role in BCa. For instance, elevated expression of miR-194 in tissue and serum from breast cancer patients has previously been associated with recurrence post-curative surgery (Hironaka-Mitsuhashi et al. 2017; Huo et al. 2016). This inconsistency may be explained by differences between the these cohorts and the Buffa et al cohort (Buffa et al. 2011) which was used in our study. Given our finding that miR-194 expression varied significantly in different PAM50 subtypes, outcomes may be affected depending on the fraction of each subtype in the study cohorts assessed to date. The cohorts also differed in treatment administered to patients and median age, which may account for variable results across studies. MiRNA expression was recently shown to differ between patients with different ages of onset (Tsai et al. 2018). Since the Hironaka-Mitsuhasi cohort had patients under 35 years of age whereas the other cohorts had median ages between 45 and 50, this might be a factor in the differences in results.

In summary, we show that miR-194 has dichotomous effects in breast and prostate cancers in terms of growth, invasion and prognosis. Tumour suppressive effects of miR-194 in BCa are likely due to its downregulation of ER via FOXA1.

Chapter 6: General discussion

6.1 General discussion of thesis findings

MicroRNAs are negative regulators of gene expression that play critical roles in cancer initiation and progression. This thesis focussed on the role of miR-194 in prostate cancer (PCa). My interest in this topic stemmed from earlier work from my host laboratory demonstrating that miR-194 is a circulating marker prognostic of PCa prognosis (Selth et al. 2013). We subsequently showed that miR-194 promotes metastasis and epithelial mesenchymal transition (EMT) in PCa, at least in part by targeting the anti-metastatic SOCS2 gene (Das et al. 2017). In this study, we aimed to understand the molecular mechanisms responsible for miR-194's oncogenic activity in PCa. Given that both breast cancer (BCa) and PCa are hormone dependant malignancies that share certain features, I have also assessed the role of miR-194 in BCa.

MiR-194 is a driver of lineage plasticity

Identification of miRNA targets relies primarily on computational prediction, assessment of gene expression changes following ectopic miRNA expression, crosslinking immunoprecipitation (CLIP) based methods and pull-down of labelled miRNA (Li & Zhang 2019). CLIP-based methods are preferred over computational prediction as they experimentally determine direct endogenous miRNA targets on a genome-wide scale. CLIP, especially in combination with gene expression analysis following miRNA perturbation, is a powerful tool for defining miRNA: target networks.

In the first part of this thesis (Chapter 3), using an integrated approach that includes high-throughput sequencing of RNA isolated by crosslinking immunoprecipitation (HITS-CLIP), RNA sequencing and bioinformatics, I identified 163 targets of miR-194. This was a ground-breaking study since, at the time of commencement of my project, no complete miRNA targetomes in PCa had been identified. Since that time the only other miRNAs whose targetomes have been identified in PCa are miR-1271-5p and miR-26a-5p (Kalofonou et al. 2019; Rizzo et al. 2017). Using the miR-194 targetome, I established that miR-194 activity was inversely related to AR activity. Consequently, using expression data from clinical cohorts and experiments in cell lines and PDX models, I have established that miR-194 promotes progression to a highly aggressive, metastatic, "AR-indifferent" neuroendocrine subtype of prostate cancer (NEPC).

NEPC is proposed to arise from prostate adenocarcinomas as an adaptive response to AR directed therapy via lineage plasticity (Akamatsu et al. 2018; Davies, Beltran & Zoubeidi 2018). Lineage or cellular plasticity, a process by which differentiated cells can change their identity to a new phenotype, is essential for cancer progression and therapy resistance (Yuan, Norgard & Stanger 2019). The induction of plasticity on treatment with ADT is attributed in part to the upregulation of several AR repressed genes. Genes such as *PEG10, SOX2, BRN2* and *lncRNA-p21* are all repressed by direct AR binding to promoter or enhancer regions of these genes (Akamatsu et al. 2015; Bishop et al. 2017; Luo et al. 2019; Mu et al. 2017). By contrast, the *MIR194* genes do not appear to have AR binding sites in their regulatory regions, and miR-194 is only downregulated at 48 hours of androgen stimulation – therefore, we believe that it is not a direct target of AR. We have previously shown that GATA2 is a direct upstream regulator of miR-194 expression (Das et al. 2017). Since GATA2 is also repressed by AR (He et al. 2014), it might serve as a link between AR signalling and miR-194, with AR-directed therapies upregulating the expression of GATA2 and consequently miR-194 (Figure 6.1).

Although the exact mechanisms underlying ADT-induced lineage plasticity remain unknown, the process of EMT is thought to transition cells into a metastable stem cell-like state that can then dedifferentiate into an AR indifferent state (Davies, Beltran & Zoubeidi 2018; Dicken, Hensley & Kyprianou 2019). Supporting a link between EMT and NEPC, EMT regulators have been found to be associated with NEPC. For instance, overexpressing the EMT transcription factor (EMT-TF) SNAIL in LNCaP cells induces neurite-like morphology and an increase in expression of neuroendocrine markers (McKeithen et al. 2010). Additionally, SNAIL and ZEB1, another EMT-TF, are upregulated during transition of a PDX model from adenocarcinoma to NEPC (Akamatsu et al. 2015). EMT is characterized by downregulated expression of epithelial markers and upregulated mesenchymal markers, reduced adhesion between cells and a more migratory phenotype (Pearson 2019). Our previous work has indicated that miR-194 promotes EMT by reducing expression of the epithelial markers CDH1 and ZO-1, and upregulating the mesenchymal marker CDH2 (Das et al. 2017). In addition, miR-194 promotes cytoskeletal rearrangements and increased migratory and invasive capacity, consistent with induction of EMT (Das et al. 2017). The STAT3 signalling pathway, which has been shown to promote the acquisition of stem cell features (Schroeder et al. 2014), is also activated by miR-194 (Das et al. 2017). My work implicating miR-194 in NEPC (Chapter

3), along with our earlier findings that link miR-194 to EMT and stem cell related pathways (Das et al. 2017), support the concept of miR-194 being a key hub regulating lineage plasticity.

Mechanistically, my data suggests that miR-194's role as a plasticity regulator is in part via miR-194 mediated downregulation of FOXA1 (Figure 6.1), a transcription factor that is important for maintaining a cellular differentiated state (Kaestner 2010). FOXA1 is an inhibitor of EMT in PCa cells, acting by supressing the EMT-TF Slug (Jin et al. 2013). FOXA1 also inhibits transition to NEPC by suppressing IL8-MEK/ERK signalling (Kim et al. 2017), a pathway that I have found is upregulated on ectopic expression of miR-194 in cell lines. Highlighting the importance of FOXA1 in NEPC, the R219 point mutation that leads to impaired FOXA1 activity is present in nearly 75% of NEPC tumours (Adams et al. 2019).

While I propose that FOXA1 is an important target by which miR-194 promotes lineage plasticity, many other target genes are likely to be involved in this process and could constitute a miR-194 "plasticity supressing targetome" (Figure 6.1). Like FOXA1, several miR-194 target genes have been identified as inhibitors of EMT in prostate and other cancers. These include ZNF516 (Li et al. 2017), ATXN1 (Kang et al. 2017), MPZL2 (Ramena et al. 2016) and ARHGAP1 (Li, Liu & Yin 2017). Notably the EMT epithelial marker ZO-1 is a direct miR-194 target. Additionally, targets such as ARHGAP1 and TRAF6 are upstream inhibitors of IL8 and EZH2, both of which are important in NE transdifferentiation (Lu et al. 2017; Satterfield et al. 2017). Pathway analysis of the miR-194 targetome indicates that it is enriched for genes involved in cytoskeletal rearrangement, adhesion, junction formation and lamellopodia formation consistent with a role in regulating cellular invasion, migration and therefore plasticity. Besides directly downregulating genes, ectopic expression of miR-194 also strongly upregulated several oncogenes. *MET*, one of the most highly upregulated genes, is of particular interest as it regulates EMT and cancer cell stemness (Jeon & Lee 2017).

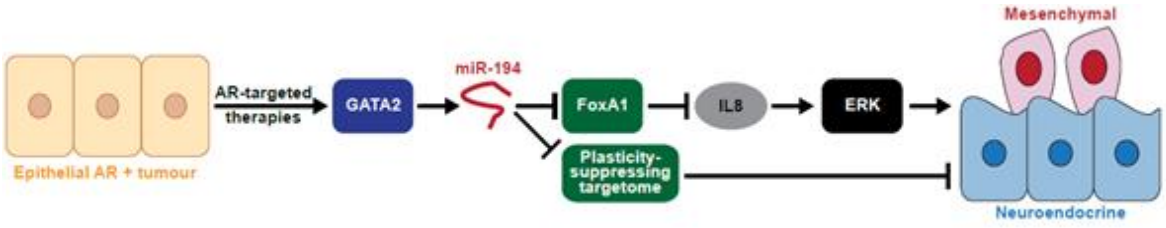

Figure 6.1 Schematic depicting the role of miR-194 in NEPC.

A key finding of this study was the cytotoxic and cytostatic effect of inhibiting miR-194 in cell lines and patient derived models of NEPC, raising the possibility of exploiting miR-194 as therapeutic target in NEPC. miRNA-based therapeutics are comprised of antagomiRs, which bind to target miRNA preventing interactions with target mRNA, and miRNA mimics, which aim to replace disease-inhibiting miRNAs lost during disease progression (Simonson & Das 2015). MiRNA-based therapeutics are advantageous since they can be used to (i) modulate multiple oncogenic genes or pathways with a single molecule and (ii) target genes whose corresponding proteins are not targetable by conventional antibodies or inhibitors (Rupaimoole et al. 2011). However, targeting miRNAs as a therapeutic strategy remain associated with many challenges, including: redundancy, since many miRNA target the same genes and inhibiting one miRNA may not result in desired effects; delivery to target tissues; cellular toxicity due to pressure on the miRNA processing machinery; activation of a non-specific immune response; and the selection of appropriate doses to maximize therapeutic effects but prevent off-target effects (Chen et al. 2015). Despite these drawbacks, miRNA-based therapeutics have had success in recent clinical trials (Kreth, Hübner & Hinske 2018; Van der Ree et al. 2016). In case of advanced prostate cancer, I envision three potential strategies in which a miR-194 inhibitor could be of benefit to treat advanced prostate cancer (Figure 6.2). First, as demonstrated in this study, targeting miR-194 using antagomiRs can be used to inhibit the growth of NEPC. Second, targeting miR-194 (likely in combination with conventional therapies) could prevent emergence of the neuroendocrine phenotype. Supporting this concept, transfection of a miR-194 inhibitor was able to prevent serum starvation induced neuroendocrine differentiation in LNCaP cells. Finally, a miR-194 inhibitor could be used to revert NEPC tumours back to an adenocarcinoma phenotype that is responsive to conventional AR-targeted therapies. These are exciting opportunities, but taking them forward clearly requires further studies in *in vitro* models and in preclinical animal models. One key study would involve using genetically engineered mouse models of NEPC such as the NPp53 model. Treatment of NPp53 mice with the anti-androgen abitraterone results in progression to an NEPC phenotype that is similar to human NEPC (Zou et al. 2017). I propose treating NPp53 mice with miR-194 locked nucleic acid inhibitors (LNA) *in vivo* by injection during abiraterone treatment to assess if this prevents progression to NEPC or after progression to determine if miR-194 inhibition reduces tumour growth.

Besides being a therapeutic target, miR-194 may have utility as a serum biomarker. Initial interest in miR-194's role in prostate cancer arose when this miRNA was identified as a circulating marker for disease recurrence (Selth et al. 2013). In advanced PCa, circulating levels of miR-194 could be used for tracking disease progression and informing treatment decisions. To assess this further, I propose a prospective study in individuals treated with ADT to determine if those who initially expressed higher levels of miR-194 are more likely to progress to CRPC and//or NEPC. Supporting such a study, I found that miR-194 trended towards higher levels in the serum of mice harbouring NEPC PDXs compared to those with adenocarcinoma PDXs (Figure 6.3). Although these results were not significant, perhaps due to the small cohort size, they suggests that tumours expressing high levels of miR-194 could release it into serum.

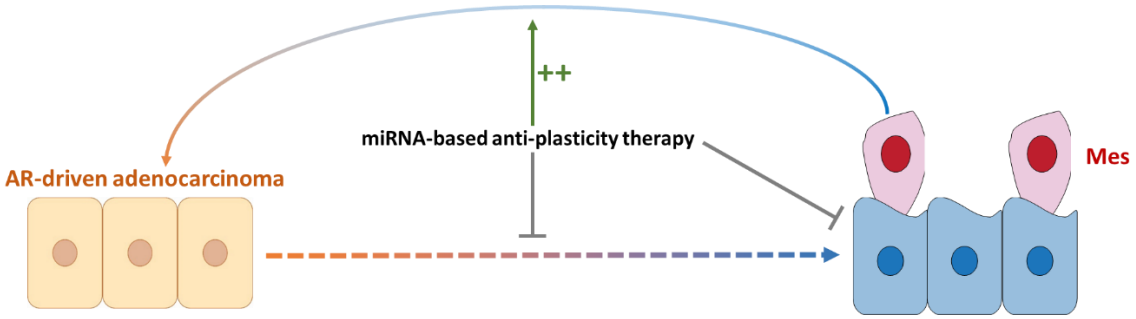

Figure 6.2 Strategies for targeting miR-194 in NEPC.

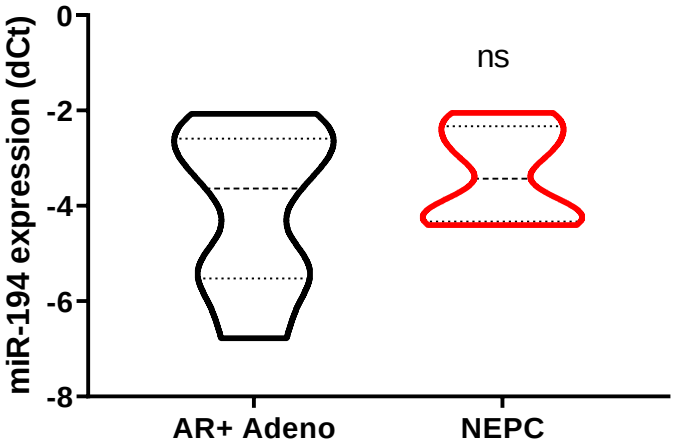

Figure 6.3 Expression of miR-194 in the serum of mice with adenocarcinoma or NEPC PDXs.

Insights into target gene regulation by miR-194

Individual miRNAs differ in their mechanism of interaction with target transcripts, and the rules governing these interaction are not completely understood (Moore et al. 2015). Data from CLIP studies has been crucial to better understanding these miRNA:target interactions, revealing previously unknown widespread diversity in regions to which miRNAs bind and enabling the identification of non-canonical miRNA regulation of target transcripts (Chi et al. 2009; Loeb et al. 2012). In Chapter 4, I used Ago-HITS-CLIP and transcriptomic data to study functional miR-194: mRNA interactions.

My results indicate that miR-194: more potently destabilized target mRNAs by binding in the 3'UTR compared to CDS sites; can more potently represses targets through multiple binding sites; and is associated with widespread non-canonical binding events. However, miR-194 does not follow the general miRNA repression hierarchy based on seed length and is not associated with common non-canonical seed types like nucleation bulges and centered sites. These findings highlight the fact that miRNAs can function through similar mechanisms, but each miRNA also has unique features.

Non-canonical binding events forms the majority of miRNA:target gene interactions, but these are often overlooked in favour of canonical binding sites in the 3'UTR and CDS. This study and others (Helwak et al. 2013; Loeb et al. 2012) have found that such interactions in the 3'UTR are functional, although they have much smaller effects on mRNA stability than canonical seed matches. Importantly, non-canonical seed matches may play crucial roles within miRNA targetomes. For instance, in the case of miR-24, downregulation of targets with non-canonical seed matches is critical for mediating its antiproliferative effects (Lal et al. 2009). In addition to 3'UTR sites, non-canonical sites in the CDS are also of interest, given that these were recently discovered to be highly functional for miR-20a (Zhang et al. 2018) and also occur in miR-194 CDS targets (Chapter 4). Although we did not incorporate non-canonical targets into the miR-194 targetome, I propose that this will be critical to comprehensively understand its function.

One drawback of this study was a lack of proteomic data corresponding to the HITS-CLIP and RNA-seq data since a significant component of miRNA regulation occurs through translational repression, particularly for non-3'UTR sites (Hausser et al. 2013). Stable Isotope Labelling by amino acids (SILAC)-based methods have previously been

used to determine changes to cellular proteomes following perturbation of miRNAs (Bargaje et al. 2012). Using this method to determine proteomic changes following ectopic expression of miR-194 would ensure a more accurate miR-194 targetome hence gaining a more complete picture of its function in prostate cancer.

The role of miR-194 in BCa

BCa is a hormone driven malignancy in which the estrogen receptor (ER) is the key driver in approximately 75% of cases. In Chapter 5, I assessed the role of miR-194 in BCa and its effect on the expression of FOXA1 and ER.

Overall, my results indicate that miR-194 is a tumour suppressor in ER-positive BCa, unlike its oncogenic role in PCa. Such context-dependant roles are common among miRNAs and depend on the genes targeted by the miRNA in that cell type (Erhard et al. 2014). As an example, a previous study of HER2 (+/-ER) BCa reported that miR-194 inhibited migration/invasion by targeting TLN2 (Le et al. 2012), but TLN2 was not a miR-194 target in PCa (Chapter 3). Differential gene targeting phenomena like these likely explain the dichotomous responses to miR-194 we observed in PCa versus BCa. Furthermore, even if the same gene is targeted in both cancers, observed phenotypes may be different depending on the role of the target gene in that context. For instance, while FOXA1 is targeted by miR-194 in both BCa and PCa, the downstream effects mediated by FOXA1 are different in these cancers. In PCa, FOXA1 represses the IL-8 gene (Kim et al. 2017), whereas in ER-positive breast cancer FOXA1 together with ER upregulates IL-8 (Fu et al. 2016). Additionally, downregulation of FOXA1 activates pathways promoting plasticity in PCa (at least partly by upregulating IL-8), whereas in BCa my work indicates that loss of FOXA1 may suppress plasticity/invasion. In order to fully elucidate the dichotomy in miR-194's roles in BCa and PCa, it would be crucial to identify a miR-194 targetome for BCa using an approach similar to that described in Chapter 3.

Given the importance of ER in growth and progression of luminal BCa, targeting ER levels and function is the most common treatment strategy for this BCa subtype (Manavathi et al. 2012). My study, which indicates ER is an indirect target of miR-194, opens up the possibility of exploring miR-194 upregulation as a therapeutic strategy in luminal BCa. The potential of such a strategy is enhanced since miR-194 also impacts on

other targets such as FOXA1, which is currently being explored as a therapeutic target in ER positive breast cancer (Jozwik and Carroll 2012).

6.2 Conclusions

Collectively, the research in this thesis has expanded on previous knowledge on the role of miR-194 in PCa, and identified a novel role for this factor in BCa. Of greater translational significance, this work provides a rationale for targeting miR-194 in this disease.

References

Abida, W, Cyrta, J, Heller, G, Prandi, D, Armenia, J, Coleman, I, Cieslik, M, Benelli, M, Robinson, D & Van Allen, EM 2019, 'Genomic correlates of clinical outcome in advanced prostate cancer', *Proceedings of the National Academy of Sciences*, vol. 116, no. 23, pp. 11428-11436.

Abrahamsson, PA 1999, 'Neuroendocrine cells in tumour growth of the prostate', *Endocr Relat Cancer*, vol. 6, no. 4, Dec, pp. 503-519.

Abrahamsson, PA & di Sant'Agnese, PA 1993, 'Neuroendocrine cells in the human prostate gland', *J Androl*, vol. 14, no. 5, Sep-Oct, pp. 307-309.

Adams, EJ, Karthaus, WR, Hoover, E, Liu, D, Gruet, A, Zhang, Z, Cho, H, DiLoreto, R, Chhangawala, S, Liu, Y, Watson, PA, Davicioni, E, Sboner, A, Barbieri, CE, Bose, R, Leslie, CS & Sawyers, CL 2019, 'FOXA1 mutations alter pioneering activity, differentiation and prostate cancer phenotypes', *Nature*, vol. 571, no. 7765, Jul, pp. 408-412.

Agarwal, V, Subtelny, AO, Thiru, P, Ulitsky, I & Bartel, DP 2018, 'Predicting microRNA targeting efficacy in Drosophila', *Genome biology*, vol. 19, no. 1, p. 152.

Aggarwal, R, Zhang, T, Small, EJ & Armstrong, AJ 2014, 'Neuroendocrine prostate cancer: subtypes, biology, and clinical outcomes', *Journal of the National Comprehensive Cancer Network*, vol. 12, no. 5, pp. 719-726.

AIHW 2019, *Cancer in Australia 2019*, Cancer series Australian Insttute of Health and Welfare , C AIHW.

Akamatsu, S, Inoue, T, Ogawa, O & Gleave, ME 2018, 'Clinical and molecular features of treatment-related neuroendocrine prostate cancer', *International Journal of Urology*, vol. 25, no. 4, pp. 345-351.

Akamatsu, S, Wyatt, AW, Lin, D, Lysakowski, S, Zhang, F, Kim, S, Tse, C, Wang, K, Mo, F & Haegert, A 2015, 'The placental gene PEG10 promotes progression of neuroendocrine prostate cancer', *Cell reports*, vol. 12, no. 6, pp. 922-936.

Albala, DM 2017, 'Imaging and treatment recommendations in patients with castrate-resistant prostate cancer', *Reviews in urology*, vol. 19, no. 3, p. 200.

Alberti, C & Cochella, L 2017, 'A framework for understanding the roles of miRNAs in animal development', *Development*, vol. 144, no. 14, pp. 2548-2559.

Ambs, S, Prueitt, RL, Yi, M, Hudson, RS, Howe, TM, Petrocca, F, Wallace, TA, Liu, C-G, Volinia, S & Calin, GA 2008, 'Genomic profiling of microRNA and messenger RNA reveals deregulated microRNA expression in prostate cancer', *Cancer research*, vol. 68, no. 15, pp. 6162-6170.

Antonarakis, ES 2013, 'Enzalutamide: the emperor of all anti-androgens', *Translational andrology and urology*, vol. 2, no. 2, p. 119.

Armandari, I, Hamid, AR, Verhaegh, G & Schalken, J 2014, 'Intratumoral steroidogenesis in castration-resistant prostate cancer: a target for therapy', *Prostate international*, vol. 2, no. 3, pp. 105-113.

Armenia, J, Wankowicz, SA, Liu, D, Gao, J, Kundra, R, Reznik, E, Chatila, WK, Chakravarty, D, Han, GC & Coleman, I 2018, 'The long tail of oncogenic drivers in prostate cancer', *Nature genetics*, vol. 50, no. 5, p. 645.

Arora, VK, Schenkein, E, Murali, R, Subudhi, SK, Wongvipat, J, Balbas, MD, Shah, N, Cai, L, Efstathiou, E & Logothetis, C 2013, 'Glucocorticoid receptor confers resistance to antiandrogens by bypassing androgen receptor blockade', *Cell*, vol. 155, no. 6, pp. 1309-1322.

Artibani, W, Porcaro, AB, De Marco, V, Cerruto, MA & Siracusano, S 2018, 'Management of biochemical recurrence after primary curative treatment for prostate cancer: a review', *Urologia internationalis*, vol. 100, no. 3, pp. 251-262.

Ayala, AG, Ro, JY, Babaian, R, Troncoso, P & Grignon, DJ 1989, 'The prostatic capsule: does it exist? Its importance in the staging and treatment of prostatic carcinoma', *The American journal of surgical pathology*, vol. 13, no. 1, pp. 21-27.

Bailey, TL, Boden, M, Buske, FA, Frith, M, Grant, CE, Clementi, L, Ren, J, Li, WW & Noble, WS 2009, 'MEME SUITE: tools for motif discovery and searching', *Nucleic acids research*, vol. 37, no. suppl_2, pp. W202-W208.

Balk, SP 2014, 'Androgen receptor functions in prostate cancer development and progression', *Asian journal of andrology*, vol. 16, no. 4, p. 561.

Banerjee, PP, Banerjee, S, Brown, TR & Zirkin, BR 2018, 'Androgen action in prostate function and disease', *American journal of clinical and experimental urology*, vol. 6, no. 2, p. 62.

Bao, C, Li, Y, Huan, L, Zhang, Y, Zhao, F, Wang, Q, Liang, L, Ding, J, Liu, L & Chen, T 2015, 'NF-kB signaling relieves negative regulation by miR-194 in hepatocellular carcinoma by suppressing the transcription factor HNF-1o', *Sci Signal*, vol. 8, p. 387.

Bardin, CW, BULLOCK, LP, SHERINS, RJ, MOWSZOWICZ, I & BLACKBURN, WR 1973, 'Part II. Androgen metabolism and mechanism of action in male pseudohermaphroditism: a study of testicular feminization', *Proceedings of the 1972 Laurentian Hormone Conference*, Elsevier, pp. 65-109.

Bargaje, R, Gupta, S, Sarkeshik, A, Park, R, Xu, T, Sarkar, M, Halimani, M, Roy, SS, Yates, J & Pillai, B 2012, 'Identification of novel targets for miR-29a using miRNA proteomics', *PloS one*, vol. 7, no. 8, p. e43243.

Bartel, DP 2004, 'MicroRNAs: genomics, biogenesis, mechanism, and function', *Cell*, vol. 116, no. 2, pp. 281-297.

Bartel, DP 2009, 'MicroRNAs: target recognition and regulatory functions', *Cell*, vol. 136, no. 2, pp. 215-233.

Baskerville, S & Bartel, DP 2005, 'Microarray profiling of microRNAs reveals frequent coexpression with neighboring miRNAs and host genes', *Rna*, vol. 11, no. 3, pp. 241-247.

Beltran, H, Prandi, D, Mosquera, JM, Benelli, M, Puca, L, Cyrta, J, Marotz, C, Giannopoulou, E, Chakravarthi, BV & Varambally, S 2016, 'Divergent clonal evolution of castration-resistant neuroendocrine prostate cancer', *Nature medicine*, vol. 22, no. 3, p. 298.

Beltran, H, Rickman, DS, Park, K, Chae, SS, Sboner, A, MacDonald, TY, Wang, Y, Sheikh, KL, Terry, S & Tagawa, ST 2011, 'Molecular characterization of neuroendocrine prostate cancer and identification of new drug targets', *Cancer discovery*, vol. 1, no. 6, pp. 487-495.

Bernardo, GM, Lozada, KL, Miedler, JD, Harburg, G, Hewitt, SC, Mosley, JD, Godwin, AK, Korach, KS, Visvader, JE & Kaestner, KH 2010, 'FOXA1 is an essential determinant of ERα expression and mammary ductal morphogenesis', *Development*, vol. 137, no. 12, pp. 2045-2054.

Beshiri, ML, Tice, CM, Tran, C, Nguyen, HM, Sowalsky, AG, Agarwal, S, Jansson, KH, Yang, Q, McGowen, KM & Yin, J 2018, 'A PDX/organoid biobank of advanced prostate cancers captures genomic and phenotypic heterogeneity for disease modeling and therapeutic screening', *Clinical Cancer Research*, vol. 24, no. 17, pp. 4332-4345.

Biagioni, F, Ben-Moshe, NB, Fontemaggi, G, Canu, V, Mori, F, Antoniani, B, Di Benedetto, A, Santoro, R, Germoni, S & De Angelis, F 2012, 'miR-10b*, a master inhibitor of the cell cycle, is down-regulated in human breast tumours', *EMBO molecular medicine*, vol. 4, no. 11, pp. 1214-1229.

Bicknell, AA, Cenik, C, Chua, HN, Roth, FP & Moore, MJ 2012, 'Introns in UTRs: why we should stop ignoring them', *Bioessays*, vol. 34, no. 12, pp. 1025-1034.

Bishop, JL, Thaper, D, Vahid, S, Davies, A, Ketola, K, Kuruma, H, Jama, R, Nip, KM, Angeles, A & Johnson, F 2017, 'The Master Neural Transcription Factor BRN2 Is an Androgen Receptor–Suppressed Driver of Neuroendocrine Differentiation in Prostate Cancer', *Cancer discovery*, vol. 7, no. 1, pp. 54-71.

Bluemn, EG, Coleman, IM, Lucas, JM, Coleman, RT, Hernandez-Lopez, S, Tharakan, R, Bianchi-Frias, D, Dumpit, RF, Kaipainen, A & Corella, AN 2017, 'Androgen receptor pathway-independent prostate cancer is sustained through FGF signaling', *Cancer cell*, vol. 32, no. 4, pp. 474-489. e476.

Bonci, D, Coppola, V, Patrizii, M, Addario, A, Cannistraci, A, Francescangeli, F, Pecci, R, Muto, G, Collura, D & Bedini, R 2016, 'A microRNA code for prostate cancer metastasis', *Oncogene*, vol. 35, no. 9, p. 1180.

Bracken, CP, Li, X, Wright, JA, Lawrence, DM, Pillman, KA, Salmanidis, M, Anderson, MA, Dredge, BK, Gregory, PA & Tsykin, A 2014, 'Genome-wide identification of miR-200 targets reveals a regulatory network controlling cell invasion', *The EMBO journal*, vol. 33, no. 18, pp. 2040-2056.

Braun, CJ, Zhang, X, Savelyeva, I, Wolff, S, Moll, UM, Schepeler, T, Ørntoft, TF, Andersen, CL & Dobbelstein, M 2008, 'p53-Responsive micrornas 192 and 215 are capable of inducing cell cycle arrest', *Cancer research*, vol. 68, no. 24, pp. 10094-10104.

Bray, F, Ferlay, J, Soerjomataram, I, Siegel, RL, Torre, LA & Jemal, A 2018, 'Global cancer statistics 2018: GLOBOCAN estimates of incidence and mortality worldwide for 36 cancers in 185 countries', *CA: a cancer journal for clinicians*.

Brinkmann, A, Jenster, G, Kuiper, G, Ris, C, Van Laar, J, Van der Korput, J, Degenhart, H, Trifiro, M, Pinsky, L & Romalo, G 1992, 'The human androgen receptor: structure/function relationship in normal and pathological situations', *The Journal of steroid biochemistry and molecular biology*, vol. 41, no. 3-8, pp. 361-368.

Brinkmann, AO, Faber, P, Van Rooij, H, Kuiper, G, Ris, C, Klaassen, P, Van der Korput, J, Voorhorst, M, Van Laar, J & Mulder, E 1989, 'The human androgen receptor: domain structure,

genomic organization and regulation of expression', *Journal of steroid biochemistry*, vol. 34, no. 1-6, pp. 307-310.

Broutier, L, Andersson-Rolf, A, Hindley, CJ, Boj, SF, Clevers, H, Koo, B-K & Huch, M 2016, 'Culture and establishment of self-renewing human and mouse adult liver and pancreas 3D organoids and their genetic manipulation', *Nature protocols*, vol. 11, no. 9, p. 1724.

Buffa, FM, Camps, C, Winchester, L, Snell, CE, Gee, HE, Sheldon, H, Taylor, M, Harris, AL & Ragoussis, J 2011, 'microRNA-associated progression pathways and potential therapeutic targets identified by integrated mRNA and microRNA expression profiling in breast cancer', *Cancer research*, vol. 71, no. 17, pp. 5635-5645.

Burdick, MJ, Reddy, CA, Ulchaker, J, Angermeier, K, Altman, A, Chehade, N, Mahadevan, A, Kupelian, PA, Klein, EA & Ciezki, JP 2009, 'Comparison of biochemical relapse-free survival between primary Gleason score 3 and primary Gleason score 4 for biopsy Gleason score 7 prostate cancer', *International Journal of Radiation Oncology* Biology* Physics*, vol. 73, no. 5, pp. 1439-1445.

Buyyounouski, MK, Choyke, PL, McKenney, JK, Sartor, O, Sandler, HM, Amin, MB, Kattan, MW & Lin, DW 2017, 'Prostate cancer–major changes in the American Joint Committee on Cancer eighth edition cancer staging manual', *CA: a cancer journal for clinicians*, vol. 67, no. 3, pp. 245-253.

Calin, GA, Dumitru, CD, Shimizu, M, Bichi, R, Zupo, S, Noch, E, Aldler, H, Rattan, S, Keating, M & Rai, K 2002, 'Frequent deletions and down-regulation of micro-RNA genes miR15 and miR16 at 13q14 in chronic lymphocytic leukemia', *Proceedings of the National Academy of Sciences*, vol. 99, no. 24, pp. 15524-15529.

Cancer Genome Atlas Research, N 2015, 'The Molecular Taxonomy of Primary Prostate Cancer', *Cell*, vol. 163, no. 4, Nov 5, pp. 1011-1025.

Chen, CD, Welsbie, DS, Tran, C, Baek, SH, Chen, R, Vessella, R, Rosenfeld, MG & Sawyers, CL 2004, 'Molecular determinants of resistance to antiandrogen therapy', *Nature medicine*, vol. 10, no. 1, p. 33.

Chen, Y, Clegg, NJ & Scher, HI 2009, 'Anti-androgens and androgen-depleting therapies in prostate cancer: new agents for an established target', *The lancet oncology*, vol. 10, no. 10, pp. 981-991.

Chen, Y, Zhao, H, Tan, Z, Zhang, C & Fu, X 2015, 'Bottleneck limitations for microRNA-based therapeutics from bench to the bedside', *Die Pharmazie-An International Journal of Pharmaceutical Sciences*, vol. 70, no. 3, pp. 147-154.

Chi, SW, Zang, JB, Mele, A & Darnell, RB 2009, 'Argonaute HITS-CLIP decodes microRNA–mRNA interaction maps', *Nature*, vol. 460, no. 7254, p. 479.

Chia, K, O'Brien, M, Brown, M & Lim, E 2015, 'Targeting the androgen receptor in breast cancer', *Current oncology reports*, vol. 17, no. 2, pp. 1-6.

Chmelar, R, Buchanan, G, Need, EF, Tilley, W & Greenberg, NM 2007, 'Androgen receptor coregulators and their involvement in the development and progression of prostate cancer', *International journal of cancer*, vol. 120, no. 4, pp. 719-733.

Choi, J-S, Nam, M-H, Yoon, S-Y & Kang, S-H 2015, 'MicroRNA-194-5p could serve as a diagnostic and prognostic biomarker in myelodysplastic syndromes', *Leukemia research*, vol. 39, no. 7, pp. 763-768.

Chong, JT, Oh, WK & Liaw, BC 2018, 'Profile of apalutamide in the treatment of metastatic castration-resistant prostate cancer: evidence to date', *OncoTargets and therapy*, vol. 11, p. 2141.

Cimmino, A, Calin, GA, Fabbri, M, Iorio, MV, Ferracin, M, Shimizu, M, Wojcik, SE, Aqeilan, RI, Zupo, S & Dono, M 2005, 'miR-15 and miR-16 induce apoptosis by targeting BCL2', *Proceedings of the National Academy of Sciences*, vol. 102, no. 39, pp. 13944-13949.

Claessens, F, Alen, P, Devos, A, Peeters, B, Verhoeven, G & Rombauts, W 1996, 'The androgen-specific probasin response element 2 interacts differentially with androgen and glucocorticoid receptors', *Journal of Biological Chemistry*, vol. 271, no. 32, pp. 19013-19016.

Clarke, CL & Graham, JD 2012, 'Non-overlapping progesterone receptor cistromes contribute to cell-specific transcriptional outcomes', *PloS one*, vol. 7, no. 4, p. e35859.

Cooke, PS, Young, P & Cunha, GR 1991, 'Androgen receptor expression in developing male reproductive organs', *Endocrinology*, vol. 128, no. 6, pp. 2867-2873.

Coutinho, I, Day, TK, Tilley, WD & Selth, LA 2016, 'Androgen receptor signaling in castration-resistant prostate cancer: a lesson in persistence', *Endocrine-Related Cancer*, vol. 23, no. 12, pp. T179-T197.

Culig, Z, Hoffmann, J, Erdel, M, Eder, I, Hobisch, A, Hittmair, A, Bartsch, G, Utermann, G, Schneider, M & Parczyk, K 1999, 'Switch from antagonist to agonist of the androgen receptor blocker bicalutamide is associated with prostate tumour progression in a new model system', *British journal of cancer*, vol. 81, no. 2, p. 242.

Cury, J, Coelho, RF & Srougi, M 2008, 'Well-differentiated prostate cancer in core biopsy specimens may be associated with extraprostatic disease', *Sao Paulo Medical Journal*, vol. 126, no. 2, pp. 119-122.

D'Amico, AV, Whittington, R, Malkowicz, SB, Schultz, D, Blank, K, Broderick, GA, Tomaszewski, JE, Renshaw, AA, Kaplan, I & Beard, CJ 1998, 'Biochemical outcome after radical prostatectomy, external beam radiation therapy, or interstitial radiation therapy for clinically localized prostate cancer', *Jama*, vol. 280, no. 11, pp. 969-974.

Dardenne, E, Beltran, H, Benelli, M, Gayvert, K, Berger, A, Puca, L, Cyrta, J, Sboner, A, Noorzad, Z & MacDonald, T 2016, 'N-Myc induces an EZH2-mediated transcriptional program driving neuroendocrine prostate cancer', *Cancer cell*, vol. 30, no. 4, pp. 563-577.

Das, R, Gregory, PA, Fernandes, RC, Denis, I, Wang, Q, Townley, SL, Zhao, SG, Hanson, AR, Pickering, MA, Armstrong, HK, Lokman, NA, Ebrahimie, E, Davicioni, E, Jenkins, RB, Karnes, RJ, Ross, AE, Den, RB, Klein, EA, Chi, KN, Ramshaw, HS, Williams, ED, Zoubeidi, A, Goodall, GJ, Feng, FY, Butler, LM, Tilley, WD & Selth, LA 2017, 'MicroRNA-194 Promotes Prostate Cancer Metastasis by Inhibiting SOCS2', *Cancer Res*, vol. 77, no. 4, Feb 15, pp. 1021-1034.

Davies, AH, Beltran, H & Zoubeidi, A 2018, 'Cellular plasticity and the neuroendocrine phenotype in prostate cancer', *Nature Reviews Urology*.

Dicken, H, Hensley, PJ & Kyprianou, N 2019, 'Prostate tumor neuroendocrine differentiation via EMT: The road less traveled', *Asian journal of urology*, vol. 6, no. 1, pp. 82-90.

Dong, Q, Meng, P, Wang, T, Qin, W, Qin, W, Wang, F, Yuan, J, Chen, Z, Yang, A & Wang, H 2010, 'MicroRNA let-7a inhibits proliferation of human prostate cancer cells in vitro and in vivo by targeting E2F2 and CCND2', *PloS one*, vol. 5, no. 4, p. e10147.

Donjacour, AA & Cunha, GR 1993, 'Assessment of prostatic protein secretion in tissue recombinants made of urogenital sinus mesenchyme and urothelium from normal or androgen-insensitive mice', *Endocrinology*, vol. 132, no. 6, pp. 2342-2350.

Eisermann, K, Wang, D, Jing, Y, Pascal, LE & Wang, Z 2013, 'Androgen receptor gene mutation, rearrangement, polymorphism', *Translational andrology and urology*, vol. 2, no. 3, p. 137.

Ellis, L & Loda, M 2018, 'LSD1: A single target to combat lineage plasticity in lethal prostate cancer', *Proceedings of the National Academy of Sciences*, vol. 115, no. 18, pp. 4530-4531.

Ellwanger, DC, Büttner, FA, Mewes, H-W & Stümpflen, V 2011, 'The sufficient minimal set of miRNA seed types', *Bioinformatics*, vol. 27, no. 10, pp. 1346-1350.

Epstein, JI 2000, 'Gleason score 2–4 adenocarcinoma of the prostate on needle biopsy: a diagnosis that should not be made', LWW.

Erhard, F, Haas, J, Lieber, D, Malterer, G, Jaskiewicz, L, Zavolan, M, Dölken, L & Zimmer, R 2014, 'Widespread context dependency of microRNA-mediated regulation', *Genome research*, vol. 24, no. 6, pp. 906-919.

Esposito, S, Russo, MV, Airoldi, I, Tupone, MG, Sorrentino, C, Barbarito, G, Di Meo, S & Di Carlo, E 2015, 'SNAI2/Slug gene is silenced in prostate cancer and regulates neuroendocrine differentiation, metastasis-suppressor and pluripotency gene expression', *Oncotarget*, vol. 6, no. 19, p. 17121.

Fang, Z & Rajewsky, N 2011, 'The impact of miRNA target sites in coding sequences and in 3′ UTRs', *PloS one*, vol. 6, no. 3, p. e18067.

Forman, JJ & Coller, HA 2010, 'The code within the code: microRNAs target coding regions', *Cell cycle*, vol. 9, no. 8, pp. 1533-1541.

Friedlander, TW & Ryan, CJ 2010, 'Adrenal Androgen Synthesis Inhibitor Therapies in Castration-Resistant Prostate Cancer', *Drug Management of Prostate Cancer*, Springer, pp. 91-100.

Friedman, RC, Farh, KK-H, Burge, CB & Bartel, DP 2009, 'Most mammalian mRNAs are conserved targets of microRNAs', *Genome research*, vol. 19, no. 1, pp. 92-105.

Fuqua, SA 2001, 'The role of estrogen receptors in breast cancer metastasis', *Journal of mammary gland biology and neoplasia*, vol. 6, no. 4, pp. 407-417.

Gaidatzis, D, Burger, L, Florescu, M & Stadler, MB 2015, 'Analysis of intronic and exonic reads in RNA-seq data characterizes transcriptional and post-transcriptional regulation', *Nature biotechnology*, vol. 33, no. 7, p. 722.

Galardi, S, Mercatelli, N, Giorda, E, Massalini, S, Frajese, GV, Ciafrè, SA & Farace, MG 2007, 'miR-221 and miR-222 expression affects the proliferation potential of human prostate carcinoma cell lines by targeting p27Kip1', *Journal of Biological Chemistry*, vol. 282, no. 32, pp. 23716-23724.

Gao, N, Ishii, K, Mirosevich, J, Kuwajima, S, Oppenheimer, SR, Roberts, RL, Jiang, M, Yu, X, Shappell, SB & Caprioli, RM 2005, 'Forkhead box A1 regulates prostate ductal morphogenesis and promotes epithelial cell maturation', *Development*, vol. 132, no. 15, pp. 3431-3443.

Gao, N, Zhang, J, Rao, MA, Case, TC, Mirosevich, J, Wang, Y, Jin, R, Gupta, A, Rennie, PS & Matusik, RJ 2003, 'The role of hepatocyte nuclear factor-3α (Forkhead Box A1) and androgen receptor in transcriptional regulation of prostatic genes', *Molecular Endocrinology*, vol. 17, no. 8, pp. 1484-1507.

Gleason, DF 1966, 'Classification of prostatic carcinomas', *Cancer Chemother. Rep.*, vol. 50, pp. 125-128.

Gleason, DF 1992, 'Histologic grading of prostate cancer: a perspective', *Human pathology*, vol. 23, no. 3, pp. 273-279.

Gordetsky, J & Epstein, J 2016, 'Grading of prostatic adenocarcinoma: current state and prognostic implications', *Diagnostic pathology*, vol. 11, no. 1, p. 25.

Gordon, K & Hodgen, GD 1992, 'Evolving role of gonadotropin-releasing hormone antagonists', *Trends in Endocrinology & Metabolism*, vol. 3, no. 7, pp. 259-263.

Goto, Y, Kojima, S, Nishikawa, R, Kurozumi, A, Kato, M, Enokida, H, Matsushita, R, Yamazaki, K, Ishida, Y & Nakagawa, M 2015, 'MicroRNA expression signature of castration-resistant prostate cancer: the microRNA-221/222 cluster functions as a tumour suppressor and disease progression marker', *British journal of cancer*, vol. 113, no. 7, p. 1055.

Grasso, CS, Wu, Y-M, Robinson, DR, Cao, X, Dhanasekaran, SM, Khan, AP, Quist, MJ, Jing, X, Lonigro, RJ & Brenner, JC 2012, 'The mutational landscape of lethal castration-resistant prostate cancer', *Nature*, vol. 487, no. 7406, p. 239.

Grimson, A, Farh, KK-H, Johnston, WK, Garrett-Engele, P, Lim, LP & Bartel, DP 2007, 'MicroRNA targeting specificity in mammals: determinants beyond seed pairing', *Molecular cell*, vol. 27, no. 1, pp. 91-105.

Grino, PB, Griffin, JE & Wilson, JD 1990, 'Testosterone at high concentrations interacts with the human androgen receptor similarly to dihydrotestosterone', *Endocrinology*, vol. 126, no. 2, pp. 1165-1172.

Gui, B, Hsieh, C-L, Kantoff, PW, Kibel, AS & Jia, L 2017, 'Androgen receptor-mediated downregulation of microRNA-221 and-222 in castration-resistant prostate cancer', *PloS one*, vol. 12, no. 9, p. e0184166.

Ha, M & Kim, VN 2014, 'Regulation of microRNA biogenesis', *Nature reviews Molecular cell biology*, vol. 15, no. 8, p. 509.

Hamdy, FC, Donovan, JL, Lane, JA, Mason, M, Metcalfe, C, Holding, P, Davis, M, Peters, TJ, Turner, EL & Martin, RM 2016, '10-year outcomes after monitoring, surgery, or radiotherapy for localized prostate cancer', *New England Journal of Medicine*, vol. 375, no. 15, pp. 1415-1424.

Han, J, Lee, Y, Yeom, K-H, Kim, Y-K, Jin, H & Kim, VN 2004, 'The Drosha-DGCR8 complex in primary microRNA processing', *Genes & development*, vol. 18, no. 24, pp. 3016-3027.

Hart, M, Nolte, E, Wach, S, Szczyrba, J, Taubert, H, Rau, TT, Hartmann, A, Grässer, FA & Wullich, B 2014, 'Comparative microRNA profiling of prostate carcinomas with increasing tumor stage by deep sequencing', *Molecular cancer research*, vol. 12, no. 2, pp. 250-263.

Hausser, J, Syed, AP, Bilen, B & Zavolan, M 2013, 'Analysis of CDS-located miRNA target sites suggests that they can effectively inhibit translation', *Genome research*, vol. 23, no. 4, pp. 604-615.

He, B, Lanz, RB, Fiskus, W, Geng, C, Yi, P, Hartig, SM, Rajapakshe, K, Shou, J, Wei, L & Shah, SS 2014, 'GATA2 facilitates steroid receptor coactivator recruitment to the androgen receptor complex', *Proceedings of the National Academy of Sciences*, vol. 111, no. 51, pp. 18261-18266.

Heinlein, CA & Chang, C 2002, 'Androgen receptor (AR) coregulators: an overview', *Endocrine reviews*, vol. 23, no. 2, pp. 175-200.

Heinlein, CA & Chang, C 2004, 'Androgen receptor in prostate cancer', *Endocr Rev*, vol. 25, no. 2, Apr, pp. 276-308.

Helpap, B, Köllermann, J & Oehler, U 1999, 'Neuroendocrine differentiation in prostatic carcinomas: histogenesis, biology, clinical relevance, and future therapeutical perspectives', *Urologia internationalis*, vol. 62, no. 3, pp. 133-138.

Helwak, A, Kudla, G, Dudnakova, T & Tollervey, D 2013, 'Mapping the human miRNA interactome by CLASH reveals frequent noncanonical binding', *Cell*, vol. 153, no. 3, pp. 654-665.

Hino, K, Tsuchiya, K, Fukao, T, Kiga, K, Okamoto, R, Kanai, T & Watanabe, M 2008, 'Inducible expression of microRNA-194 is regulated by HNF-1α during intestinal epithelial cell differentiation', *Rna*, vol. 14, no. 7, pp. 1433-1442.

Hironaka-Mitsuhashi, A, Matsuzaki, J, Takahashi, R-u, Yoshida, M, Nezu, Y, Yamamoto, Y, Shiino, S, Kinoshita, T, Ushijima, T & Hiraoka, N 2017, 'A tissue microRNA signature that predicts the prognosis of breast cancer in young women', *PloS one*, vol. 12, no. 11, p. e0187638.

Hoefert, JE, Bjerke, GA, Wang, D & Yi, R 2018, 'The microRNA-200 family coordinately regulates cell adhesion and proliferation in hair morphogenesis', *J Cell Biol*, vol. 217, no. 6, pp. 2185-2204.

Hörnberg, E, Ylitalo, EB, Crnalic, S, Antti, H, Stattin, P, Widmark, A, Bergh, A & Wikström, P 2011, 'Expression of androgen receptor splice variants in prostate cancer bone metastases is associated with castration-resistance and short survival', *PloS one*, vol. 6, no. 4, p. e19059.

Huggins, C & Hodges, CV 1941, 'Studies on prostatic cancer. I. The effect of castration, of estrogen and of androgen injection on serum phosphatases in metastatic carcinoma of the prostate', *Cancer research*, vol. 1, no. 4, pp. 293-297.

Humphrey, PA 2004, 'Gleason grading and prognostic factors in carcinoma of the prostate', *Modern pathology*, vol. 17, no. 3, p. 292.

Huo, D, Clayton, WM, Yoshimatsu, TF, Chen, J & Olopade, OI 2016, 'Identification of a circulating MicroRNA signature to distinguish recurrence in breast cancer patients', *Oncotarget*, vol. 7, no. 34, p. 55231.

Isaacs, JT & Coffey, DS 1989, 'Etiology and disease process of benign prostatic hyperplasia', *The prostate*, vol. 15, no. S2, pp. 33-50.

Jalava, S, Urbanucci, A, Latonen, L, Waltering, K, Sahu, B, Jänne, OA, Seppälä, J, Lähdesmäki, H, Tammela, T & Visakorpi, T 2012, 'Androgen-regulated miR-32 targets BTG2 and is overexpressed in castration-resistant prostate cancer', *Oncogene*, vol. 31, no. 41, p. 4460.

Jang, TL, Patel, N, Faiena, I, Radadia, KD, Moore, DF, Elsamra, SE, Singer, EA, Stein, MN, Eastham, JA & Scardino, PT 2018, 'Comparative effectiveness of radical prostatectomy with adjuvant radiotherapy versus radiotherapy plus androgen deprivation therapy for men with advanced prostate cancer', *Cancer*, vol. 124, no. 20, pp. 4010-4022.

Jenster, G, Trapman, J & Brinkmann, A 1993, 'Nuclear import of the human androgen receptor', *Biochemical Journal*, vol. 293, no. 3, pp. 761-768.

Jenster, G, van der Korput, HA, van Vroonhoven, C, van der Kwast, TH, Trapman, J & Brinkmann, AO 1991, 'Domains of the human androgen receptor involved in steroid binding, transcriptional activation, and subcellular localization', *Molecular Endocrinology*, vol. 5, no. 10, pp. 1396-1404.

Jeon, H-M & Lee, J 2017, 'MET: roles in epithelial-mesenchymal transition and cancer stemness', *Annals of translational medicine*, vol. 5, no. 1.

Jernberg, E, Bergh, A & Wikström, P 2017, 'Clinical relevance of androgen receptor alterations in prostate cancer', *Endocrine connections*, vol. 6, no. 8, pp. R146-R161.

Jeselsohn, R, Buchwalter, G, De Angelis, C, Brown, M & Schiff, R 2015, 'ESR1 mutations [mdash] a mechanism for acquired endocrine resistance in breast cancer', *Nature Reviews Clinical Oncology*.

Jin, H-J, Zhao, JC, Ogden, I, Bergan, RC & Yu, J 2013, 'Androgen receptor-independent function of FoxA1 in prostate cancer metastasis', *Cancer research*, vol. 73, no. 12, pp. 3725-3736.

Jin, H-J, Zhao, JC, Wu, L, Kim, J & Yu, J 2014, 'Cooperativity and equilibrium with FOXA1 define the androgen receptor transcriptional program', *Nature communications*, vol. 5, p. 3972.

Jozwik, KM & Carroll, JS 2012, 'Pioneer factors in hormone-dependent cancers', *Nature Reviews Cancer*, vol. 12, no. 6, p. 381.

Kabekkodu, SP, Shukla, V, Varghese, VK, D'Souza, J, Chakrabarty, S & Satyamoorthy, K 2018, 'Clustered miRNAs and their role in biological functions and diseases', *Biological Reviews*, vol. 93, no. 4, pp. 1955-1986.

Kaestner, KH 2010, 'The FoxA factors in organogenesis and differentiation', *Current opinion in genetics & development*, vol. 20, no. 5, pp. 527-532.

Kallio, HM, Hieta, R, Latonen, L, Brofeldt, A, Annala, M, Kivinummi, K, Tammela, TL, Nykter, M, Isaacs, WB & Lilja, HG 2018, 'Constitutively active androgen receptor splice variants AR-V3, AR-V7 and AR-V9 are co-expressed in castration-resistant prostate cancer metastases', *British journal of cancer*, vol. 119, no. 3, p. 347.

Kalofonou, F, Leach, D, Hamilton, M, Mcguire, SE, Fletcher, C, Waxman, J & Bevan, CL 2019, 'MiR-1271-5p: An AR-modulatory microRNA with a distinct role in prostate cancer progression, through SND1 and MORF4L1 interaction', American Society of Clinical Oncology.

Kang, A-R, An, H-T, Ko, J & Kang, S 2017, 'Ataxin-1 regulates epithelial–mesenchymal transition of cervical cancer cells', *Oncotarget*, vol. 8, no. 11, p. 18248.

Kapatia, G, Attri, VS, Mete, UK & Rastogi, P 2018, 'Metastatic basal cell carcinoma of prostate in a young adult: A rare aggressive entity', *African Journal of Urology*, vol. 24, no. 4, pp. 287-290.

Kauffmann, G & Liauw, SL 2017, 'The use of Hormonal Therapy to Augment Radiation Therapy in Prostate Cancer: An Update', *Current urology reports*, vol. 18, no. 7, p. 50.

Kemppainen, JA & Wilson, EM 1996, 'Agonist and antagonist activities of hydroxyflutamide and Casodex relate to androgen receptor stabilization', *Urology*, vol. 48, no. 1, pp. 157-163.

Khella, HW, Bakhet, M, Allo, G, Jewett, MA, Girgis, AH, Latif, A, Girgis, H, Von Both, I, Bjarnason, GA & Yousef, GM 2013, 'miR-192, miR-194 and miR-215: a convergent microRNA network suppressing tumor progression in renal cell carcinoma', *Carcinogenesis*, vol. 34, no. 10, pp. 2231-2239.

Kim, J & Coetzee, GA 2004, 'Prostate specific antigen gene regulation by androgen receptor', *J Cell Biochem*, vol. 93, no. 2, Oct 1, pp. 233-241.

Kim, J, Jin, H, Zhao, JC, Yang, YA, Li, Y, Yang, X, Dong, X & Yu, J 2017, 'FOXA1 inhibits prostate cancer neuroendocrine differentiation', *Oncogene*, vol. 36, no. 28, p. 4072.

Kobayashi, H & Tomari, Y 2016, 'RISC assembly: Coordination between small RNAs and Argonaute proteins', *Biochimica et Biophysica Acta (BBA)-Gene Regulatory Mechanisms*, vol. 1859, no. 1, pp. 71-81.

Koivisto, P, Kononen, J, Palmberg, C, Tammela, T, Hyytinen, E, Isola, J, Trapman, J, Cleutjens, K, Noordzij, A & Visakorpi, T 1997, 'Androgen receptor gene amplification: a possible molecular mechanism for androgen deprivation therapy failure in prostate cancer', *Cancer research*, vol. 57, no. 2, pp. 314-319.

Kreth, S, Hübner, M & Hinske, LC 2018, 'MicroRNAs as clinical biomarkers and therapeutic tools in perioperative medicine', *Anesthesia & Analgesia*, vol. 126, no. 2, pp. 670-681.

Krützfeldt, J, Rösch, N, Hausser, J, Manoharan, M, Zavolan, M & Stoffel, M 2012, 'MicroRNA-194 is a target of transcription factor 1 (Tcf1, HNF1α) in adult liver and controls expression of frizzled-6', *Hepatology*, vol. 55, no. 1, pp. 98-107.

Ku, SY, Rosario, S, Wang, Y, Mu, P, Seshadri, M, Goodrich, ZW, Goodrich, MM, Labbé, DP, Gomez, EC & Wang, J 2017, 'Rb1 and Trp53 cooperate to suppress prostate cancer lineage plasticity, metastasis, and antiandrogen resistance', *Science*, vol. 355, no. 6320, pp. 78-83.

Kumar, A, Coleman, I, Morrissey, C, Zhang, X, True, LD, Gulati, R, Etzioni, R, Bolouri, H, Montgomery, B & White, T 2016, 'Substantial interindividual and limited intraindividual genomic diversity among tumors from men with metastatic prostate cancer', *Nature medicine*, vol. 22, no. 4, p. 369.

Labrie, F, BÉLANGER, A, CUSAN, L, SEGUIN, C, PELLETIER, G, KELLY, PA, REEVES, JJ, LEFEBVRE, FA, LEMAY, A & GOURDEAU, Y 1980, 'Antifertility effects of LHRH agonists in the male', *Journal of Andrology*, vol. 1, no. 5, pp. 209-228.

Labrie, F, Belanger, A, Luu-The, V, Labrie, C, Simard, J, Cusan, L, Gomez, J & Candas, B 2005, 'Gonadotropin-releasing hormone agonists in the treatment of prostate cancer', *Endocrine reviews*, vol. 26, no. 3, pp. 361-379.

Lal, A, Navarro, F, Maher, C, Maliszewski, LE, Yan, N, O'Day, E, Chowdhury, D, Dykxhoorn, DM, Tsai, P & Hofman, O 2009, 'miR-24 inhibits cell proliferation by suppressing expression of E2F2, MYC and other cell cycle regulatory genes by binding to "seedless" 3′ UTR microRNA recognition elements', *Molecular cell*, vol. 35, no. 5, p. 610.

Lawrence, MG, Obinata, D, Sandhu, S, Selth, LA, Wong, SQ, Porter, LH, Lister, N, Pook, D, Pezaro, CJ & Goode, DL 2018, 'Patient-derived models of abiraterone-and enzalutamide-resistant prostate cancer reveal sensitivity to ribosome-directed therapy', *European urology*, vol. 74, no. 5, pp. 562-572.

Le Magnen, C, Shen, MM & Abate-Shen, C 2018, 'Lineage plasticity in cancer progression and treatment', *Annual review of cancer biology*, vol. 2, pp. 271-289.

Le, X-F, Almeida, MI, Mao, W, Spizzo, R, Rossi, S, Nicoloso, MS, Zhang, S, Wu, Y, Calin, GA & Bast Jr, RC 2012, 'Modulation of MicroRNA-194 and cell migration by HER2-targeting trastuzumab in breast cancer', *PloS one*, vol. 7, no. 7, p. e41170.

Lee, AR, Gan, Y, Tang, Y & Dong, X 2018, 'A novel mechanism of SRRM4 in promoting neuroendocrine prostate cancer development via a pluripotency gene network', *EBioMedicine*, vol. 35, pp. 167-177.

Lee, JJ, Thomas, IC, Nolley, R, Ferrari, M, Brooks, JD & Leppert, JT 2015, 'Biologic differences between peripheral and transition zone prostate cancer', *The prostate*, vol. 75, no. 2, pp. 183-190.

Lee, RC, Feinbaum, RL & Ambros, V 1993, 'The C. elegans heterochronic gene lin-4 encodes small RNAs with antisense complementarity to lin-14', *Cell*, vol. 75, no. 5, pp. 843-854.

Lee, Y, Ahn, C, Han, J, Choi, H, Kim, J, Yim, J, Lee, J, Provost, P, Rådmark, O & Kim, S 2003, 'The nuclear RNase III Drosha initiates microRNA processing', *Nature*, vol. 425, no. 6956, p. 415.

Lee, Y, Kim, M, Han, J, Yeom, KH, Lee, S, Baek, SH & Kim, VN 2004, 'MicroRNA genes are transcribed by RNA polymerase II', *The EMBO journal*, vol. 23, no. 20, pp. 4051-4060.

Leung, AK, Young, AG, Bhutkar, A, Zheng, GX, Bosson, AD, Nielsen, CB & Sharp, PA 2011, 'Genome-wide identification of Ago2 binding sites from mouse embryonic stem cells with and without mature microRNAs', *Nature structural & molecular biology*, vol. 18, no. 2, p. 237.

Li, J-p, Liu, Y & Yin, Y-h 2017, 'ARHGAP1 overexpression inhibits proliferation, migration and invasion of C-33A and SiHa cell lines', *OncoTargets and therapy*, vol. 10, p. 691.

Li, J & Zhang, Y 2019, 'Current experimental strategies for intracellular target identification of microRNA', *ExRNA*, vol. 1, no. 1, p. 6.

Li, L, Liu, X, He, L, Yang, J, Pei, F, Li, W, Liu, S, Chen, Z, Xie, G & Xu, B 2017, 'ZNF516 suppresses EGFR by targeting the CtBP/LSD1/CoREST complex to chromatin', *Nature communications*, vol. 8, no. 1, p. 691.

Linder, S, van der Poel, H, Bergman, AM, Zwart, W & Prekovic, S 2018, 'Enzalutamide therapy for advanced prostate cancer: efficacy, resistance and beyond', *Endocrine-Related Cancer*, vol. 1, no. aop.

Liu, T, Ortiz, JA, Taing, L, Meyer, CA, Lee, B, Zhang, Y, Shin, H, Wong, SS, Ma, J & Lei, Y 2011, 'Cistrome: an integrative platform for transcriptional regulation studies', *Genome biology*, vol. 12, no. 8, p. R83.

Loeb, GB, Khan, AA, Canner, D, Hiatt, JB, Shendure, J, Darnell, RB, Leslie, CS & Rudensky, AY 2012, 'Transcriptome-wide miR-155 binding map reveals widespread noncanonical microRNA targeting', *Molecular cell*, vol. 48, no. 5, pp. 760-770.

Logothetis, CJ & Lin, S-H 2005, 'Osteoblasts in prostate cancer metastasis to bone', *Nature Reviews Cancer*, vol. 5, no. 1, pp. 21-28.

Lonergan, PE & Tindall, DJ 2011, 'Androgen receptor signaling in prostate cancer development and progression', *Journal of carcinogenesis*, vol. 10, no. 1, p. 20.

López-Otín, C & Diamandis, EP 1998, 'Breast and prostate cancer: an analysis of common epidemiological, genetic, and biochemical features', *Endocrine reviews*, vol. 19, no. 4, pp. 365-396.

Lu, W, Liu, S, Li, B, Xie, Y, Izban, M, Ballard, BR, Sathyanarayana, S, Adunyah, S, Matusik, RJ & Chen, Z 2017, 'SKP2 loss destabilizes EZH2 by promoting TRAF6-mediated ubiquitination to suppress prostate cancer', *Oncogene*, vol. 36, no. 10, p. 1364.

Lubahn, DB, Joseph, DR, Sullivan, PM, Willard, HF, French, FS & Wilson, EM 1988, 'Cloning of human androgen receptor complementary DNA and localization to the X chromosome', *Science*, vol. 240, no. 4850, pp. 327-330.

Luna, JM, Barajas, JM, Teng, K-y, Sun, H-L, Moore, MJ, Rice, CM, Darnell, RB & Ghoshal, K 2017, 'Argonaute CLIP defines a deregulated miR-122-bound transcriptome that correlates with patient survival in human liver cancer', *Molecular cell*, vol. 67, no. 3, pp. 400-410. e407.

Lund, E, Güttinger, S, Calado, A, Dahlberg, JE & Kutay, U 2004, 'Nuclear export of microRNA precursors', *Science*, vol. 303, no. 5654, pp. 95-98.

Luo, J, Wang, K, Yeh, S, Sun, Y, Liang, L, Xiao, Y, Xu, W, Niu, Y, Cheng, L & Maity, SN 2019, 'LncRNA-p21 alters the antiandrogen enzalutamide-induced prostate cancer neuroendocrine differentiation via modulating the EZH2/STAT3 signaling', *Nature communications*, vol. 10, no. 1, p. 2571.

M Witkos, T, Koscianska, E & J Krzyzosiak, W 2011, 'Practical aspects of microRNA target prediction', *Current molecular medicine*, vol. 11, no. 2, pp. 93-109.

Martens-Uzunova, E, Jalava, S, Dits, N, Van Leenders, G, Møller, S, Trapman, J, Bangma, C, Litman, T, Visakorpi, T & Jenster, G 2012, 'Diagnostic and prognostic signatures from the small non-coding RNA transcriptome in prostate cancer', *Oncogene*, vol. 31, no. 8, p. 978.

Mathé, EA, Nguyen, GH, Bowman, ED, Zhao, Y, Budhu, A, Schetter, AJ, Braun, R, Reimers, M, Kumamoto, K & Hughes, D 2009, 'MicroRNA expression in squamous cell carcinoma and adenocarcinoma of the esophagus: associations with survival', *Clinical Cancer Research*, vol. 15, no. 19, pp. 6192-6200.

Mayran, A & Drouin, J 2018, 'Pioneer transcription factors shape the epigenetic landscape', *Journal of Biological Chemistry*, vol. 293, no. 36, pp. 13795-13804.

McGeary, SE, Lin, KS, Shi, CY, Bisaria, N & Bartel, DP 2018, 'The biochemical basis of microRNA targeting efficacy', *BioRxiv*, p. 414763.

McKeithen, D, Graham, T, Chung, LW & Odero-Marah, V 2010, 'Snail transcription factor regulates neuroendocrine differentiation in LNCaP prostate cancer cells', *The prostate*, vol. 70, no. 9, pp. 982-992.

McNeal, JE 1978, 'Origin and evolution of benign prostatic enlargement', *Investigative urology*, vol. 15, no. 4, pp. 340-345.

McNeal, JE 1981, 'The zonal anatomy of the prostate', *The prostate*, vol. 2, no. 1, pp. 35-49.

McNeal, JE 1988, 'Normal histology of the prostate', *The American journal of surgical pathology*, vol. 12, no. 8, pp. 619-633.

McNeal, JE, Redwine, EA, Freiha, FS & Stamey, TA 1988, 'Zonal distribution of prostatic adenocarcinoma. Correlation with histologic pattern and direction of spread', *The American journal of surgical pathology*, vol. 12, no. 12, pp. 897-906.

Meng, Y, Shao, C, Ma, X & Wang, H 2013, 'Introns targeted by plant microRNAs: a possible novel mechanism of gene regulation', *Rice*, vol. 6, no. 1, p. 8.

Merseburger, AS, Bellmunt, J, Jenkins, C, Parker, C & Fitzpatrick, JM 2013, 'Perspectives on treatment of metastatic castration-resistant prostate cancer', *The oncologist*, vol. 18, no. 5, pp. 558-567.

Miller, KD, Siegel, RL, Lin, CC, Mariotto, AB, Kramer, JL, Rowland, JH, Stein, KD, Alteri, R & Jemal, A 2016, 'Cancer treatment and survivorship statistics, 2016', *CA Cancer J Clin*, vol. 66, no. 4, Jul, pp. 271-289.

Mirosevich, J, Bentel, J, Zeps, N, Redmond, S, D'antuono, M & Dawkins, H 1999, 'Androgen receptor expression of proliferating basal and luminal cells in adult murine ventral prostate', *Journal of Endocrinology*, vol. 162, no. 3, pp. 341-350.

Mishra, S, Lin, C-L, Huang, TH, Bouamar, H & Sun, L-Z 2014, 'MicroRNA-21 inhibits p57 Kip2 expression in prostate cancer', *Molecular cancer*, vol. 13, no. 1, p. 212.

Monteys, AM, Spengler, RM, Wan, J, Tecedor, L, Lennox, KA, Xing, Y & Davidson, BL 2010, 'Structure and activity of putative intronic miRNA promoters', *Rna*, vol. 16, no. 3, pp. 495-505.

Montgomery, RB, Mostaghel, EA, Vessella, R, Hess, DL, Kalhorn, TF, Higano, CS, True, LD & Nelson, PS 2008, 'Maintenance of intratumoral androgens in metastatic prostate cancer: a mechanism for castration-resistant tumor growth', *Cancer research*, vol. 68, no. 11, pp. 4447-4454.

Moore, MJ, Scheel, TK, Luna, JM, Park, CY, Fak, JJ, Nishiuchi, E, Rice, CM & Darnell, RB 2015, 'miRNA–target chimeras reveal miRNA 3′-end pairing as a major determinant of Argonaute target specificity', *Nature communications*, vol. 6, p. 8864.

Mosquera, JM, Beltran, H, Park, K, MacDonald, TY, Robinson, BD, Tagawa, ST, Perner, S, Bismar, TA, Erbersdobler, A & Dhir, R 2013, 'Concurrent AURKA and MYCN gene amplifications are harbingers of lethal treatment-related neuroendocrine prostate cancer', *Neoplasia (New York, NY)*, vol. 15, no. 1, p. 1.

Mostaghel, EA 2013, 'Steroid hormone synthetic pathways in prostate cancer', *Translational andrology and urology*, vol. 2, no. 3, p. 212.

Mostaghel, EA & Plymate, S 2011, 'New hormonal therapies for castration-resistant prostate cancer', *Endocrinology and Metabolism Clinics*, vol. 40, no. 3, pp. 625-642.

Mottet, N, Bellmunt, J, Bolla, M, Briers, E, Cumberbatch, MG, De Santis, M, Fossati, N, Gross, T, Henry, AM & Joniau, S 2017, 'EAU-ESTRO-SIOG guidelines on prostate cancer. Part 1: screening, diagnosis, and local treatment with curative intent', *European urology*, vol. 71, no. 4, pp. 618-629.

Mu, P, Zhang, Z, Benelli, M, Karthaus, WR, Hoover, E, Chen, C-C, Wongvipat, J, Ku, S-Y, Gao, D & Cao, Z 2017, 'SOX2 promotes lineage plasticity and antiandrogen resistance in TP53-and RB1-deficient prostate cancer', *Science*, vol. 355, no. 6320, pp. 84-88.

Nabavi, N, Saidy, NRN, Venalainen, E, Haegert, A, Parolia, A, Xue, H, Wang, Y, Wu, R, Dong, X & Collins, C 2017, 'miR-100-5p inhibition induces apoptosis in dormant prostate cancer cells and prevents the emergence of castration-resistant prostate cancer', *Scientific reports*, vol. 7, no. 1, p. 4079.

Nam, RK, Benatar, T, Amemiya, Y, Wallis, CJ, Romero, JM, Tsagaris, M, Sherman, C, Sugar, L & Seth, A 2018, 'MicroRNA-652 induces NED in LNCaP and EMT in PC3 prostate cancer cells', *Oncotarget*, vol. 9, no. 27, p. 19159.

National Cancer Control Indicators, CA 2019, *Distribution of cancer stage*, <https://ncci.canceraustralia.gov.au/diagnosis/distribution-cancer-stage/distribution-cancer-stage>.

Neame, E 2009, 'HITS-CLIP hits the microRNA target', *Nature Reviews Genetics*, vol. 10, 08/01/online, p. 510.

Nouri, M, Caradec, J, Lubik, AA, Li, N, Hollier, BG, Takhar, M, Altimirano-Dimas, M, Chen, M, Roshan-Moniri, M & Butler, M 2017, 'Therapy-induced developmental reprogramming of prostate cancer cells and acquired therapy resistance', *Oncotarget*, vol. 8, no. 12, p. 18949.

O'Donnell, H & Parker, C 2008, 'What is low-risk prostate cancer and what is its natural history?', *World journal of urology*, vol. 26, no. 5, pp. 415-422.

Oh, M, Alkhushaym, N, Fallatah, S, Althagafi, A, Aljadeed, R, Alsowaida, Y, Jeter, J, Martin, JR, Babiker, HM & McBride, A 2019, 'The association of BRCA1 and BRCA2 mutations with prostate cancer risk, frequency, and mortality: A meta-analysis', *The prostate*, vol. 79, no. 8, pp. 880-895.

Ørom, UA, Nielsen, FC & Lund, AH 2008, 'MicroRNA-10a binds the 5′ UTR of ribosomal protein mRNAs and enhances their translation', *Molecular cell*, vol. 30, no. 4, pp. 460-471.

Ovando-Vázquez, C, Lepe-Soltero, D & Abreu-Goodger, C 2016, 'Improving microRNA target prediction with gene expression profiles', *BMC genomics*, vol. 17, no. 1, p. 364.

Ozsolak, F, Poling, LL, Wang, Z, Liu, H, Liu, XS, Roeder, RG, Zhang, X, Song, JS & Fisher, DE 2008, 'Chromatin structure analyses identify miRNA promoters', *Genes & development*, vol. 22, no. 22, pp. 3172-3183.

Packer, JR & Maitland, NJ 2016, 'The molecular and cellular origin of human prostate cancer', *Biochimica et Biophysica Acta (BBA)-Molecular Cell Research*, vol. 1863, no. 6, pp. 1238-1260.

Parker, C, Nilsson, S, Heinrich, D, Helle, SI, O'sullivan, J, Fosså, SD, Chodacki, A, Wiechno, P, Logue, J & Seke, M 2013, 'Alpha emitter radium-223 and survival in metastatic prostate cancer', *New England Journal of Medicine*, vol. 369, no. 3, pp. 213-223.

Pearson, GW 2019, 'Control of invasion by epithelial-to-mesenchymal transition programs during metastasis', *Journal of clinical medicine*, vol. 8, no. 5, p. 646.

Peng, Y & Croce, CM 2016, 'The role of MicroRNAs in human cancer', *Signal transduction and targeted therapy*, vol. 1, p. 15004.

Perou, CM, Sørlie, T, Eisen, MB, van de Rijn, M, Jeffrey, SS, Rees, CA, Pollack, JR, Ross, DT, Johnsen, H & Akslen, LA 2000, 'Molecular portraits of human breast tumours', *Nature*, vol. 406, no. 6797, pp. 747-752.

Peterson, SM, Thompson, JA, Ufkin, ML, Sathyanarayana, P, Liaw, L & Congdon, CB 2014, 'Common features of microRNA target prediction tools', *Frontiers in genetics*, vol. 5, p. 23.

Phillips, I, Shah, SI, Duong, T, Abel, P & Langley, RE 2014, 'Androgen deprivation therapy and the re-emergence of parenteral estrogen in prostate cancer', *Oncology & hematology review*, vol. 10, no. 1, p. 42.

Pichiorri, F, Suh, S-S, Rocci, A, De Luca, L, Taccioli, C, Santhanam, R, Zhou, W, Benson, DM, Hofmainster, C & Alder, H 2010, 'Downregulation of p53-inducible microRNAs 192, 194, and 215 impairs the p53/MDM2 autoregulatory loop in multiple myeloma development', *Cancer cell*, vol. 18, no. 4, pp. 367-381.

Pienta, KJ & Bradley, D 2006, 'Mechanisms underlying the development of androgen-independent prostate cancer', *Clinical Cancer Research*, vol. 12, no. 6, pp. 1665-1671.

Pike, MC, Spicer, DV, Dahmoush, L & Press, MF 1993, 'Estrogens progestogens normal breast cell proliferation and breast cancer risk', *Epidemiologic reviews*, vol. 15, no. 1, pp. 17-35.

Pillman, KA, Scheer, KG, Hackett-Jones, E, Saunders, K, Bert, AG, Toubia, J, Whitfield, HJ, Sapkota, S, Sourdin, L & Pham, H 2019b, 'Extensive transcriptional responses are co-ordinated by microRNAs as revealed by Exon–Intron Split Analysis (EISA)', *Nucleic acids research*, vol. 47, no. 16, pp. 8606-8619.

Piper, C, Porres, D, Pfister, D & Heidenreich, A 2014, 'The role of palliative surgery in castration-resistant prostate cancer', *Current opinion in supportive and palliative care*, vol. 8, no. 3, pp. 250-257.

Porkka, KP, Pfeiffer, MJ, Waltering, KK, Vessella, RL, Tammela, TL & Visakorpi, T 2007, 'MicroRNA expression profiling in prostate cancer', *Cancer research*, vol. 67, no. 13, pp. 6130-6135.

Pratt, AJ & MacRae, IJ 2009, 'The RNA-induced silencing complex: a versatile gene-silencing machine', *Journal of Biological Chemistry*, vol. 284, no. 27, pp. 17897-17901.

Prescott, J & Coetzee, GA 2006, 'Molecular chaperones throughout the life cycle of the androgen receptor', *Cancer letters*, vol. 231, no. 1, pp. 12-19.

Prins, GS & Birch, L 1993, 'Immunocytochemical analysis of androgen receptor along the ducts of the separate rat prostate lobes after androgen withdrawal and replacement', *Endocrinology*, vol. 132, no. 1, pp. 169-178.

Qu, Y, Dai, B, Ye, D, Kong, Y, Chang, K, Jia, Z, Yang, X, Zhang, H, Zhu, Y & Shi, G 2015, 'Constitutively active AR-V7 plays an essential role in the development and progression of castration-resistant prostate cancer', *Sci Rep*, vol. 5, Jan 7, p. 7654.

Ramena, G, Yin, Y, Yu, Y, Walia, V & Elble, RC 2016, 'CLCA2 interactor EVA1 is required for mammary epithelial cell differentiation', *PloS one*, vol. 11, no. 3, p. e0147489.

Rathkopf, DE, Antonarakis, ES, Shore, ND, Tutrone, RF, Alumkal, JJ, Ryan, CJ, Saleh, M, Hauke, RJ, Bandekar, R & Maneval, EC 2017, 'Safety and antitumor activity of apalutamide (ARN-509) in metastatic castration-resistant prostate cancer with and without prior abiraterone acetate and prednisone', *Clinical Cancer Research*.

Reese, AC 2016, 'Clinical and Pathologic Staging of Prostate Cancer', *Prostate Cancer*, Elsevier, pp. 353-360.

Reinhart, BJ, Slack, FJ, Basson, M, Pasquinelli, AE, Bettinger, JC, Rougvie, AE, Horvitz, HR & Ruvkun, G 2000, 'The 21-nucleotide let-7 RNA regulates developmental timing in Caenorhabditis elegans', *Nature*, vol. 403, no. 6772, p. 901.

Risbridger, GP, Davis, ID, Birrell, SN & Tilley, WD 2010, 'Breast and prostate cancer: more similar than different', *Nature Reviews Cancer*, vol. 10, no. 3, p. 205.

Rizzo, M, Berti, G, Russo, F, Fazio, S, Evangelista, M, D'Aurizio, R, Pellegrini, M & Rainaldi, G 2017, 'Discovering the miR-26a-5p targetome in prostate cancer cells', *Journal of Cancer*, vol. 8, no. 14, p. 2729.

Robinson, D, Van Allen, EM, Wu, Y-M, Schultz, N, Lonigro, RJ, Mosquera, J-M, Montgomery, B, Taplin, M-E, Pritchard, CC & Attard, G 2015, 'Integrative clinical genomics of advanced prostate cancer', *Cell*, vol. 161, no. 5, pp. 1215-1228.

Rupaimoole, R, Han, H-D, Lopez-Berestein, G & Sood, AK 2011, 'MicroRNA therapeutics: principles, expectations, and challenges', *Chinese journal of cancer*, vol. 30, no. 6, p. 368.

Sahu, B, Laakso, M, Pihlajamaa, P, Ovaska, K, Sinielnikov, I, Hautaniemi, S & Jänne, OA 2013, 'FoxA1 specifies unique androgen and glucocorticoid receptor binding events in prostate cancer cells', *Cancer research*, vol. 73, no. 5, pp. 1570-1580.

Sanchez, AM, Flamini, MI, Baldacci, C, Goglia, L, Genazzani, AR & Simoncini, T 2010, 'Estrogen receptor-α promotes breast cancer cell motility and invasion via focal adhesion kinase and N-WASP', *Molecular Endocrinology*, vol. 24, no. 11, pp. 2114-2125.

Sathianathen, NJ, Konety, BR, Crook, J, Saad, F & Lawrentschuk, N 2018, 'Landmarks in prostate cancer', *Nature Reviews Urology*, p. 1.

Satterfield, L, Shuck, R, Kurenbekova, L, Allen-Rhoades, W, Edwards, D, Huang, S, Rajapakshe, K, Coarfa, C, Donehower, LA & Yustein, JT 2017, 'miR-130b directly targets ARHGAP1 to drive activation of a metastatic CDC42-PAK1-AP1 positive feedback loop in Ewing sarcoma', *International journal of cancer*, vol. 141, no. 10, pp. 2062-2075.

Scher, HI, Buchanan, G, Gerald, W, Butler, LM & Tilley, WD 2004, 'Targeting the androgen receptor: improving outcomes for castration-resistant prostate cancer', *Endocrine-Related Cancer*, vol. 11, no. 3, pp. 459-476.

Schmitz, U, Pinello, N, Jia, F, Alasmari, S, Ritchie, W, Keightley, M-C, Shini, S, Lieschke, GJ, Wong, JJ & Rasko, JE 2017, 'Intron retention enhances gene regulatory complexity in vertebrates', *Genome biology*, vol. 18, no. 1, p. 216.

Schroeder, A, Herrmann, A, Cherryholmes, G, Kowolik, C, Buettner, R, Pal, S, Yu, H, Müller-Newen, G & Jove, R 2014, 'Loss of androgen receptor expression promotes a stem-like cell phenotype in prostate cancer through STAT3 signaling', *Cancer research*, vol. 74, no. 4, pp. 1227-1237.

Seashols-Williams, S, Budd, W, Clark, G, Wu, Q, Daniel, R, Dragoescu, E & Zehner, Z 2016, 'miR-9 acts as an oncomiR in prostate cancer through multiple pathways that drive tumour progression and metastasis', *PloS one*, vol. 11, no. 7, p. e0159601.

Selth, L, Townley, S, Bert, A, Stricker, P, Sutherland, P, Horvath, L, Goodall, G, Butler, L & Tilley, W 2013, 'Circulating microRNAs predict biochemical recurrence in prostate cancer patients', *British journal of cancer*, vol. 109, no. 3, pp. 641-650.

Seok, H, Ham, J, Jang, E-S & Chi, SW 2016, 'MicroRNA target recognition: insights from transcriptome-wide non-canonical interactions', *Molecules and cells*, vol. 39, no. 5, p. 375.

Shah, RB & Zhou, M 2012, 'Anatomy and Normal Histology of the Prostate Pertinent to Biopsy Practice', *Prostate Biopsy Interpretation: An Illustrated Guide*, Springer Berlin Heidelberg, Berlin, Heidelberg, pp. 1-10.

Shin, C, Nam, J-W, Farh, KK-H, Chiang, HR, Shkumatava, A & Bartel, DP 2010, 'Expanding the microRNA targeting code: functional sites with centered pairing', *Molecular cell*, vol. 38, no. 6, pp. 789-802.

Siiteri, PK & Wilson, JD 1974, 'Testosterone formation and metabolism during male sexual differentiation in the human embryo', *The Journal of Clinical Endocrinology & Metabolism*, vol. 38, no. 1, pp. 113-125.

Simonson, B & Das, S 2015, 'MicroRNA therapeutics: the next magic bullet?', *Mini reviews in medicinal chemistry*, vol. 15, no. 6, pp. 467-474.

Song, Y, Zhao, F, Wang, Z, Liu, Z, Chiang, Y, Xu, Y, Gao, P & Xu, H 2012, 'Inverse association between miR-194 expression and tumor invasion in gastric cancer', *Annals of surgical oncology*, vol. 19, no. 3, pp. 509-517.

Steinkamp, MP, O'Mahony, OA, Brogley, M, Rehman, H, LaPensee, EW, Dhanasekaran, S, Hofer, MD, Kuefer, R, Chinnaiyan, A & Rubin, MA 2009, 'Treatment-dependent androgen receptor mutations in prostate cancer exploit multiple mechanisms to evade therapy', *Cancer research*, vol. 69, no. 10, pp. 4434-4442.

Stephenson, AJ, Kattan, MW, Eastham, JA, Dotan, ZA, Bianco Jr, FJ, Lilja, H & Scardino, PT 2006, 'Defining biochemical recurrence of prostate cancer after radical prostatectomy: a proposal for a standardized definition', *J Clin Oncol*, vol. 24, no. 24, pp. 3973-3978.

Sweeney, CJ, Chen, Y-H, Carducci, M, Liu, G, Jarrard, DF, Eisenberger, M, Wong, Y-N, Hahn, N, Kohli, M & Cooney, MM 2015, 'Chemohormonal therapy in metastatic hormone-sensitive prostate cancer', *New England Journal of Medicine*, vol. 373, no. 8, pp. 737-746.

Tan, H-L, Sood, A, Rahimi, HA, Wang, W, Gupta, N, Hicks, J, Mosier, S, Gocke, CD, Epstein, JI & Netto, GJ 2014, 'Rb loss is characteristic of prostatic small cell neuroendocrine carcinoma', *Clinical Cancer Research*, vol. 20, no. 4, pp. 890-903.

Tan, S, Guo, J, Huang, Q, Chen, X, Li-Ling, J, Li, Q & Ma, F 2007, 'Retained introns increase putative microRNA targets within 3′ UTRs of human mRNA', *FEBS letters*, vol. 581, no. 6, pp. 1081-1086.

Taplin, M-E, Bubley, GJ, Shuster, TD, Frantz, ME, Spooner, AE, Ogata, GK, Keer, HN & Balk, SP 1995, 'Mutation of the androgen-receptor gene in metastatic androgen-independent prostate cancer', *New England Journal of Medicine*, vol. 332, no. 21, pp. 1393-1398.

Taylor, BS, Schultz, N, Hieronymus, H, Gopalan, A, Xiao, Y, Carver, BS, Arora, VK, Kaushik, P, Cerami, E & Reva, B 2010, 'Integrative genomic profiling of human prostate cancer', *Cancer cell*, vol. 18, no. 1, pp. 11-22.

Taylor, RA, Toivanen, R & Risbridger, GP 2010, 'Stem cells in prostate cancer: treating the root of the problem', *Endocrine-Related Cancer*, vol. 17, no. 4, pp. R273-R285.

Thompson, IM 2001, 'Flare associated with LHRH-agonist therapy', *Reviews in urology*, vol. 3, no. Suppl 3, p. S10.

Tilley, WD, Marcelli, M, Wilson, JD & McPhaul, MJ 1989, 'Characterization and expression of a cDNA encoding the human androgen receptor', *Proceedings of the National Academy of Sciences*, vol. 86, no. 1, pp. 327-331.

Toivanen, R & Shen, MM 2017, 'Prostate organogenesis: tissue induction, hormonal regulation and cell type specification', *Development*, vol. 144, no. 8, pp. 1382-1398.

Tong, A, Fulgham, P, Jay, C, Chen, P, Khalil, I, Liu, S, Senzer, N, Eklund, A, Han, J & Nemunaitis, J 2009, 'MicroRNA profile analysis of human prostate cancers', *Cancer gene therapy*, vol. 16, no. 3, pp. 206-216.

Tran, C, Ouk, S, Clegg, NJ, Chen, Y, Watson, PA, Arora, V, Wongvipat, J, Smith-Jones, PM, Yoo, D & Kwon, A 2009, 'Development of a second-generation antiandrogen for treatment of advanced prostate cancer', *Science*, vol. 324, no. 5928, pp. 787-790.

Tsai, H-P, Huang, S-F, Li, C-F, Chien, H-T & Chen, S-C 2018, 'Differential microRNA expression in breast cancer with different onset age', *PloS one*, vol. 13, no. 1, p. e0191195.

Turo, R, Smolski, M, Esler, R, Kujawa, ML, Bromage, SJ, Oakley, N, Adeyoju, A, Brown, SC, Brough, R & Sinclair, A 2014, 'Diethylstilboestrol for the treatment of prostate cancer: past, present and future', *Scandinavian journal of urology*, vol. 48, no. 1, pp. 4-14.

Van der Ree, M, Van Der Meer, A, Van Nuenen, A, De Bruijne, J, Ottosen, S, Janssen, H, Kootstra, N & Reesink, H 2016, 'Miravirsen dosing in chronic hepatitis C patients results in decreased micro RNA-122 levels without affecting other micro RNA s in plasma', *Alimentary pharmacology & therapeutics*, vol. 43, no. 1, pp. 102-113.

Van Laar, J, Bolt-de Vries, J, Voorhorst-Ogink, M & Brinkmann, A 1989, 'The human androgen receptor is a 110 kDa protein', *Molecular and cellular endocrinology*, vol. 63, no. 1-2, pp. 39-44.

Van Leenders, G & Schalken, J 2001, 'Stem cell differentiation within the human prostate epithelium: implications for prostate carcinogenesis', *BJU international*, vol. 88, pp. 35-42.

Vasudevan, S 2012, 'Posttranscriptional upregulation by microRNAs', *Wiley Interdisciplinary Reviews: RNA*, vol. 3, no. 3, pp. 311-330.

Visakorpi, T, Hyytinen, E, Koivisto, P, Tanner, M, Keinänen, R, Palmberg, C, Palotie, A, Tammela, T, Isola, J & Kallioniemi, O-P 1995, 'In vivo amplification of the androgen receptor gene and progression of human prostate cancer', *Nature genetics*, vol. 9, no. 4, p. 401.

Walter, BA, Valera, VA, Pinto, PA & Merino, MJ 2013, 'Comprehensive microRNA profiling of prostate cancer', *Journal of Cancer*, vol. 4, no. 5, p. 350.

Wang, B, Shen, Z-l, Gao, Z-d, Zhao, G, Wang, C-y, Yang, Y, Zhang, J-z, Yan, Y-c, Shen, C & Jiang, K-w 2015, 'MiR-194, commonly repressed in colorectal cancer, suppresses tumor growth by regulating the MAP4K4/c-Jun/MDM2 signaling pathway', *Cell cycle*, vol. 14, no. 7, pp. 1046-1058.

Wang, L, Liu, C, Li, C, Xue, J, Zhao, S, Zhan, P, Lin, Y, Zhang, P, Jiang, A & Chen, W 2015, 'Effects of microRNA-221/222 on cell proliferation and apoptosis in prostate cancer cells', *Gene*, vol. 572, no. 2, pp. 252-258.

Wang, M, Wang, W, Zhang, P, Xiao, J, Wang, J & Huang, C 2014, 'Discrimination of the expression of paralogous microRNA precursors that share the same major mature form', *PloS one*, vol. 9, no. 3, p. e90591.

Wang, X, Kruithof-de Julio, M, Economides, KD, Walker, D, Yu, H, Halili, MV, Hu, Y-P, Price, SM, Abate-Shen, C & Shen, MM 2009, 'A luminal epithelial stem cell that is a cell of origin for prostate cancer', *Nature*, vol. 461, no. 7263, p. 495.

Wang, Y, Hayward, SW, Cao, M, Thayer, KA & Cunha, GR 2001, 'Cell differentiation lineage in the prostate', *Differentiation*, vol. 68, no. 4-5, pp. 270-279.

Ward, JF, Vogelzang, N, Davis, BJ & Richie, JP 2015, 'Initial management of regionally localized intermediate-, high-, and very high-risk prostate cancer and those with clinical lymph node involvement', *J Clin Oncol [Internet]*, pp. 5019-5019.

Wee, LM, Flores-Jasso, CF, Salomon, WE & Zamore, PD 2012, 'Argonaute divides its RNA guide into domains with distinct functions and RNA-binding properties', *Cell*, vol. 151, no. 5, pp. 1055-1067.

Wilson, JD, Griffin, JE & Russell, DW 1993, 'Steroid 5α-reductase 2 deficiency', *Endocrine reviews*, vol. 14, no. 5, pp. 577-593.

Wong, CI, Zhou, ZX, Sar, M & Wilson, EM 1993, 'Steroid requirement for androgen receptor dimerization and DNA binding. Modulation by intramolecular interactions between the NH2-terminal and steroid-binding domains', *Journal of Biological Chemistry*, vol. 268, no. 25, pp. 19004-19012.

Xu, G, Fewell, C, Taylor, C, Deng, N, Hedges, D, Wang, X, Zhang, K, Lacey, M, Zhang, H & Yin, Q 2010, 'Transcriptome and targetome analysis in MIR155 expressing cells using RNA-seq', *Rna*, vol. 16, no. 8, pp. 1610-1622.

Xu, J, Kang, Y, Liao, W-m & Yu, L 2012, 'MiR-194 regulates chondrogenic differentiation of human adipose-derived stem cells by targeting Sox5', *PloS one*, vol. 7, no. 3, p. e31861.

Yamamura, S, Saini, S, Majid, S, Hirata, H, Ueno, K, Deng, G & Dahiya, R 2012, 'MicroRNA-34a modulates c-Myc transcriptional complexes to suppress malignancy in human prostate cancer cells', *PloS one*, vol. 7, no. 1, p. e29722.

Yang, Y, Chen, R, Sun, T, Zhao, L, Liu, F, Ren, S, Wang, H, Lu, X, Gao, X & Xu, C 2019, 'Efficacy and safety of combined androgen blockade with antiandrogen for advanced prostate cancer', *Current Oncology*, vol. 26, no. 1, p. e39.

Yang, YA & Yu, J 2015, 'Current perspectives on FOXA1 regulation of androgen receptor signaling and prostate cancer', *Genes & diseases*, vol. 2, no. 2, pp. 144-151.

Yuan, S, Norgard, RJ & Stanger, BZ 2019, 'Cellular plasticity in cancer', *Cancer discovery*, vol. 9, no. 7, pp. 837-851.

Zaret, KS & Carroll, JS 2011, 'Pioneer transcription factors: establishing competence for gene expression', *Genes & development*, vol. 25, no. 21, pp. 2227-2241.

Zhang, J, Zhao, C-Y, Zhang, S-H, Yu, D-H, Chen, Y, Liu, Q-H, Shi, M, Ni, C-R & Zhu, M-H 2014, 'Upregulation of miR-194 contributes to tumor growth and progression in pancreatic ductal adenocarcinoma', *Oncology reports*, vol. 31, no. 3, pp. 1157-1164.

Zhang, K, Zhang, X, Cai, Z, Zhou, J, Cao, R, Zhao, Y, Chen, Z, Wang, D, Ruan, W & Zhao, Q 2018, 'A novel class of microRNA-recognition elements that function only within open reading frames', *Nature structural & molecular biology*, vol. 25, no. 11, p. 1019.

Zhang, M, Zhuang, Q & Cui, L 2016, 'MiR-194 inhibits cell proliferation and invasion via repression of RAP2B in bladder cancer', *Biomedicine & Pharmacotherapy*, vol. 80, pp. 268-275.

Zhao, SG, Chang, SL, Erho, N, Yu, M, Lehrer, J, Alshalalfa, M, Speers, C, Cooperberg, MR, Kim, W & Ryan, CJ 2017, 'Associations of luminal and basal subtyping of prostate cancer with prognosis and response to androgen deprivation therapy', *JAMA oncology*, vol. 3, no. 12, pp. 1663-1672.

Zhou, L, Di, Q, Sun, B, Wang, X, Li, M & Shi, J 2016, 'MicroRNA-194 restrains the cell progression of non-small cell lung cancer by targeting human nuclear distribution protein C', *Oncology reports*, vol. 35, no. 6, pp. 3435-3444.

Zou, M, Toivanen, R, Mitrofanova, A, Floch, N, Hayati, S, Sun, Y, Le Magnen, C, Chester, D, Mostaghel, EA & Califano, A 2017, 'Transdifferentiation as a mechanism of treatment resistance in a mouse model of castration-resistant prostate cancer', *Cancer discovery*, vol. 7, no. 7, pp. 736-749.

Zumsteg, ZS, Spratt, DE, Pei, I, Zhang, Z, Yamada, Y, Kollmeier, M & Zelefsky, MJ 2013, 'A new risk classification system for therapeutic decision making with intermediate-risk prostate cancer patients undergoing dose-escalated external-beam radiation therapy', *European urology*, vol. 64, no. 6, pp. 895-902.